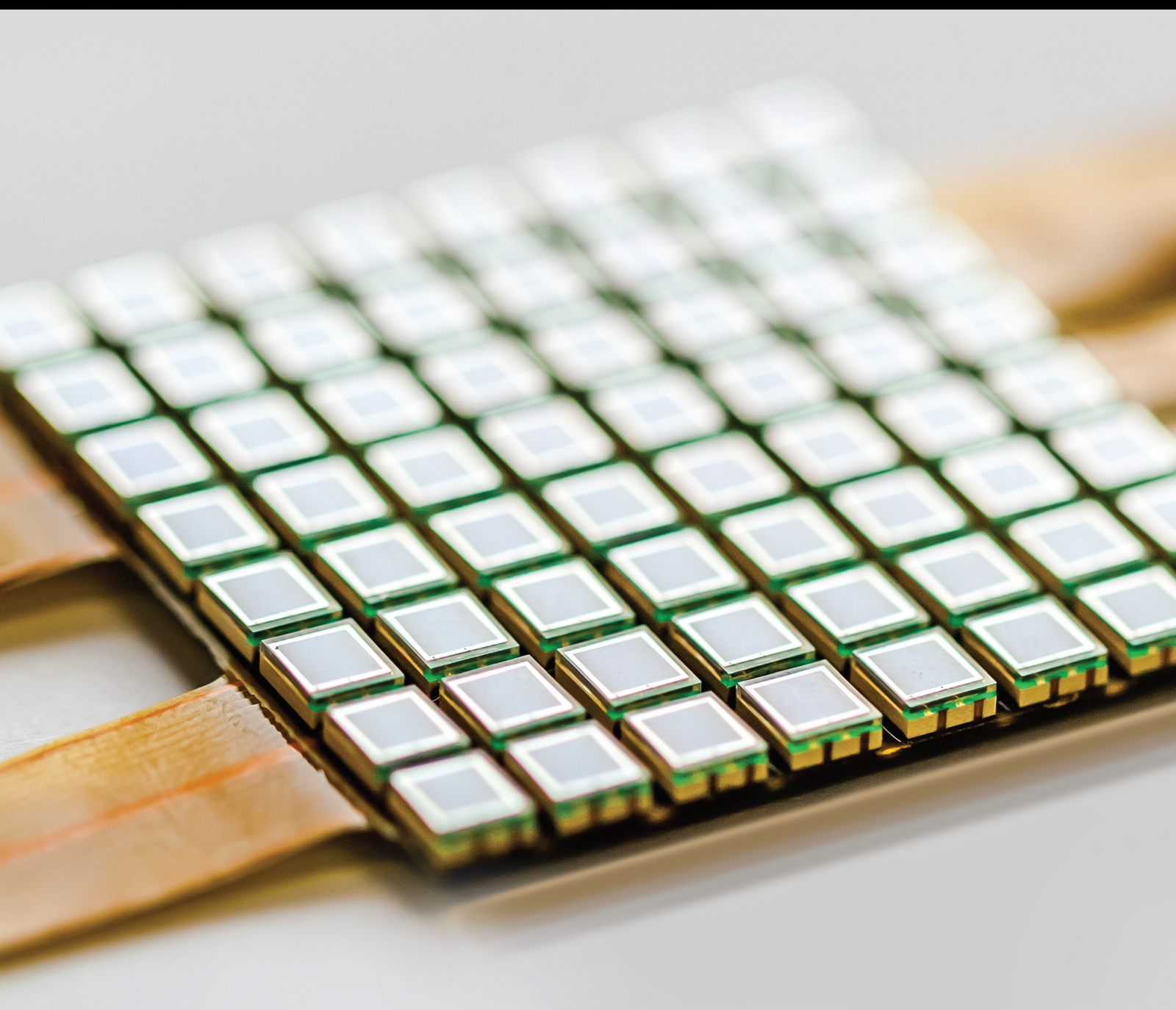# Physical Layer Security for Sensor-enabled Heterogeneous Networks

Lead Guest Editor: Rupak Kharel
Guest Editors: Kashif Naseer and Omprakash Kaiwartya

Physical Layer Security for Sensor-enabled Heterogeneous Networks

Physical Layer Security for Sensor-enabled Heterogeneous Networks

Lead Guest Editor: Rupak Kharel
Guest Editors: Kashif Naseer and Omprakash Kaiwartya

Ehsan Namaziandost (iD), Iran
Heinz C. Neitzert (iD), Italy
Sing Kiong Nguang (iD), New Zealand
Calogero M. Oddo (iD), Italy
Tinghui Ouyang, Japan
SANDEEP KUMAR PALANISWAMY (iD),
India
Alberto J. Palma (iD), Spain
Davide Palumbo (iD), Italy
Abinash Panda (iD), India
Roberto Paolesse (iD), Italy
Akhilesh Pathak (iD), Thailand
Giovanni Pau (iD), Italy
Giorgio Pennazza (iD), Italy
Michele Penza (iD), Italy
Sivakumar Poruran, India
Stelios Potirakis (iD), Greece
Biswajeet Pradhan (iD), Malaysia
Giuseppe Quero (iD), Italy
Linesh Raja (iD), India
Maheswar Rajagopal (iD), India
Valerie Renaudin (iD), France
Armando Ricciardi (iD), Italy
Christos Riziotis (iD), Greece
Ruthber Rodriguez Serrezuela (iD), Colombia
Maria Luz Rodriguez-Mendez (iD), Spain
Jerome Rossignol (iD), France
Maheswaran S, India
Ylias Sabri (iD), Australia
Sourabh Sahu (iD), India
José P. Santos (iD), Spain
Sina Sareh, United Kingdom
Isabel Sayago (iD), Spain
Andreas Schütze (iD), Germany
Praveen K. Sekhar (iD), USA
Sandra Sendra, Spain
Sandeep Sharma , India
Sunil Kumar Singh Singh (iD), India
Yadvendra Singh (iD), USA
Afaque Manzoor Soomro (iD), Pakistan
Vincenzo Spagnolo, Italy
Kathiravan Srinivasan (iD), India
Sachin K. Srivastava (iD), India
Stefano Stassi (iD), Italy

Danfeng Sun, China
Ashok Sundramoorthy, India
Salvatore Surdo (iD), Italy
Roshan Thotagamuge (iD), Sri Lanka
Guiyun Tian (iD), United Kingdom
Sri Ramulu Torati (iD), USA
Abdellah Touhafi (iD), Belgium
Hoang Vinh Tran (iD), Vietnam
Aitor Urrutia (iD), Spain
Hana Vaisocherova - Lisalova (iD), Czech
Republic
Everardo Vargas-Rodriguez (iD), Mexico
Xavier Vilanova (iD), Spain
Stanislav Vítek (iD), Czech Republic
Luca Vollero (iD), Italy
Tomasz Wandowski (iD), Poland
Bohui Wang, China
Qihao Weng, USA
Penghai Wu (iD), China
Qiang Wu, United Kingdom
Yuedong Xie (iD), China
Chen Yang (iD), China
Jiachen Yang (iD), China
Nitesh Yelve (iD), India
Aijun Yin, China
Chouki Zerrouki (iD), France

Contents

Research Article

Dual-Hop Transmission and Multiple Relays for Performance Analysis of Designing Physical Layer Security for IoT Networks

Nhan Duc Nguyen ⬤,[1] **Anh-Tu Le** ⬤,[2] **Dinh-Thuan Do** ⬤,[3] and **Munyaradzi Munochiveyi** ⬤[4]

[1]*Faculty of Mechanical-Electrical and Computer Engineering, School of Engineering and Technology, Van Lang University, 69/ 68 Dang Thuy Tram Street, Ward 13, Binh Thanh District, Ho Chi Minh City 70000, Vietnam*
[2]*Faculty of Electronics Technology, Industrial University of Ho Chi Minh City, Vietnam*
[3]*Department of Computer Science and Information Engineering, Asia University, Taichung 41354, Taiwan*
[4]*Electrical and Electronic Engineering Department, University of Zimbabwe, Mount Pleasant, Harare, Zimbabwe*

Correspondence should be addressed to Munyaradzi Munochiveyi; mmunochiveyi@eng.uz.ac.zw

This article presents a secure performance metric of a downlink nonorthogonal multiple access (NOMA) in the presence of interference from the traditional user. In the context of NOMA, we deploy two-hop transmission to improve the performance of destinations. Further, multiple relays are implemented to aid robust signal-to-interference-plus-noise ratio (SINR) at destinations. We derive a closed-form expression of secure outage probability (SOP) to characterize security concerns in the case an eavesdropper exists in the overage of second hop transmission. We verify all expressions by employing Monte Carlo simulations.

1. Introduction

1.1. Motivation. The nonorthogonal multiple access (NOMA) procedures can progress the effectiveness of the spectrum since it can allocate the same frequency band to multiple users by differentiating the power levels of each user in the cluster [1–5]. Successive interference cancellation (SIC) is a technique that is achieved at the receiver's end to distinguish the received signals [6]. The addition of the NOMA technique into cognitive radio (CR) networks has shown advantages like improving better spectral efficiency and also serving increased numerous secondary users, realizing 5th generation (5G) communication systems [7]. In [8], the author mentioned repetition-based NOMA, which can achieve high diversity gain by utilizing repetition. This method is different compared to the conventional power domain NOMA as all users possess the same power level but a diverse number of repetitions. Since it has high diversity gain, we can achieve low outage probability with no need for instant channel state information (CSI) response for

power allocation. The key parameters are constrained to sustain the outage probability (OP) lesser than the target value by deriving a closed-form expression of OP. Moreover, in [9] the authors examined the impact of imperfect CSI and imperfect SIC on NOMA-enabled coordinated direct and relay transmission (CDRT) network consisting of a base station communicating directly with a cell-centered user and an FD relay responsible for communicating with a user located at the cell-edge. Here, the authors obtained exact OP and ergodic rates for the users under the assumption of imperfect CSI and SIC. Also, the authors considered the channel links to be operating under Nakagami-m fading conditions. Numerical results demonstrated the adverse impact of imperfect CSI and SIC on the OP performance of the system. To remedy this, the authors determined a suitable base-station power allocation coefficient to ensure fair outage for both network users under imperfect CSI and SIC conditiIn [10], the authors studied the performance of downlink NOMA in vehicular communication over double Rayleigh fading channels, where a base station communicates with a

far-user and a near-user. Due to the impact of mobility, the authors derived OP expressions of the individual users as well as for the overall system considering the scenario of when the NOMA rate falls below the system target rate and when Orthogonal Multiple Access (OMA) outperforms the NOMA system. Additionally, the authors derived ergodic capacity and Average Bit Error Rate (ABER) expressions. Numerical results showed that in terms of OP and ergodic capacity, NOMA outperforms OMA, however in terms of ABER, OMA outperforms NOMA as OMA users lack inter-user interferences.

In the presence of massive communications, security becomes the major apprehension among the users. Because of the diverse nature of radio propagation, the communication networks are exposed to the eavesdropper, and this also becomes a major challenge for researchers to overcome [11]. We know that cognitive radio (CR) networks permit unlicensed users in the spectrum that increases the risk of wiretapping, particularly when the users are malicious. In previous generations, cryptographic algorithms are utilized in the top layers to protect the data. But these algorithms are time-consuming and complicated since they have to perform encryption and decryption to protect the data [12]. Whereas, Physical Layer Security (PLS) has become the single utmost significant tactic to secure the data. Since the evolution of CR networks, there has been a giant exploration going on to enhance the performance of PLS [13–20]. Authors in [13, 14] have designed CR networks user-scheduling schemes, to improve the secrecy performance by achieving multiuser diversity for a primary user under the Quality of Service (QoS) limitation. Authors in [13] have shown that the scheme can achieve maximum diversity, whereas in [14], the three user-scheduling schemes show that the secrecy performance rate is significantly enhanced by growing the number of cognitive users. Authors in [15] have employed multiple relay selection policies where one relay aids in transmitting the information and the other acts as a friendly jammer. This way, the authors were able to obtain efficient performance in terms of secrecy outage of the cognitive transmission system. In [16], the authors proposed an Artificial Noise (AN) assisted optimal beamforming scheme, in which the ergodic secrecy rate is maximized by obtaining optimal power allocation among data and AN signal.

Until now, all the works discussed are based on Rayleigh fading channels, whereas the works in [17–20] are based on Nakagami-m fading channels. In [17] the authors have provided a consistent method to identify the secrecy performance of the framework by determining the mathematical expression of Secrecy Outage Probability (SOP) and nonzero secrecy capacity probability. Authors in [18] have considered a multiantenna networks approach by proposing optimal and suboptimal antenna selecting schemes for secured underlay CR networks. The authors have also derived mathematical descriptions of the exact and asymptotic SOP of both schemes. In [19], the authors considered enhancing the secrecy performance by increasing the number of relays or legitimate channel Nakagami parameters. In [20], the authors considered PLS in a CR network with multiple primary and secondary users. PLS also plays a pivotal role in NOMA communications in terms of secure transmission [20–25]. Especially, the authors in [24–26] mentioned that the secrecy performance of the NOMA technique outperforms the Orthogonal Multiple Access (OMA) technique. Authors in [24] optimized the transmit power to achieve a maximum secrecy rate. Along with these techniques, authors in [25, 26] have adopted beamforming and power allocation policies. In [25], the authors considered a NOMA-assisted multicast-unicast system and studied the risk of multicast receivers intercepting the unicasting messages. Whereas, in [26], the cell-edge user is considered an eavesdropper who spies on the data and information of a cell-center user. Authors in [27] have considered the user pairing method to improve the security of the NOMA system. In this model, the users are arranged according to their channel gains and paired with unlike channel gains to achieve the NOMA protocol. The outcomes explain that the secrecy diversity order of the user is equal to the ascending direction of channel ordering.

1.2. Related Works. Recently, several authors have been interested in studying secrecy in NOMA-aided Full-Duplex (FD) systems in the vicinity of eavesdroppers. One of these works is found in [28], where the authors investigated the SOP of NOMA-assisted dual-hop FD amplify-and-forward networks in the presence of a colluding and noncolluding wiretapping eavesdropper. This system comprised a base station, a multiple antenna FD relay, an eavesdropper, and multiple users. In [29], the authors studied the trade-off between reliability and security of PLS techniques in cooperative NOMA-enabled dual-hop Internet-of-Things (IoT) systems under in-phase and quadrature-phase imbalance (IQI) conditions at the transceivers. The system consisted of a single source, a relay, an eavesdropper, and multiple devices. Here, the authors derived closed-form OP and Intercept Probability (IP) expressions. The simulation results showed that IQI increases OP while reducing IP, demonstrating that reliability is impacted but security is enhanced. In [30], the author considered the PLS of a dual-hop NOMA system consisting of a single source, relay, an eavesdropper, and numerous users. The authors maximized the system's secure sum rate over different source subcarriers with optimal power allocation. Further, the authors solved the nonconvex and mixed-integer programming problem via duality theory. Simulation results demonstrated that the proposed system outperforms OMA systems. In [31], the authors examined the Strictly Positive Secrecy Capacity (SPSC) and SOP of a NOMA-aided dual-hop DF system under different scenarios of untrusted and trusted relays. Here, the network is made up of a base station, a DF relay, an eavesdropper, and a multiple users. The authors derived exact expressions for SPSC and SOP under independent Rayleigh fading. Moreover, numerical results compared the secrecy performance of the proposed system against OMA. Similarly, in [32], the authors examined the secrecy performance of cooperative downlink and uplink NOMA-aided network with an untrusted relay. To minimize secrecy failure at the untrusted relay, the authors proposed adaptive downlink and uplink jamming strategies. For each strategy, the authors derived lower bound ergodic secrecy sum rates

for the proposed system. Furthermore, in [33], the authors considered different scenarios of single and multiple antenna relay configurations at the source and the untrusted relay. In this work, the authors derived closed-form lower bound ergodic secrecy sum rate (ESSR) and proved via simulation results how the proposed system outperforms OMA systems.

Differently, in [34], the authors considered the SOP of a cooperative NOMA-aided system with multiple relays over Nakagami-m fading channels in the presence of an eavesdropper. Here, the authors proposed three different types of relay selection (RS) strategies which are Optimal Single Relay Selection (OSRS), Two-Step Single Relay Selection (TSRS), and Optimal Dual Relay Selection (ODRS). The authors obtained closed-form SOP expressions under different RS strategies. Similarly, in [35], the authors considered the asymptotic SOP of NOMA-assisted multiple-DF relay network over Rayleigh fading channels with two RS schemes—OSRS and TSRS. The authors also derived exact asymptotic SOP for both RS schemes considering fixed and dynamic power allocations. In [36], the authors investigated a cooperative NOMA network with multiple relays, where one relay transmits information and the other relays act as jammers. Here, the authors considered two RS schemes, random and max–min RS. The authors derived closed-form SOP for both RS schemes. Simulation results proved that in the moderate to high signal-to-noise ratio (SNR) region, the proposed scheme obtains a lower SOP than systems without jammers. Also, the max-min RS scheme enhances the SOP in the low SNR range.

However, it would be unreasonable for us not to mention the hidden cost of multiple relays in NOMA-aided massive IoT networks. Large CSI signaling overhead, power allocation feedback, and computational complexity emerge when there are a massive number of devices and relays in NOMA-enabled multiple-relay networks [37, 38]. In such a scenario, feedback delay from the multiple relays becomes a critical issue resulting in channel estimation and synchronization errors in the uplink [37, 38]. Therefore, obtaining perfect CSI is difficult to achieve [37, 38]. These issues are still open research problems, and we welcome more research in this area to enable NOMA-enabled multiple relay networks to be implemented practically.

Furthermore, another area of interest this research work did not consider, but is also worth researching, is the security in simultaneous wireless information and power transfer- (SWIPT-) enabled IoT networks. The authors in [39, 40] proposed a PLS approach for SWIPT-enabled multiple relays IoT network. Additionally, the authors investigated the impact of static power splitting relaying (SPSR) and dynamic power splitting relaying (DPSR) on secure communications in the presence of an eavesdropper. Similarly, in [41], the authors also considered the impact of SPSR and DPSR on the outage and throughput performance for a DF relay SWIPT system, consisting of a single source, multiple relays, and a destination. Differently, in [42], the authors proposed partial and full relay selection techniques for self-energy recycling (S-ER) FD multiple-relay networks, in which the self-interference energy is harvested back at the relay for future use.

1.3. Contributions. In several works, such as [34–36], the authors considered systems with multiple relays and different RS strategies when examining the SOP of such proposed systems. However, the practical issue of interference was not investigated in those works. Therefore, in this work, we propose a NOMA-enabled multiple-relay communication network reliant on partial relay selection (PRS) and investigate the SOP performance of the proposed system. In particular, we take into consideration the aspect of interferences on the NOMA-aided communication system. Table 1 provides a comparison of this work versus the works in [28–36]. Our contributions are listed as follows:

(i) We consider transmission assisted by NOMA where a single antenna base station communicates with two devices arranged in a near and far position from the base station in the presence of an eavesdropper, multiple relays, and interference causing conventional user equipment (CUE). The proposed system employs a partial relay selection (PRS) scheme. We study the secrecy performance to determine the downlink SOP and SPSC performance under Rayleigh fading channels

(ii) We then determine the signal-to-interference-plus-noise ratios (SINRs) of the two devices and use them to formulate exact SOP and SPSC formulas over Rayleigh fading channels. The derived expressions are validated by Monte Carlo simulations

(iii) We analyze and compare the SOP and SPSC under various conditions. In particular, we find that transmit SNR at source, interference channel, the number of relays, and power allocation factors are the main impacts on SOP and SPSC. The obtained numerical results demonstrate that the proposed scheme can increase secrecy and achieve significant SOP via many practical scenarios

1.4. Organization. The rest of this paper is organized as follows. Section 2 describes the downlink NOMA under Rayleigh channels in the dual-hop multiple-relay network in the presence of an eavesdropper and interference. In Section 3, we consider the scenario of NOMA in terms of secrecy outage performance. In Section 4, we consider strictly positive secrecy capacity. In Section 5, we provide extensive numerical simulations, and Section 6 concludes the paper.

2. System Model

A downlink NOMA cooperative relay network is studied, as shown in Figure 1. In particular, we consider a base station (S), a K DF relays, two main destinations (D_i), an eavesdropper (E), and a conventional user equipment (CUE). This CUE causes interference to the two main users (D_i) as in Figure 1. In addition, the channel coefficient from S to R_k, ($k = 1, \cdots, K$), from R_k to D_i, from R_k to E, and from the CUE to D_i are g_{SR_k}, $g_{R_k D_i}$, $g_{R_k E}$, and g_{CU_i}, respectively. All channels experience Rayleigh fading, i.e., channel g with

TABLE 1: A comparison of existing works on PLS for dual-hop transmission and multiple relays.

System setup	Reference	Major contributions	Scenario
Dual-hop FD-AF-NOMA	[28]	Closed-form SOP expressions	Colluding and noncolluding wiretapping eavesdropper
Dual-hop DF-NOMA-IoT	[29]	Closed-form OP and IP expressions	In-phase and quadrature-phase imbalance (IQI) conditions at the transceivers
Dual-hop AF-NOMA	[30]	Secure sum rate maximization over different source subcarriers with optimal power allocation	Single eavesdropper
Dual-hop untrusted DF-NOMA	[31]	Closed-form SPSC and SOP expressions	Untrusted and trusted relays
Dual-hop untrusted AF-NOMA	[32]	Closed-form lower bound ESSR	Untrusted AF relay engaged in both relaying and eavesdropping
Dual-hop untrusted AF-NOMA	[33]	Closed-form lower bound ESSR	Untrusted relay
Dual-hop relay-selection DF-HD-NOMA	[34]	Closed-form SOP expressions under different RS strategies	Single eavesdropper
Dual-hop relay-selection DF-NOMA	[35]	Closed-form asymptotic SOP for both RS schemes considering fixed and dynamic power allocations.	Single eavesdropper
Dual-hop jamming HD-DF-NOMA	[36]	Closed-form SOP under different RS schemes	Jamming relay
Dual-hop interference DF-NOMA-IoT	Our work	Closed-form SOP and SPSC under PRS setup	Single eavesdropper, interference causing conventional user equipment (CUE)
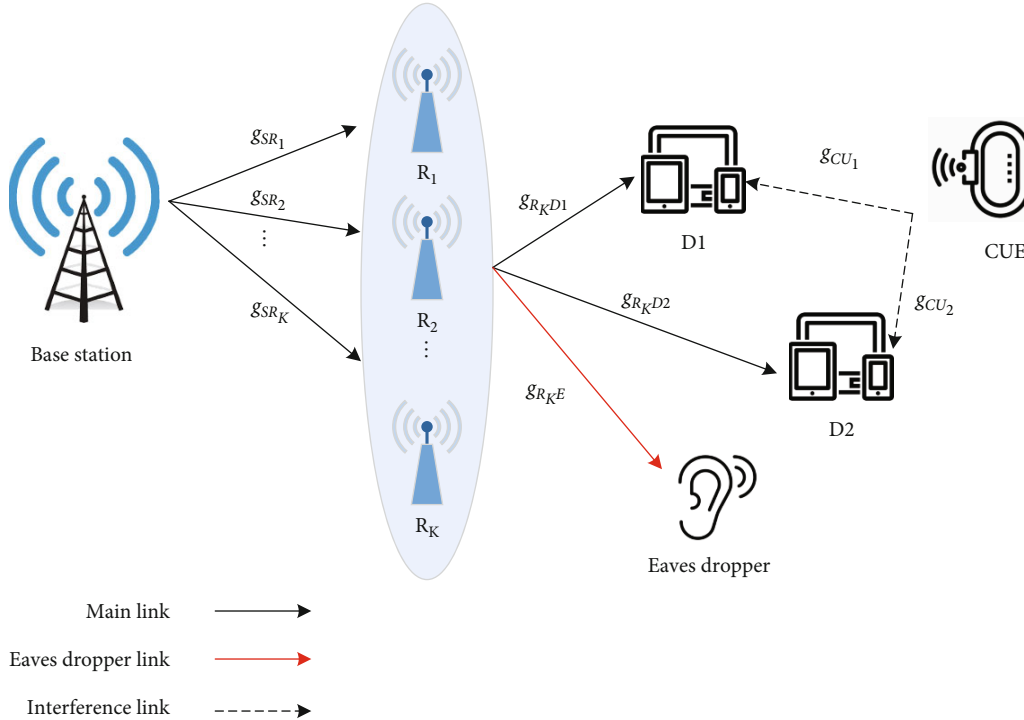
FIGURE 1: Downlink dual-hop NOMA-aided multiple-relay network in the presence of an eavesdropper and interference.

parameter $CN(0, \Omega)$. Moreover, we assume all channels follow perfect CSI as in [4].

In the first time slot, the source (S) transmits the signal $\sqrt{a_1}x_1 + \sqrt{a_2}x_2$ to the selected relay R_k in which a_1 and a_2 are the power allocation coefficient and $a_1 < a_2$, and x_i is the signal dedicated to D_i. Therefore, the received signal R_k is given by

$$r_{SR_k} = \sqrt{P_S}(\sqrt{a_1}x_1 + \sqrt{a_2}x_2)g_{SR_k} + n_{R_k}, \quad (1)$$

where P_S is the transmit power at S, and n_{R_k} is $CN(0, \sigma_{R_k}^2)$. When R_k decodes x_2, the signal-to-interference-plus-noise ratio (SINR) is formulated by

$$\vartheta_{R_k \longrightarrow x_2} = \frac{P_S a_2 \left| g_{SR_k} \right|^2}{P_S a_1 \left| g_{SR_k} \right|^2 + \sigma_{R_k}^2} = \frac{\rho_S a_2 \left| g_{SR_k} \right|^2}{\rho_S a_1 \left| g_{SR_k} \right|^2 + 1}, \quad (2)$$

where $\rho_S = ((P_S)/(\sigma_{R_k}^2))$. Following the principle of the NOMA scheme [4], the instantaneous signal-to-noise-ratio (SNR) after using successive interference cancellation (SIC) to detect x_1 at R_k is given by

$$\vartheta_{R_k \longrightarrow x_1} = \rho_S a_1 \left| g_{SR_k} \right|^2. \quad (3)$$

In the second time slot, the relay R_k forwards the signal from source S to D_i. As a result, the received signal D_i is formulated by

$$r_{RD_i} = \sqrt{P_R} (\sqrt{a_1} x_1 + \sqrt{a_2} x_2) g_{R_k D_i} + P_{CE} g_{CU_i} + n_i, \quad (4)$$

where P_R is the transmit power at R_k, P_{CE} is the power of the CUE, and n_i is $CN(0, \sigma_i^2)$. Next, the SINR at D_2 when detecting its own signal x_2 is given as

$$\vartheta_{D_2 \longrightarrow x_2} = \frac{P_R a_2 \left| g_{R_k D_2} \right|^2}{P_R a_1 \left| g_{R_k D_2} \right|^2 + P_{CE} \left| g_{CU_2} \right|^2 + \sigma_2^2}$$

$$= \frac{\rho_R a_2 \left| g_{R_k D_2} \right|^2}{\rho_R a_1 \left| g_{R_k D_2} \right|^2 + \rho_{CE} \left| g_{CU_2} \right|^2 + 1}, \quad (5)$$

where $\rho_R = ((P_R)/(\sigma_i^2))$, $\rho_{CE} = ((P_{CE})/(\sigma_i^2))$. Next the SINR at D_1 when detecting signal x_2 is expressed by

$$\vartheta_{D_1 \longrightarrow x_2} = \frac{\rho_R a_2 \left| g_{R_k D_1} \right|^2}{\rho_R a_1 \left| g_{R_k D_1} \right|^2 + \rho_{CE} \left| g_{CU_1} \right|^2 + 1}. \quad (6)$$

By conducting SIC, the SINR to detect signal x_1 at D_1 is expressed by

$$\vartheta_{D_1 \longrightarrow x_1} = \frac{\rho_R a_1 \left| g_{R_k D_1} \right|^2}{\rho_{CE} \left| g_{CU_1} \right|^2 + 1}. \quad (7)$$

To consider the impact of the eavesdropper, we need to compute the received signal at E as

$$r_E = \sqrt{P_R} (\sqrt{a_1} x_1 + \sqrt{a_2} x_2) g_{R_k E} + n_E, \quad (8)$$

where n_E is $CN(0, \sigma_E^2)$ and $\rho_E = ((P_E)/(\sigma_E^2))$. Similar to [43], the instantaneous SNR of detecting the signal D_i are given as

$$\vartheta_{E \longrightarrow x_i} = \rho_E a_i \left| g_{R_k E} \right|^2. \quad (9)$$

By employing partial relay selection (PRS), the selected relay R_k is chosen as follows based on criteria [44].

$$k^* = \arg \max_{k=1,\cdots,K} \left| g_{SR_k} \right|^2. \quad (10)$$

3. Performance Analysis

In this section, we derive the closed-form of Secrecy Outage Probability (SOP) for D_i. The secrecy rate of D_i is given as

$$C_i = \left[\frac{1}{2} \log_2 \left(1 + \min \left(\vartheta_{R_{k^*} \longrightarrow x_2}, \vartheta_{D_2 \longrightarrow x_2} \right) \right) - \frac{1}{2} \log_2 \left(1 + \vartheta_{E \longrightarrow x_2} \right) \right]^+, \quad (11)$$

where $[x]^k = \max(x, 0)$.

3.1. Secrecy Outage Probability of D_2. Following the result reported in [45], the cumulative distribution functions (CDF) of $\left| g_{SR_{k^*}} \right|^2 = \max_{k=1,\cdots,K} \left| g_{SR_k} \right|^2$ is given as

$$F_{\left| g_{SR_{k^*}} \right|^2}(x) = \left(1 - e^{-(x/(\Omega_{SR_{k^*}}))} \right)^K$$

$$= 1 - \sum_{k=1}^K \binom{K}{k} (-1)^{k-1} e^{-((kx)/(\Omega_{SR_{k^*}}))}. \quad (12)$$

Then, the SOP of D_2 is computed by

$$\text{SOP}_{D_2} = \Pr(C_2 < R_2)$$

$$= \Pr \left(\frac{1 + \min \left(\vartheta_{R_{k^*} \longrightarrow x_2}, \vartheta_{D_2 \longrightarrow x_2} \right)}{1 + \vartheta_{E \longrightarrow x_2}} < \gamma_2 \right) \quad (13)$$

$$= 1 - \Pr \left(\frac{1 + \vartheta_{R_{k^*} \longrightarrow x_2}}{1 + \vartheta_{E \longrightarrow x_2}} > \gamma_2, \frac{1 + \vartheta_{D_2 \longrightarrow x_2}}{1 + \vartheta_{E \longrightarrow x_2}} > \gamma_2 \right),$$

where $\gamma_i = 2^{2R_i}$ and R_i is the targeted secrecy rate. Substituting (2), (5), and (9) into (12), it can be written such SOP for D_2 as

$$\text{SOP}_{D_2} = 1 - \Pr\left(\vartheta_{R_{k*}\longrightarrow x_2} > \delta_2 + \gamma_2 \vartheta_{E\longrightarrow x_2}, \vartheta_{D_2\longrightarrow x_2} > \delta_2 + \gamma_2 \vartheta_{E\longrightarrow x_2}\right)$$

$$= 1 - \Pr\left(\left|g_{SR_{k*}}\right|^2 > \frac{\delta_2 + \beta_2 \left|g_{R_{k*}E}\right|^2}{a_1 \rho_S \beta_2 \left(\chi_2 - \left|g_{R_{k*}E}\right|^2\right)}, \left|g_{R_{k*}D_2}\right|^2 > \frac{\left(\delta_2 + \beta_2 \left|g_{R_{k*}E}\right|^2\right)\left(\rho_{CE}\left|g_{CU_2}\right|^2 + 1\right)}{a_1 \rho_R \beta_2 \left(\chi_2 - \left|g_{R_{k*}E}\right|^2\right)}\right), \tag{14}$$

where $\beta_i = \gamma_i a_i \rho_E$, $\delta_i = \gamma_i - 1$. Then, the SOP of D_2 can be rewritten by

$$\text{SOP}_{D_2} = 1 - \sum_{k=1}^{K}\binom{K}{k}\frac{(-1)^{k-1}}{\Omega_{CU_2}\Omega_{R_{k*}E}}\int_0^{\chi_2} e^{-(((\delta_2+\beta_2 z)k)/(\theta_2(\chi_2-z)))} e^{-((\delta_2+\beta_2 z)/(\theta_1(\chi_2-z)))} e^{-\left(z/(\Omega_{R_{k*}E})\right)} \int_0^{\infty} e^{-((\rho_{CE}(\delta_2+\beta_2 z)y)/(\theta_1(\chi_2-z)))} e^{-\left(y/(\Omega_{CU_2})\right)} dy dz$$

$$= 1 - \sum_{k=1}^{K}\binom{K}{k}\frac{(-1)^{k-1}}{\Omega_{R_{k*}E}}\int_0^{\chi_2} \frac{e^{-(((\delta_2+\beta_2 z)k)/(\theta_2(\chi_2-z)))} e^{-((\delta_2+\beta_2 z)/(\theta_1(\chi_2-z)))} e^{-\left((z)/(\Omega_{R_{k*}E})\right)}}{1 + (\theta_3(\delta_2+\beta_2 z)/\chi_2 - z)} dz, \tag{15}$$

where $\chi_2 = (1/(a_1\beta_2)) - ((\gamma_2)/(\beta_2))$, $\theta_1 = \Omega_{R_{k*}D_2}a_1\rho_R\beta_2$, $\theta_2 = \Omega_{SR_{k*}}a_1\rho_S\beta_2$, and $\theta_3 = ((\Omega_{CU_2}\rho_{CE})/(\theta_1))$. Using

Gaussian-Chebyshev Quad with $\phi_n = \cos((2n-1)/(2N))$, SOP_{D_2} is given by

$$\text{SOP}_{D_2} \approx 1 - \frac{\pi}{2N}\sum_{k=1}^{K}\binom{K}{k}\frac{\chi_2(-1)^{k-1}}{\Omega_{R_{k*}E}}\sum_{n=1}^{N}\sqrt{1-\phi_n^2}\frac{e^{-(((2\delta_2+\beta_2\chi_2(1+\phi_n))k)/(\theta_2\chi_2(1-\phi_n)))} e^{-((2\delta_2+\beta_2\chi_2(1+\phi_n))/(\theta_1\chi_2(1-\phi_n)))} e^{-\left(\chi_2(1+\phi_n)()/(2\Omega_{R_{k*}E})\right)}}{1 + ((\theta_3(2\delta_2+\beta_2\chi_2(1+\phi_n)))/(\chi_2(1-\phi_n)))}. \tag{16}$$

3.2. Secrecy Outage Probability of D_1. In here, the SOP of D_1 is given by

$$\begin{aligned}\text{SOP}_{D_1} &= \Pr(C_1 < R_1)\\ &= \Pr\left(\frac{1 + \min\left(\vartheta_{R_{k*}\longrightarrow x_1}, \vartheta_{D_1\longrightarrow x_1}\right)}{1 + \vartheta_{E\longrightarrow x_1}} < \gamma_1\right)\\ &= 1 - \Pr\left(\vartheta_{R_{k*}\longrightarrow x_1} > \gamma_1\left(1 + \vartheta_{E\longrightarrow x_1}\right) - 1, \vartheta_{D_1\longrightarrow x_1} > \gamma_1\left(1 + \vartheta_{E\longrightarrow x_1}\right) - 1\right).\end{aligned} \tag{17}$$

Proposition 1. *The expression SOP of D_1 is given by*

$$\begin{aligned}SOP_{D_1} = 1 &+ \sum_{k=1}^{K}\binom{K}{k}\frac{(-1)^{k-1}\mu_2 e^{-\delta_1\mu_1}}{\Omega_{R_{k*}E}}\\ &\cdot e^{\left((\mu_3(\beta_1\mu_1\Omega_{R_{k*}E}+1))/(\Omega_{R_{k*}E})\right)}Ei\left(-\frac{\mu_3(\beta_1\mu_1\Omega_{R_{k*}E}+1)}{\Omega_{R_{k*}E}}\right).\end{aligned} \tag{18}$$

Proof. Putting (3), (7), and (9) into (17), we have

$$\text{SOP}_{D_1} = 1 - \Pr\left(\left|g_{SR_{k*}}\right|^2 > \frac{\delta_1 + \beta_1\left|g_{R_{k*}E}\right|^2}{a_1\rho_S}, \left|g_{R_{k*}D_1}\right|^2 > \frac{\left(\delta_1 + \beta_1\left|g_{R_{k*}E}\right|^2\right)\left(\rho_{CE}\left|g_{CU_1}\right|^2 + 1\right)}{a_1\rho_R}\right),$$

$$= 1 - \int_0^{\infty}\int_0^{\infty} f_{\left|g_{R_{k*}E}\right|^2}(z) f_{\left|g_{CU_1}\right|^2}(y)\left(1 - F_{\left|g_{SR_{k*}}\right|^2}\left(\frac{\delta_1 + \beta_1 z}{a_1\rho_S}\right)\right)\left(1 - F_{\left|g_{R_{k*}D_1}\right|^2}\left(\frac{(\delta_1 + \beta_1 z)(\rho_{CE}y + 1)}{a_1\rho_R}\right)\right) dy dz. \tag{19}$$

After some variable substitutions and manipulations, (19) can be transformed by

$$
\begin{aligned}
\mathrm{SOP}_{D_1} &= 1 - \sum_{k=1}^{K} \binom{K}{k} \frac{(-1)^{k-1} e^{-\delta_1 \mu_1}}{\Omega_{CU_1} \Omega_{R_{k*}E}} \int_0^\infty e^{-\beta_1 \mu_1 z} e^{-\left(z/\left(\Omega_{R_{k*}E}\right)\right)} \\
&\quad \cdot \int_0^\infty e^{-\left(\left(\rho_{CE}(\delta_1 + \beta_1 z)\right)/\left(\Omega_{R_{k*}D_1} a_1 \rho_R\right)\right)y} e^{-\left(y/\left(\Omega_{CU_1}\right)\right)} dy d \\
&= 1 - \sum_{k=1}^{K} \binom{K}{k} \frac{(-1)^{k-1} \mu_2 e^{-\delta_1 \mu_1}}{\Omega_{R_{k*}E}} \int_0^\infty \frac{e^{-\left(\beta_1 \mu_1 + \left(1/\left(\Omega_{R_{k*}E}\right)\right)\right)z}}{\mu_3 + z} dz,
\end{aligned}
\tag{20}
$$

where $\mu_1 = \left(1/\left(\Omega_{SR_{k*}} a_1 \rho_S\right)\right) + \left(1/\left(\Omega_{R_{k*}D_1} a_1 \rho_R\right)\right), \mu_2 = \left(\left(\Omega_{R_{k*}D_1} a_1 \rho_R\right)/\left(\rho_{CE} \Omega_{CU_1} \beta_1\right)\right)$, and $\mu_3 = \mu_2 + \left(\left(\delta_1\right)/\left(\beta_1\right)\right)$. Using ([46], 3.352.4), (18) can be obtained.

The proof is completed. □

3.3. Asymptotic SOP Analysis.

In this section, the asymptotic SOP expression could be derived at high SNR $\rho_S = \rho_R \longrightarrow \infty$ to provide more insights of performance analysis. It can be performed by applying the first-order Maclaurin's series expansions $e^{-x} = 1 - x$ and use $Ei(-x) = \ln(x) + C$ as [46]. The asymptotic SOP of D_2 and D_1 are expressed as, respectively,

$$
\begin{aligned}
\mathrm{SOP}_{D_2} &\approx 1 - \frac{\pi}{2N} \sum_{k=1}^{K} \binom{K}{k} \frac{\chi_2 (-1)^{k-1}}{\Omega_{R_{k*}E}} \sum_{n=1}^{N} \sqrt{1 - \phi_n^2} \\
&\quad \cdot \left(1 + \frac{\theta_3(2\delta_2 + \beta_2 \chi_2(1 + \phi_n))}{\chi_2(1 - \phi_n)}\right)^{-1} \\
&\quad \times \left(1 - \frac{(2\delta_2 + \beta_2 \chi_2(1 + \phi_n))(k+1)}{\theta_2 \chi_2(1 - \phi_n)} - \frac{\chi_2(1 + \phi_n)}{2\Omega_{R_{k*}E}}\right),
\end{aligned}
\tag{21}
$$

$$
\begin{aligned}
\mathrm{SOP}_{D_1} &= 1 + \sum_{k=1}^{K} \binom{K}{k} \frac{(-1)^{k-1} \mu_2}{\Omega_{R_{k*}E}} \left(1 + \frac{\mu_3(\beta_1 \mu_1 \Omega_{R_{k*}E} + 1)}{\Omega_{R_{k*}E}} - \delta_1 \mu_1\right) \\
&\quad \cdot \left(\ln\left(\frac{\mu_3(\beta_1 \mu_1 \Omega_{R_{k*}E} + 1)}{\Omega_{R_{k*}E}}\right) + C\right).
\end{aligned}
\tag{22}
$$

4. Strictly Positive Secrecy Capacity Analysis

In this section, we analyze the strictly positive secrecy capacity (SPSC). Then, the SPSC of the system is given as [47].

$$
\mathrm{SPCP}_{out} = \Pr(C_1 > 0, C_2 > 0).
\tag{23}
$$

TABLE 2: Table of parameter.

System parameters	Value
The power allocation	$a_1 = 0.2$ and $a_2 = 0.8$
The number of relay	$K = 2$
The power of CUE	$\rho_{CU} = 1$
The parameter of channel	$\Omega_{SR_{k*}} = \Omega_{R_{k*}D_i} = \Omega_{R_{k*}E} = \Omega_{CU_1} = \Omega_{CU_2} = 1$
The target rate	$R_1 = 1$ and $R_2 = 0.1$ bit per channel use

Proposition 2. *The close-form of SPSC is given by*

$$
\begin{aligned}
\mathrm{SPCP}_{out} &= - \sum_{k=1}^{K} \binom{K}{k} \frac{(-1)^{k-1} \Omega_{R_{k*}D_i} \rho_R}{\rho_{CE} \rho_E \Omega_{CU_1} \Omega_{R_{k*}E}} e^{\left(\varpi_1/\left(\Omega_{CU_1}\right)\right)} Ei \\
&\quad \cdot \left(-\frac{\varpi_1}{\Omega_{CU_1}}\right) \times \sum_{k_1=1}^{K} \binom{K}{k_1} \frac{(-1)^{k_1-1}}{2\rho_E a_1 \Omega_{R_{k*}E}} \frac{\pi}{N} \sum_{n=1}^{N} \\
&\quad \cdot \frac{\sqrt{1 - \phi_n^2} e^{-\varpi_2(1 + \phi_n)}}{1 + \left(\left((1 + \phi_n)\rho_{CE}\Omega_{CU_2}\right)/\left((1 - \phi_n)\rho_R a_1 \Omega_{R_{k*}D_2}\right)\right)}.
\end{aligned}
\tag{24}
$$

Proof. See Appendix. □

5. Simulation Results

In this section, we present the numerical analysis of our SOP of D_i along with the corroboration of analytical results. The parameters of the system can be expressed in Table 2.

Figure 2 considers the SOP versus transmit SNR while varying K DF relays. Different values of SOP can be seen for the two destinations. For D_1 and D_2, the best SOP is achieved with $K = 2$. This shows that the addition of more relays is beneficial to SOP. Furthermore, we observe that the different values of SOP for D_2 converge to a single floor at high SNR values. This is due to the absence of SIC at D_2, therefore, the SOP is impacted in high SNR regions despite the number of relays. In addition, D_2 NOMA performs better than OMA in the range of SNR from 0 to 30 dB. And D_1 NOMA performs better than OMA in all SNR.

In Figure 3, we consider the SOP versus transmit SNR while varying ρ_E. Different values of SOP can be seen for the two destinations. For D_1 and D_2, the best SOP is achieved with $\rho_E = -5$(dB). This shows that increasing ρ_E impacts on SOP. Also, in Figure 3, the analytical and simulated results closely match. Looking closely at the results, we can see that the SOP of D_2 is impacted the most by larger ρ_E values. Furthermore, we observe that the SOP for D_2 approaches a floor at high SNR values for $\rho_E = 1$ (dB). As in Figure 2, this can be attributed to the lack of SIC at D_2.
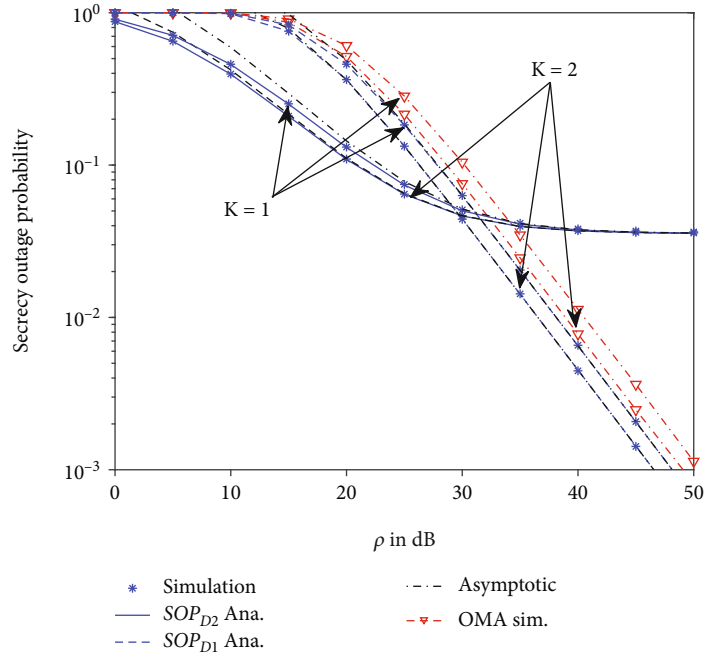
FIGURE 2: The SOP versus ρ in dB varying K with $\rho_E = 1$ (dB).
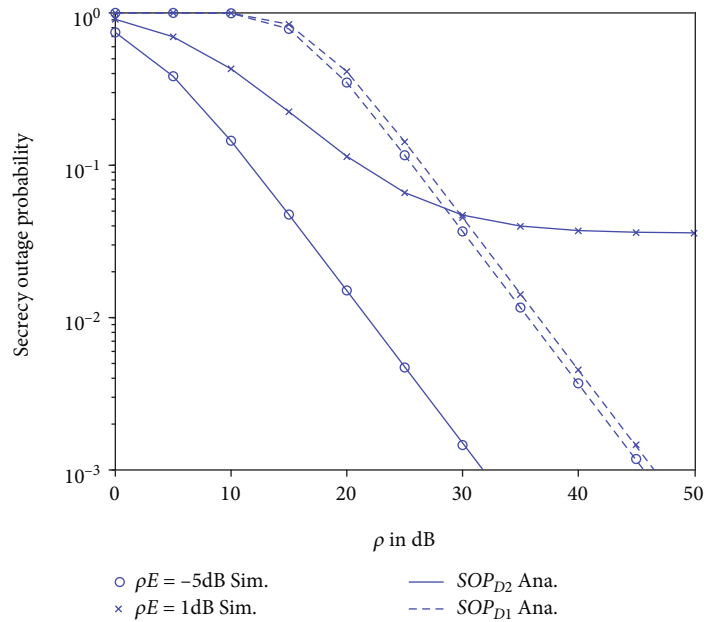
FIGURE 3: The SOP versus ρ in dB varying ρ_E.

In Figure 4, we consider the SOP versus transmit SNR while varying ρ_{CU}. Different values of SOP can be seen for the two destinations. For D_1 and D_2, the best SOP is achieved with $\rho_{CU} = -5$ (dB). In Figure 4, the analytical and simulated results closely match. Furthermore, we observe that the different SOP values for D_2 converge at a floor at high SNR values, this is due to the absence of SIC at the far user D_2. Hence, D_2 is impacted by the interference of the CUE, unlike D_1 which employs SIC. Figure 4, clearly shows the impact of SIC on SOP at the different NOMA devices.

In Figure 5, we consider the SOP versus a_2 varying ρ in dB with $\rho_E = 1$ (dB). Different values of SOP can be seen for the two destinations. For D_1 and D_2, the best SOP is achieved with an SNR of 30 dB. Furthermore, the analytical and simulated results closely match. Figure 5 clearly shows the impact of power allocation on SOP at the different NOMA devices.
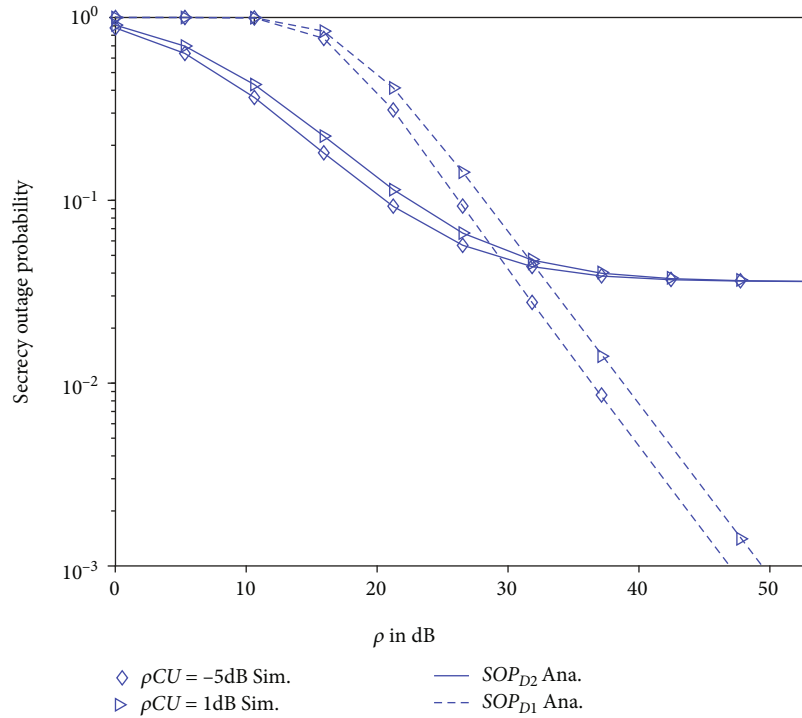
FIGURE 4: The SOP versus ρ in dB varying ρ_{CU} with $\rho_E = 1$ (dB).
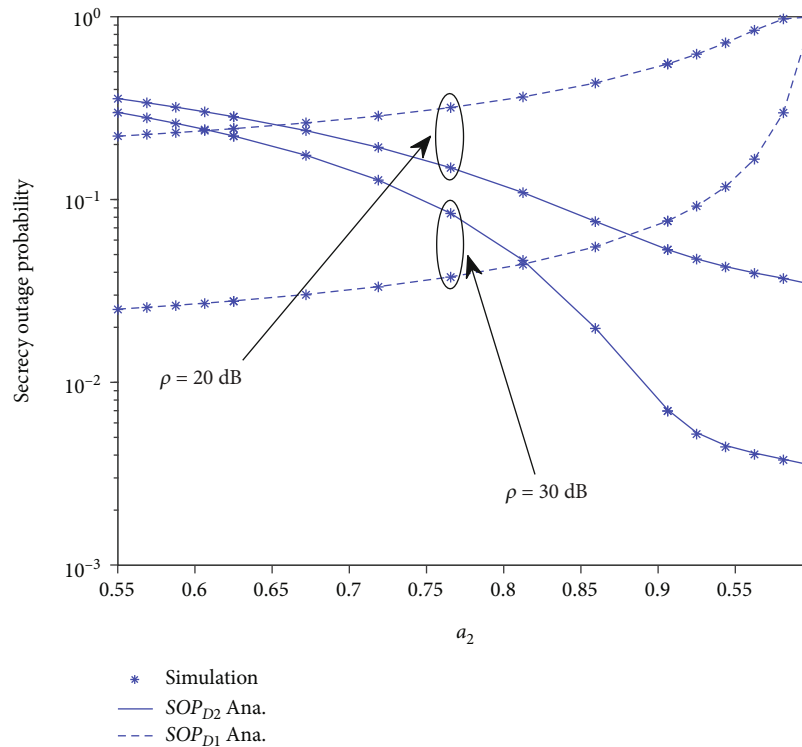
FIGURE 5: The SOP versus a_2 in dB varying ρ with $\rho_E = 1$ (dB).

In Figure 6, we consider the SPSC versus transmit SNR while varying K. Different values of SPSC can be observed depending on the value of K. The best SPSC curve is achieved with $K = 3$. In Figure 6, the analytical and simulated results closely match. Furthermore, we observe that the different SPSC values converge at a ceiling at high SNR
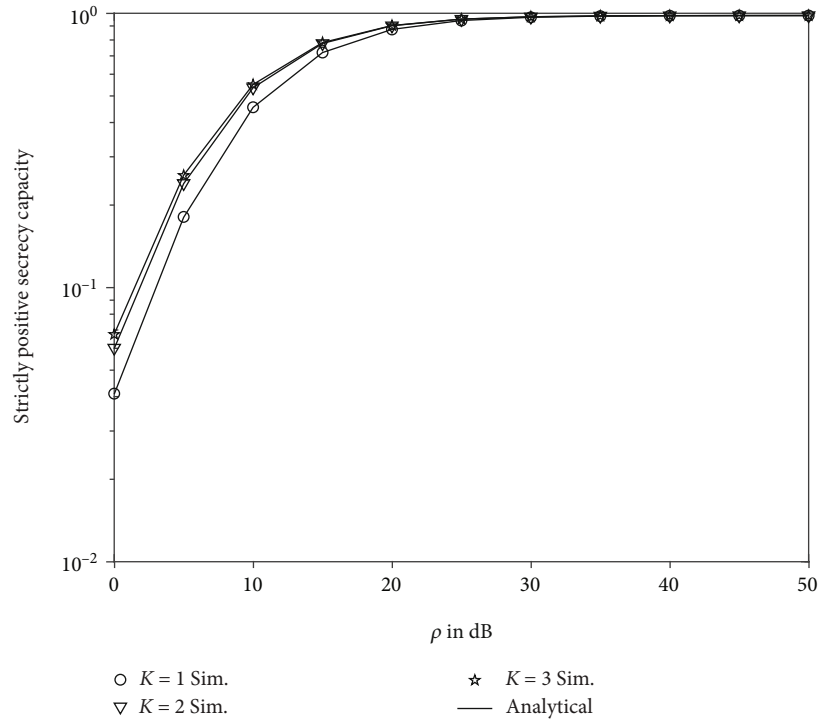
FIGURE 6: The SPSC versus ρ in dB varying K with $\rho_E = 1$ (dB).
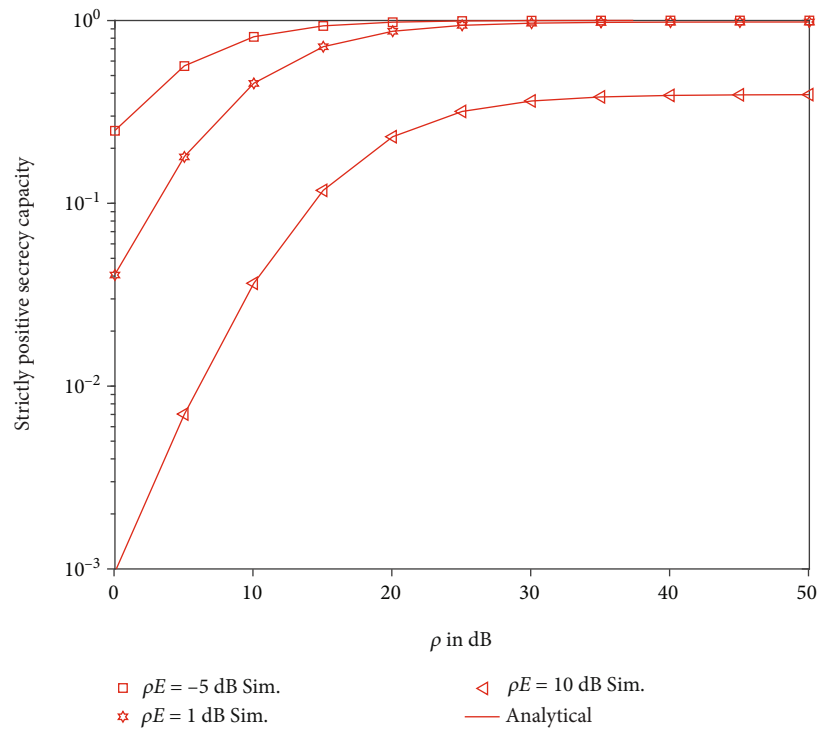
FIGURE 7: The SPSC versus ρ in dB varying ρ_E.

values. Demonstrating that at moderate to high SNR values, the number of relays has no significant impact on the SPSC of the proposed system.

In Figure 7, we consider the SPSC versus transmit SNR while varying ρ_E. Different values of SPSC can be observed depending on the value of ρ_E. In Figure 7, the analytical
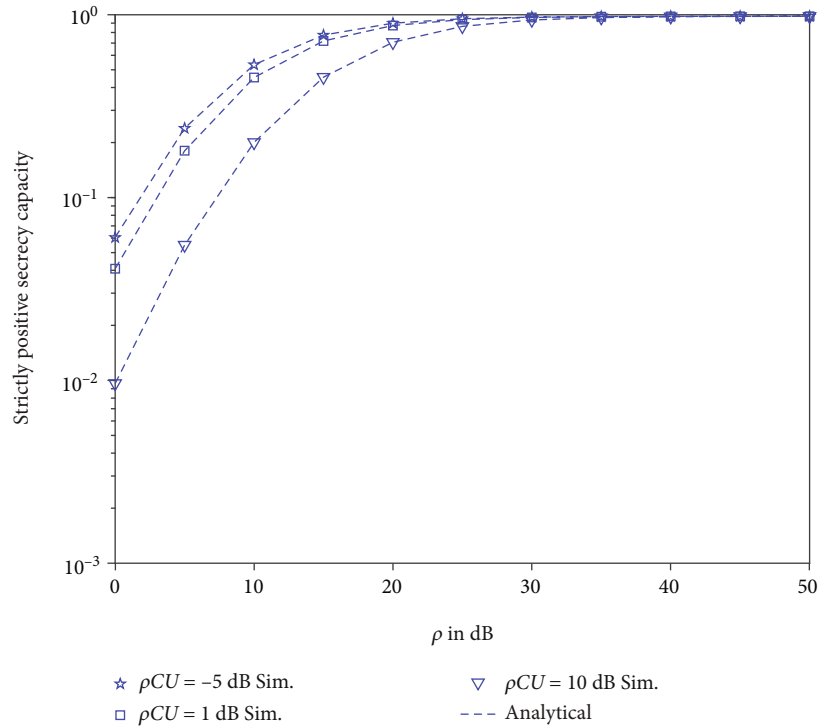
FIGURE 8: The SPSC versus ρ in dB varying ρ_{CU} with $\rho_E = 1$ (dB).

and simulated results closely match. Furthermore, we observe that the different SPSC values approach ceilings at high SNR values. Also, for Figure 7, it is clear that a tenfold increase in ρ_E significantly reduces the ceiling of SPSC of our system in the moderate to high SNR region. This is due to the increased signal strength at the eavesdropper affecting the proposed system.

In Figure 8, we consider the SPSC versus transmit SNR while varying ρ_{CU}. Different values of SPSC can be observed depending on the value of ρ_{CU}. In Figure 8, the analytical and simulated results closely match. Furthermore, we observe that the different SPSC values converge at a similar ceiling at high SNR values. For this figure, unlike in Figure 6, a tenfold increase in interference power ρ_{CU} does not significantly reduce the ceiling of the SPSC of our system. Demonstrating the reliability and security of our proposed system in the moderate to high SNR region in the presence of interference.

6. Conclusions

In this paper, the PLS problem of two destinations (NOMA users) has been studied in the context of downlink NOMA network under the presence of interference from traditional user CUE. Once an eavesdropper can overhear a signal in second hop transmission, SOP can be evaluated to verify the security of the dual-hop downlink transmission. By designing multiple relays, we can have a higher chance to improve SOP. We found that better SOP can be achieved by having more relays to forward signals. We derived the closed-form expressions SOP and lots of scenarios are presented in numerical simulation to confirm the impact of the studied parameters on secrecy performance. Simulation results are presented to examine the impact of the following parameters, i.e., transmit SNR at source, interference channel, the number of relays, and power allocation factors, on system performance. In future work, we may consider the secure performance of multiple NOMA users.

Appendix

A. Proof of Proposition 2

The SPSC can be expressed as

$$\mathrm{SPCP}_{\mathrm{out}} = \underbrace{\mathrm{Pr}\left(\min\left(\vartheta_{R_{k_*}\longrightarrow x_1}, \vartheta_{D_1\longrightarrow x_1}\right) > \vartheta_{E\longrightarrow x_1}\right)}_{I_1} \underbrace{\mathrm{Pr}\left(\min\left(\vartheta_{R_{k_*}\longrightarrow x_2}, \vartheta_{D_1\longrightarrow x_2}\right) > \vartheta_{E\longrightarrow x_2}\right)}_{I_2}. \tag{A.1}$$

Next, the first term of I_1 can be calculated by

$$
\begin{aligned}
I_1 &= \Pr\left(\min\left(\vartheta_{R_{k*}\rightarrow x_1}, \vartheta_{D_1\rightarrow x_1}\right) > \vartheta_{E\rightarrow x_1}\right) \\
&= \Pr\left(\vartheta_{R_{k*}\rightarrow x_1} > \vartheta_{E\rightarrow x_1}, \vartheta_{D_1\rightarrow x_1} > \vartheta_{E\rightarrow x_1}\right) \\
&= \Pr\left(\left|g_{SR_{k*}}\right|^2 > \frac{\rho_E\left|g_{R_{k*}E}\right|^2}{\rho_S}, \left|g_{R_{k*}D_1}\right|^2 > \frac{\rho_E\left|g_{R_{k*}E}\right|^2\left(\rho_{CE}\left|g_{CU_1}\right|^2+1\right)}{\rho_R}\right).
\end{aligned}
$$
(A.2)

Then, it can be calculated as

$$
\begin{aligned}
I_1 &= \int_0^\infty\int_0^\infty f_{|g_{CU_1}|^2}(y) f_{|g_{R_{k*}E}|^2}(x) \\
&\quad \cdot \left(1 - F_{|g_{SR_{k*}}|^2}\left(\frac{\rho_E x}{\rho_S}\right)\right)\left(1 - F_{|g_{SR_{k*}}|^2}\left(\frac{\rho_E x(\rho_{CE}y+1)}{\rho_R}\right)\right) dxdy \\
&= \sum_{k=1}^K \binom{K}{k} \frac{(-1)^{k-1}}{\Omega_{CU_1}\Omega_{R_{k*}E}} \int_0^\infty\int_0^\infty e^{-\left(y/\left(\Omega_{CU_1}\right)\right)} \\
&\quad \cdot e^{-\left(\left((\rho_E kx)/\left(\Omega_{SR_{k*}}\rho_S\right)\right)+\left(1/\left(\Omega_{R_{k*}E}\right)\right)+\left((\rho_E(\rho_{CE}y+1))/\left(\Omega_{R_{k*}D_1}\rho_R\right)\right)\right)x} dxdy \\
&= \sum_{k=1}^K \binom{K}{k} \frac{(-1)^{k-1}\Omega_{R_{k*}D_1}\rho_R}{\rho_{CE}\rho_E\Omega_{CU_1}\Omega_{R_{k*}E}} \int_0^\infty \frac{e^{-\left(y/\left(\Omega_{CU_1}\right)\right)}}{\varpi_1 + y} dy,
\end{aligned}
$$
(A.3)

where $\varpi_1 = \left(\left(\Omega_{R_{k*}D_1}\rho_R k\right)/\left(\Omega_{SR_{k*}}\rho_{CE}\rho_S\right)\right) + \left(\left(\Omega_{R_{k*}D_1}\rho_R\right)/\left(\Omega_{R_{k*}E}\rho_E\rho_{CE}\right)\right) + \left(1/\left(\rho_{CE}\right)\right)$. Similarly, we can obtain I_1 as

$$
I_1 = -\sum_{k=1}^K \binom{K}{k} \frac{(-1)^{k-1}\Omega_{R_{k*}D_1}\rho_R}{\rho_{CE}\rho_E\Omega_{CU_1}\Omega_{R_{k*}E}} e^{\left(\varpi_1/\left(\Omega_{CU_1}\right)\right)} Ei\left(-\frac{\varpi_1}{\Omega_{CU_1}}\right).
$$
(A.4)

In addition, the second term I_2 is given by

$$
\begin{aligned}
I_2 &= \Pr\left(\min\left(\vartheta_{R_{k*}\rightarrow x_2}, \vartheta_{D_2\rightarrow x_2}\right) > \vartheta_{E\rightarrow x_2}\right) \\
&= \Pr\left(\left|g_{SR_{k*}}\right|^2 > \frac{\rho_E\left|g_{R_{k*}E}\right|^2}{\rho_S - \rho_S\rho_E a_1\left|g_{R_{k*}E}\right|^2}, \left|g_{R_{k*}D_2}\right|^2 > \frac{\rho_E\left|g_{R_{k*}E}\right|^2\left(\rho_{CE}\left|g_{CU_1}\right|^2+1\right)}{\rho_R - \rho_R\rho_E a_1\left|g_{R_{k*}E}\right|^2}\right).
\end{aligned}
$$
(A.5)

Similar in above, it can be rewritten by

$$
\begin{aligned}
I_2 &= \int_0^\infty\int_0^{\left(1/(\rho_E a_1)\right)} f_{|g_{CU_2}|^2}(y) f_{|g_{R_{k*}E}|^2}(x) \\
&\quad \cdot \left(1 - F_{|g_{SR_{k*}}|^2}\left(\frac{\rho_E x}{\rho_S - \rho_S\rho_E a_1 x}\right)\right) \\
&\quad \cdot \left(1 - F_{|g_{R_{k*}D_2}|^2}\left(\frac{\rho_E x(\rho_{CE}y+1)}{\rho_R - \rho_R\rho_E a_1 x}\right)\right) dxdy. \\
&= \sum_{k_1=1}^K \binom{K}{k_1} \frac{(-1)^{k_1-1}}{\Omega_{CU_2}\Omega_{R_{k*}E}} \int_0^\infty\int_0^{\left(1/(\rho_E a_1)\right)} e^{-\left(y/\left(\Omega_{CU_2}\right)\right)} \\
&\quad \cdot e^{-\left(x/\left(\Omega_{R_{k*}E}\right)\right)} e^{-\left((\rho_E k_1 x)/\left(\rho_S\Omega_{SR_{k*}}(1-\rho_E a_1 x)\right)\right)} \\
&\quad \cdot e^{-\left((\rho_E x(\rho_{CE}y+1))/\left(\rho_R\Omega_{R_{k*}D_2}(1-\rho_E a_1 x)\right)\right)} dxdy.
\end{aligned}
$$
(A.6)

Then, using Gaussian-Chebyshev Quad we can approximate I_2 as

$$
\begin{aligned}
I_2 &\approx \sum_{k_1=1}^K \binom{K}{k_1} \frac{(-1)^{k_1-1}}{2\rho_E a_1\Omega_{CU_2}\Omega_{R_{k*}E}} \frac{\pi}{N} \sum_{n=1}^N \sqrt{1-\phi_n^2}\, e^{-\varpi_2(1+\phi_n)} \\
&\quad \cdot \int_0^\infty e^{-\left(y/\left(\Omega_{CU_2}\right)\right)} e^{-\left(((1+\phi_n)\rho_{CE}y)/\left((1-\phi_n)\rho_R a_1\Omega_{R_{k*}D_2}\right)\right)} dy \\
&\approx \sum_{k_1=1}^K \binom{K}{k_1} \frac{(-1)^{k_1-1}}{2\rho_E a_1\Omega_{R_{k*}E}} \frac{\pi}{N} \sum_{n=1}^N \\
&\quad \cdot \frac{\sqrt{1-\phi_n^2}\, e^{-\varpi_2(1+\phi_n)}}{1 + \left(((1+\phi_n)\rho_{CE}\Omega_{CU_2})/\left((1-\phi_n)\rho_R a_1\Omega_{R_{k*}D_2}\right)\right)},
\end{aligned}
$$
(A.7)

where $\varpi_2 = \left(1/\left(2\rho_E a_1\Omega_{R_{k*}E}\right)\right) + \left(k_1/\left((1-\phi_n)\rho_S a_1\Omega_{SR_{k*}}\right)\right) + \left(1/\left((1-\phi_n)\rho_R a_1\Omega_{R_{k*}D_2}\right)\right)$. Putting (A.5) and (A.7) into (A.1), the proof is completed.

Data Availability

No data were used to support this study.

Conflicts of Interest

The authors declare that they have no conflicts of interest.

Acknowledgments

References

[1] M. Coşandal, E. B. Koca, and H. Sari, "NOMA-2000 versus PD-NOMA: an outage probability comparison," *IEEE Communications Letters*, vol. 25, no. 2, pp. 427–431, 2021.

[2] B. Xu, Z. Xiang, P. Ren, and X. Guo, "Outage performance of downlink full-duplex network-coded cooperative NOMA," *IEEE Wireless Communications Letters*, vol. 10, no. 1, pp. 26–29, 2021.

[3] M.-S. Van Nguyen, S. Dinh-Thuan Do, S. Al-Rubaye, A. A.-D. Mumtaz, and O. Dobre, "Exploiting impacts of antenna selection and energy harvesting for massive network connectivity," *IEEE Transactions on Communications*, vol. 69, no. 11, pp. 7587–7602, 2021.

[4] D.-T. Do, A. Le, and B. M. Lee, "NOMA in cooperative underlay cognitive radio networks under imperfect SIC," *IEEE Access*, vol. 8, pp. 86180–86195, 2020.

[5] D.-T. Do, M. -S. V. Nguyen, F. Jameel, R. Jäntti, and I. S. Ansari, "Performance evaluation of relay-aided CR-NOMA for beyond 5G communications," *IEEE Access*, vol. 8, pp. 134838–134855, 2020.

[6] D.-T. Do, A.-T. Le, Y. Liu, and A. Jamalipour, "User grouping and energy harvesting in UAV-NOMA system with AF/DF relaying," *IEEE Transactions on Vehicular Technology*, vol. 70, no. 11, pp. 11855–11868, 2021.

[7] F. Zhou, Y. Wu, Y.-C. Liang, Z. Li, Y. Wang, and K.-K. Wong, "State of the art, taxonomy, and open issues on cognitive radio networks with NOMA," *IEEE Wireless Communications*, vol. 25, no. 2, pp. 100–108, 2018.

[8] J. Choi, "Repetition-based NOMA transmission and its outage probability analysis," *IEEE Transactions on Vehicular Technology*, vol. 69, no. 6, pp. 5913–5922, 2020.

[9] V. Aswathi and A. V. Babu, "Full/half duplex cooperative NOMA under imperfect successive interference cancellation and channel state estimation errors," *IEEE Access*, vol. 7, pp. 179961–179984, 2019.

[10] N. Jaiswal and N. Purohit, "Performance of downlink NOMA-enabled vehicular communications over double Rayleigh fading channels," *IET Communications*, vol. 14, no. 20, pp. 3652–3660, 2020.

[11] Y. Zou, J. Zhu, X. Wang, and L. Hanzo, "A survey on wireless security: technical challenges, recent advances, and future trends," *Proceedings of the IEEE*, vol. 104, no. 9, pp. 1727–1765, 2016.

[12] Y. Liu, H. H. Chen, and L. Wang, "Physical layer security for next generation wireless networks: theories, technologies, and challenges," *IEEE Communications Surveys & Tutorials*, vol. 19, no. 1, pp. 347–376, 2017.

[13] Y. Zou, X. Wang, and W. Shen, "Physical-layer security with multiuser scheduling in cognitive radio networks," *IEEE Transactions on Communications*, vol. 61, no. 12, pp. 5103–5113, 2013.

[14] Y. Zou, X. Li, and Y. C. Liang, "Secrecy outage and diversity analysis of cognitive radio systems," *IEEE Journal on Selected Areas in Communications*, vol. 32, no. 11, pp. 2222–2236, 2014.

[15] Y. Liu, L. Wang, T. T. Duy, M. Elkashlan, and T. Q. Duong, "Relay selection for security enhancement in cognitive relay networks," *IEEE Wireless Communications Letters*, vol. 4, no. 1, pp. 46–49, 2015.

[16] A. Al-Nahari, G. Geraci, M. Al-Jamali, M. H. Ahmed, and N. Yang, "Beamforming with artificial noise for secure MIS-OME cognitive radio transmissions," *IEEE Transactions on Information Forensics and Security*, vol. 13, no. 8, pp. 1875–1889, 2018.

[17] C. Tang, G. Pan, and T. Li, "Secrecy outage analysis of underlay cognitive radio unit over Nakagami-m fading channels," *IEEE Wireless Communications Letters*, vol. 3, no. 6, pp. 609–612, 2014.

[18] H. Lei, C. Gao, I. S. Ansari et al., "Secrecy outage performance of transmit antenna selection for MIMO underlay cognitive radio systems over Nakagami-m channels," *IEEE Transactions on Vehicular Technology*, vol. 66, no. 3, pp. 2237–2250, 2017.

[19] R. Zhao, Y. Yuan, L. Fan, and Y. C. He, "Secrecy performance analysis of cognitive decode-and-forward relay networks in Nakagami-m fading channels," *IEEE Transactions on Communications*, vol. 65, no. 2, pp. 549–563, 2017.

[20] Z. Xiang, W. Yang, G. Pan, Y. Cai, and Y. Song, "Physical layer security in cognitive radio inspired NOMA network," *IEEE Journal of Selected Topics in Signal Processing*, vol. 13, no. 3, pp. 700–714, 2019.

[21] B. Zheng, M. Wen, C. X. Wang et al., "Secure NOMA based two-way relay networks using artificial noise and full duplex," *IEEE Journal on Selected Areas in Communications*, vol. 36, no. 7, pp. 1426–1440, 2018.

[22] L. Lv, Z. Ding, Q. Ni, and J. Chen, "Secure MISO-NOMA transmission with artificial noise," *IEEE Transactions on Vehicular Technology*, vol. 67, no. 7, pp. 6700–6705, 2018.

[23] J. Chen, L. Yang, and M. S. Alouini, "Physical layer security for cooperative NOMA systems," *IEEE Transactions on Vehicular Technology*, vol. 67, no. 5, pp. 4645–4649, 2018.

[24] B. He, A. Liu, N. Yang, and V. K. N. Lau, "On the design of secure non-orthogonal multiple access systems," *IEEE Journal on Selected Areas in Communications*, vol. 35, no. 10, pp. 2196–2206, 2017.

[25] Z. Ding, Z. Zhao, M. Peng, and H. V. Poor, "On the spectral efficiency and security enhancements of NOMA assisted multicast-unicast streaming," *IEEE Transactions on Communications*, vol. 65, no. 7, pp. 3151–3163, 2017.

[26] Y. Li, M. Jiang, Q. Zhang, Q. Li, and J. Qin, "Secure beamforming in downlink MISO nonorthogonal multiple access systems," *IEEE Transactions on Vehicular Technology*, vol. 66, no. 8, pp. 7563–7567, 2017.

[27] X. Li, M. Zhao, M. Zeng et al., "Hardware impaired ambient backscatter NOMA systems: reliability and security," *IEEE Transactions on Communications*, vol. 69, no. 4, pp. 2723–2736, 2021.

[28] N. Zaghdoud, A. B. Mnaouer, H. Boujemaa, and F. Touati, "Secrecy performance of cooperative NOMA system with multiple full-duplex relays against non-colluding/colluding eavesdroppers," in *2020 IEEE 45th LCN Symposium on Emerging Topics in Networking (LCN Symposium)*, pp. 70–77, Sydney, Australia, 2020.

[29] X. Li, M. Zhao, X. C. Gao et al., "Physical layer security of cooperative NOMA for IoT networks under I/Q imbalance," *IEEE Access*, vol. 8, pp. 51189–51199, 2020.

[30] W. U. Khan, "Maximizing physical layer security in relay-assisted multicarrier nonorthogonal multiple access transmission," *Internet Technology Letters*, vol. 2, no. 2, 2019.

[31] M.-S. Van Nguyen and D.-T. Do, "Evaluating secrecy performance of cooperative NOMA networks under existence of relay link and direct link," *International Journal of Communication Systems*, vol. 33, no. 6, 2020.

[32] L. Lv, H. Jiang, Z. Ding, L. Yang, and J. Chen, "Secrecy-enhancing design for cooperative downlink and uplink NOMA with an untrusted relay," *IEEE Transactions on Communications*, vol. 68, no. 3, pp. 1698–1715, 2020.

[33] L. Lv, F. Zhou, J. Chen, and N. Al-Dhahir, "Secure cooperative communications with an untrusted relay: a NOMA-inspired jamming and relaying approach," *IEEE Transactions on Information Forensics and Security*, vol. 14, no. 12, pp. 3191–3205, 2019.

[34] H. Lei, Z. Yang, K. H. Park et al., "Secrecy outage analysis for cooperative NOMA systems with relay selection schemes," *IEEE Transactions on Communications*, vol. 67, no. 9, pp. 6282–6298, 2019.

[35] H. Lei, Z. Yang, K. Park, I. S. Ansari, G. Pan, and M. Alouini, "On physical layer security of multiple-relay assisted NOMA systems," in *2019 IEEE International Conference on Communications Workshops (ICC Workshops)*, Shanghai, China, 2019.

[36] C. Yu, H. Ko, X. Peng, W. Xie, and P. Zhu, "Jammer-aided secure communications for cooperative NOMA systems," *IEEE Communications Letters*, vol. 23, no. 11, pp. 1935–1939, 2019.

[37] D. Wan, M. Wen, F. Ji, H. Yu, and F. Chen, "Non-orthogonal multiple access for cooperative communications: challenges, opportunities, and trends," *IEEE Wireless Communications*, vol. 25, no. 2, pp. 109–117, 2018.

[38] X. Chen, R. Jia, and D. W. K. Ng, "The application of relay to massive non-orthogonal multiple access," *IEEE Transactions on Communications*, vol. 66, no. 11, pp. 5168–5180, 2018.

[39] T. N. Nguyen, D. H. Tran, T. V. Chien et al., "Security-reliability trade-off analysis for SWIPT-and AF-based IoT networks with friendly jammers," 2022, http://arxiv.org/abs/2206.04428.

[40] V.-D. Phan, T. N. Nguyen, A. V. Le, and M. Voznak, "A study of physical layer security in SWIPT-based decode-and-forward relay networks with dynamic power splitting," *Sensors*, vol. 21, no. 17, p. 5692, 2021.

[41] T. N. Nguyen, D. H. Tran, V. D. Phan et al., "Throughput enhancement in FD- and SWIPT-enabled IoT networks over nonidentical Rayleigh fading channels," *IEEE Internet of Things Journal*, vol. 9, no. 12, pp. 10172–10186, 2022.

[42] T. N. Nguyen, T. T. Duy, P. T. Tran, M. Voznak, X. Li, and H. V. Poor, "Partial and full relay selection algorithms for AF multi-relay full-duplex networks with self-energy recycling in non-identically distributed fading channels," *IEEE Transactions on Vehicular Technology*, vol. 71, no. 6, pp. 6173–6188, 2022.

[43] Y. Liu, Z. Qin, M. Elkashlan, Y. Gao, and L. Hanzo, "Enhancing the physical layer security of non-orthogonal multiple access in large-scale networks," *IEEE Transactions on Wireless Communications*, vol. 16, no. 3, pp. 1656–1672, 2017.

[44] D.-T. Do and A.-T. Le, "NOMA based cognitive relaying: transceiver hardware impairments, relay selection policies and outage performance comparison," *Computer Communications*, vol. 146, pp. 144–154, 2019.

[45] I. Krikidis, J. Thompson, S. Mclaughlin, and N. Goertz, "Amplify-and-forward with partial relay selection," *IEEE Communications Letters*, vol. 12, no. 4, pp. 235–237, 2008.

[46] I. S. Gradshteyn and I. M. Ryzhik, *Table of Integrals, Series, and Products*, Academic Press, San Diego, CA, 2000.

[47] N. M. S. Do DT and T. A. Hoang, "Exploiting secure performance in power domain–based multiple access: impacts of relay link/direct link and secure analysis," *International Journal of Communication Systems*, vol. 32, no. 15, 2019.

Review Article

Mitigating Hotspot Issues in Heterogeneous Wireless Sensor Networks

Osamah Ibrahim Khalaf ⓘ,[1] Carlos Andrés Tavera Romero ⓘ,[2] Shahzad Hassan ⓘ,[3] and Muhammad Taimoor Iqbal[3]

[1]*Al-Nahrain University, Baghdad, Iraq*
[2]*COMBA R&D Laboratory, Faculty of Engineering, Universidad Santiago de Cali, Cali 76001, Colombia*
[3]*Computer Engineering Department, Bahria University Islamabad, Pakistan*

Correspondence should be addressed to Shahzad Hassan; shassan.buic@bahria.edu.pk

Wireless Sensor Networks (WSNs) consist of a spatially distributed set of autonomous connected sensor nodes. The deployed sensor nodes are extensively used for sensing and monitoring for environmental surveillance, military operations, transportation monitoring, and healthcare monitoring. The sensor nodes in these networks have limited resources in terms of battery, storage, and processing. In some scenarios, the sensor nodes are deployed closer to the base station and responsible to forward their own and neighbor nodes' data towards the base station and depleted energy. This issue is called a hotspot in the network. Hotspot issues mainly appear in those locations where traffic load is more on the sensor nodes. The dynamic and unequal clustering techniques have been used and mitigate the hotspot issues. However, with few benefits, these solutions have suffered from coverage overhead, network connection issues, unbalanced energy utilization among the sink nodes, and network stability issues. In this paper, a comprehensive review of various equal clustering, unequal clustering, and hybrid clustering approaches with their clustering attributes is presented to mitigate hotspot issues in heterogeneous WSNs by using various parameters such as cluster head selection, number of clusters, zone formation, transmission, and routing parameters. This review provides a detailed platform for new researchers to explore the new and novel solutions to solve the hotspot issues in these networks.

1. Introduction

Wireless Sensor Networks (WSNs) are developed for sensing and monitoring vital signs of the environment and area by using distributed and connected sensor nodes. The sensor nodes are further classified into normal nodes, sink nodes (SNs), and Gateway Nodes (GN). The sensor nodes are tiny in size and have inadequate resources in terms of energy, processing, and storage space [1–3]. In most cases, the sensor nodes are deployed in a very intense and harsh environment [4, 5]. The main objective of this deployment is to sense the data remotely and forward it to the end-user or system for decision-making. For data forwarding, there is a need for more efficient mechanisms to manage the node's energy system and improve the network lifetime [6].

The sensor nodes are sensing and perceiving the information from the surrounding environment and process and transmit it to the closest node till the data reached the base station (BS) [7]. In WSN, due to the limited energy resources of sensor nodes, there is an essential requirement of well-efficient and balanced data aggregation mechanism and energy-efficient routing protocols [8]. The energy factor is always one of the considerable factors to design any solution for WSNs [9, 10]. Several types of routing protocols have been proposed to conserve the sensor nodes' energy [7, 11, 12]. The clustering technique is an efficient

topological control mechanism that can effectively improve the scalability period and lifespan of WSNs [10]. The WSN applications have gained popularity including target tracking [13, 14], environmental monitoring [8], security [15–19], disaster response [5], and health monitoring [20, 21].

In a clustering environment, the data is engaged from one node to another node and causes hotspots or energy hole problems. A hotspot is caused by the node deployed closest to the BS and quickly drains its energy due to traffic coming from other nodes and forwarded from it. These sensor nodes do not only send their data but also transmit the data from other sources due to which early death of nodes causes hotspot issues. In this paper, Heterogeneous Wireless Sensor Networks (HWSN) are discussed in terms of network lifetime primarily based on hotspot issues [22]. Figure 1 shows the architecture of WSN.

The other objectives of this paper are as follows.

Clustering is the most popular energy-efficient technique and has proven benefits, but it also suffered from hotspot issues.

- (i) The absence of current and detailed survey articles on hotspot approaches motivated us to accomplish this research. To the best of our knowledge, this is the only review performed on hotspot issues

- (ii) First, we introduce a detailed classification of HWSN considering all the foremost characteristics of clustering algorithms, which includes types of clustering protocol, clustering design process, and data transmission for general understanding of clustering algorithms

- (iii) Secondly, an assessment of the clustering protocols is executed and highlights the hotspot issues based on equal, unequal, and hybrid cluster size, considering all the design and data transmission aspects of the protocols, i.e., cluster size, CH selection, data transmission, data aggregation, type of clustering, and zones

The rest of the paper is organized as follows: Section 2 presents the introduction to clustering. Section 3 presents the clustering attribute classification. Section 4 addresses the hotspot issue and classification of protocols based on equal, unequal, and hybrid clustering protocols. The last section concludes the paper with a future direction.

2. Clustering in WSN

In WSNs, clustering refers to the division of nodes into groups based on some characteristics. Clusters could be formed based on residual energy [23], location [7], and network topology. Normally, a node that takes more responsibilities is called the CH. The CH formation techniques are distributed [8] or centralized [23] in WSNs. In the former techniques, every node broadcasts information (residual energy) to the one-hop neighbor, and eventually, the node with greater value becomes CH. In the latter techniques, every node is responsible for sharing information back to BS which does computation and selects CHs in the network. BS then informs all the nodes about their respective CHs.
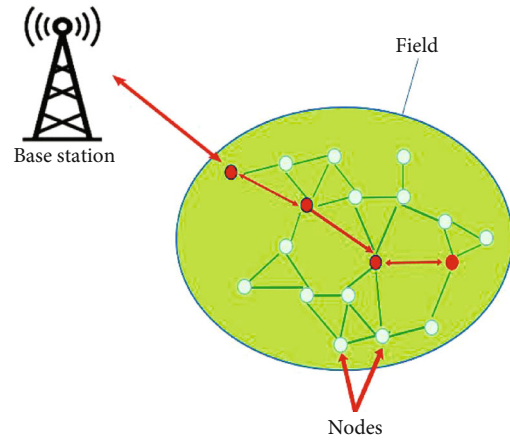
Figure 1: Wireless Sensor Network architecture [7].

WSN is comprised of nested clusters in a supercluster. CHs in small clusters gather data from sensor nodes and forward to super CH in a hierarchy. By using this way, the network works in a multihop fashion, and the role of the node as CH is rotated in a cluster, depending on the hierarchy.

After deployment of the sensor nodes in the network, there are normally two ways to transmit sensed data to the BS. First is direct communication or single-hop [8] between the sensor nodes and the BS. This consumes more energy of the sensor node and shortens the network lifetime. The second one is multihop communication [23], in which the sensor node forwards the data to another nearby node that is comparatively nearer to the BS. The nodes near the BS always serve as intermediate nodes, creating energy holes, which is a problem in WSN when a node cannot find the next forwarder node for multihop communication. Figure 2 shows the clustering process in WSNs.

2.1. Why Clustering Is Needed? The clustering mechanism provides a hierarchal grouping of the sensor nodes and provides scalability, efficiency, and collaboration in the network. It is a promising approach which not only decreases the total number of transmissions required towards BS but also saves energy in the clusters [10], because CHs aggregate data from its cluster members and forward it to BS. Furthermore, maintenance costs are incurred by dynamic topology after using the clustering technique. Reconfiguration is normally done on the CH level where the remaining cluster nodes are not affected. In short, clustering achieves the following objectives:

- (i) Better utilization of resources

- (ii) Scalability improvements

The network life can be enhanced to a greater extent if utilizing the network energy uniformly.

3. Clustering Attribute Classification

The categorization of cluster protocols is based on various clustering mechanisms, clustering types, and cluster design processes.
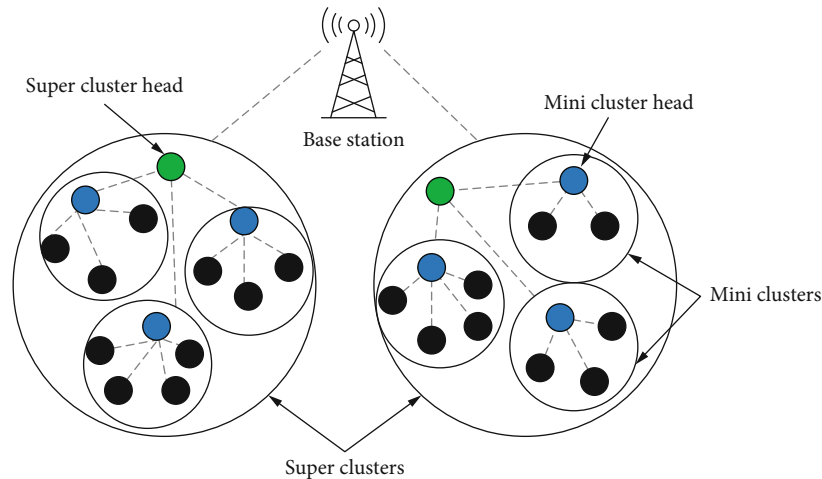
FIGURE 2: Clustering in WSNs [24].

3.1. Clustering Mechanism. Topology control is one of the most significant issues in ad hoc networks due to the massive number of sensor nodes and the inconsistency of the network infrastructure. In ad hoc networks, topology management strategies, choosing appropriate neighbors to establish links, and selecting the optimal neighbors for hop-by-hop data delivery are vital to enhancing scalability, resource utilization, and stability [25]. The clustering mechanism [10] is one of the most vital solutions which has been developed and proposed by a lot of researchers in WSNs. To enhance the network lifespan and network stability, the clustering technique is improving resource utilization. The clustering mechanism can manage and organized the network system into a set of clusters for topological control. Figure 3 shows the clustering protocol classification.

3.2. Clustering Types. The clustering protocols are divided into two types including homogenous [26] and heterogeneous [27]. In the former, all network nodes have the same initial energy while in the latter, network nodes are equipped with different initial energy levels. In the homogenous type of clustering, the network nodes have the same initial energy, processing capabilities, and sensing range. The homogenous networks require high hardware costs. To overcome the limitation of homogenous networks, heterogeneous networks are proposed in which two types of sensor nodes are introduced. Generally, the heterogeneous network has two types of nodes having different energy levels termed as high energy or advanced nodes and low energy or normal nodes. The advanced nodes have maximum energy than the normal nodes. Depending on node heterogeneity, the heterogeneous network can be classified into two-tier or multi-tier heterogeneous networks.

3.3. Clustering Design Process. The clustering process in WSN maximizes the network lifetime, and it is mainly due to the whole network being partitioned into different clusters and each set of a cluster-defined set of nodes. The cluster formation process and the number of clusters are very important factors in clustering protocols. The clusters should be well balanced, and the number of messages exchanged during cluster formation should be minimized. The complexity of the algorithm should increase linearly when the network grows. CH selection is another important challenge that directly affects network performance. The best possible node should be selected so that the network stability period and overall network lifetime should be maximized [27]. The clustering process is divided into three steps, i.e., CH selection, cluster formation, and data transmission [27].

3.3.1. Cluster Head Selection. As CH is primarily used for aggregating and distributing the information to the SN, CH selection plays a very crucial part in optimizing energy consumption. However, the appropriate CH selection enhances the network lifetime. In a cluster-based network, CH near the BS quickly exhausts its energy, which leads to hotspot problems. Unequal clustering algorithms are utilized [28] to overcome this problem. The CH selection is based on various parameters such as probability [29], distance [30], residual energy [23], RSSI [31], cluster density [32], node degree [33], initial energy [34], threshold [35], and hybrid method [36]. The energy utilization of the CH is more extensive as compared to the normal sensor nodes. After the CH selection, nodes joined their CH based on the minimum distance forming a cluster. Figure 4 shows the clustering design process.

3.3.2. Cluster Formation. The cluster formation can be classified into two categories, centralization by the BS or distributive by the nodes themselves [37]. The clustering algorithm uses the network's global knowledge in centralized approaches, while in distributed approaches, local knowledge is used to create clusters. In the distributive approach, the CHs declare their selection to the network nodes by broadcasting advertisement messages where each network node responds by sending a join message to the CH. Each type of cluster comprises a cluster member (CM), and each cluster has a leader whose task is to transmit the data to the other neighbor nodes or BS. The cluster size can be equal, unequal, or hybrid. After the cluster formation, the

Clustering
protocols

Heterogeneous

Homogeneous

Clustering design
process

Cluster head
selection

Cluster
formation
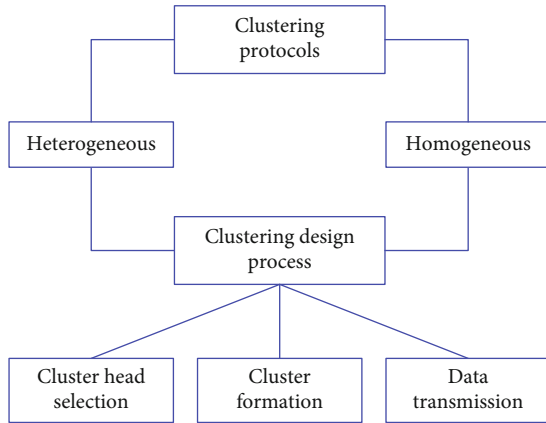
Data
transmission

FIGURE 3: Clustering protocol classification [26, 27].

CH receives the data from the CM, and after, the data aggregation/fusion process forwards the data to the BS via single or multihop transmission for the end-user processing.

3.3.3. Data Transmission. In the clustering technique, both communication models such as single [8] and multihop [23] communication, chain-based [38], or tree-based [39] have unavoidable energy dissipation among the cluster members. This situation arises when some sensor nodes die permanently and hence reduces the lifespan of the network. In clustering protocols, the energy depletion of the sensor nodes which are deployed near to the BS is higher as compared to other nodes, which leads to a hotspot problem [40] or energy hole problem. Due to this hotspot problem, a set of data is forwarded to the BS and collapse the complete network system. Experiment results in [26] indicated the vital information that over ninety percent (90%) of the energy of the whole network remains unutilized if the lifetime of the network is dropped out due to the hotspot issues.

4. Hotspot Issue

The hotspot problem [40] degrades the network transmission. Transmission is interrupted because the number of nodes drains out their energy due to the excess of transmission from that nodes. To alleviate the hotspot issue, many authors have discussed the energy imbalance issue by implementing the unequal type of clustering techniques. Most of the dynamic unequal cluster techniques improve the hotspot issues, but they have also a lot of other issues like overhead along with coverage, connectivity, and network stability issues. So, static or equal clustering [41] technique is used, and this technique can consume a minimal amount of energy and less overhead. But static clustering techniques also have issues while mitigating hotspot and balancing the energy utilization among the SNs. The number of clusters in a zone is the main issue in the static clustering technique while mitigating the hotspot problem increases the lifetime and the network. Increasing the cluster size makes the node closest to the BS deplete their energy fast and causes hotspot issues. A decrease in cluster size increases the intracluster

communication cost where nodes die due to excess communication and the cause of hotspot issues. Figure 5 shows the classification of protocols.

In this paper, we present some parameters of architectures and investigate the hotspot issues. Conducting research based on eliminating hotspot or energy hole issues, we classified protocols according to different clustering techniques including equal [41], unequal [28], and hybrid [36]. In equal clustering, the size of the clusters is consistent throughout the network. Conversely, in unequal clustering, the size of clusters differs throughout the network based on the distance to the BS.

4.1. Equal/Static Clustering Protocols. In this section, equal clustering protocols are discussed whereas Table 1 summarizes static protocols and their performance parameters and comparison.

4.1.1. HUCL. The HUCL [42] protocol comprises both dynamic and unequal clustering static and equal clustering. In this protocol, CHs are nominated based on the principle of residual energy, distance from the BS, and the number of engaged SMS. To avoid the overhead in the network, the set of data transmission stages consists of major slots, and slots are partitioned into several minor slots, and each set of minor slots has sets of CMs, which forward the data to the CH. This CH sends the aggregated data to the BS, and each major slot consists of a new CH, and also, the current CH informs the new CH about its sensor nodes and all information in the transmission phase.

4.1.2. EADUC. An efficient clustering protocol for elevating hotspot or energy hole issues is discussed in [43], in which the authors proposed the protocol called Energy-Aware Distributed Unequal Clustering (EADUC). This protocol elects the CH on the principle of average residual energy of the surrounding sensor nodes and the residual energy of the SN itself. It developed a cluster of uneven sizes to mitigate the hotspot issues. The CH which is closest to the BS has a smaller number of clusters which are used to efficiently balance the energy consumption and make the network energy preserved for intercluster communication.

4.1.3. IEADUC. In [44], the authors proposed an Improved Energy-Aware Distributed Unequal Clustering protocol (IEADUC) as an improved version of [43]. In IEADUC, one step is included when electing CH, and that is considering the neighbor nodes. In this protocol, the selection of the next hop for data forwarding the Relay Node (RN) is used. The RN can formulate the set of tables that consists of energy utilization of nodes instead of location and distance information used in the EADUC protocol.

4.1.4. ZECR. In [45], the authors proposed a protocol called Zone divided and Energy Balanced Clustering Routing protocol (ZECR). This algorithm partitions the area into several types of zones and uses unequal clustering techniques to alleviate the hotspot issues. These types of hotspot issues are produced by the nodes which are closer to the BS and send the data passing through it. Due to this factor, nodes
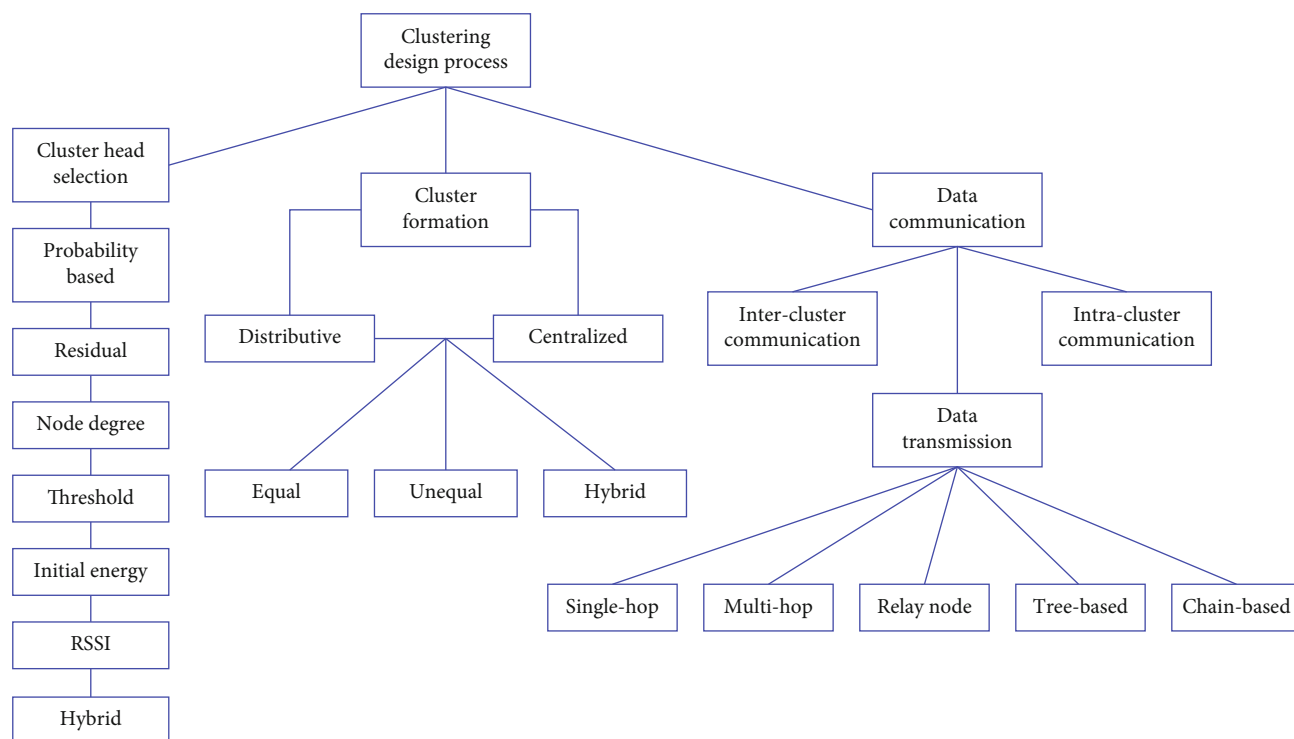
FIGURE 4: Clustering design process [23, 29–36].

deplete their energy faster and created hotspot issues. The technique of CH selection is based on the principle where the nodes can only be selected as a CH that has an energy that is defined in the protocol. The energy should be equal to the respective standard defined in the protocol. RN for intercluster communication is selected based on high residual energy, and data is transferred to the BS efficiently.

4.1.5. IEEUC. In [46], the authors proposed Improved Energy-Efficient Unequal Clustering (IEEUC). The IEEUC protocol is the improved and extended version of the EEUC protocol [33], which does not only depend upon the physical orientation of the SNs but also depend upon the distance of the SNs to the BS. The number of clusters closest to the BS has a small size and preserves more energy in contrast to the cluster far away from the BS.

4.1.6. LUCA. In [47], the authors proposed a Location-based Unequal Clustering Algorithm (LUCA). In this protocol, there is an unequal cluster mechanism that is established based on the location factor. Due to this location factor, the clusters are changed, respectively. The cluster size in the protocol changes concerning the distance of the SNs from the BS. This protocol forms the smaller clusters close to the BS to preserve the energy and balances the energy among the sensor nodes whereas the larger clusters are distant from the BS and the whole process is done to alleviate the hotspot issues.

4.1.7. EBCAG. An efficient clustering protocol called Energy Balancing Unequal Clustering Approach for Gradient-based routing (EBCAG) using gradient-based routing for eliminat-

ing the hotspot issue is discussed in [48]. The protocol divided the nodes into an unequal set of clusters where each set of SNs can preserve a gradient value. The gradient value in the protocol is set to be formulated as the minimum number of hops to BS. The size of the cluster in this protocol is depending on the set of gradient values of the CH of respective clusters. The selection of the CH is based on the principle that first a tentative CH is selected with a random probability of the nodes and becoming a CH. If a CH that is tentatively selected has maximum remaining energy, it is set to be updated as a final CH. The CH in an unequal clustering collects the data from the SNs of its respective clusters and sends the data to the BS on the descendent gradient of the CH.

4.1.8. EBUCP. In [49], the authors suggested an algorithm called the Energy Balanced Unequal Clustering Protocol (EBUCP). This algorithm confirms the nonexistence of isolated nodes for the formation of unequal clusters. This protocol consists of two steps, where in the first step the radius of the cluster is formulated. In the second step, the CH selection process is contained and provides the detail that there are no isolated nodes in the network system. The protocol is partitioned into a multilayer mechanism in which the circular area is divided into a set of multilayers. In these types of multilayers in circular rings, each layer has a balanced energy consumption mechanism.

4.1.9. Dynamic Unequal Clustering Protocol. In [50], the researchers proposed an energy-aware protocol called the dynamic unequal clustering protocol. The main purpose of this protocol is to avoid hotspot issues and prolong the
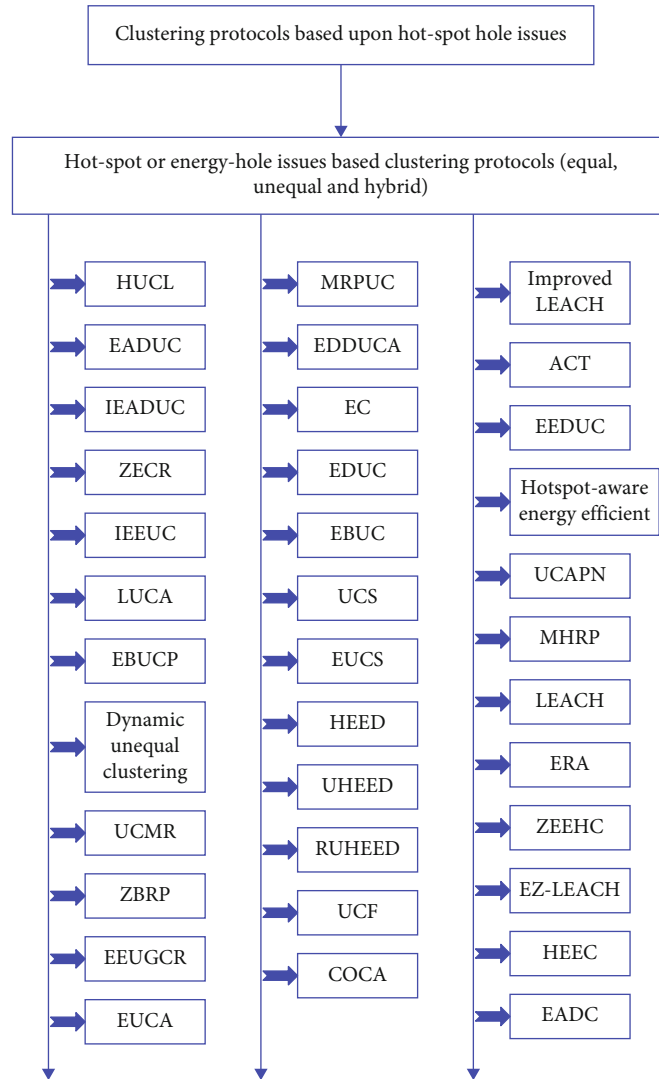
FIGURE 5: Classification of protocols.

network lifetime and network stability. In this protocol, the cluster size is variable. It means that unequal clustering is used for preserving the energy of the sensor nodes. In this protocol, the CH selection mechanism is based on the node's residual energy and the distance of the nodes to the BS. The CH nomination mechanism is established on the remaining energy and the distance of the nodes to the BS.

4.1.10. UCMR. In [51], the authors proposed a protocol called the Unequal Clustering Multihop Routing protocol (UCMR). In this protocol, each set of the cluster has different cluster sizes; this cluster size is grounded on its distance from the BS. This protocol reduces the hotspot or energy hole issues with the help of an unequal clustering process. In this protocol, the unequal clustering process manages the network with cluster sizes. The cluster near the BS has a small size to preserve energy as likened to the cluster which is distant away from the BS. Table 1 shows the comparison of the static protocol.

4.1.11. ZBRP. In [52], the authors proposed a protocol called the Zone-Based Routing Protocol (ZBRP). It consists of clustering technique and network space aspect to eliminate the hotspot issues. In this protocol, the CH selection is depending on the random back of time in each round. The set of nodes closer to the BS having higher residual energy and previously sending less data is selected as the RN. The protocol formulates uneven-sized clusters, and these types of clusters have very small overhead while considering the location information.

4.1.12. EEUGCR. In [53], the authors proposed a protocol called the Energy-Efficient Uneven Grid-based Clustering Routing protocol (EEUGCR). This protocol uses a centralized technique in which the BS is responsible for all types of tasks such as CH nomination, cluster establishment, and RN selection criteria. The BS in this protocol partitioned the entire network into a set of unequal-sized clusters. The cluster size is based on its distance from the BS. Greater

TABLE 1: Static protocols.

Sr. no.	Protocol	Data transmission	Node type	Clustering type	CH selection
1	HUCL	Multihop	Homogeneous	Hybrid clustering	Distance to the BS and adjacent nodes, energy
2	EADUC	Multihop	Heterogeneous	Unequal clustering	Deterministic
3	IEADUC	Multihop	Heterogeneous	Unequal clustering	Residual energy, surrounding nodes
4	ZECR	Multihop	Heterogeneous	Unequal clustering	Residual energy
5	IEEUC	Multihop	Homogeneous	Unequal clustering	Hybrid
6	LUCA	Multihop	Homogeneous	Unequal clustering	Random
7	EBCAG	Multihop	Homogeneous	Unequal clustering	Deterministic
8	EBUCP	Multihop	Heterogeneous	Unequal clustering	Remaining energy, average energy
9	Dynamic unequal clustering protocol	Multihop	Homogeneous	Unequal clustering	Remaining energy
10	UCMR	Multihop	Homogeneous	Unequal clustering	Deterministic
11	ZBRP	Multihop	Homogeneous	Hybrid clustering	Remaining energy
12	EEUGCR	Multihop	Homogeneous	Unequal clustering	Centrality factor
13	EUCA	Multihop	Homogeneous	Unequal clustering	Residual energy
14	MRPUC	Multihop	Homogeneous	Unequal clustering	Deterministic

distance from the BS increases the size of clusters, and closer to the BS decreases the size of the cluster for preserving more energy. Due to a lot of energy dissipation of the cluster near the BS, the grid clustering method is introduced where the hotspot issues are alleviated. In the end, data is sent to the most upper-level layer, and from this layer, data is sent to the BS through data mules.

4.1.13. EUCA. In [54], the authors suggested a protocol called the Enhanced Unequal Clustering Algorithm (EUCA) based on the UCA protocol. In this protocol, the authors have enhanced the UCA protocol to overcome the hotspot issue. The basic idea behind this solution is placing the BS closer to the clusters and BS nodes which are tiny in size placed far away from the clusters. This strategy enhances the network lifetime by consuming less energy in the network.

4.1.14. MRPUC. In [55], the authors proposed the protocol called Multihop Routing Protocol with Unequal Clustering (MRPUC). The main purpose of this protocol is to develop an unequal clustering technique to enhance the network lifetime and network stability. Nodes nearer the BS have a tiny cluster size to evade hotspot issues. The selection of CH is based on the node which has higher residual energy in the

system. The number of clusters that are closest to the BS is kept small where they preserved the energy in intracluster communication and forward the packets for intercluster communication.

4.2. Unequal Clustering Protocol. In this section, unequal clustering protocols are discussed.

4.2.1. EDDUCA. In [56], the authors suggested a protocol called Energy Degree Distance-based Unequal Clustering (EDDUCA). CH election is centered on outstanding energy, the degree of the node, and the distance of the CH from the BS. This solution consists of an unequal clustering technique for preserving the energy of the nodes closer to the BS. Due to the unequal clustering mechanism, the size of the cluster closer to the BS is kept smaller as compared to the clusters which are far away from the BS.

4.2.2. EC. In [57], the authors presented a disseminated protocol called Energy-efficient Clustering (EC). This solution maintains the sizes of the clusters founded on the distance of the clusters from the BS. In this protocol, uncertain CHs are selected arbitrarily, and the concluding CH is selected based on the highest leftover energy. The intercluster routing protocol developed the balanced energy scenario and

produces less amount of overhead due to the route discovery mechanism.

4.2.3. EDUC. In [58], the authors presented an Energy-Driven Unequal-based Clustering protocol (EDUC). The protocol consists of the unequal clustering method and CH rotation mechanism. In this solution, an unequal set of clustering methods is responsible for the balance of energy consumption among the nodes. The CH rotation mechanism is used for the dissipation of energy among the cluster nodes. The number of clusters that are contiguous to the BS has a smaller size and thus preserves the energy. While in another case, the clusters which are distant from the BS have a larger size.

4.2.4. EBUC. In [59], the authors proposed and evaluated an algorithm called the Energy Balance Unequal Clustering (EBUC). This algorithm consists of an unequal clustering technique that is most often used for periodic data collection. This protocol provides the mechanism in which the CH preserves more energy and avoided hotspot issues. This protocol adopts both inter- and intracluster routing. For intercluster routing, the CH can relay the data with the help of RN. This RN gathers the accumulated data from the CHs and relays this data to the BS.

4.2.5. UCS. In [60], the authors proposed a protocol called Unequal Clustering Size (UCS). The protocol provides the mechanism that CH nodes can completely adjust their location and the cluster size and the load balancing among different CHs should be managed properly.

4.2.6. EUCS. In [61], the authors presented an Enhanced Unequal Clustering (EUCS). In [61], the clusters which are closer to the BS have tiny cluster sizes as related to the clusters which are distant from the BS. The CH selection mechanism consists of the nodes which have the highest residual energy and also the distance of it from the BS, to balance the energy utilization between the SNs and the CH reelection mechanism. So, in this scheme, the CH reelection mechanism is initiated when the CH energy becomes less than the set threshold. Table 2 shows the static protocols, their performance parameters, and their comparison.

4.2.7. HEED. In [62], the authors proposed a Hybrid Energy-Efficient Distributed clustering (HEED). The HEED protocol uses a hybrid scheme for CH selection and comprises outstanding power of the nodes and the degree of the respected nodes in an equal clustering manner.

4.2.8. UHEED. In [63], the authors presented an algorithm called Unequal Clustering Hybrid Energy-Efficient Distributed (UHEED) based on [62]. This protocol can mitigate the hotspot issues and improve the energy utilization among the nodes and prolong the network lifespan and stability. In [63], the CH selection is based on the unequal size cluster mechanism. These types of clusters are formed with a set of parameters such as distance among CH and BS. In this scheme, the size of the clusters is kept smaller near the BS as compared to the size of the clusters which are far away from the BS. Due to this type of cluster formation, the intracluster communication cost closer to the BS reduces. The clusters are smaller near the BS, and there is less burden on the CHs as compared to the CHs which are far away from the BS.

4.2.9. RUHEED. In [64], the authors proposed a Rotated Unequal clustering protocol (RUHEED). This protocol is the extended form of [63], with a more rotating CH node for the CH election mechanism. The CH is rotated in a specific manner among the nodes of the identical cluster. This CH rotation is depending upon the node which has the highest outstanding energy in the cluster.

4.2.10. Fuzzy-Based Clustering. In [65], the authors proposed a protocol called fuzzy-based clustering mechanism for mitigating hotspot issues in WSNs. This protocol can develop a systematic unequal clustering technique using the fuzzy logic mechanism. In this protocol, the selection of CH is not only dependent upon the residual energy of the nodes but also dependent upon other systematic information of the set of nodes. In this protocol, the cluster size adjacent to the BS is lesser in contrast to the clusters which are distant from the BS. These adjacent clusters preserved their energy in intracluster routing and use this energy for intercluster communication and balance the load among the nodes.

4.2.11. COCA. In [66], the authors proposed a Construction of Optimal Clustering Architecture (COCA) for WSNs. This protocol developed a mechanism for optimal cluster formation in which the energy utilization mechanism in all clusters is even. Due to this even energy utilization, the hotspot issues are alleviated systematically. In the second part of the protocol, a CH rotation mechanism is developed in such a way that the energy which is consumed during intracluster communication lessens, and hence, it overcomes the hotspot issues.

4.2.12. Improved LEACH. In [67], the authors proposed a protocol called the Improved Low Energy Adaptive Clustering Hierarchy (Improved LEACH) protocol for WSNs. The CH sends the data directly to the BS without any assistance from any other nodes. The CH selection is centered on the round-robin principle, and the selection of time slots is predefined. In the data transmission phase, the SNs of the respective cluster use the TDMA time slot scheme to send the data to the CHs and the CHs use the CSMA technique to send the collected data to the BS.

4.2.13. ACT. In [68], the authors proposed a protocol called Arranging Cluster size and Transmission range (ACT) for WSNs. This protocol provides an extension mechanism for arranging the set of clusters and their transmission. This scheme describes that size of clusters is depending upon the distance of the clusters from the BS. Clusters that are closer to the BS have a tiny cluster size in contrast to the clusters which are distant from the BS which reduces the extra burden on the nodes near the BS.

TABLE 2: Unequal clustering protocols.

Sr. no.	Protocol	Data transmission	Node type	Clustering type	CH election
1	EDDUCA	Multihop	Homogeneous	Unequal clustering	Compound
2	EC	Multihop	Homogeneous	Unequal clustering	Hybrid
3	EDUC	Multihop	Heterogeneous	Unequal clustering	Random
4	EBUC	Multihop	Homogeneous	Unequal clustering	Heuristic
5	UCS	Multihop	Homogeneous and heterogeneous	Unequal clustering	Preset
6	EUCS	Multihop	Homogeneous	Unequal clustering	High residual energy
7	HEED	Multihop	Homogeneous	Static and equal clustering	Hybrid
8	UHEED	Multihop	Homogeneous	Unequal clustering	Hybrid
9	RUHEED	Multihop	Homogeneous	Unequal clustering	Hybrid
10	UCF	Multihop	Homogeneous	Unequal clustering	Fuzzy
11	COCA	Multihop	Homogeneous	Unequal clustering	Hybrid
12	Improved LEACH	Single-hop	Homogeneous	Unequal clustering	Hybrid
13	ACT	Multihop	Homogeneous	Unequal clustering	Deterministic
14	EEDUC	Multihop	Homogeneous	Unequal clustering	Hybrid

4.2.14. EEDUC. In [69], the author suggested a protocol called Energy-Efficient Distributed Unequal Clustering (EEDUC) for WSN. The protocol systematically collects the periodical data to balance the energy utilization among the SNs. In this protocol, CH is selected based upon some type of efficient intracluster parameters. Each type of SN in a cluster established a waiting time. This waiting time consists of the residual energy of the SNs and also the number of adjacent nodes in a cluster. With the help of this waiting time selection, the CH is selected. While removing the hotspot, there is an unequal clustering mechanism that clusters adjacent to the BS have reduced cluster size as matched to the clusters which are distant from the BS, and hence, load on CHs near the BS is lessened. But there is a defect in this technique which is a lot of energy utilization while relaying the data from CH to RN and RN to BS.

4.3. Hybrid Protocols. In this section, hybrid clustering protocols are discussed.

4.3.1. Hotspot Aware Energy. In [70], the authors proposed a hotspot aware energy resourceful clustering approach for WSN. In this protocol, an unequal clustering mechanism is formulated where unequal clustering depends upon the distance from the BS. In this protocol, there is a two-tier mechanism in which CH is put under the higher tier and the SNs put under the lower tier. Each set of SNs can send the data to the higher tier which is CH, and the CH can send the gathered data to the BS. Initially, the CH is selected centered on the remaining energy of the node. If a node fell in more than the individual cluster range, then sensor nodes can select the CH which has low intracluster communication.

4.3.2. UCAPN. In [71], the authors proposed an energy responsive imbalanced clustering algorithm for prolonging the network lifetime (UCAPN). This protocol partitioned the network into unequal cluster sizes. This protocol selects the CHs built on the set of outstanding energy of the adja-

cent nodes and developed an unequal clustering mechanism. In this protocol, the set of clusters that are close to the BS has smaller cluster sizes as compared to the clusters which are distant from the BS and minimized the energy consumption.

4.3.3. MHRP. In [72], the author proposed energy effective Multi-Hop Routing Protocol (MHRP) for WSNs. In [72], the CH election process is based on SNs with the highest outstanding energy and a systematic set of routing paths that are selected for the outstanding energy and the distance among the nodes. This protocol divides the network area into a different set of regions or zones where CH is selected based on the remaining energy of the SNs and for the data forwarding process. This protocol has a mechanism for multihop communication.

4.3.4. ERA. In [73], the authors proposed an Energy-conscious Routing Algorithm (ERA) for WSNs. The CH selection is established on the remaining energy. For the selection of CHs, initially, each node uses a time slot based on the set of residual energy of the nodes. For the cluster formation process, this protocol uses the set of SNs which are sending a message to the adjacent CH created on the remaining energy and its distance from the BS. Data forwarding from CH to BS is based on a series of CHs where the data is forwarded and reached the BS.

4.3.5. ZEEHC. In [74], the authors presented a Zone-based Energy Proficient Hierarchical Clustering convention (ZEEHC) protocol for WSNs. In this type of protocol, the network system is divided efficiently into the desirable size of zones to raise the stability and network lifetime of the network system. In this protocol, there is a concept of multihop propagation of information from CH or ZH to RN and then to BS. Table 3 shows the hybrid protocol comparison and performance metrics.

4.3.6. EZ-LEACH. In [75], the authors proposed an improvement on LEACH called Energy-Zone-LEACH (EZ-LEACH)

TABLE 3: Hybrid protocols.

Sr. no.	Protocol	Data transmission	Node type	Clustering type	CH election
1	[52]	Multihop	Homogeneous	Unequal clustering	Residual energy
2	UCAPN	Multihop	Homogeneous	Unequal clustering	Residual energy
3	MHRP	Multihop	Homogeneous	Optimal and equal clustering	Residual energy
4	LEACH	Single-hop	Homogeneous	Dynamic clustering	Random
5	ERA	Multihop	Homogeneous	Optimal clustering	Hybrid
6	ZEEHC	Multihop	Homogeneous	Static and equal clustering	Residual energy
7	EZ-LEACH	Multihop	Homogeneous	Static and equal clustering	Hybrid
8	HEEC	Multihop	Homogeneous	Optimal clustering	Hybrid
9	EADC	Multihop	Heterogeneous	Dynamic clustering	Hybrid
10	DHCS	Multihop	Homogeneous	Dynamic clustering	Hybrid
11	ESDCH	Multihop	Homogeneous	Optimal clustering	Hybrid
12	DHCM	Multihop	Homogeneous	Optimal clustering	Hybrid
13	DCH-NPSO	Multihop	Homogeneous	Optimal clustering	Hybrid
14	PSO-DH	Multihop	Homogeneous	Optimal clustering	Hybrid

protocol for WSNs. The first step of the protocol is network formation in which the network is divided into a set of four logical zones. CH is selected in this protocol where the node which has a centrality factor can send its location to the BS. Then, BS selects the CH node which is closed to the central node. The residual and average energy is also considered for the selection of CH.

4.3.7. HEEC. In [76], the authors proposed a Hierarchical Energy-Efficient Clustering algorithm (HEEC) for WSNs. The CH is selected grounded on the set of outstanding energy of the SNs and the distance to the BS. The CH selection process also consists of the node alive status where the node can transmit data to the BS. This protocol also introduces the reelecting of the CH. The BS check after the first round the energy status of the CH and compare it to the other node. If it has less energy like aliveness and residual energy, then the reelecting process is continued. This load balance makes the network system energy efficient.

4.3.8. EADC Scheme. In [77], the authors presented a protocol with nonuniform node distribution for WSNs. This scheme consists of two main parts: the first is the Energy-Aware Clustering algorithm (EADC) and the second is cluster-based routing phenomena. This EADC scheme has the ability to establish clusters that are even sized and use the process of competition ranges. There are balanced energy consumptions among the node systematically. In the second part of the protocol, to balance the energy consumption among the CHs, a cluster-based systematic routing protocol is developed. In this protocol, to systematically balance the energy consumption among the CH, there is a set of mechanisms that are established for intracluster and intercluster energy consumption adjustment. The CH selection mechanism consists of nodes with the highest residual energy, and also, the average remaining energy of the adjacent node is set to be considered for the selection of CH.

4.3.9. DHCS. In [78], the authors proposed the energy resourceful Dual-Head Clustering Scheme (DHCS) for WSNs. The dual CH mechanism is established in which two CHs are considered which has the ability of network route management, data relaying, data aggregation process, cluster maintenance process, and set of intracluster and intercluster communication mechanisms. The addition of these two CHs makes the network system efficient, and there is a load balance in the network system, and also, the CH reelection mechanism is removed. The dual CH selection mechanism consists of a set of criteria in which the first CH is selected based on the residual energy of the node. The node with maximum residual energy is selected as the first CH. The second CH which is called the aggregated head is selected by the first CH and is used for data aggregation, cluster formation, and another set of clustering operations.

4.3.10. ESDCH. In [79], the authors proposed an Energy-Saving Dual-Cluster Head protocol (ESDCH) for WSNs. In this protocol, each set of SNs can arrange itself into clusters and set the states of the SN into sleep state or active state established on the outstanding energy of the nodes. This protocol considers the dual CH mechanism, and the purpose of this dual CH is to balance the load in the whole network system systematically. Primary CH is chosen which has the maximum remaining energy in the cluster, and after that, secondary CH is chosen from the remaining nodes in the cluster which are nearer to the primary CH. Primary CH can collect all the data from the SNs and provide some aggregation mechanism and send this to the BS. Secondary CH is only active when the working of the primary CH is interrupted. This protocol can balance the energy intake among the nodes systematically.

4.3.11. DHCM. In [80], the authors proposed a protocol called the Dual-Head Clustering Mechanism (DHCM) for WSNs. This protocol can use the dual CH mechanism. This dual CH mechanism balances the load in the whole network

system and makes the network system energy efficient. The set of communication between CHs and the BS uses the multihop mechanism, and due to this, CHs which are nearer to the BS get burden with heavy relay traffic where nodes die out, and the network system gets partitioned. To overcome these issues, the authors developed a dual CH mechanism, and this mechanism balanced the load and makes the network system energy efficient. Both CHs have different responsibilities in the network system. One CH is used for data collection from all the nodes; then, another CH has the responsibility of data relaying and also data aggregation mechanism.

4.3.12. DCH-NPSO. In [24], the authors presented Dual Cluster Heads using Niching Particle Swarm Optimization (DCH-NPSO). In this protocol dual CH, the mechanism is established and balances the energy utilization in the whole network system. Two CHs are selected in the individual cluster, and these CHs balanced the load in each cluster. Master CH and Slave CH are two CHs that are selected in each cluster. Master CH can collect all the data from the CMs and provide some type of aggregation mechanism and send this data to the Slave CH. Slave CH can send the data to the BS. Master CH cannot transfer data straight to the BS and hence balance the energy utilization in the network system.

4.3.13. PSO-DH. In [31], the authors proposed a protocol called the Double Cluster Heads clustering algorithm using Particle Swarm Optimization (PSO-DH). This protocol provides a mechanism for selecting two CHs using the PSO technique. This protocol does not only provide a systematic mechanism for CH selection but also provide a balanced energy consumption mechanism among the nodes. Two types of CHs are selected which are master CH and vice CH. Master CH collects the data from all the CMs and provides some aggregation mechanism and sends it to the vice CH. Vice CH receives this aggregated data and relays it to the BS. Master CH cannot directly communicate with the BS, and in this case, there is a balance of energy consumption in the clusters.

5. Conclusion

We may deduce from the aforesaid analyses that routing strategies may improve sensor network energy efficiency or extend network life. However, the hotspot issues are still under consideration. This research alleviated the hotspot problem in WSN. The hotspot problem refers to that where the sensor nodes are close to the BS and consume more energy and depleted faster than the other placed sensor nodes. Due to significant data traffic from CMs and other CHs towards the BS, the areas around BS are hotspots. In WSNs, hotspot issues are still an open challenge. Hotspot or energy hole issues make the network system halt, partition the network system, disappear the coverage area, reduce the efficiency of the system, and in addition decrease the network lifetime. Many existing clustering protocols like dynamic and unequal clustering techniques have tried to

overcome hotspot issues. However, while tackling the hotspot issue, these protocols have suffered from other issues like overhead and connectivity. This research reveals that static and equal clustering techniques are more efficient for avoiding hotspots. There is a pressing need to design a more efficient and smart clustering protocol for WSN to tackle the hotspot issue. In the future, we will review some other issues in WSN and relate those with hotspot issues.

Conflicts of Interest

The authors declare no conflict of interest.

Acknowledgments

References

[1] I. F. Akyildiz, W. Su, Y. Sankarasubramaniam, and E. Cayirci, "A survey on sensor networks," *IEEE Communications Magazine*, vol. 40, no. 8, pp. 102–114, 2002.

[2] W. Abidi and T. Ezzedine, "Effective clustering protocol based on network division for heterogeneous wireless sensor networks," *Computing*, vol. 102, no. 2, pp. 413–425, 2020.

[3] G. M. Abdulsahib and O. I. Khalaf, "Accurate and effective data collection with minimum energy path selection in wireless sensor networks using mobile sinks," *Journal of Information Technology Management*, vol. 13, pp. 139–153, 2021.

[4] J. Toledo-Castro, P. Caballero-Gil, N. Rodríguez-Pérez, I. Santos-González, C. Hernández-Goya, and R. Aguasca-Colomo, "Forest fire prevention, detection, and fighting based on fuzzy logic and wireless sensor networks," *Complexity*, vol. 2018, 17 pages, 2018.

[5] M. A. Ghaida and I. K. Osamah, "An improved algorithm to fire detection in forest by using wireless sensor networks," *International Journal of Civil Engineering and Technology*, vol. 9, pp. 369–377, 2018.

[6] I. K. Osamah, M. A. Ghaida, I. K. Osamah, and S. Muayed, "A modified algorithm for improving lifetime WSN," *Journal of Engineering and Applied Sciences*, vol. 13, pp. 9277–9282, 2018.

[7] R. Pachlor and D. Shrimankar, "VCH-ECCR: a centralized routing protocol for wireless sensor networks," *Journal of Sensors*, vol. 2017, 10 pages, 2017.

[8] T. M. Behera, S. K. Mohapatra, U. C. Samal, M. S. Khan, M. Daneshmand, and A. H. Gandomi, "I-SEP: an improved routing protocol for heterogeneous WSN for IoT-based environmental monitoring," *IEEE Internet of Things Journal*, vol. 7, no. 1, pp. 710–717, 2020.

[9] A. F. Subahi, Y. Alotaibi, O. I. Khalaf, and F. Ajesh, "Packet drop battling mechanism for energy aware detection in wireless networks," *Computers, Materials and Continua*, vol. 66, no. 2, pp. 2077–2086, 2021.

[10] S. K. Singh, M. Singh, and D. Singh, "Energy efficient homogenous clustering algorithm for wireless sensor networks," *International Journal of Wireless & Mobile Networks (IJWMN)*, vol. 2, no. 3, pp. 49–61, 2010.

[11] A. Sarkar and T. M. Senthil, "Cluster head selection for energy efficient and delay-less routing in wireless sensor network," *Journal of Wireless Networks*, vol. 25, no. 1, pp. 303–320, 2019.

[12] O. I. Khalaf and B. Sabbar, "An overview on wireless sensor networks and finding optimal location of nodes," *Periodicals of Engineering and Natural Sciences*, vol. 7, no. 3, pp. 1096–1101, 2019.

[13] O. I. Khalaf, G. M. Abdulsahib, and B. M. Sabbar, "Optimization of wireless sensor network coverage using the bee algorithm," *Journal of Information Science and Engineering*, vol. 36, pp. 377–386, 2020.

[14] O. I. Khalaf, F. Ajesh, A. A. Hamad, G. N. Nguyen, and D. N. Le, "Efficient dual-cooperative bait detection scheme for collaborative attackers on mobile ad-hoc networks," *IEEE Access*, vol. 8, pp. 227962–227969, 2020.

[15] S. Kavianpour, B. Shanmugam, S. Azam, M. Zamani, G. Narayana Samy, and F. De Boer, "A systematic literature review of authentication in internet of things for heterogeneous devices," *Journal of Computer Networks and Communications*, vol. 2019, 14 pages, 2019.

[16] S. Rajasoundaran, A. V. Prabu, J. B. V. Subrahmanyam et al., "Secure watchdog selection using intelligent key management in wireless sensor networks," *Materials Today*, 2021.

[17] A. D. Salman, O. I. Khalaf, and G. M. Abdulsahib, "An adaptive intelligent alarm system for wireless sensor network," *Science*, vol. 15, no. 1, pp. 142–147, 2019.

[18] N. Shah, Y. Ali, N. Ullah, and I. García-Magariño, "Internet of Things for healthcare using effects of mobile computing: a systematic literature review," *Wireless Communications & Mobile Computing (Online)*, vol. 2019, pp. 1–20, 2019.

[19] M. S. Aliero, K. N. Qureshi, M. F. Pasha, I. Ghani, and R. A. Yauri, "Systematic review analysis on SQLIA detection and prevention approaches," *Wireless Personal Communications*, vol. 112, no. 4, pp. 2297–2333, 2020.

[20] C. A. Tavera, J. H. Ortiz, O. I. Khalaf, D. F. Saavedra, and T. H. Aldhyani, "Wearable wireless body area networks for medical applications," *Computational and Mathematical Methods in Medicine*, vol. 2021, 9 pages, 2021.

[21] M. Abdulkarem, K. Samsudin, F. Z. Rokhani, and A. M. F. Rasid, "Wireless sensor network for structural health monitoring: a contemporary review of technologies, challenges, and future direction," *Structural Health Monitoring*, vol. 19, no. 3, pp. 693–735, 2020.

[22] A. Verma, S. Kumar, P. R. Gautam, T. Rashid, and A. Kumar, "Fuzzy logic based effective clustering of homogeneous wireless sensor networks for mobile sink," *IEEE Sensors Journal*, vol. 20, no. 10, pp. 5615–5623, 2020.

[23] M. Sajwan, D. Gosain, and A. K. Sharma, "CAMP: cluster aided multi-path routing protocol for wireless sensor networks," *Wireless Networks*, vol. 25, no. 5, pp. 2603–2620, 2019.

[24] D. Ma and P. Xu, "An energy distance aware clustering protocol with dual cluster heads using niching particle swarm optimization for wireless sensor networks," *Journal of Control Science and Engineering*, vol. 2015, 6 pages, 2015.

[25] A. Shahraki, A. Taherkordi, Ø. Haugen, and F. Eliassen, "Clustering objectives in wireless sensor networks: a survey and research direction analysis," *Computer Networks*, vol. 180, article 107376, 2020.

[26] X. Zhao, S. Ren, H. Quan, and Q. Gao, "Routing protocol for heterogeneous wireless sensor networks based on a modified grey wolf optimizer," *Sensors*, vol. 20, no. 3, p. 820, 2020.

[27] L. Kong, Q. Xiang, X. Liu et al., "ICP: instantaneous clustering protocol for wireless sensor networks," *Computer Networks*, vol. 101, pp. 144–157, 2016.

[28] A. A. Jasim, M. Y. I. Idris, S. Razalli Bin Azzuhri, N. R. Issa, M. T. Rahman, and M. F. . Khyasudeen, "Energy-efficient wireless sensor network with an unequal clustering protocol based on a balanced energy method (EEUCB)," *Sensors*, vol. 21, no. 3, p. 784, 2021.

[29] P. Rawat and S. Chauhan, "Probability based cluster routing protocol for wireless sensor network," *Journal of Ambient Intelligence and Humanized Computing*, vol. 12, no. 2, pp. 2065–2077, 2021.

[30] E. Pei, J. Pei, S. Liu, W. Cheng, Y. Li, and Z. Zhang, "A heterogeneous nodes-based low energy adaptive clustering hierarchy in cognitive radio sensor network," *IEEE Access*, vol. 7, pp. 132010–132026, 2019.

[31] Z. Ruihua, J. Zhiping, L. Xin, and H. Dongxue, "Double cluster-heads clustering algorithm for wireless sensor networks using PSO," in *2011 6th IEEE conference on industrial electronics and applications*, Beijing, China, 2011.

[32] S. Singh, "Energy efficient multilevel network model for heterogeneous WSNs," *Engineering Science and Technology, an International Journal*, vol. 20, no. 1, pp. 105–115, 2017.

[33] B. Baranidharan and B. Santhi, "DUCF: distributed load balancing unequal clustering in wireless sensor networks using fuzzy approach," *Applied Soft Computing*, vol. 40, pp. 495–506, 2016.

[34] E. M. Borujeni, D. Rahbari, and M. Nickray, "Fog-based energy-efficient routing protocol for wireless sensor networks," *The Journal of Supercomputing*, vol. 74, no. 12, pp. 6831–6858, 2018.

[35] K. A. Darabkh, W. S. Al-Rawashdeh, M. Hawa, and R. Saifan, "MT-CHR: a modified threshold-based cluster head replacement protocol for wireless sensor networks," *Computers and Electrical Engineering*, vol. 72, pp. 926–938, 2018.

[36] F. A. Khan, M. Khan, M. Asif, A. Khalid, and I. U. Haq, "Hybrid and multi-hop advanced zonal-stable election protocol for wireless sensor networks," *IEEE Access*, vol. 7, pp. 25334–25346, 2019.

[37] A. Hamzah, M. Shurman, O. Al-Jarrah, and E. Taqieddin, "Energy-efficient fuzzy-logic-based clustering technique for hierarchical routing protocols in wireless sensor networks," *Sensors*, vol. 19, no. 3, p. 561, 2019.

[38] N. Ramluckun and B. Vandana, "Energy-efficient chain-cluster based intelligent routing technique for wireless sensor networks," *Applied Computing and Informatics*, vol. 16, no. 1/2, pp. 39–57, 2020.

[39] W. Osamy, A. M. Khedr, A. Aziz, and A. A. El-Sawy, "Cluster-tree routing based entropy scheme for data gathering in wireless sensor networks," *IEEE Access*, vol. 6, pp. 77372–77387, 2018.

[40] R. Elkamel, A. Messouadi, and A. Cherif, "Extending the lifetime of wireless sensor networks through mitigating the hot spot problem," *Journal of Parallel and Distributed Computing*, vol. 133, pp. 159–169, 2019.

[41] H. Shin, S. Moh, I. Chung, and M. Kang, "Equal-size clustering for irregularly deployed wireless sensor networks," *Wireless Personal Communications*, vol. 82, no. 2, pp. 995–1012, 2015.

[42] L. Malathi, R. K. Gnanamurthy, and K. Chandrasekaran, "Energy efficient data collection through hybrid unequal clustering for wireless sensor networks," *Computers and Electrical Engineering*, vol. 48, pp. 358–370, 2015.

[43] J. Yu, Y. Qi, G. Wang, Q. Guo, and X. Gu, "An energy-aware distributed unequal clustering protocol for wireless sensor networks," *International Journal of Distributed Sensor Networks*, vol. 7, no. 1, Article ID 202145, 2011.

[44] V. Gupta and R. Pandey, "An improved energy aware distributed unequal clustering protocol for heterogeneous wireless sensor networks," *Engineering Science and Technology, an International Journal*, vol. 19, no. 2, pp. 1050–1058, 2016.

[45] Y. Zou, H. Zhang, and X. Jia, "Zone-divided and energy-balanced clustering routing protocol for wireless sensor networks," in *2011 4th IEEE International Conference on Broadband Network and Multimedia Technology*, Shenzhen, China, 2011..

[46] P. Liu, T.-L. Huang, X.-Y. Zhou, and G.-X. Wu, "An improved energy efficient unequal clustering algorithm of wireless sensor network," in *2010 International Conference on Intelligent Computing and Integrated Systems*, Guilin, China, 2010.

[47] S. Lee, H. Choe, B. Park, Y. Song, and C.-K. Kim, "LUCA: an energy-efficient unequal clustering algorithm using location information for wireless sensor networks," *Wireless Personal Communications*, vol. 56, no. 4, pp. 715–731, 2011.

[48] T. Liu, Q. Li, and P. Liang, "An energy-balancing clustering approach for gradient-based routing in wireless sensor networks," *Computer Communications*, vol. 35, no. 17, pp. 2150–2161, 2012.

[49] N. Bao, G. Han, L. Liu, X. Jiang, and L. Shu, "An unequal clustering routing protocol for energy-heterogeneous wireless sensor networks," in *2015 IEEE/CIC International Conference on Communications in China-Workshops (CIC/ICCC)*, Shenzhen, China, 2015.

[50] X. Qin, X. Wang, F. Ouyang, T. Wang, X. Gan, and X. Tian, "A dynamic unequal energy efficient clustering in wireless sensor network," in *2016 8th International Conference on Wireless Communications & Signal Processing (WCSP)*, Yangzhou, China, 2016.

[51] U. Hari, B. Ramachandran, and C. Johnson, "An unequally clustered multihop routing protocol for wireless sensor networks," in *2013 International Conference on Advances in Computing, Communications, and Informatics (ICACCI)*, Mysore, India, 2013.

[52] M. Venkateswarlu Kumaramangalam, K. Adiyapatham, and C. Kandasamy, "Zone-based routing protocol for wireless sensor networks," *International scholarly research notices*, vol. 2014, Article ID 798934, 9 pages, 2014.

[53] B. Prince, P. Kumar, M. P. Singh, and J. P. Singh, "An energy efficient uneven grid clustering based routing protocol for wireless sensor networks," in *2016 International Conference on Wireless Communications, Signal Processing and Networking (WiSPNET)*, Chennai, India, 2016.

[54] S. Talbi and L. Zaouche, "Enhanced unequal clustering algorithm for wireless sensor networks," in *2015 IEEE/ACS 12th International Conference of Computer Systems and Applications (AICCSA)*, Marrakech, Morocco, 2015.

[55] B. Gong, L. Li, S. Wang, and X. Zhou, "Multihop routing protocol with unequal clustering for wireless sensor networks," in *2008 ISECS International Colloquium on Computing, Communication, Control, and Management*, Guangzhou, China, 2008.

[56] A. B. F. Guiloufi, N. Nasri, and A. Kachouri, "An energy-efficient unequal clustering algorithm using 'Sierpinski triangle' for WSNs," *Wireless Personal Communications*, vol. 88, no. 3, pp. 449–465, 2016.

[57] D. Wei, Y. Jin, S. Vural, K. Moessner, and R. Tafazolli, "An energy-efficient clustering solution for wireless sensor networks," *IEEE Transactions on Wireless Communications*, vol. 10, no. 11, pp. 3973–3983, 2011.

[58] J. Yu, Y. Qi, and G. Wang, "An energy-driven unequal clustering protocol for heterogeneous wireless sensor networks," *Journal of Control Theory and Applications*, vol. 9, no. 1, pp. 133–139, 2011.

[59] C.-J. Jiang, W.-R. Shi, M. Xiang, and X.-L. Tang, "Energy-balanced unequal clustering protocol for wireless sensor networks," *The Journal of China Universities of Posts and Telecommunications*, vol. 17, no. 4, pp. 94–99, 2010.

[60] S. Soro and W. B. Heinzelman, "Prolonging the lifetime of wireless sensor networks via unequal clustering," in *19th IEEE international parallel and distributed processing symposium*, Denver, CO, USA, 2005.

[61] G. V. Selvi and R. Manoharan, "Enhanced unequal clustering scheme for wireless sensor networks," *International Journal of Computer Applications*, vol. 75, no. 4, pp. 24–28, 2013.

[62] O. Younis and S. Fahmy, "HEED: a hybrid, energy-efficient, distributed clustering approach for ad hoc sensor networks," *IEEE Transactions on Mobile Computing*, vol. 3, no. 4, pp. 366–379, 2004.

[63] E. Ever, R. Luchmun, L. Mostarda, A. Navarra, and P. Shah, "UHEED-an unequal clustering algorithm for wireless sensor networks," in *Proceedings of the 1st International Conference on Sensor Networks*no. 1, pp. 185–193, Rome, Italy, 2012.

[64] N. Aierken, R. Gagliardi, L. Mostarda, and Z. Ullah, "RUHEED-rotated unequal clustering algorithm for wireless sensor networks," in *2015 IEEE 29th International Conference on Advanced Information Networking and Applications Workshops*, Gwangju, Korea (South), 2015.

[65] M. Naghibzadeh, H. Taheri, and P. Neamatollahi, "Fuzzy-based clustering solution for hot spot problem in wireless sensor networks," in *7th International Symposium on Telecommunications (IST'2014)*, Tehran, Iran, 2014.

[66] H. Li, Y. Liu, W. Chen, W. Jia, B. Li, and J. Xiong, "COCA: constructing optimal clustering architecture to maximize sensor network lifetime," *Computer Communications*, vol. 36, no. 3, pp. 256–268, 2013.

[67] P. Ren, J. Qian, L. Li, Z. Zhao, and X. Li, "Unequal clustering scheme based LEACH for wireless sensor networks," in *2010 Fourth International Conference on Genetic and Evolutionary Computing*, Shenzhen, China, 2010.

[68] W. K. Lai, C. S. Fan, and L. Y. Lin, "Arranging cluster sizes and transmission ranges for wireless sensor networks," *Information Sciences*, vol. 183, no. 1, pp. 117–131, 2012.

[69] S. Lee, "An energy-efficient distributed unequal clustering protocol for wireless sensor networks," *World Academy of Science, Engineering and Technology*, vol. 48, 2008.

[70] M. K. Joshi, L. Osborne, B. Sun, and S. K. Makki, "Hot spot aware energy efficient clustering approach for wireless sensor networks," in *2011 IEEE consumer communications and networking conference (CCNC)*, Las Vegas, NV, USA, 2011.

[71] G. V. Selvi and R. Manoharan, "Unequal clustering algorithm for WSN to prolong the network lifetime (UCAPN)," in *2013 4th International Conference on Intelligent Systems, Modelling and Simulation*, Bangkok, Thailand, 2013.

[72] J. Wang, "An energy-efficient multi-hop hierarchical routing protocol for wireless sensor networks," *International Journal*

of Future Generation Communication and Networking, vol. 5, pp. 89–98, 2012.

[73] T. Amgoth and P. K. Jana, "Energy-aware routing algorithm for wireless sensor networks," *Computers and Electrical Engineering*, vol. 41, pp. 357–367, 2015.

[74] N. Swathi, S. S. Kumar, K. S. Kumar, and P. R. Prasad, "Zone based hierarchical energy efficient clustering scheme for WSN," in *2016 IEEE International Conference on Recent Trends in Electronics, Information & Communication Technology (RTEICT)*, Bangalore, India, 2016.

[75] H. Salmabadi, M. A. Sarram, and F. Adibnia, "An improvement on LEACH protocol (EZ-LEACH)," in *2015 2nd International Conference on Knowledge-Based Engineering and Innovation (KBEI)*, Tehran, Iran, 2015.

[76] P. Rajeshwari, B. Shanthini, and M. Prince, "Hierarchical energy efficient clustering algorithm for WSN," *Middle-East Journal of Scientific Research*, vol. 23, pp. 108–117, 2015.

[77] J. Yu, Y. Qi, G. Wang, and X. Gu, "A cluster-Based routing protocol for wireless sensor networks with nonuniform node distribution," *International Journal of Electronics and Communications*, vol. 66, no. 1, pp. 54–61, 2012.

[78] F. Khan, F. Bashir, and K. Nakagawa, "Dual head clustering scheme in wireless sensor networks," in *2012 International Conference on Emerging Technologies*, Islamabad, Pakistan, 2012.

[79] K. Sundaran and V. Ganapathy, "Energy efficient wireless sensor networks using dual cluster head with sleep/active mechanism," *Journal of Science and Technology*, vol. 9, no. 41, 2016.

[80] M. Alam and J. Rodriguez, "A dual head clustering mechanism for energy efficient WSNs," in *Lecture Notes of the Institute for Computer Sciences, Social Informatics and Telecommunications Engineering*, pp. 380–387, Springer Berlin Heidelberg, Berlin, Heidelberg, 2010.

Research Article

Eco-Environmental Civilization Construction System in Remote Areas Based on Multiple Data Collection and the Internet of Things

Xinyi Du [ORCID] **and Haijun Ma**

School of Marxism, China University of Geosciences, Beijing 100083, China

Correspondence should be addressed to Xinyi Du; 2018190005@cugb.edu.cn

For a long time, the development strategy of remote areas is basically resource-oriented. Large-scale exploitation of resources not only damages the corresponding balance of resource reserves but also causes serious damage to the ecological environment. To this end, this paper has carried out research on the construction of ecological environment civilization in remote areas based on multidata collection and edge computing. Based on the understanding of the connotation, composition, and characteristics of ecological civilization, this paper selects representative indicators to reflect the specific requirements of ecological civilization, constructs an evaluation index system for the construction of ecological civilization in remote areas, and uses the evaluation indicators analysis and sorting. Second, edge computing and sensor technologies are applied to the process of data collection and information transmission and providing solutions for data collection and transmission in remote areas. This paper also presents the security method to protect the information transmission. Through testing, the program has shown good adaptability and can provide ideas for the construction of ecological environment in remote areas.

1. Introduction

New technologies are implemented in every field of life and make the services more convenient and feasible for people life. Wireless sensor networks (WSN), Internet of Things (IoT), smart cities, and cloud/edge based networks are few examples of technologies. These technologies are also adopted for eco-environmental civilization construction systems for data monitoring and analysis [1]. In the industrial society, the productivity of human society has been greatly improved and huge wealth has been created, and a major social transformation has been fundamentally completed. The economic, political, cultural, spiritual, social structure, and the way of life have all been greatly changed. Human beings have the ability to plunder the natural resources [2, 3]. In the middle of the last century, as the conflict between humans and the environment intensified, a series of environmental problems brought serious consequences, and humans began to reflect on the impact of industrial civiliza-

tion [4]. Righteousness has entered a new stage. Mankind recognizes that in the choice of development path, it is necessary to take the path of sustainable development that is in harmony with the ecological environment, and a new way of civilization should be established [5, 6]. Therefore, ecological civilization came into being. Ecological civilization is a choice made by mankind on the basis of reflection on industrial civilization. The index system of ecological civilization plays a very important role in measuring and evaluating the development status and situation of various regions, especially remote areas, helping decision-makers to monitor and evaluate past and present development, and formulating future development goals [7].

At the same time, the establishment of ecological civilization development ideas has also raised a new major issue for the academic community, how to define the theoretical, and how to better implement the practice of ecological civilization. Some other challenges are data analysis, data monitoring, security, and resource allocations. Roy Morrison of

the United States clearly put forward the concept of "ecological civilization" in 1995. He regarded "ecological civilization" as a form of civilization after "industrial civilization". [8]. Since the 1960s and 1970s, Western countries have taken the lead in environmental protection and ecological construction. International organizations such as the United Nations (UN) have subsequently put forward the concept of sustainable development. More and more countries have joined the ranks of ecological civilization construction, although they may not use the term "ecological civilization" [9]. There are many studies on ecological civilization, mainly focusing on the sustainable development indicator system. After entering the 21st century, Albert Weir proposed a new theory "Ecological Modernization Theory," which changed people's views on environmental policy [10]. The ecological footprint method is the concept and model proposed in [11] to calculate the carrying capacity of the ecosystem to humans. Authors in [12] believed that the construction of ecological civilization is the inevitable path of national development and suggestions from the aspects of improving ecological awareness and developing circular economy. Authors in [13] pointed out that it is necessary to establish an ecological civilization development mechanism from the perspective of the country, society, enterprises, and the whole people. In the quantitative analysis, the fuzzy neural network model is mainly used to screen the indicators, and the set pair analysis and the direct value method are used to carry out the static evaluation construction [14].

The main purpose of this paper is to introducing the background and significance of constructing. Construct an evaluation index system for the construction of ecological civilization in remote areas on the basis of understanding the connotation, composition, and characteristics of ecological civilization. This evaluation index is used to analyze and rank the level of ecological civilization construction among regions. In addition, this paper discusses the main factors that affect the changes in the remote areas from the growth of various indicators and comprehensive levels of construction. Using spatial statistical analysis in this study to level the ecological civilization construction, and introducing a data development model to dynamically simulate the operation trajectory of ecological civilization construction, good results have been achieved. This paper also discusses the technologies aspect and its security issues for data monitoring and analysis. The main contributions of this paper are as follows:

(i) Proposed a model for construction of ecological environment civilization in remote areas based on multidata collection and edge computing

(ii) Proposed a model based on edge computing and sensor technologies for data processing and collection

(iii) Proposed a security model to protect the process and analyzed data at the edge computing side

The rest of the paper is organized as follows: Section 2 presents the related technologies. Section 3 discusses the ecological environment monitoring based on fuzzy neural network. Section 4 presents the model evaluation based on data development. The paper concludes with future direction in the last section.

2. Related Technologies

2.1. Edge Computing and Sensor Technology. Edge computing and sensor technologies are applied to the process of data collection and information transmission, providing solutions for data collection and transmission in remote areas [15]. Traditional cloud computing requires front-end equipment to return the collected data from the network to the cloud. As computing nodes increase, it will inevitably lead to increased network load and insufficient bandwidth resources, which will lead to system response delays. This is in the era of high real-time requirements for the Internet of Everything. It is a fatal flaw [16, 17]. Edge computing is to offload part of the computing tasks in the cloud center to the edge of the network, effectively reducing the loss of network bandwidth and improving the real-time response of the system. Edge computing and sensor technology are applied in the process of data collection and information transmission, providing solutions for data collection and transmission in remote areas [18, 19]. Use edge computing to build an efficient network computing paradigm, comprehensively analyze and process data collected by smart devices in different fields, realize information query, prediction, abnormal signal detection, and other functions, and provide city managers with comprehensive and practical information that is conducive to decision-making. Realize the optimization and promotion of urban management and also provide low-latency and high-quality services for the majority of users [20, 21]. Figure 1 describes the risk monitoring process from the cloud to the edge and then to the user end.

Node monitoring system and edge computing network system architecture, this paper constructs a three-tier container risk monitoring model from the cloud to the edge to the user side, as shown in Figure 1. This article makes full use of network resources and meets all user needs, achieving the goal of the least total deployment cost [22, 23]. Different from the service function chain deployment problem under the traditional single platform, the underlying network elements of the heterogeneous NFV environment are diversified. Each NFV platform can be installed on a common server to realize multiple types of virtual network functions. However, the processing power, resource consumption, deployment cost, and distribution of the data are not the same [24].

2.2. Construction of Ecological Environment Civilization. The establishment of indicators for ecological civilization construction is not only a concrete manifestation of the civilization but also an assessment of the current success of ecological civilization construction [25]. By referring to a large number of documents, this article will start from three aspects: ecological economy, ecological environment, and
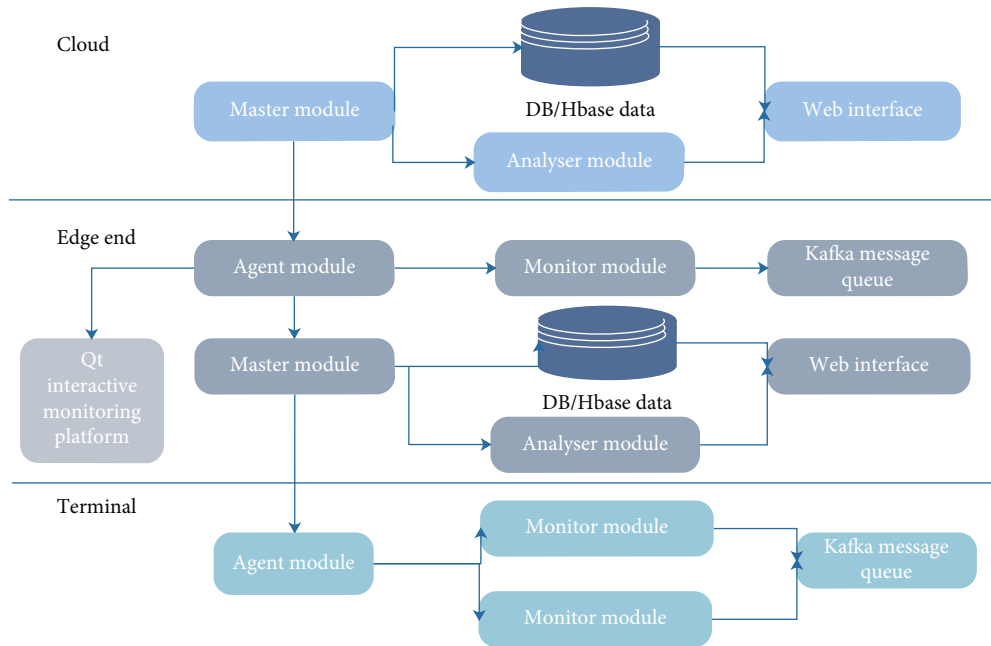
FIGURE 1: Risk monitoring from the cloud to the edge to the client.

ecological people's livelihood. The research methods used in this article include comprehensive literature analysis, investigation, empirical research, and quantitative analysis. In the quantitative analysis, the fuzzy neural network model is mainly used to screen the indicators, the set pair analysis and the direct value method are used to carry out the static evaluation, the spatial statistical analysis is used to study the spatial distribution pattern of the level of ecological civilization construction, and the data package is introduced. The network model dynamically simulates the operation trajectory and has achieved good results [26, 27]. The sustainable development evaluation index system is the basic content of sustainable development research and the core issue of sustainable development guiding regional development practice. Many scholars have been committed to establishing a more scientific and accurate evaluation index system, but there is still no set of truly widely accepted and recognized index system [28]. At present, two types, four main research directions, and three types of construction models have emerged in the international sustainable development evaluation index system. Figure 2 describes the technical roadmap for the construction of ecological environment civilization.

Through the combing of foreign sustainable development evaluation research, we can learn from the successful experience of some researches. First of all, we must adhere to the process of national economic development and fully implement it in the whole process of government decision-making, social progress, and economic development. It can be reflected in people's daily life and in national policies and regulations [28]. Second, sustainable development evaluation focuses on coordinated development, whether it is urban and rural overall or regional coordination, it can be reflected in the indicator system.

3. Ecological Environment Monitoring Based on Fuzzy Neural Network

As a systematic project, regional ecological civilization involves the construction of many aspects such as society, economy, and culture. The effectiveness of regional ecological civilization is difficult to directly measure with a single indicator, and the simple aggregation of multiple indicator sets cannot be reflected [29]. Therefore, the establishment of a scientific and effective evaluation model, and the integration of the selected evaluation index system into a whole, has become an important content of the evaluation of the construction of regional ecological civilization [30, 31]. The basic neural network structure is shown in Figure 3.

The second stage adjusts the connection weights between nodes according to the propagation direction opposite to stage one, that is, according to the error between the actual output and the expected output of the output layer, and finally makes the error to the minimum value. In order to make the function continuous and differentiable, the root mean square difference is minimized here, and the loss function is defined as follows:

$$L(e) = \frac{1}{2}\text{SSE} = \frac{1}{2}\sum_{j=0}^{k} e_j^2 = \frac{1}{2}\sum_{j=0}^{k} \left(\overline{y_j} - y_j\right)^2. \tag{1}$$

This paper uses stochastic gradient descent to minimize L, that is, for each training sample, the weight changes in the direction of its negative gradient. We use the following formula to solve the gradient of L to the connection weight W. The critical value can be determined according to the average value of the corresponding index in the area, that
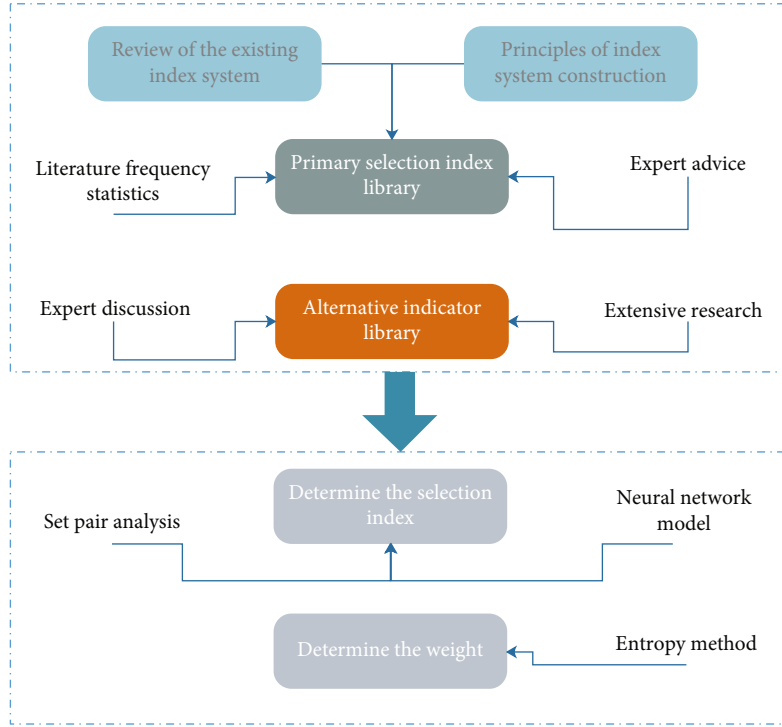
FIGURE 2: Technical roadmap for the ecological environment civilization.

Input layer   *Hidden layer*   *Output layer*
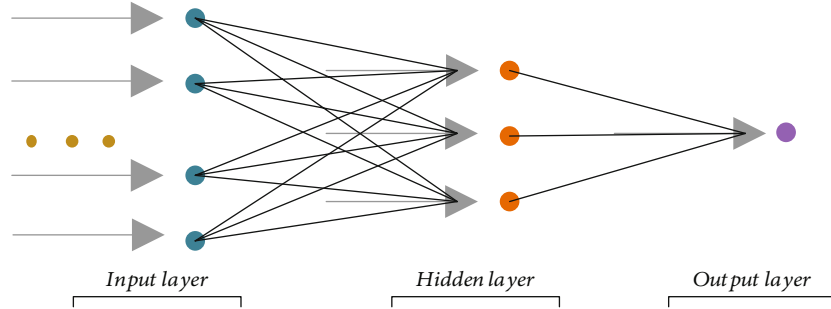
FIGURE 3: Schematic diagram of the basic neural network structure.

is, the average level of the index in the study area.

$$\frac{\vartheta L}{\vartheta \omega_{ij}^1} = \frac{\vartheta L}{\vartheta s_j^1} \bullet \frac{\vartheta s_j^1}{\vartheta \omega_{ij}^1}. \tag{2}$$

Among them, s_{2j} represents the input of the jth node of the output layer, where 1 represents the connection weight of the first layer.

$$s_j^2 = \sum_{i=1}^m x_i \bullet \omega_{ij}^1, \tag{3}$$

$$\frac{\vartheta s_j^1}{\vartheta \omega_{ij}^1} = x_i. \tag{4}$$

Substituting the previous formula can get

$$\frac{\vartheta L}{\vartheta \omega_{ij}^1} = x_i \frac{\vartheta L}{\vartheta s_j^1}. \tag{5}$$

Then, just ask for $\vartheta L / \vartheta s_j^1$. Since s_j^1 has an effect on all output layers, so

$$\frac{\vartheta L}{\vartheta s_j^1} = \sum_{i=1}^k \frac{\vartheta L}{\vartheta s_j^2} \bullet \frac{\vartheta s_j^1}{\vartheta s_j^2}, \tag{6}$$

$$s_i^2 = \sum_{j=0}^n \theta\left(s_j^1\right) \bullet \omega_{ij}^1, \tag{7}$$

$$\frac{\vartheta s_i^1}{\vartheta s_j^1} = \frac{\vartheta s_i^2}{\vartheta \theta\left(s_j^1\right)} \bullet \frac{\vartheta \theta\left(s_j^1\right)}{\vartheta s_j^1} = \omega_{ij}^1 \theta'\left(s_j^1\right). \tag{8}$$

Substituting the previous formula can get

$$\frac{\vartheta L}{\vartheta s_j^1} = \sum_{i=1}^{k} \frac{\vartheta L}{\vartheta s_i^2} \bullet \omega_{ij}^2 \theta'\left(s_j^1\right) = \theta'\left(s_j^1\right) \cdot \sum_{i=1}^{k} \frac{\vartheta L}{\vartheta s_i^2} \bullet \omega_{ij}^2, \quad (9)$$

$$\delta_j^1 = \frac{\vartheta L}{\vartheta s_i^1}. \quad (10)$$

The hidden layer is

$$\delta_j^1 = \theta'\left(s_j^1\right) \sum_{i=1}^{k} \delta_j^1 \bullet \omega_{ij}^2. \quad (11)$$

The output layer δ is

$$\delta_j^1 = \frac{\vartheta L}{\vartheta s_i^1} = e_i \bullet \theta'\left(s_i^1\right). \quad (12)$$

The back propagation process is that each node in the output layer will get an error e, and use e as the reverse input of the output layer. At this time, then the output layer δ is transmitted to the hidden layer according to the connection weight.

$$s_j^1 = \theta'\left(s_j^1\right) \cdot \sum_{i=1}^{k} \delta_i^1 \omega_{ij}^2. \quad (13)$$

Now let us look at the gradient of the first layer of weight:

$$\frac{\vartheta L}{\vartheta \omega_{ij}^2} = x_i \bullet \delta_j^1. \quad (14)$$

The second layer of weight gradient:

$$\frac{\vartheta L}{\vartheta \omega_{ij}^2} = \frac{\vartheta L}{\vartheta s_j^2} \bullet \frac{\vartheta s_j^2}{\vartheta \omega_{ij}^2} = \delta_j^1 \cdot \theta\left(s_i^1\right). \quad (15)$$

You can see a rule: the gradient of each weight is equal to the output of the node of the previous layer connected to it multiplied by the output of the backpropagation of the next layer connected to it. Some of the rule knowledge bases formulated on this basis are shown in Table 1.

From the given rules through multiple learning, all possible combinations of rules are obtained, and take the learning rate $\alpha = 0.7$, $\beta = 0.8$, and iteratively follow the learning rules to get the following randomly selected the predicted value of the optimal unit price of the task package.

4. Security Model

In section presents the security model by using the neural network due to its more powerful features and high accuracy and classification mechanism [32]. This method also uses its internal state which is also called memory to process variables length for the sequence of inputs. The output value of the input sequence depends on past computed value [33]. In the proposed security model, the first step is dataset collection and creation. The used dataset contains twelve classes and called CICDDOS 2019. This dataset already has a number of distributed denial of services (DDoS) attacks and categorized as either exploitation-based or reflection-based attacks at edge computing level. Figure 4 shows the proposed security model.

Dataset exists sin raw form and has many redundant values and zeros. The feature extraction is started and then selection process began by using different learning algorithms. For the filter method, the univariant is selected to identify the significant features from dataset. The SVM, LSTM, and Naive Bayes methods are used in to select the k best features from dataset. Feature selection is applied on twenty-two data mining and ML applications to remove the overfitting, reducing training time and improve accuracy [34]. The different feature method is used to check the accuracy and remove the columns which are greater than the given threshold, which has only one unique value and remove collinear features which are greater than the given value and remove the features which have 0.0 importance from a gradient boosting machine. The proposed security model performs better in terms of accuracy by using five classification methods and different feature ranges. The accuracy achieved between total instances analyzed and total correctly identified instances in a dataset. Accuracy is compared against every algorithm in each data set.

5. Model Evaluation Based on Data Development

This module takes remote areas as an application case. Based on the collection of a large amount of statistical data, the use of data envelopment and fuzzy neural network is used to filter and obtain the evaluation index system of regional ecological civilization construction, and the entropy method is used to assign weights to the index system. The sustainable development evaluation index system is the basic content of sustainable development research and the core issue of sustainable development guiding regional development practice as shown in Equations (16) and (17).

$$\max h_{j0} = \frac{\sum_{r=1}^{n} u_r y_{rj0}}{\sum_{i=1}^{m} v_r x_{rj0}}, \quad (16)$$

$$t = \frac{1}{\sum_{i=1}^{m} v_i x_{ij}}, w_i = tv_i, \mu_r = tu_r. \quad (17)$$

By referring to a large number of documents, this article will start from three aspects: ecological economy, ecological environment, and ecological people's livelihood. Different from the service function chain deployment problem under the traditional single platform, the underlying network elements of the heterogeneous NFV environment are diversified. Sustainable development evaluation focuses on coordinated development, whether it is urban and rural overall or regional coordination, it can be reflected in the

TABLE 1: Part of the rule knowledge base.

Serial number	$x_1\lambda_1 = 1$	$x_2\lambda_2 = 1$	$x_3\lambda_3 = 1$	$x_4\lambda_4 = 0.95$	$x_5\lambda_5 = 0.45$	$x_6\lambda_6 = 0.84$	$x_7\lambda_7 = 0.91$	Then
1	1							1
2		1						1
3			1					-1
4				1				-1
5					1			-1
6						1		1
7							1	-1

FIGURE 4: Proposed security model.
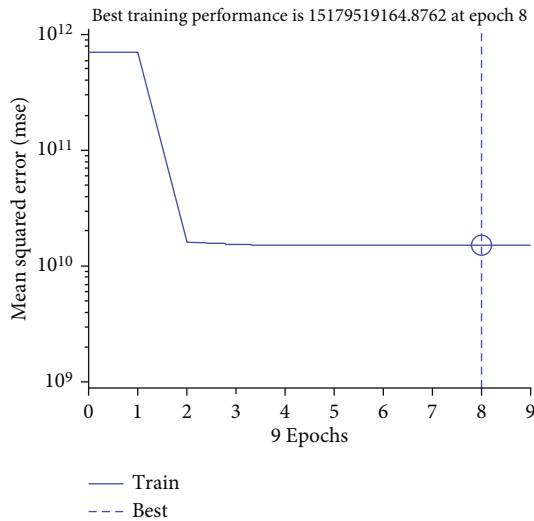
FIGURE 5: Training accuracy of original data.
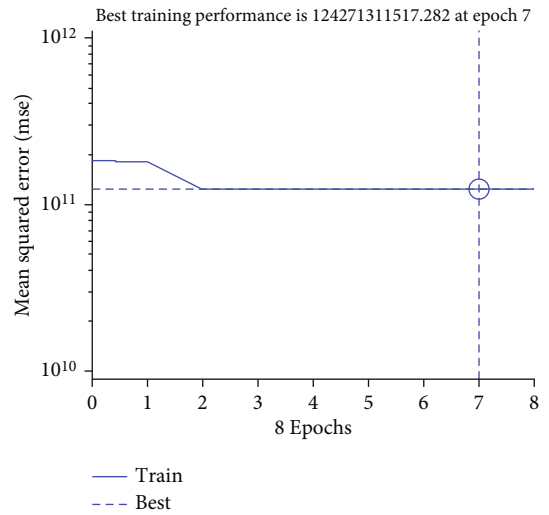
FIGURE 6: Training accuracy of new variable data.

indicator system. Figures 5 and 6, respectively, show the training accuracy of the original data and the training accuracy of the newly added variable data.

The indicators designed in this paper not only meet the needs of the government's macromanagement but also be widely recognized by the society, and should not be too much; it should not only be combined with the actual economic and social development of the western region in recent years but also consider its future development. It is necessary not only to objectively and dynamically reflect the remote areas but also from the perspective of adapting and perfecting the weights of indicators with changes in

TABLE 2: Analysis of relevant variables in environment civilization.

| | B | S.E. | Wals | DF | Sig. | Exp (B) | 95% of EXP(B) C.I. | |
							Lower limit	Upper limit
V1	-0.609	0.076	63.549	1	0.000	0.544	0.468	0.632
V2	0.036	0.007	24.422	1	0.000	1.036	1.022	1.051
V3	-0.326	0.084	14.962	1	0.000	0.722	0.612	0.851
V4	-0.202	0.060	11.098	1	0.001	0.817	0.726	0.920
V5	0.174	0.080	4.747	1	0.029	1.190	1.018	1.392
V6	-0.310	0.122	6.433	1	0.011	0.733	0.577	0.932
V7	-0.468	0.191	5.998	1	0.014	0.627	0.431	0.911
V8	-0.309	0.122	6.382	1	0.012	0.734	0.578	0.933
Constant	2.693	0.654	16.963	1	0.000	14.775		

economic and social development, making them representative, maneuverable, and innovative, guiding, practical, scientific, and forward-looking indicator system for the construction of ecological civilization. Many scholars have been committed to establishing a more scientific and accurate evaluation index system, but there is still no set of truly widely accepted and recognized index system. This paper uses SPSS software to process a large amount of data to get the following analysis (Table 2). Table 2 describes the results of the analysis of variables related environmental civilization.

This module takes remote areas as an application case. Based on the collection of a large amount of statistical data, the use of data envelopment and fuzzy neural network is used to filter and obtain the evaluation index system of regional ecological civilization construction, and the entropy method is used to assign weights to the index system. Using the evaluation index system of regional ecological civilization construction in this remote area, an evaluation model of regional ecological civilization construction based on set pair analysis was established, and the evaluation results of each subsystem and the overall were obtained. It can be seen from Table 2 that each indicator has an upper limit, a lower limit, and a value; compared with the traditional simple weighting method, there is no need for the size of the expert's subjective judgment weight coefficient, and to reduce subjective arbitrariness. Righteousness has entered a new stage. Mankind recognizes that in the choice of development path, it is necessary to take the path of sustainable development that is in harmony with the ecological environment, and a new way of civilization should be established.

The lower limit of the index can be determined according to the minimum value of the corresponding index in the study area, the upper limit of the index can be determined according to the highest target, and the critical value can be determined according to the average value of the corresponding index in the area, that is, the average level of the index in the study area. Each value can also be determined according to the planning goal and make appropriate adjustments to local conditions. The last attempt of this chapter introduces a simplified data envelopment model to simulate the development. Actual calculations show that the data envelopment model can be applied to complex systems such as regional ecological civilization construction. The analysis results obtained are not only helpful for grasping the development direction of regional ecological civilization construction but also for analyzing the evolution of the complex system of economic-society-ecological environment provides new ideas.

6. Conclusion

At present, the theoretical research on the civilization construction is almost all from the perspective of traditional ecology and economics, and the conclusions drawn have two biases, one is biased towards ecological protection, and the other is biased towards development. Traditional cloud computing requires front-end equipment to return collected data from the network to the cloud. As computing nodes increase, it will inevitably lead to increased network load and insufficient bandwidth resources, which will lead to system response delays. A large number of studies are homogenized seriously, and simply apply indicators and methods, and the evaluation results obtained cannot guide the work and practice of ecological civilization construction. Based on the understanding of the connotation, composition, and characteristics of ecological civilization, this paper selects representative indicators to reflect the specific requirements of ecological civilization, constructs an evaluation index system for the construction of ecological civilization in remote areas, and analysis and sorting. The model constructed by the indicator system is still subjective. How to further improve the scientificity of indicator construction and strengthen the reliability of the constructed model is still the focus of research work for a long time. How to strike a balance between the availability, applicability, and scientificity of the indicators, how to make the indicators meet the needs of future development, and have better foresight and guidance, are all difficult points for research. Although this paper tries to introduce fuzzy neural network and data envelopment model, it is only a simple model that simplifies the conversion rules. It can not only further improve the application of this model but also can be combined with other models to achieve more powerful analysis and evaluation capabilities. The paper also presented the security

model by using some methods at the edge network side to protect the data from unauthorized access and users.

Data Availability

The data of this article is already included in the article.

Conflicts of Interest

The authors declare that they have no conflicts of interest.

References

[1] K. N. Qureshi and A. H. Abdullah, "Industrial wireless sensor network architecture standards, applications," in *AsiaSense, the sixth international conference 2013*, Melaka, Malaysia, 2013.

[2] X. Zhang, Y. Wang, Y. Qi et al., "Evaluating the trends of China's ecological civilization construction using a novel indicator system," *Journal of Cleaner Production*, vol. 133, pp. 910–923, 2016.

[3] J.-Y. Heurtebise, "Sustainability and ecological civilization in the age of Anthropocene: an epistemological analysis of the psychosocial and "culturalist" interpretations of global environmental risks," *Sustainability*, vol. 9, no. 8, 2017.

[4] J. Chai, L. Zhang, M. Yang, Q. Nie, and L. Nie, "Investigation on the coupling coordination relationship between electric power green development and ecological civilization construction in China: a case study of Beijing," *Sustainability*, vol. 12, no. 21, 2020.

[5] X. Sun, L. Gao, H. Ren et al., *China's Progress towards Sustainable Land Development and Ecological Civilization*, Springer, 2018.

[6] X. Lu, S. Zhang, J. Xing et al., "Progress of air pollution control in China and its challenges and opportunities in the ecological civilization era," *Engineering*, vol. 6, no. 12, pp. 1423–1431, 2020.

[7] A. E. Frazier, B. A. Bryan, A. Buyantuev et al., *Ecological Civilization: Perspectives from Landscape Ecology and Landscape Sustainability Science*, Springer, 2019.

[8] X. Wang, S. Ren, and B. Yuan, "Index system and process design of classification assessment of ecological civilization construction in China," *Journal of Central South University (Social Science)*, vol. 1, 2016.

[9] J. Wu, X. Li, Y. Luo, and D. Zhang, *Spatiotemporal Effects of Urban Sprawl on Habitat Quality in the Pearl River Delta from 1990 to 2018, Scientific Reports*, 2021.

[10] M. Hu, S. Sarwar, and Z. Li, "Spatio-temporal differentiation mode and threshold effect of Yangtze River Delta urban ecological well-being performance based on network DEA," *Sustainability*, vol. 13, no. 8, 2021.

[11] W. Zhang, X. Zhang, L. Li, and Z. Zhang, "Urban forest in Jinan City: distribution, classification and ecological significance," *Catena*, vol. 69, no. 1, pp. 44–50, 2007.

[12] K. L. Brown, "The basin of Mexico: ecological processes in the evolution of a civilization. William T. Sanders, Jeffrey R. Parsons and Robert S. Santley. Academic Press, New York, 1979. Xiii+418 pp., 5 appendices, maps," *American Antiquity*, vol. 45, no. 4, pp. 884–886, 1980.

[13] F. Wei, S. Cui, N. Liu et al., "Ecological civilization: China's effort to build a shared future for all life on earth," *National Science Review*, vol. 8, no. 7, 2021.

[14] P. Zhou and T. Qu, "Management of the marine economy: an ecological civilization perspective," *Journal of Coastal Research*, vol. 106, pp. 69–72, 2020.

[15] R. W. Anwar, M. Bakhtiari, A. Zainal, and K. N. Qureshi, "Wireless sensor network performance analysis and effect of blackhole and sinkhole attacks," *Jurnal Teknologi*, vol. 78, no. 4-3, 2016.

[16] X. Chen and J. Zheng, "Countermeasures for marine environmental pollution governance: an ecological civilization perspective," *Journal of Coastal Research*, vol. 106, no. sp1, pp. 355–358, 2020.

[17] M. Xie, H. Duan, P. Kang, Q. Qiao, and L. Bai, "Toward an ecological civilization: China's progress as documented by the second national general survey of pollution sources," *Engineering*, vol. 7, no. 9, pp. 1336–1341, 2021.

[18] W. Shi and S. Dustdar, "The promise of edge computing," *Computer*, vol. 49, no. 5, pp. 78–81, 2016.

[19] F. Wang, J. Xu, X. Wang, and S. Cui, "Joint offloading and computing optimization in wireless powered mobile-edge computing systems," *IEEE Transactions on Wireless Communications*, vol. 17, no. 3, pp. 1784–1797, 2017.

[20] Z. Xiong, Y. Zhang, D. Niyato, P. Wang, and Z. Han, "When mobile blockchain meets edge computing," 2017, https://arxiv.org/abs/1711.05938.

[21] Y. Liu, C. Xu, Y. Zhan, Z. Liu, J. Guan, and H. Zhang, "Incentive mechanism for computation offloading using edge computing: a Stackelberg game approach," *Computer Networks*, vol. 129, pp. 399–409, 2017.

[22] Z. Li, W. M. Wang, G. Liu, L. Liu, J. He, and G. Q. Huang, "Toward open manufacturing," *Industrial Management & Data Systems*, vol. 118, no. 1, pp. 303–320, 2018.

[23] Y. Tao, W. Yin, W. Zhang, Y. Zhao, C. Ktistis, and A. J. Peyton, "A very-low-frequency electromagnetic inductive sensor system for workpiece recognition using the magnetic polarizability tensor," *IEEE Sensors Journal*, vol. 17, no. 9, pp. 2703–2712, 2017.

[24] T.-C. Chang, C.-H. Lin, K. C.-J. Lin, and W.-T. Chen, "Traffic-aware sensor grouping for IEEE 802.11 ah networks: regression based analysis and design," *IEEE Transactions on Mobile Computing*, vol. 18, no. 3, pp. 674–687, 2018.

[25] G. Maier, F. Pfaff, M. Wagner et al., "Real-time multitarget tracking for sensor-based sorting," *Journal of Real-Time Image Processing*, vol. 16, no. 6, pp. 2261–2272, 2019.

[26] N. Maouche, B. Nessark, and I. Bakas, "Platinum electrode modified with polyterthiophene doped with metallic nanoparticles, as sensitive sensor for the electroanalysis of ascorbic acid (AA)," *Arabian Journal of Chemistry*, vol. 12, no. 8, pp. 2556–2562, 2019.

[27] Y. Yang, Y. Xia, G. Wang, L. Tao, J. Yu, and L. Ai, "Effects of boiling, ultra-high temperature and high hydrostatic pressure on free amino acids, flavor characteristics and sensory profiles in Chinese rice wine," *Food Chemistry*, vol. 275, pp. 407–416, 2019.

[28] M. Zhang, Y. Liu, J. Wu, and T. Wang, "Index system of urban resource and environment carrying capacity based on ecological civilization," *Environmental Impact Assessment Review*, vol. 68, pp. 90–97, 2018.

[29] M. Halskov Hansen and Z. Liu, "Air pollution and grassroots echoes of "ecological civilization" in rural China," *The China Quarterly*, vol. 234, pp. 320–339, 2018.

[30] F. Shi, D. Weaver, Y. Zhao, M.-F. Huang, C. Tang, and Y. Liu, "Toward an ecological civilization: mass comprehensive ecotourism indications among domestic visitors to a Chinese wetland protected area," *Tourism Management*, vol. 70, pp. 59–68, 2019.

[31] M. Faure, "The export of ecological civilization: reflections from law and economics and law and development," *Sustainability*, vol. 12, no. 24, article 10409, 2020.

[32] S. Li, W. Li, C. Cook, C. Zhu, and Y. Gao, "Independently recurrent neural network (indrnn): building a longer and deeper rnn," in *Proceedings of the IEEE conference on computer vision and pattern recognition*, pp. 5457–5466, Salt Lake City, UT, USA, 2018.

[33] M. S. Elsayed, N.-A. Le-Khac, S. Dev, and A. D. Jurcut, "Ddos-net: a deep-learning model for detecting network attacks," in *2020 IEEE 21st International Symposium on" A World of Wireless, Mobile and Multimedia Networks"(WoWMoM)*, pp. 391–396, Cork, Ireland, 2020.

[34] I. Sharafaldin, A. H. Lashkari, S. Hakak, and A. A. Ghorbani, "Developing realistic distributed denial of service (DDoS) attack dataset and taxonomy," in *2019 International Carnahan Conference on Security Technology (ICCST)*, pp. 1–8, Chennai, India, 2019.

Research Article

LT Codes with Double Encoding Matrix Reorder Physical Layer Secure Transmission

Hang Zhang ⓘ, Fanglin Niu ⓘ, Ling Yu ⓘ, and Si Zhang ⓘ

School of Electronics and Information Engineering, Liaoning University of Technology, Jinzhou, Liaoning 121001, China

Correspondence should be addressed to Fanglin Niu; dx_niufl@lnut.edu.cn

In traditional wireless sensor networks, information transmission usually uses data encryption methods to prevent information from being stolen illegally. However, once the encryption methods are leaked, eavesdropping nodes can easily obtain information. LT codes are rateless codes; if it is attacked by random channel noise, the decoding process will change and the decoding overhead will also randomly change. When it is used for physical layer communication of wireless sensor networks, it ensures that the destination node recovers all the information without adding the key, while the eavesdropping node can only obtain part of the information to achieve wireless information security transmission. To reduce the intercept efficiency of eavesdropping nodes, a physical layer security (PLS) method of LT codes with double encoding matrix reorder (DEMR-LT codes) is proposed. This method performs two consecutive LT code concatenated encoding on the source symbol, and part of the encoding matrix is reordered according to the degree value of each column from large to small, which reduces the probability of eavesdropping nodes recovering the source information. Experimental results show that compared with other LT code PLS schemes, DEMR-LT codes only increase the decoding overhead by a small amount. However, it can effectively reduce the intercept efficiency of eavesdropping nodes and improve information transmission security.

1. Introduction

In wireless sensor networks, limited by the cost of current sensor equipment and computing power, traditional encryption technology cannot effectively secure information transmission in wireless sensor networks. As a result of this problem, PLS technology based on information theory [1–3] has attracted increasing attention from researchers because PLS technology can realize secure transmission without keys. In contrast to the traditional encryption methods used in the network layer and in the above layers, PLS utilizes the wireless channel's characteristics combined with wireless communication technology to reduce the eavesdroppers' signal receiving quality to realize the secure transmission of information.

The concept of PLS can be traced back to 1949. Shannon proposed the principle of secure communication and the concept of perfect secrecy in [4]. Later, Wyner proposed the wiretap channel model [5] and defined the secrecy capacity of degraded wiretap channels based on information

theory in 1975. These two works set the information theory foundation for the development of PLS technology. According to the definition of secrecy capacity, secure communication can be realized in the transmission process of the wiretap channel when the channel capacity of the main channel is higher than that of the wiretap channel. Therefore, most of the existing PLS technologies is aimed at improving the security capacity. The commonly used methods include artificial noise [6], cooperative relay [7], and beamforming [8]. Among them, artificial noise is an important application direction of PLS. Putting artificial noise in the null space of the main channel can reduce the eavesdroppers' signal reception quality without affecting the signal reception of legitimate receivers. For example, an artificial noise design method based on secrecy capacity optimization was proposed in [9]. On the basis of the traditional artificial noise method, local artificial noise was added to transform the antinoise ability of the wireless communication system into secrecy capacity. [10] proposed a PLS scheme based on joint feedback and artificial noise without

any eavesdropper's channel state information, and the secrecy capacity was maximized by optimizing the power distribution ratio between the secret information and artificial noise.

In recent years, PLS technology has become an important solution to the problem with the security of wireless sensor networks. For example, [11] proposed a cooperative jamming scheme for wireless sensor networks, where cooperative jamming nodes disturb the eavesdropper by sending noise, and legitimate receivers can effectively eliminate the noise by using the orthogonality of orthogonal vectors, thus improving the confidentiality of information transmission. [12] proposed a physical layer network coding scheme for confidential data transmission in wireless sensor networks, where the source node sends data to the destination node through the relay node. By applying physical layer network coding, the signal received by the relay node is guaranteed to be inseparable to prevent attacks by external eavesdroppers. Compared with traditional encryption technology, although PLS technology can achieve stronger security performance, it has transmission rate defects. [13] proposed that under the limitation of physical layer security capacity, the information transmission rate would be considerably reduced, which would cause the delay of the legitimate receiver's information reception. To solve this problem, [14] first introduced fountain codes [15] into PLS technology and proposed a transmit power control strategy to improve the signal-to-noise ratio of legitimate receivers. When the quality of the main channel is worse than that of the wiretap channel, the legitimate receiver can have a faster rate of information reception. According to the working principle of fountain codes, supposing that the source symbols have been grouped, each group of sources contains k symbols. After fountain code encoding, an infinite number of encoded symbols can be generated. As long as the receivers receive n encoded symbols, k source symbols can be recovered, and n is only slightly higher than k. In the wiretap channel, the security of information transmission in the main channel can be guaranteed as long as the legitimate receiver receives n encoded symbols before the eavesdropper and completes the decoding by taking advantage of this characteristic of fountain codes.

To reduce the intercept efficiency of eavesdropping nodes in wireless sensor networks, a PLS scheme is proposed based on encoding matrix reordering according to the degree value of each column from large to small and through secondary LT concatenated encoding. The main contributions of this work can be summarized as follows:

(1) This paper proposes a PLS transmission method of wireless sensor networks using LT codes as antieavesdropping codes and establishes a DEMR-LT code PLS encoding model. In addition, an encoding matrix reorder method in DEMR-LT codes is proposed to reduce the probability that the eavesdropping node completes the decoding before the destination node in each decoding

(2) In this paper, the decoding start time and the number of decoding symbols of DEMR-LT codes are deduced and verified by simulation experiments. It is proven that DEMR-LT codes can reduce the intercept efficiency of eavesdropping nodes while increasing the decoding overhead by a small amount

The rest of this paper is organized as follows. Section 2 introduces the related work of the latest research on wireless sensor networks. Section 3 briefly introduces the system model and LT codes. Section 4 presents the encoding and decoding method design of DEMR-LT codes. Section 5 provides the performance analysis of DEMR-LT codes. The final conclusions are provided in Section 6.

All mathematical symbols used in this paper are shown in Table 1.

2. Related Work

Traditional wireless sensor network security technology is mostly based on cryptography. For example, [16] proposed a secure efficient hierarchical key management scheme (SEHKM) for wireless sensor networks. In this scheme, a network key, group key, and pairwise key are established to encrypt messages sent among sensor nodes, which not only ensures the security of information transmission but also improves the computing and storage efficiency of wireless sensor networks. [17] proposed an efficient dynamic authentication and key management scheme for heterogeneous wireless sensor networks (HWSNs). The key distribution algorithm generates dynamic keys based on existing information without any secure channel and sharing phase and improves the security of information transmission. [18] proposed a local dynamic scheme based on the layer cluster topology to complete the key management process in wireless sensor networks, and the number of nodes that need to update the key during the dynamic key agreement process is reduced under the conditions to protect the security of the network.

With the development of computer technology, the attack ability of eavesdroppers is also constantly improving, and thus, more complex encryption algorithms are required to maintain the information security between sensor nodes. However, in the actual working process of sensor nodes, due to its weak computing power, a single node is unable to carry out complex encryption calculations. Thus, the traditional encryption algorithm faces great challenges. In recent years, PLS has gradually become a common research topic within wireless sensor network security due to its low computational complexity and the ability to directly apply existing PLS technologies, such as artificial noise and cooperative relay for sensor networks. For example, [19] applied cooperative communication technology in PLS to wireless sensor networks and designed a security protocol suitable for sensor networks, which improved the performance of information security transmission between nodes. [20] proposed exploiting opportunistic scheduling schemes and wireless power transmission based on multihop transmission to improve the PLS in wireless sensor networks, enabling the data to be safely transmitted in the presence of an eavesdropper.

TABLE 1: Mathematical symbols and descriptions.

Mathematical symbols	Descriptions
$\rho(d)$	The probability of degree d in ISD degree distribution function
$\tau(d)$	Enhancement factor in RSD degree distribution function
$\mu(d)$	The probability of degree d in RSD degree distribution function
M	Source symbol
k	After the source symbols are grouped, the number of source symbols in each group
P_{AB}	Legitimate channel erasure probability in Figures 1 and 2
P_{AE}	Wiretap channel erasure probability in Figures 1 and 2
$G_1{}'$	LT-1 encoding matrix in DEMR-LT codes
G_{11}	The first $k/(1 - P_{AB})$ columns of the LT-1 encoding matrix $G_1{}'$
G_{12}	Columns $k/(1 - P_{AB}) + 1$ to w_1 in the LT-1 encoding matrix $G_1{}'$
G_{11-1}	The nondegree 1 columns in the partial LT-1 encoding matrix G_{11}
G_{11-2}	The degree 1 columns in the partial LT-1 encoding matrix G_{11}
w_1	The number of columns in the LT-1 encoding matrix $G_1{}'$
$\mu(1)$	The probability of degree 1 in the RSD degree distribution function
$G_2{}'$	LT-2 encoding matrix of DEMR-LT codes
G_{21}	The first $k(1 - \mu_1(1))/(1 - P_{AB})^2$ columns in the LT-2 encoding matrix $G_2{}'$
G_{22}	Columns $\left(k(1 - \mu_1(1))/(1 - P_{AB})^2\right) + 1$ to w_2 in the LT-2 encoding matrix $G_2{}'$
w_2	The number of columns in the LT-2 encoding matrix $G_2{}'$
C_{11}	The partial LT-1 encoding symbols obtained by G_{11-1}
C_1	The partial LT-1 encoding symbols obtained by G_{11-2} and G_{12}
C_2	LT-2 encoding symbols obtained by $G_2{}'$
$\widehat{C}_1$	The symbol of C_1 received by Bob after being transmitted through the legitimate channel
$\widehat{C}_2$	The symbol of C_2 received by Bob after being transmitted through the legitimate channel
$C\wedge_1{}'$	The symbol of C_1 received by Eve after being transmitted through the wiretap channel
$C\wedge_2{}'$	The symbol of C_2 received by Eve after being transmitted through the wiretap channel
ACK1	Feedback information after LT-1 decoding in the DEMR-LT codes
ACK2	Feedback information after LT-2 decoding in the DEMR-LT codes
t_{LT}	Decoding start time of traditional LT codes
t_{LT-1}	Decoding start time of LT-1 codes
t_{LT-2}	The time that the degree 1 symbol first appeared in LT-2 decoding
$t_{LT-2(degree-1)}$	LT-2 degree 1 symbol reception time in DEMR-LT codes
$t_{DEMR-LT}$	Decoding start time of DEMR-LT codes
m_{LT}	The number of decoding symbols in traditional LT codes
m_{LT-1}	The number of decoding symbols in LT-1 codes
m_1	The number of $\widehat{C}_1$ symbols in LT-1 decoding
m_{LT-2}	The number of $\widehat{C}_2$ symbols in LT-2 decoding
$m_{DEMR-LT}$	The number of decoding symbols in DEMR-LT codes
ε	Decoding overhead of traditional LT codes
ε_1	Decoding overhead of LT-1 decoding in DEMR-LT codes
ε_2	Decoding overhead of LT-2 decoding in DEMR-LT codes

Combining fountain codes with PLS technology can increase the information transmission rate while ensuring the security of the system. For example, [21] proposed a PLS method based on fountain coding aided by combining fountain codes with cooperative interference technology. The signal reception quality of eavesdroppers is reduced, and a constellation rotation approach is used to reduce the impact of interference on legitimate receivers. [22, 23] proposed using the feedback information of legitimate receivers to dynamically adjust the encoding mechanism of fountain codes to improve the decoding rate of legitimate receivers. [24] proposed a fountain coding-aided secure transmission scheme with delay and content awareness, which also used feedback to adjust the number and priority of encoded symbols, and successfully applied this scheme to image transmission. In [25, 26], the authors proposed sending the degree 1 symbol in advance by reordering the encoding matrix of the fountain code according to the degree value of each column from small to large. The start of the decoding was advanced to improve the recovery rate of intermediate symbols of online fountain codes. Therefore, combining the advantages of fountain codes and PLS technology could further improve the information security transmission performance of wireless sensor networks.

3. System Model and LT Codes

3.1. Wiretap Channel Model of Wireless Sensor Networks Based on LT Codes.
The wireless sensor network is a wireless network composed of a large number of sensors in a self-organizing and multihop manner. The source node (Alice) collects information and sends the information to the destination node (Bob) through the wireless network, while the eavesdropping node (Eve) uses the open structure of the wireless network to obtain a large amount of information by monitoring the wireless sensor networks. LT codes are a kind of fountain code that has the advantages of simple encoding and decoding and low decoding overhead. When combined with the wiretap channel model [5], channel coding at the physical layer of wireless transmission can achieve a better antieavesdropping effect. The wiretap channel model of wireless sensor networks based on LT codes is shown in Figure 1.

In Figure 1, the wiretap channel model of wireless sensor networks based on LT codes mainly consists of the source node Alice, the destination node Bob, and the eavesdropping node Eve. The channel between Alice and Bob is called the legitimate channel, and the channel between Alice and Eve is called the wiretap channel. LT codes are selected as the antieavesdropping code, and the receiver nodes use belief propagation (BP) decoding. Assume that Eve knows all the decoding rules of Bob. In Figure 1, Alice first groups the source symbols and then continuously sends the encoded symbols to Bob through the LT encoder, while Eve steals the LT encoded symbols in the legitimate channel through the wiretap channel. When Bob receives enough LT encoded symbols and finishes decoding, Bob sends an ACK instruction to Alice and tells Alice to stop sending source symbols. If Eve has not fully recovered the source information at this time, the incomplete LT encoded symbols received by Eve cannot continue the decoding process, thus reducing Eve's intercept efficiency.

3.2. LT Code Degree Distribution.
LT codes are a kind of fountain code designed by using the robust soliton distribution (RSD) degree distribution function [15], and the RSD degree distribution function is composed of the ideal soliton distribution (ISD) and the enhancement factor $\tau(d)$ after normalization. The definition of ISD is shown in

$$\rho(d) = \begin{cases} \dfrac{1}{k}, & d = 1, \\ \dfrac{1}{d(d-1)}, & d = 2, 3, \cdots, k, \end{cases} \tag{1}$$

where k represents the number of original source symbols and d represents the degree of encoded symbols.

$\tau(d)$ is expressed as follows:

$$\tau(d) = \begin{cases} \dfrac{s}{k} \cdot \dfrac{1}{d}, & d = 1, 2, 3, \cdots, \left(\dfrac{k}{s}\right) - 1, \\ \dfrac{s}{k} \ln\left(\dfrac{s}{\delta}\right), & d = k/s, \\ 0, & d > k/s, \end{cases} \tag{2}$$

where $s = c \ln(k/\delta)\sqrt{k}$, c is a constant, $c > 0$, and δ represents the maximum probability of decoding failure.

Normalize equations (1) and (2), and the RSD degree distribution function can be obtained as follows:

$$\mu(d) = \frac{\rho(d) + \tau(d)}{z}, \ d = 1, 2, \cdots, k, \tag{3}$$

where $z = \sum_d (\rho(d) + \tau(d))$ and $\mu(1)$ represents the probability of degree 1 symbols.

3.3. LT Code Encoding Matrix in the Erasure Channel.
We group the source symbols, and each group of source symbols M contains k symbols. In the channel with the erasure probability P_{AB}, the LT encoding matrix G is designed according to equation (3), which is shown in

$$G = \begin{pmatrix} 1 & 1 & 0 & 1 & 0 & \cdots & 1 & \cdots \\ 0 & 0 & 1 & 1 & 0 & \cdots & 1 & \cdots \\ \vdots & \vdots & \vdots & \vdots & \vdots & \vdots & \vdots & \vdots \\ 1 & 0 & 1 & 0 & 1 & \cdots & 0 & \cdots \end{pmatrix}_{k \times w}. \tag{4}$$

In equation (4), G is the $k \times w$ matrix, the position of element "1" in each column of the LT encoding matrix G represents the position of the corresponding source symbol, and the number represents the degree value of the corresponding encoded symbol.
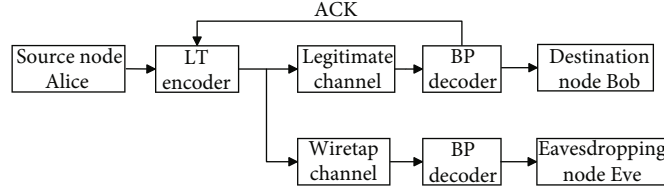
FIGURE 1: Wiretap channel model of wireless sensor networks based on LT codes.

LT codes encode symbols $C = M \times G$. To recover a group of source symbols, the number of correctly encoded symbols that the destination node needs to receive is $a(a \geq k)$. However, affected by the erasure channel, the number of encoded symbols received by the destination node is $m = a/(1 - P_{AB})$. Since the LT codes are rateless codes, to ensure that there are enough encoded symbols for decoding, the number of columns in G satisfies $w \gg m$.

4. The Encoding and Decoding Method Design of DEMR-LT Codes

In the traditional LT code antieavesdropping method, since the degree 1 symbol appears early, it takes a long time for the destination node Bob to decode from the beginning to the end. Therefore, the eavesdropping node Eve is given more time to receive the encoded symbols for decoding, and Eve may complete the decoding before Bob. In response to this problem, this paper proposes DEMR-LT codes on the basis of Figure 1. Since we need to carry out secondary LT cascade encoding for k source symbols, the first LT encoding process is called LT-1 encoding. Then, the second LT encoding process for the first $k(1 - \mu_1(1))/(1 - P_{AB})$ encoding symbols obtained in LT-1 encoding is called LT-2 encoding, and part of the encoding matrix is reordered according to the degree value of each column from large to small in two encoding processes, to delay the decoding start time of the receiving node and achieve antieavesdropping.

4.1. The DEMR-LT Code Encoding Matrix Design for the Erasure Channel. To obtain the encoding symbols of the DEMR-LT codes, the encoding matrix needs to be designed. First, the source symbols are grouped, the number of source symbols in each group is k, and the number of encoding symbols required to complete LT-1 and LT-2 decoding is m_{LT-1} and m_{LT-2}, respectively. The number of encoding symbols is determined by the number of encoding matrix columns, in order to ensure that the destination node receives enough decoding symbols for decoding, the number of LT-1 encoding matrix columns $w_1 \gg m_{LT-1}$, and the number of LT-2 encoding matrix columns $w_2 \gg m_{LT-2}$.

4.1.1. LT-1 Encoding Matrix. According to equation (4) to obtain the encoding matrix G_1, the encoding matrix G_{11} is obtained by reordering the encoding matrix of the first column $k/(1 - P_{AB})$ in G_1 according to the degree value of each column from large to small. To ensure that the k source symbols in LT-1 can be fully recovered in the final decoding, we continue to obtain the encoding matrix G_{12} of columns

$(k/(1 - P_{AB})) + 1$ to $m_1/(1 - P_{AB})$ in G_1 according to the RSD degree distribution. Thus, we can get the LT-1 encoding matrix $G_1{}'$ as follows:

$$G_1{}' = (G_{11}, G_{12})_{k \times w_1}, \qquad (5)$$

where G_{11} is the $k \times (k/(1 - P_{AB}))$ matrix and G_{12} is the $k \times (w_1 - (k/(1 - P_{AB})))$ matrix.

In equation (5), after the encoding matrix G_{11} is reordered according to the degree value, the degree 1 column is arranged in the latter part of the encoding matrix G_{11}. By setting the nondegree 1 column and the degree 1 column matrix reordered according to the degree value as G_{11-1} and G_{11-2}, respectively, the LT-1 encoding matrix $G_1{}'$ of equation (5) can be written as follows:

$$G_1{}' = (G_{11-1}, G_{11-2}, G_{12})_{k \times w_1}, \qquad (6)$$

where G_{11-1} is the $k \times (k(1 - \mu_1(1))/(1 - P_{AB}))$ matrix, G_{11-2} is the $k \times (k\mu_1(1)/(1 - P_{AB}))$ matrix, and $\mu_1(1)$ is the probability distribution of degree $d = 1$ obtained from equation (3) when the number of source symbols is k.

4.1.2. LT-2 Encoding Matrix. The number of LT encoding symbols cannot be determined. This paper proposes selecting the first $k(1 - \mu_1(1))/(1 - P_{AB})$ encoding symbols of LT-1 as the source symbols to conduct the second LT encoding. The number of LT-2 decoding symbols m_{LT-2} is also difficult to determine, but it is greater than or equal to $k(1 - \mu_1(1))/(1 - P_{AB})$, according to equation (4) to obtain the encoding matrix G_2, and G_2 is the $(k(1 - \mu_1(1))/(1 - P_{AB})) \times w_2$ matrix.

Similar to the construction of the LT-1 encoding matrix, we divide G_2 into two parts and reorder the first $k(1 - \mu_1(1))/(1 - P_{AB})^2$ columns in G_2 according to the degree value d of each column from large to small to obtain G_{21}. In order to recover the source symbol of LT-2, i.e., the first $k(1 - \mu_1(1))/(1 - P_{AB})$ encoding symbol of LT-1, according to the RSD degree distribution function, to obtain the $(k(1 - \mu_1(1))/(1 - P_{AB})^2) + 1$ to w_2 columns encodes matrix G_{22}. Then, we obtain the LT-2 encoding matrix $G_2{}'$ as follows:

$$G_2{}' = (G_{21}, G_{22})_{k(1 - \mu_1(1))/(1 - P_{AB}) \times w_2}, \qquad (7)$$

where G_{21} is the $k(1 - \mu_1(1))/(1 - P_{AB}) \times k(1 - \mu_1(1))/(1 - P_{AB})^2$ matrix and G_{22} is the $k(1 - \mu_1(1))/(1 - P_{AB}) \times (w_2 - (k(1 - \mu_1(1))/(1 - P_{AB})^2))$ matrix.

4.2. The DEMR-LT Code Encoding and Decoding Method. Suppose the source symbol is M, the LT-1 encoding matrix $G_1{}'$ is composed of G_{11-1}, G_{11-2}, and G_{12}, and the LT-2 encoding matrix is $G_2{}'$. C_{11} is the partial LT-1 encoded symbol obtained through encoding matrix G_{11-1}; C_1 is the another partial LT-1 encoded symbol obtained through the encoding matrix G_{11-2} and G_{12}; C_2 is the LT-2 encoded symbol obtained from C_{11} through the LT-2 encoding matrix $G_2{}'$; ACK1 and ACK2 are the feedback information after the decoding of the LT-1 codes and LT-2 codes, respectively. The DEMR-LT codes' physical layer security encoding model is shown in Figure 2.

The specific encoding and decoding methods of the DEMR-LT codes are as follows:

(1) We group the source symbols, and each group contains k symbols. We obtain the LT-1 encoding symbol C_{11} according to G_{11-1} and obtain C_1 according to G_{11-2} and G_{12}. Then, we use C_{11} as the LT-2 source to obtain the LT-2 encoding symbol C_2 through the encoding matrix $G_2{}'$

(2) The Alice control switch first selects "2." Then, Alice sends C_2 to Bob and checks whether ACK2 has been received; if not, Alice keeps sending C_2 to Bob

(3) The Bob control switch selects "2" to receive $\widehat{C}_2$ over the legitimate channel and chooses the correct symbol $\widehat{C}_2$ for BP decoding. When C_{11} is recovered, ACK2 is sent to Alice, and at the same time, the Bob control switch selects "1"

(4) When Alice receives ACK2, it stops sending C_2; at the same time, the Alice control switch selects "1" and starts sending C_1 to Bob

(5) Bob receives $\widehat{C}_1$ through the legitimate channel and combines C_{11} recovered in step (3) for LT-1 decoding together. When the message M is recovered, Bob sent ACK1 to Alice

(6) Alice stops sending C_1 after receiving ACK1 and continues to send the next group of DEMR-LT code encoding symbols

(7) Repeat the above steps until the source symbols of all groups are recovered

The algorithm flowchart of the DEMR-LT codes' physical layer security encoding is shown in Figure 3.

Due to wireless communication, when Alice sends encoded symbols, both Eve and Bob can receive Alice's encoded symbols. Suppose Eve knows the decoding rules with Bob and decodes the received Alice encoding symbols. According to the DEMR-LT code decoding rule, the Eve con-

trol switch selects "2" first to receive the encoded symbol $C\wedge_2{}'$ sent by Alice through the wiretap channel and decodes $\widehat{C}_{11}$ as much as possible before Bob sends ACK2. After receiving ACK2 sent by Bob, the Eve control switch selects "1," then receives $C\wedge_1{}'$ through the wiretap channel, and recovers the message M together with the translated part of $\widehat{C}_{11}$.

During the process of Alice sending a group of encoded symbols, due to the influence from the noise of the legal channel and the wiretap channel, there are some errors in the $\widehat{C}_2$ received by Bob and the $C\wedge_2{}'$ received by Eve. However, the randomness of the noise leads to different error symbols received by Bob and Eve, and the differences also occur in the process of BP decoding, which makes it difficult for Eve and Bob to recover C_{11} at the same time.

If Bob recovers all C_{11} symbols and decodes them together with $\widehat{C}_1$, Eve only recovers part of $\widehat{C}_{11}$ symbols. Since there is no degree 1 encoded symbol in $\widehat{C}_{11}$, Eve cannot start decoding before Bob and needs to continue receiving $C\wedge_1{}'$ for decoding together. Then, there is a situation where Bob's decoding ends, but Eve has not yet acquired enough symbols, and thus, Eve cannot continue to receive $C\wedge_1{}'$ and enter the "waterfall area" of BP decoding to recover a large number of source symbols. As a result, Eve can only obtain a small intercept rate or even zero. Of course, there are also cases where Eve recovers information before Bob and obtains a 100% intercept rate, but it is usually necessary to send multiple groups of symbols to transmit a complete message. Therefore, Eve can only intercept a fraction of the total source message.

5. Performance Analysis of DEMR-LT Codes

The hardware environment required for the simulation experiment in this section is as follows: Intel™Core™ i5, 8 GB running memory, Windows™ 10 operating system, and MATLAB™ R2016a application software.

Experimental conditions: we assume that the wireless sensor network model structure is shown in Figure 1, where there is a source node Alice, a destination node Bob, and an eavesdropping node Eve existing around them to steal the information between Alice and Bob. In addition, we do not consider the data encryption between sensor nodes. Both Bob and Eve use the BP decoding method for LT decoding, and Eve knows all of Bob's decoding rules.

Experimental parameters: the source symbol number is $k = 2000$, the transmission group number is 5000, RSD degree distribution is set to $c = 0.03$, and $\delta = 0.05$.

5.1. Decoding Start Time of Destination Node. LT codes generally adopt BP decoding and begin decoding when the degree 1 symbol is received. In the traditional LT code encoding matrix, the columns of degree 1 are not reordered, and the starting decoding time t_{LT} is uncertain, but the number of columns in the LT encoding matrix is greater than or equal to $k/(1 - P_{AB})$. According to equation (5), the number of degree 1 columns in the first $k/(1 - P_{AB})$ columns is $k\mu(1)/(1 - P_{AB})$. If there is no rearrangement of the degree 1 column, then the decoding start time t_{LT} is as follows:
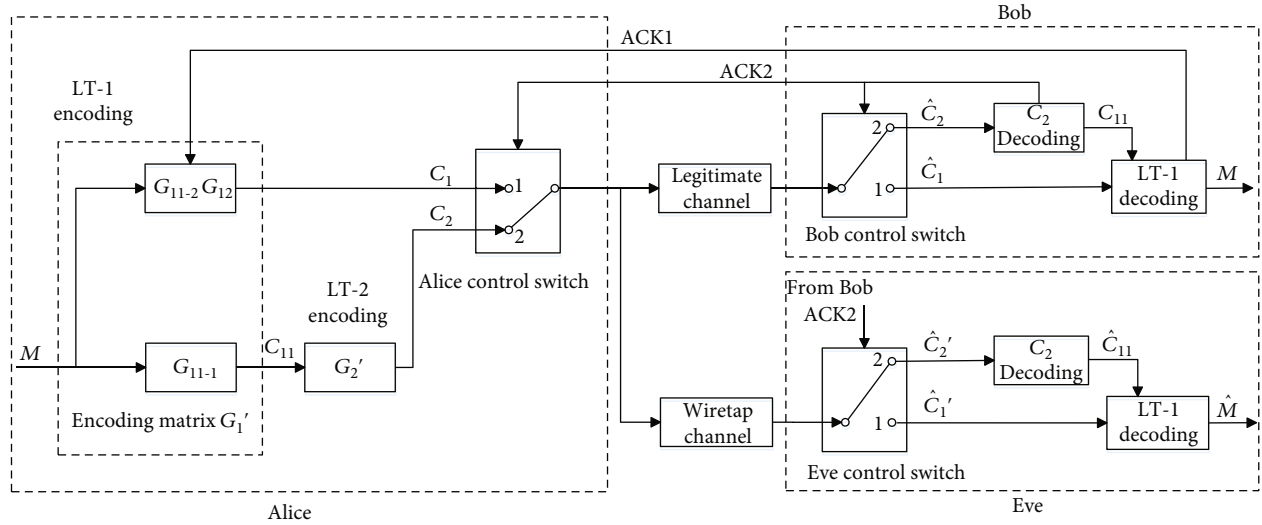
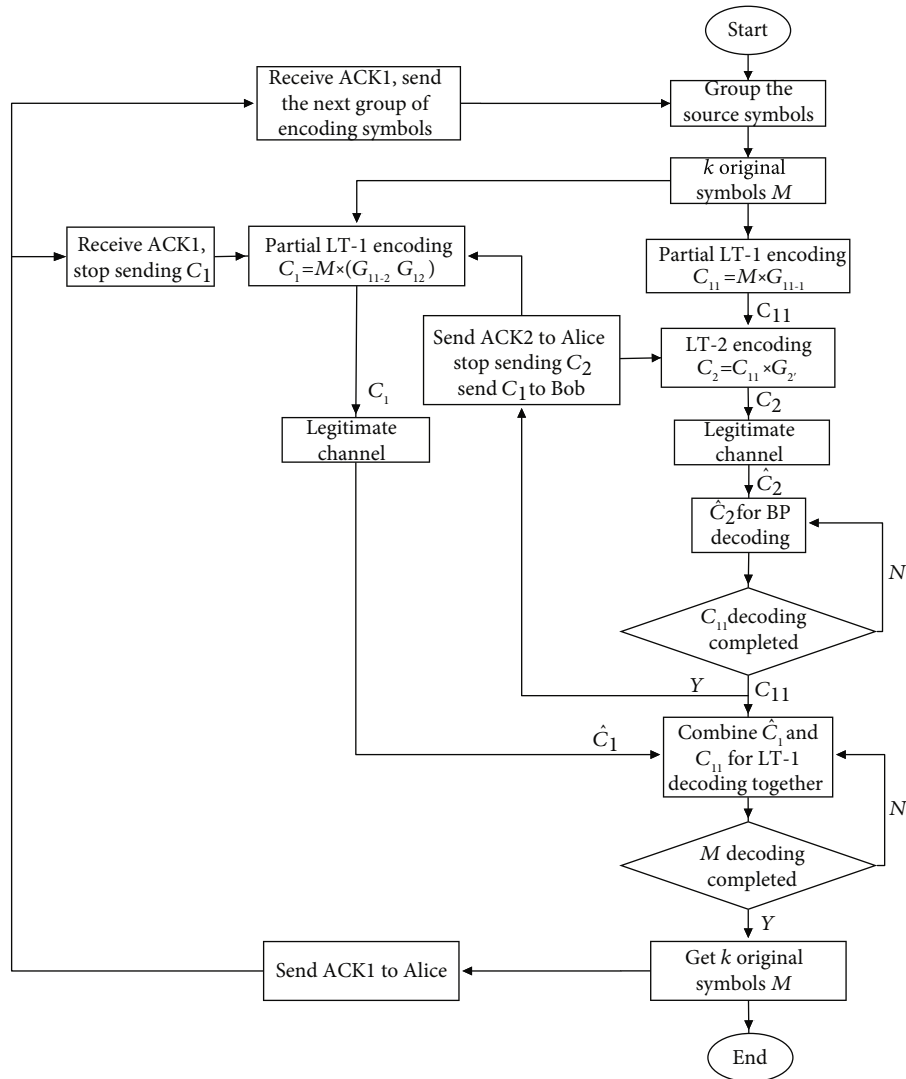FIGURE 2: DEMR-LT codes' physical layer security encoding model.

FIGURE 3: The algorithm flowchart of the DEMR-LT codes' physical layer security encoding.

$$t_{LT} \leq \left(\frac{k(1 - \mu(1))}{1 - P_{AB}} + 1 \right) T, \tag{8}$$

where $\mu(1)$ represents the degree 1 probability that the number of the source symbols is k.

If only LT-1 codes are used for transmission, the number of columns with degree 1 in the first $k/(1 - P_{AB})$ columns of equation (5) is $k\mu_1(1)/(1 - P_{AB})$. After rearrangement, degree 1 columns are listed in columns $((k(1 - \mu_1(1))/(1 - P_{AB})) + 1) \sim k/(1 - P_{AB})$ of equation (6). Affected by the erasure channel, the destination node receives the degree 1 symbol with errors, so the decoding start time t_{LT-1} of LT-1 codes satisfies

$$t_1 \geq \left(\frac{k(1 - \mu_1(1))}{1 - P_{AB}} + 1 \right) T, \tag{9}$$

where T is the time period of each symbol and $\mu_1(1)$ represents the probability distribution of degree $d = 1$ obtained by equation (3) when the number of source symbols is k.

In the LT-2 encoding of DEMR-LT codes, C_{11} is the source of LT-2, the number of source symbols is $k(1 - \mu_1(1))/(1 - P_{AB})$, and the time of the first appearance of the degree 1 encoding symbol is t_{LT-2}. Then, t_{LT-2} satisfies

$$t_{LT-2} \geq \left(\frac{k(1 - \mu_1(1))(1 - \mu_2(1))}{(1 - P_{AB})^2} + 1 \right) T, \tag{10}$$

where $\mu_2(1)$ represents the probability distribution of degree $d = 1$ obtained by equation (3) when the number of source symbols is $k(1 - \mu_1(1))/(1 - P_{AB})$.

In the process of DEMR-LT code decoding, first, it is necessary to receive the LT-2 degree 1 symbol to start LT-1 decoding, and the number of decoded symbols required is greater than or equal to $k(1 - \mu_1(1))/(1 - P_{AB})$. Since there is no degree 1 encoded symbol in C_{11}, LT-1 decoding cannot be started, and thus, it is necessary to obtain the degree 1 symbol from C_1 to start LT-1 decoding. LT-2 degree 1 symbol reception time is $t_{LT-2(degree-1)} = (k(1 - \mu_1(1))\mu_2(1)/(1 - P_{AB})^2)T$, and the decoding start time of DEMR-LT codes satisfies

$$\begin{aligned} t_{DEMR-LT} &\geq t_{LT-2} + t_{LT-2(degree-1)} \\ &= \left(\frac{k(1 - \mu_1(1))(1 - \mu_2(1))}{(1 - P_{AB})^2} + \frac{k(1 - \mu_1(1))\mu_2(1)}{(1 - P_{AB})^2} + 1 \right) T \\ &= \left(\frac{k(1 - \mu_1(1))}{(1 - P_{AB})^2} + 1 \right) T. \end{aligned} \tag{11}$$

Equations (9) and (11) are taken as equal signs to compare their sizes, i.e.,

$$t_{DEMR-LT} - t_{LT-1} = \left(\frac{k(1 - \mu_1(1))}{(1 - P_{AB})^2} - \frac{k(1 - \mu_1(1))}{1 - P_{AB}} \right) T = \frac{k(1 - \mu_1(1))}{(1 - P_{AB})} \left(\frac{1}{(1 - P_{AB})} - 1 \right) T. \tag{12}$$

According to equation (12), when $P_{AB} = 0$, then $t_{DEMR-LT} = t_{LT-1}$, and with the increase in P_{AB}, then $t_{DEMR-LT} > t_{LT-1}$. Thus, there is a case where DEMR-LT codes start decoding later than LT-1 codes or decoding simultaneously.

Comparing equations (8), (9), and (12), we can get the following: $t_{DEMR-LT} \geq t_{LT-1} \geq t_{LT}$.

When the legitimate channel erasure probability is $P_{AB} = 0.3$ and the wiretap channel erasure probability is P_{AE}, the comparison result of the decoding start time of the traditional LT codes, LT-1 codes, and DEMR-LT codes is shown in Figure 4.

According to Figure 4, traditional LT codes, LT-1 codes, and DEMR-LT codes receive on average 252, 2822, and 2824 symbols to begin decoding, and the decoding time of DEMR-LT codes is delayed by 2 symbols compared with LT-1 codes.

In traditional LT codes, the receiving nodes can start decoding as long as the degree 1 symbol is received, and the decoding start time is earlier. In LT-1 codes, the receiving time of the degree 1 symbol is delayed because the encoding matrix is reordered once. Thus, the decoding success probability before receiving the degree 1 symbol is 0, and the decoding start time is later than that of traditional LT codes. However, in DEMR-LT codes, the receiving time of the degree 1 symbol is further delayed due to the reordering of matrixes G_1 and G_2. Therefore, the decoding start time is the latest compared with that of the other two schemes.

In addition, Figure 4 shows that the curves of DEMR-LT codes and LT-1 codes basically coincide before the 2822nd symbol is received. The main reason for this is that both of these encoding methods rearrange part of the encoding matrix for different times. Thus, the decoding process cannot start before receiving the symbol of degree 1, and the probability of success of decoding is 0.

5.2. Intercept Efficiency of the Eavesdropping Node. The experimental conditions are the same as above and compare the influence of changes in the wiretap channel erasure probability and the legitimate channel erasure probability of three different LT code schemes on the intercept efficiency of the eavesdropping node. The experimental results are shown in Figures 5 and 6.

According to Figure 5, when $P_{AB} = 0.3$, the Eve intercept efficiencies of the three schemes all decrease with increasing P_{AE}, and the Eve intercept efficiencies of the DEMR-LT codes are the lowest.

Figure 6 shows that the value of P_{AB} ranges from 0 to 0.8, and the difference between P_{AB} and P_{AE} is different; the relationship between Eve's intercept efficiency and P_{AB} is compared using three different schemes. As shown in Figure 6, Eve has the lowest intercept efficiency compared with the other two schemes in three channel conditions. In Figure 6(a), under the condition of the degraded wiretap channel, Eve's intercept efficiency always decreases with increasing P_{AB}. In Figure 6(b), the intercept efficiency of Eve decreases first and then slightly increases with increasing P_{AB}. However, as shown in Figure 6(c), even under the
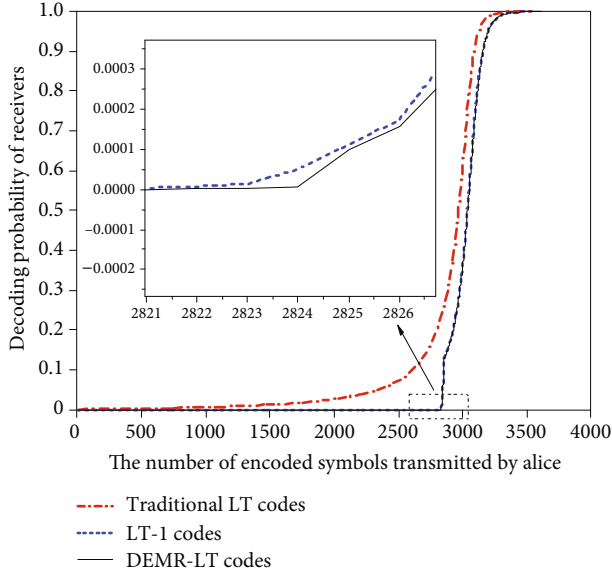
FIGURE 4: The relationship between the decoding probability of receiving nodes and the number of encoded symbols transmitted by Alice.
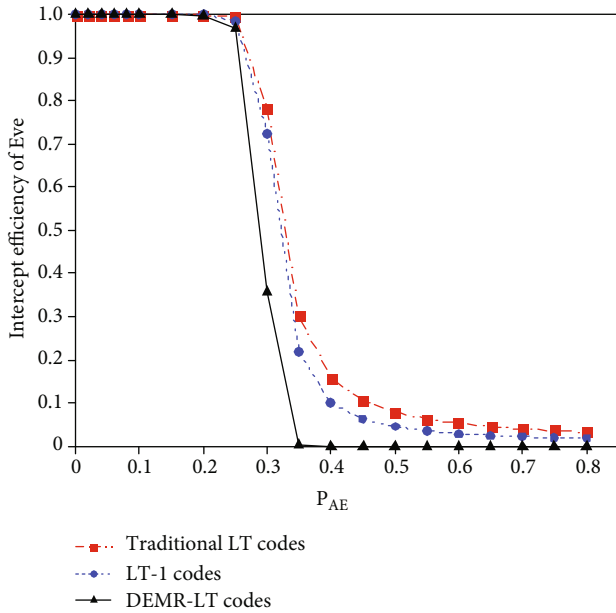

FIGURE 5: The relationship between intercept efficiency of Eve and P_{AE}.

condition that the wiretap channel condition is superior to the legitimate channel, DEMR-LT codes can also considerably reduce Eve's intercept efficiency.

According to the experimental results in Figures 5 and 6, the scheme proposed in this paper makes the intercept efficiency of eavesdropping nodes low. The main reason for this is that DEMR-LT codes contain two decoding stages in total. In LT-2, Bob receives the encoded symbol $\widehat{C}_2$ and decodes C_{11}. Then, it sends ACK2 to Alice and stops sending C_2. Eve can only decode the $\widehat{C}_{11}$ symbol by stealing enough

$C\wedge_2{}'$ before Bob sends ACK2 and continues with LT-1 decoding; otherwise, the message M cannot be recovered. By reordering the encoding matrixes $G_1{}'$ and $G_2{}'$ in descending order according to the degree value of each column, DEMR-LT codes delay the receiving time of degree 1 symbols and shorten the receiving time for Eve to receive more $C\wedge_2{}'$ symbols. As a result, the probability that Eve completes decoding before Bob is reduced, leading to a further decline in Eve's intercept efficiency.

In addition, the reason for the phenomenon that Eve's intercept efficiency first drops and then rises in the other schemes of Figure 6 is that the encoded symbols received by Eve and Bob are the same when $P_{AB} = P_{AE} = 0$. Both of them have the same decoding process and complete decoding at the same time, and thus, Eve's intercept efficiency is 100%. With the increase in P_{AB} and P_{AE}, the difference between the encoded symbols received by Eve and Bob gradually increases; Eve cannot continue to decode according to Bob's decoding order, which may be earlier or later than Bob's decoding. Thus, Eve' intercept efficiency begins to decrease. When P_{AB} and P_{AE} increase to a large value, the correct symbol intercepted by Eve is quite different from Bob. As long as Eve receives the degree 1 symbol before Bob, it can decode according to its own decoding order. Then, Eve's intercept efficiency increases to a certain extent. In addition, the increase range is affected by the difference between P_{AB} and P_{AE}. According to Figure 6, the better the wiretap channel is, the higher the probability that Eve will receive the degree 1 symbol before Bob and the greater the increase in intercept efficiency.

5.3. DEMR-LT Code Decoding Symbol Number. In the traditional LT code, assuming that a group of source symbol numbers is k, decoding overhead is ε ($\varepsilon \geq 1$ and $\varepsilon \longrightarrow 1$), and the legitimate channel erasure probability is P_{AB}. Then, the number of decoding symbols m_{LT} required to decode the message M is as follows:

$$m_{LT} = \frac{k\varepsilon}{1 - P_{AB}}. \tag{13}$$

In LT-1 decoding, we assume that a group of source symbol numbers is k and the decoding overhead is ε_1 ($\varepsilon_1 \geq 1$). The number of LT code decoding symbols has nothing to do with the order of received symbols, and LT-1 codes only change the order of decoded symbols, so $\varepsilon_1 \approx \varepsilon$. If only LT-1 codes are used for encoding, the number of decoding symbols m_{LT-1} is as follows:

$$m_{LT-1} = \frac{k\varepsilon}{1 - P_{AB}}. \tag{14}$$

According to Figure 2, the decoding symbol of DEMR-LT codes is composed of $\widehat{C}_2$ and $\widehat{C}_1$. Then, the number of decoded symbols m_1 for $\widehat{C}_1$ is as follows:

$$m_1 = \frac{k\mu_1(1)}{1 - P_{AB}} + \frac{k\varepsilon_1 - k}{1 - P_{AB}}. \tag{15}$$

(a) $P_{AE} = P_{AB} + 0.01$

(b) $P_{AE} = P_{AB}$

(c) $P_{AE} = P_{AB} - 0.01$
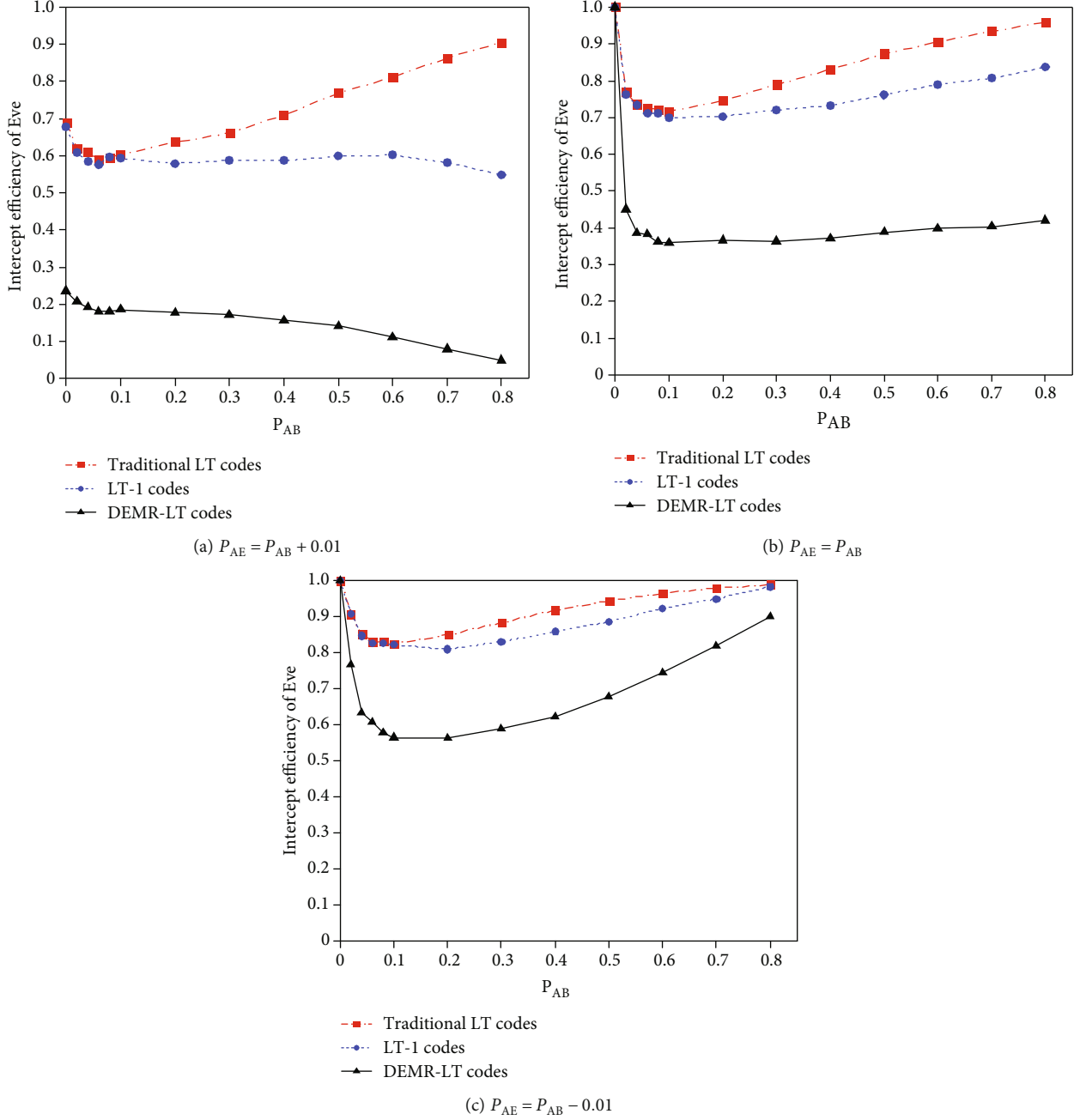
Figure 6: The influence of the difference between P_{AB} and P_{AE} on Eve's intercept efficiency.

In LT-2 decoding, we let $k(1 - \mu_1(1))/(1 - P_{AB})$ encoding symbol C_{11} be the source, and the decoding overhead is ε_2 ($\varepsilon_2 \geq 1$ and $\varepsilon_2 \longrightarrow 1$). In LT-2 decoding, according to equation (13), the number of $\widehat{C}_2$ required to recover encoded symbol C_{11} can be expressed as follows:

$$m_{\text{LT-2}} = \frac{k(1 - \mu_1(1))\varepsilon_2}{(1 - P_{AB})^2}. \tag{16}$$

After combining equations (15) and (16), the number of decoding symbols $m_{\text{DEMR-LT}}$ required to decode the message M with the DEMR-LT codes is as follows:

$$m_{\text{DEMR-LT}} = m_1 + m_{\text{LT-2}}$$
$$= \frac{k\mu_1(1)}{1 - P_{AB}} + \frac{k\varepsilon_1 - k}{1 - P_{AB}} + \frac{k(1 - \mu_1(1))\varepsilon_2}{(1 - P_{AB})^2}. \tag{17}$$
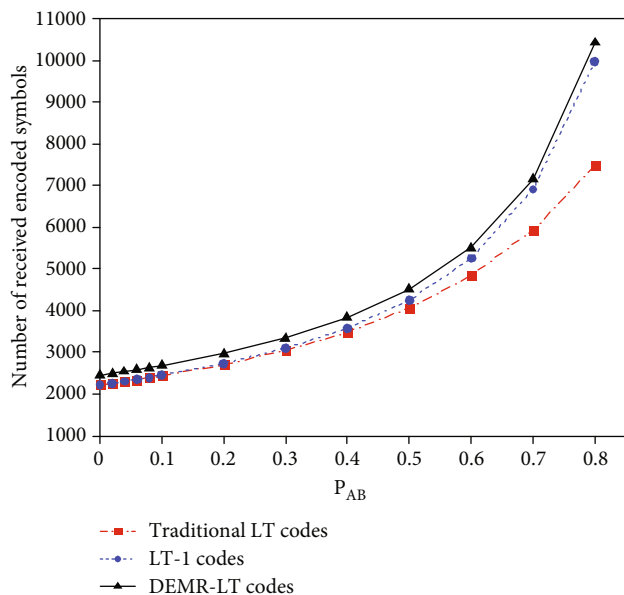
FIGURE 7: The relationship between the number of encoded symbols to be received for decoding and P_{AB}.

According to equations (13), (14), and (17), the numbers of decoded symbols of the three encoding schemes all increase with increasing P_{AB}. According to equation (16), when $P_{AB} \longrightarrow 0$, $m_{DEMR-LT} = k(\varepsilon_1 + \varepsilon_2 + \mu_1(1)(1 - \varepsilon_2) - 1)$; DEMR-LT codes have the largest value. According to equation (3), the value of $\mu_1(1)$ is small, $\varepsilon \approx \varepsilon_1 \longrightarrow 1$, and $\varepsilon_2 \longrightarrow 1$, and thus, $m_{DEMR-LT}$ is close to LT codes and LT-1 codes. However, since the square term $(1 - P_{AB})^2$ of the denominator in equation (17) is less than 1, with the increase in P_{AB}, the increase rate of $m_{DEMR-LT}$ is faster than that of m_{LT-1} and m_{LT}. Therefore, when the legitimate channel is good, the number of DEMR-LT code decoding symbols is close to m_{LT}. In contrast, when the channel is poor, the number of decoding symbols is larger.

Figure 7 studies the number of encoded symbols that the destination node needs to receive to complete the decoding under the different P_{AB} in three schemes, where P_{AB} ranges from 0 to 0.8, and other conditions remain unchanged.

According to Figure 7, the number of decoding symbols in the three schemes all increases with the increase in P_{AB}, and the number of decoding symbols from small to large is traditional LT codes, LT-1 codes, and DEMR-LT codes. When P_{AB} is larger, DEMR-LT codes increase faster.

6. Conclusions

In wireless sensor networks, aiming at the problem that traditional encryption algorithms are easy to decipher or leak, this paper proposes a DEMR-LT code PLS transmission scheme and gives the DEMR-LT code encoding matrix design method, as well as the encoding and decoding method. The research results are as follows:

(1) By comparing the start-to-end time of the DEMR-LT codes with other LT codes, the decoding process time is shortened, which shows that this method can effectively prevent eavesdropping node Eve from recovering the message symbol

(2) By comparing the intercept efficiency of DEMR-LT codes with other LT code schemes, this scheme can further reduce the intercept efficiency of Eve. Even if the wiretap channel is better than the legitimate channel, it can also reduce the intercept efficiency of eavesdroppers

(3) The mathematical expression of the decoded symbol number of DEMR-LT codes is derived. According to the experimental simulation results, the number of decoded symbols in this method increases slightly compared with those in other methods, but the number of decoded symbols does not increase much under the condition of low channel erasure probability. While ensuring the secure transmission of information, it will not excessively increase the information transmission delay of the wireless sensor networks

It can be concluded that for wireless sensor network information transmission, when the eavesdropping node obtains the same decoding conditions as the destination node, the scheme in this paper can ensure the secure transmission of information.

In future work, considering the limited computing capacity of sensor nodes, further improvements can be made in reducing the encoding and decoding complexity of the DEMR-LT codes to ensure secure information transmission performance of sensor nodes and improve transmission efficiency. In terms of future applications, the proposed encoding scheme can provide a reference for other physical layer encoding methods in wireless sensor networks to further improve the security performance of wireless sensor networks.

Data Availability

The data used to support the findings of this study are available from the corresponding author upon request.

Conflicts of Interest

The authors declare that there are no conflicts of interest regarding the publication of this article.

Acknowledgments

References

[1] K. Moara-Nkwe, Q. Shi, G. M. Lee, and M. H. Eiza, "A novel physical layer secure key generation and refreshment scheme for wireless sensor networks," *IEEE Access*, vol. 6, pp. 11374–11387, 2018.

[2] S. Atapattu, N. Ross, Y. D. Jing, Y. Y. He, and J. S. Evans, "Physical-layer security in full-duplex multi-hop multi-user wireless network with relay selection," *IEEE Transactions on Wireless Communications*, vol. 18, no. 2, pp. 1216–1232, 2019.

[3] R. Chopra, C. R. Murthy, and R. Annavajjala, "Physical layer security in wireless sensor networks using distributed co-phasing," *IEEE Transactions on Information Forensics and Security*, vol. 14, no. 10, pp. 2662–2675, 2019.

[4] C. E. Shannon, "Communication theory of secrecy systems," *The Bell System Technical Journal*, vol. 28, no. 4, pp. 656–715, 1949.

[5] A. D. Wyner, "The wire-tap channel," *Bell System Technical Journal*, vol. 54, no. 8, pp. 1355–1387, 1975.

[6] S. H. Yan, N. Yang, I. Land, R. Malaney, and J. H. Yuan, "Three artificial-noise-aided secure transmission schemes in wiretap channels," *IEEE Transactions on Vehicular Technology*, vol. 67, no. 4, pp. 3669–3673, 2018.

[7] L. Yang, J. Chen, H. Jiang, S. A. Vorobyov, and H. L. Zhang, "Optimal relay selection for secure cooperative communications with an adaptive eavesdropper," *IEEE Transactions on Wireless Communications*, vol. 16, no. 1, pp. 26–42, 2017.

[8] H. Y. Guo, Z. Yang, L. H. Zhang, J. Zhu, and Y. L. Zou, "Joint cooperative beam-forming and jamming for physical-layer security of decode-and-forward relay networks," *IEEE Access*, vol. 5, pp. 19620–19630, 2017.

[9] Y. B. Gu, Z. L. Wu, Z. D. Yin, and X. J. Zhang, "The secrecy capacity optimization artificial noise: a new type of artificial noise for secure communication in MIMO system," *IEEE Access*, vol. 7, pp. 58353–58360, 2019.

[10] H. L. He, P. Y. Ren, Q. H. Du, and H. Lin, "Joint feedback and artificial noise design for secure communications over fading channels without Eavesdropper's CSI," *IEEE Transactions on Vehicular Technology*, vol. 66, no. 12, pp. 11414–11418, 2017.

[11] T. Zhu and F. Tong, "A cluster-based cooperative jamming scheme for secure communication in wireless sensor network," in *2020 IEEE 92nd Vehicular Technology Conference (VTC2020-Fall)*, pp. 1–5, Victoria, BC, Canada, 2020.

[12] Q. Liu, Y. Wang, W. J. Zhang, and H. Li, "Secret data transmission in wireless sensor network with physical layer network coding," *Journal of Information Science & Engineering*, vol. 33, no. 4, pp. 1055–1067, 2017.

[13] L. Sun and H. B. Xu, "Fountain-coding-based secure communications exploiting outage prediction and limited feedback," *IEEE Transactions on Vehicular Technology*, vol. 68, no. 1, pp. 740–753, 2019.

[14] H. Niu, M. Iwai, K. Sezaki, L. Sun, and Q. H. Du, "Exploiting fountain codes for secure wireless delivery," *IEEE Communications Letters*, vol. 18, no. 5, pp. 777–780, 2014.

[15] D. J. C. MacKay, "Fountain codes," *IEE Proceedings-Communications*, vol. 152, no. 6, pp. 1062–1068, 2005.

[16] X. Zhang and J. Wang, "An efficient key management scheme in hierarchical wireless sensor networks," *2015 International Conference on Computing, Communication and Security (ICCCS)*, 2015, pp. 1–7, Pamplemousses, Mauritius, 2015.

[17] S. Athmani, A. Bilami, and D. E. Boubiche, "EDAK: an efficient dynamic authentication and key management mechanism for heterogeneous WSNs," *Future Generation Computer Systems*, vol. 92, pp. 789–799, 2019.

[18] B. Sun, Q. Li, and B. Tian, "Local dynamic key management scheme based on layer-cluster topology in WSN," *Wireless Personal Communications*, vol. 103, no. 1, pp. 699–714, 2018.

[19] A. Al Hayajneh, M. Z. A. Bhuiyan, and I. McAndrew, "A novel security protocol for wireless sensor networks with cooperative communication," *Computers*, vol. 9, no. 1, p. 4, 2020.

[20] K. Shim, T. V. Nguyen, and B. An, "Exploiting opportunistic scheduling schemes and WPT-based multi-hop transmissions to improve physical layer security in wireless sensor networks," *Sensors*, vol. 19, no. 24, p. 5456, 2019.

[21] L. Sun, P. Ren, Q. H. Du, and Y. C. Wang, "Fountain-coding aided strategy for secure cooperative transmission in industrial wireless sensor networks," *IEEE Transactions on Industrial Informatics*, vol. 12, no. 1, pp. 291–300, 2015.

[22] W. Y. Li, Q. H. Du, L. Sun, P. Y. Ren, and Y. C. Wang, "Security enhanced via dynamic fountain code design for wireless delivery," in *2016 IEEE Wireless communications and networking conference*, pp. 1–6, Doa, Qatar, 2016.

[23] D. T. Huang and L. Sun, "Secure communication based on fountain code and channel feedback," in *2019 11th International Conference on Wireless Communications and Signal Processing (WCSP)*, pp. 1–5, Xi'an, China, 2019.

[24] L. Sun, D. T. Huang, and A. L. Swindlehurst, "Fountain-coding aided secure transmission with delay and content awareness," *IEEE Transactions on Vehicular Technology*, vol. 69, no. 7, pp. 7992–7997, 2020.

[25] Y. L. Zhao, Y. Zhang, F. C. M. Lau, H. Yu, and Z. L. Zhu, "Improved online fountain codes," *IET Communications*, vol. 12, no. 18, pp. 2297–2304, 2018.

[26] J. X. Huang, Z. S. Fei, C. Z. Cao, and M. Xiao, "Design and analysis of online fountain codes for intermediate performance," *IEEE Transactions on Communications*, vol. 68, no. 9, pp. 5313–5325, 2020.

Hindawi

Research Article

Evaluation and of University Building Design Effect Based on Multisensor Perception and Data Security

Xusheng Xie,[1] **Junling Zhou** (ID)**,**[1] **and Xin Wen**[2]

[1]*Guangdong Polytechnic Normal University, Gaungzhou, Guangdong Province, 528000, China*
[2]*Lingnan Normal University, Zhanjiang, Guangdong Province, 524048, China*

Correspondence should be addressed to Junling Zhou; sevencatcat@gpnu.edu.cn

The development of the smart cities with new and integrated information and communication technologies has changed the traditional industries' processes. One of the domains is construction industry which plays an important supporting role for the economic development of a country, but at the same time, the construction industry is also an industry with high energy consumption and high pollution. Therefore, in order to alleviate the contradiction between economic development and resources and the environment, the construction industry must achieve sustainable development and take the road of green construction. In order to carry out the evaluation of the design effect of colleges and universities, this paper introduces the multisensor perception and fuzzy comprehensive evaluation methods. First, through the design and analysis of the sensor perception system used in the building environment, the collection, acquisition, analysis, and processing of complex information of heterogeneous multiterminals are obtained. Secondly, cluster analysis and genetic algorithms are used in the processing and analysis process of building multiterminal sensor data. The security aspect is also taking into account to design the methods. The system test verifies the performance of the university building design effect evaluation model, which can provide a reference for the sustainable development of the construction industry.

1. Introduction

People's requirements for buildings are getting higher and higher, and the complexity of buildings is increasing. Huge changes have taken place in the types, scales, and forms of modern architecture. This is also the requirement of the rapid development of modern sciences and technologies and social economy and is the inevitable result of the development of the discipline of architecture [1–3]. The complexity of building functions and the diversification of usage requirements have increased the technical problems involved in the use of indoor spaces. The development of architecture inevitably requires the cooperation of various disciplines. In the design stage, different disciplines are considered the construction of buildings from different angles, so as to continuously improve indoor space environment [4, 5]. The work related to building construction includes construction, structure, water supply and drainage, electrical, heating, ventilation, and other professional content. All

majors determine all aspects of the building in the design, and most of the energy-related design decisions occur in the early design stage [6]. When a building reaches the construction stage, the significance of building energy saving and emission reduction is only whether it can meet the requirements of building design. The characteristics of the building have been basically determined in the design stage and realized through the construction process [7–9].

Modern technologies have gradually refined the division of human activities. Architectural design is also completed by the cooperation of multiple disciplines, and more and more factors are considered by each discipline. Architects should not only consider space requirements and architecture. The aesthetic principles of form also need to consider building energy-saving design [10]. Authors in [11] analyzed the energy consumption costs of 12 types of buildings in 16 cities and calculated that traditional energy-saving technologies can save energy by 20% to 30%, and some buildings can even achieve energy saving of 40%. Further, confirm the

necessity and feasibility of energy saving and emission reduction. Authors in [12] discussed the sensitivity of building envelopes, including the impact of multilayered wall buildings (36 categories) and different sizes of glass (10-90%) on building energy consumption, and studied the impact of envelopes on building low-carbon impact of development. Authors in [13] took the development of a community in Northern Europe as an example, studied the resource input and carbon emissions of high-energy-efficiency buildings in the construction phase, and proposed excessively improving the energy efficiency of buildings, increasing the input of building materials and energy during the construction phase. Increasing carbon emissions during the construction period and forming a peak of carbon emissions before the building are used and are not conducive to the realization of the short-term carbon reduction target. Attention should be paid to the emission reduction during the construction phase and included in relevant policy formulation. Shaikh et al. [14] conducted research and verification on existing building energy consumption simulation software and believed that climate parameters are the main parameters that affect building energy consumption simulation. For the energy consumption simulation of the entire building, accurate climate data is to achieve accurate quantification. It is an important component of the analysis and discusses that different simulation targets should be selected by different climate data.

Architectural design, as planning before building construction, integrates the requirements of architectural function, architectural technology, and architectural art and is a comprehensive display of various technical means on the basis of satisfying the use of functions [15, 16]. Human requirements for the indoor and outdoor space functions of buildings always change with the development of the times. To meet these ever-changing and increasing requirements, all participants are researching and improving the design. From ancient craftsmen at home and abroad to today's engineers and scholars in many fields such as architecture, engineering, environment, and materials, a lot of research on architectural design has been carried out [17, 18]. However, the construction industry is also an industry with high energy consumption and high pollution. Therefore, in order to alleviate the contradiction between economic development and resources and environment, the construction industry must achieve sustainable development and take the road of green building. In order to carry out the evaluation of the design effect of colleges and universities, this paper introduces the multisensor perception and fuzzy comprehensive evaluation methods. The system test verifies the performance of the university building design effect evaluation model, which can provide a reference for the sustainable development of the construction industry. The paper also presents the security architecture to secure the data of the model. The main objectives of this paper are as follows:

(i) Design multisensor perception and fuzzy comprehensive evaluation methods for the sustainable development of the construction industry

(ii) Design a security model for the sustainable development-related data security

The rest of the paper is organized as follows: Section 2 discusses the architecture design effects and its evaluation. Section 3 presents the multisensor sensing model. Section 4 discusses the evaluation of the effect of college building design based on multisensor perception. Section 5 presents the security model for development data. Section 6 concludes the paper with future direction.

2. Overview of Architectural Design Effect Evaluation

Due to the lack of bottom-up postuse evaluation applications, the above-mentioned problems have further lost the opportunity to give feedback to planning builders and designers. Friedman defined it as a "degree" evaluation in his POE (Post Occupancy Evaluation) book [19, 20]. How to support and meet people's expressly or implicitly expressed needs after the completion of the environment. Each construction practice project is a complete system composed of five stages, which is divided into construction project approval, stationing planning, architectural design, building construction, building operation, and post-use evaluation [21]. The postuse evaluation of penetration at various stages continuously provides feedback and corrections for the smooth implementation and good operation of an engineering construction project [4, 22]. However, as far as the existing research is concerned, the postuse evaluation is mainly used by architects, and only feeds back to the "architectural design" stage, while ignoring the remaining four stages. But only if these five stages are consistently revised can the final architectural quality be improved. Figure 1 shows the closed-loop diagram of the whole process of architectural creation.

Postuse evaluation has three values: short-term, midterm, and long-term. The short-term value lies in the timely assessment of the existing problems in the building and the proposal of targeted correction strategies to avoid loss and expansion; the medium-term value lies in the collection of preliminary project data for large-scale renovation or reconstruction; the long-term value lies in summarizing the design experience of the same type of project and forming available reference basis or industry norms [23, 24]. The evaluation method includes two aspects: quantitative analysis and qualitative analysis. For the construction industry, quantitative analysis is the main method adopted for objective evaluation, while qualitative analysis is the main method adopted for subjective evaluation. The objective evaluation is based on the building design specification documents of different building types, and the data contained in the specifications are determined in a certain period of time. Subjective evaluation refers to the psychological feelings of people entering the building after it is completed. Subjective evaluation has individual differences and is related to people's educational level, personal accomplishment, experience, and rationality. Evaluation is based on people, and people's subjective evaluation of a commercial building is often more direct and
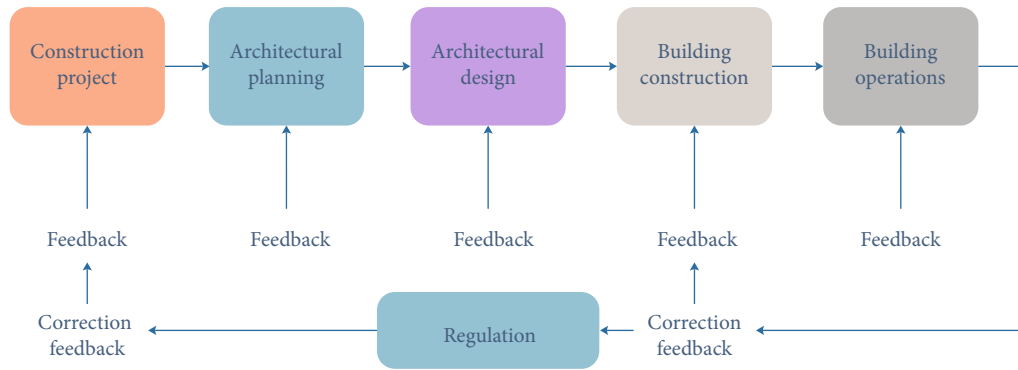
Figure 1: Closed-loop diagram of the whole process of architectural creation.

specific. This is something that designers tend to ignore. The content of the evaluation for commercial buildings includes the age of the evaluator, culture, outdoor environment design of the building, the integrated design of the traffic around the building, the circulation, space, function of the building, the parking design of the building, and the age of the evaluator.

3. Multisensor Sensing

Sensors play an important role in smart transportation, smart home, smart agriculture, and national defense security. These applications have one thing in common, that is, a wide coverage. Therefore, in order to realize these distributed applications, the system must first have a key function, that is, the information sharing capability of the sensor [25]. At present, most sensor application systems usually use different devices to build sensors, which is an important part of the wireless sensor network. It can be seen from the above that the realization of perception depends on sensitive devices, although researchers in the field of materials have been striving to find suitable production materials. However, sensitive devices will be greatly affected in certain environments, such as high temperature, corrosion, humidity, dust, and electromagnetic fields [26]. Figure 2 shows a schematic diagram of a typical sensor component.

Therefore, static characteristics can use range and measurement range, linearity, hysteresis, repeatability, sensitivity, etc., as its indicators. The dynamic characteristic refers to the response characteristic that the output of the sensor changes accordingly when the input quantity changes dynamically with time [27]. The dynamic characteristic of the sensor firstly depends on the sensor itself, which is determined by the dynamic characteristic of the link that plays a major role in the sensor. The bottom node directly contacts the analog signal in the physical world environment to collect and uses the embedded processor architecture to realize the perception function [28]. The middle layer is responsible for the collection and integration of the bottom-level section information with only a single intelligent combination and high-speed real-time upload. At the same time, the high-level decision information is downloaded to the corresponding node and executed. This layer can be a module, or it can be set as a powerful module according to system require-

ments. The uppermost layer gathers all perceptual information and has threshold judgment and decision-making functions, and the PC can be used as a decision support node.

4. Evaluation of the Effect of College Building Design Based on Multisensor Perception

4.1. Cluster Analysis of Building Location. This paper selects the data of the geographical location of the completed building and makes a cluster analysis of its latitude and longitude. Cluster analysis is a multivariate statistical analysis to quantitatively study classification problems according to the characteristics of things themselves [29]. It is a classification method of multivariate statistics "things to cluster." The basic idea is to divide the location into several categories according to the distance, so that the difference of the data within the category is as small as possible, and the difference between the categories is as large as possible.

Step 1. Data standardization.

Supposing domain $x = \{x_1, x_2, \cdots x_n\}$ is the object to be classified, and each object is represented by m indicators, then each variable can be expressed as x_{ij}.

Mean:

$$x_j = \frac{1}{n} \sum_{i=1}^{n} x_{ij}.$$ (1)

Standard deviation:

$$s_{ij} = \sqrt{\frac{1}{n-1} \sum_{i=1}^{n} (x_{ij} - x_{ij})^2}.$$ (2)

After standardization:

$$x_{ij}^* = \frac{x_{ij} - x_j}{s_j} (s_j \neq 0).$$ (3)

Step 2. Determine the similarity coefficient r_{ij} using the Euclidean distance method for cluster analysis.

Each task position can be regarded as a point in the three-dimensional space. The task position constitutes the
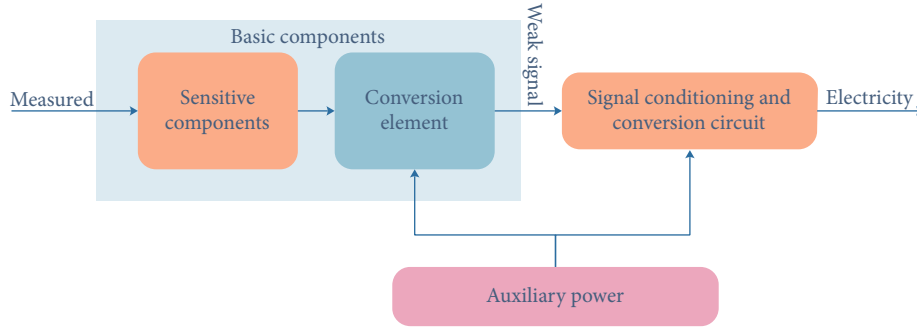
FIGURE 2: Schematic diagram of sensor components.

TABLE 1: The latitude and longitude coordinates of the clustering points and the number of various tasks.

Cluster points	1	2	3	4	5
Latitude of cluster points	23.066	23.565	22.958	22.713	23.101
Cluster point longitude	113.03	113.55	113.75	114.06	113.30
Number of buildings in cluster area	80	23	159	72	187

point in the three-dimensional space. A matrix is formed between the task position and the cluster center, and the Euclidean distance between the task position and the cluster center is calculated. Let x_i denote the ith cluster center $i = 1, 2, 3, 4, 5$ and denote the distance between the ith cluster point and the jth task position, the Euclidean distance calculation method is

$$d_{ij}(2) = \left[\sum_{k=1}^{n} \left(x_{ik} - x_{jk} \right)^2 \right]^{1/2} \quad (i, j = 1, 2, \cdots, n). \tag{4}$$

Step 3. Use SPSS to analyze the data completed by the tasks in Annex 1, and we have obtained the latitude and longitude coordinates of the cluster center point and the number of tasks in each category. The latitude and longitude coordinates of the clustering points and the number of tasks are shown in Table 1.

4.2. Establishment and Solution of Multiple Regression Model. First, analyze the Pearson correlation coefficient of the four indicators to determine whether they are linearly correlated [30]. First, integrate the data to calculate the Pearson correlation coefficient of each indicator and the rest of the indicators, and then obtain the average of the square sum of the Pearson correlation coefficients of a certain indicator and the rest of the indicators and obtain the A of each indicator R_{vi}^2.

The definition of Pearson's correlation coefficient is B:

$$R = \frac{1}{n} \sum_{i=1}^{n} \left(\frac{y_i - y}{s_y} \right) \left(\frac{x_i - x}{s_x} \right) = \frac{\text{cov}\,(Y, X)}{s_y s_x}. \tag{5}$$

If $|R| \approx 0$, it indicates that there is no linear correlation between the two variables. If $|R| \approx 1$, it shows that the two variables are completely linearly related. The direction of linear correlation is indicated by the sign of the correlation

TABLE 2: The mean value of the sum of squares of the correlation coefficients of each indicator and the other indicators.

Index	v_1	v_2	v_3	v_4
Mean sum of squares	0.856	0.758	0.625	0.791

coefficient, "+" means positive correlation, and "-" means negative correlation.

$$\bar{R}_{vi}^2 = \frac{\sum_{j=1}^{m} R_{vivj}^2}{m - 1}, \quad j = 1, 2, \cdots m, j \neq i. \tag{6}$$

In the formula, v_i is the index code, v_1 is the task location, v_2 is the member density, v_3 is the distance between the task and the member, and v_4 is the reputation value within a certain range. $\bar{R}_{vi}^2$ represents the average of the sum of squares of the Pearson correlation coefficient R of the indicator v_i and the remaining variables $v_j (i \neq j)$. m is the number of variables.

Finally, it is determined whether there is a linear relationship between the three indicators of building geographic location, personnel density, and the distance between building geographic location and personnel and task pricing. The postuse evaluation of penetration at various stages continuously provides feedback and corrections for the smooth implementation and good operation of an engineering construction project. Table 2 describes the mean value of the sum of squares of the correlation coefficients of each indicator and the other indicators.

It can be seen from Table 2 that the minimum value of $\bar{R}_{vi}^2$ is 0.625, and the linear relationship between various variables is strong. The linear relationship between v_1, v_2, v_3, and v_4 and task pricing y can be expressed by the linear regression equation.

$$y = b_0 + b_1 x_1 + \cdots + b_p x_p + \varepsilon, \quad \varepsilon \sim N\left(0, \sigma^2\right). \tag{7}$$

In the formula, $b_0, b_1, \cdots b_p, \sigma$ is an unknown parameter that has nothing to do with $x_1, x_2, \cdots, x_p$.

Let $(x_{11}, x_{12}, \cdots, x_{1p}, y_1), \cdots (x_{n1}, x_{n2}, \cdots, x_{np}, y_n)$ be a sample. Estimate the parameters using the least square method.

$$Q = \sum_{i=1}^{n} \left(y_i - b_0 - b_1 x_n - \cdots - b_p x_{1p} \right)^2. \qquad (8)$$

Take the partial derivatives of Q with respect to $b_0, b_1, \cdots b_p$, and set them equal to zero, we get

$$\frac{\partial Q}{\partial b_j} = -2 \sum_{i=0}^{n} \left(y_i - b_0 - b_1 x_{i1} - \cdots - b_p x_{ip} \right) x_{ij} = 0, \quad (j = 1, 2, \cdots, p). \qquad (9)$$

Simplify the above formula to

$$b_0 \sum_{i=1}^{n} x_{i1} + b_1 \sum_{i=1}^{n} x_{i1}^2 + b_2 \sum_{i=1}^{n} x_{i2} x_{i1} + \cdots + b_p \sum_{i=1}^{n} x_{ip} x_{i1} = \sum_{i=1}^{n} y_i x_{i1}, \qquad (10)$$

that is, the maximum likelihood estimation of the unknown parameter $(b_0, b_1, \cdots, b_p)$. So the linear regression equation is

$$\hat{y} = b_0 + b_1 x_1 + \cdots + b_p x_p. \qquad (11)$$

Calculated with SPSS19.0 software:

$$y = -23.56 + 0.35 v_1 - 0.64 v_2 + 0.26 v_3 + 0.15 v_4,$$
$$R^2 = 0.58. \qquad (12)$$

$R^2 = 0.58$ indicates that 58% of the relationship between the geographic location of the building and the four indicators can be determined by the regression equation.

Assume that the functional relationship between task pricing on the 4 indicators is

$$y = a_1 v_1 + a_2 v_2 + a_3 v_3 + a_4 v_4 + b. \qquad (13)$$

Among them, a_i is the parameter to be estimated, and b is a constant. Estimated by the least square method: $y = -23.56 + 0.35 v_1 - 0.64 v_2 + 0.26 v_3 + 0.15 v_4$; the p value corresponding to parameter v_1, v_2, v_3, and v_4 is 0.46, 0.47, 0.008, and 0.097. Perform a heteroscedasticity test on the model to get $p = 0.891$. The original hypothesis is that the model is homoscedastic. Accept the original condition, that is, there is no heteroscedasticity. The serial correlation test $DW = d = 1.85$, $d_u = 1.83$ satisfies $d_u < d < 4 - d_u$, and it is judged that there is no serial autocorrelation in this regression equation. Use the least square method to find the regression estimation equations for each explanatory variable one by one, and the results are shown in Table 3.

When the significance level is 0.05, $F(1, 29) = 4.18$ is found. Because the independent variable v_4 is $F = 1.41 <$

TABLE 3: Results of the first regression.

Equation	R^2	The estimated p value of the parameter	F	Residual sum of squares
$y = 23.16 + 56.12 v_1$	0.056	0.2589	14.55	304.12
$y = 14.23 - 15.89 v_2$	0.325	0.2345	9.36	204.23
$y = 0.258 + 0.68 v_3$	0.256	0.025	17.58	160.25

TABLE 4: The second regression analysis.

Equation	R^2	The estimated p value of the parameter	F	Residual sum of squares
$y = 0.561 v_1 - 0.398 v_2 + 0.256$	0.741	0.063	42.1	58.1
$y = 0.38 v_1 + 0.24 v_3 - 0.368$	0.76	0.025	51.2	87.9

$F_{0.05}(1, 29) = 4.18$, and the p value of the parameter estimation is too large, it shows that the regression model of v_4 to y is not significant, indicating that the member reputation value has no great relationship with task pricing. Regarding the independent variable v_2, the regression significance is not high, but for the variable v_1, you can continue to the next step of regression. Select v_1 with better test results in all aspects as the first selected variable, remove the influence of v_4 on y, and do the second time return. Table 4 shows the results of the second regression analysis.

When the significance level is 0.05, $F_{0.05}(2, 28) = 3.34$ and $F_{0.05}(1, 28) = 4.20$ are obtained by looking up the table. As the variables are added one by one, the improvement of the variable y equation is basically unchanged. Since $F_1 = 42.1$ and $F_2 = 51.2$, and both are greater than $F_{0.05}(1, 18) = 4.41$, it shows that the model is significant as a whole. The heterogeneous test of the model is $p = 0.87$, which means that there is no variance in the model; the serial correlation test is performed on the model. Since $DW = d = 2.02$ and $d_u = 1.67$ meet $d_u < d < 4 - d$, it means that the model does not have serial autocorrelation. So this model is the optimal model.

4.3. Optimization of Geographical Location of Buildings Based on Genetic Algorithm. Objective function expression:

$$\max f = \sum_{i \in m} \sum_{j \in m} x_{jk} y_{ijk} z - \sum_{g \in n} p_g \forall k \in p, \qquad (14)$$

where m is the node set, $\{0, 1, 2 \cdots i\}$, n is the node collection of the task point, $\{1, 2, \cdots, g\}$, p is a collection of crowdsourced member tasks participating in the task, $\{1, 2, , \cdots, k\}$, x_{jk} is the amount of tasks the member accepts at the task point, and z is the member's income for each task completed.

Constraints on task points, membership amount, and completion ability at each point. The amount of tasks
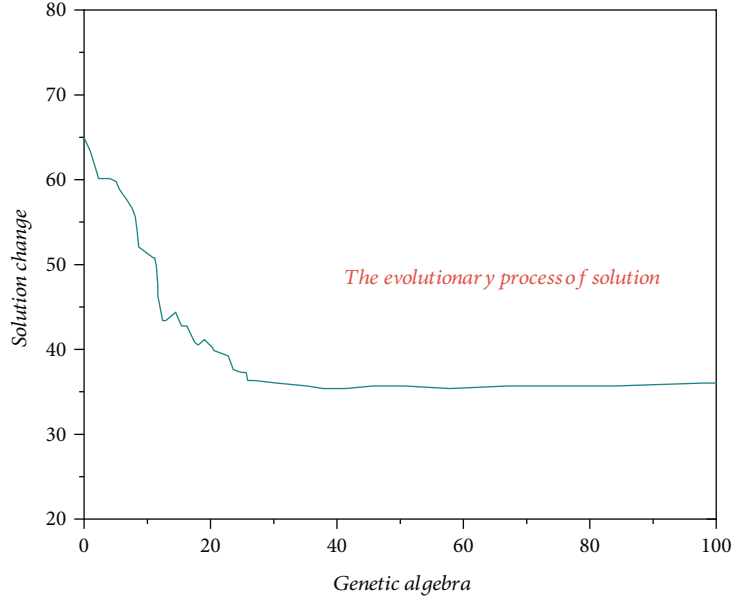
FIGURE 3: Evolution process of genetic algorithm.

completed by new members in a single time must not be less than the minimum amount of tasks completed:

$$\sum_{i \in m} \sum_{j \in m} x_{jk} y_{jk} \geq N. \tag{15}$$

The sum of the tasks accepted by all members is not greater than the sum of the tasks generated by the positions of all the characters:

$$\sum_{i \in m} \sum_{j \in m} \sum_{k \in p} x_{jk} y_{jk} \leq Q. \tag{16}$$

The task accepted by each task person is not greater than its maximum task completion ability:

$$\sum_{i \in m} \sum_{j \in m \cup N^*} \sum_{k \in p} x_{jk} y_{jk} \leq M. \tag{17}$$

Time window constraints:

$$T_{jk} = y_{jk} \left(T_{jk} + t_{ij} + t_i' \right), \tag{18}$$

$$T_{jk} = y_{jgk} t_{jg} T_{hk} = y_{ghk} \left(T_{jk} + T_{jgk} + t_{gh} \right) t_{oj} = 0. \tag{19}$$

Relational constraints between sets:

$$
\begin{aligned}
L &= L' + \sum_{e \in E} L_e, \\
R &= R' + \sum_{e \in E} L_e.
\end{aligned}
\tag{20}
$$

Penalty function constraint:

$$P_g = \begin{cases} \beta \times (T_{hk} - LT_h), & T_{hk} > LT_h, \\ 0, & T_{hk} \leq LT_h. \end{cases} \tag{21}$$

Decision variable constraints:

$$
\begin{aligned}
y_{jgk} &= \min \left\{ y_{ijk}, y_{ghk} \right\}, \\
y_{ijk}, y_{jgk}, y_{ghk} &\in \{0, 1\}.
\end{aligned}
\tag{22}
$$

The genetic algorithm is used to solve the problem by programming, and the iterative process of the solution of the model is shown in Figure 3.

The genetic algorithm used in this paper has been iterated 100 times and found that after roughly 27 iterations, the solution obtained has stabilized. The results obtained clearly solve the problems of optimizing paths and merging tasks. Table 5 shows the solution results of the optimization model.

According to the above optimization results, a comparison between before and after optimization can be obtained. Table 6 shows the comparison between before and after optimization.

Cluster analysis and genetic algorithm are used in the processing and analysis process of building multiterminal sensor data. In this paper, a genetic algorithm is used to process and optimize the sensor information, and the performance of the university building design effect evaluation model is verified through system testing, which can provide a reference for the sustainable development of the construction industry.

TABLE 5: Solution results of the optimized model.

Personnel number	Member task completion path after optimization	Number of tasks	Member income	Completion
1	$A9 \longrightarrow A1 \longrightarrow B1 \longrightarrow B3 \longrightarrow B11$	5	325	$1+1+1+1+1$
2	$A8 \longrightarrow A9 \longrightarrow A2$	3	210	$1+1+1$
3	$A9 \longrightarrow A6 \longrightarrow B4 \longrightarrow B1$	4	199.5	$1+1+1$
4	$A3 \longrightarrow A5 \longrightarrow A4 \longrightarrow B5 \longrightarrow B2$	5	268	$1+1+1+1$
5	$A1 \longrightarrow A6 \longrightarrow B3 \longrightarrow B10$	4	240	$1+1+1$

TABLE 6: Comparison of before and after optimization.

	Before optimization	Optimized
The number of members needed (person)	68	46
Average single task evaluation (%)	66.5	86
Mission completion	62.39%	60.23%
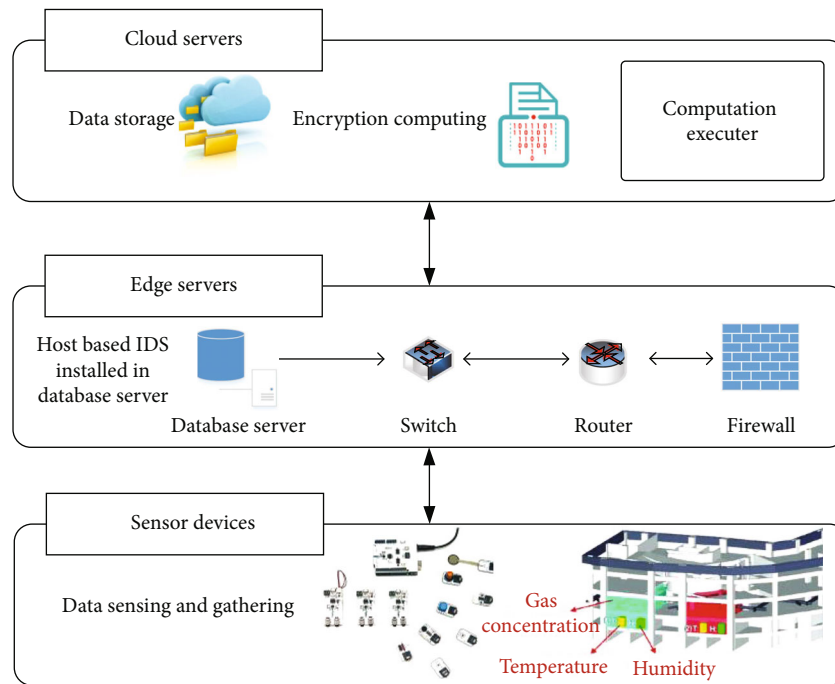
FIGURE 4: IDS system for edge computing.

5. Security Model for the Sustainable Development-Related Data Security

The huge data is collected from the systems and sensor nodes. The centralized database stores all the data for further processing and analyzing. The data is collected from the construction activities that start from planning and completion phases [31, 32]. As security is one of the challenge especially when the data transmitted to the edge computing or to the cloud for further decision making, we proposed a IDS solution at the edge computing side to protect all the data coming from ground network and sensor devices. The Intrusion Detection System (IDS) is installed at the edge computing side to filter the data and detection and prevent the data

from any sort of malicious activities in the network. Figure 4 shows the IDS deployment at the edge side to protect the building data from unauthorized access.

6. Conclusion

The buildings obtained from the construction activities according to the drawings are the true manifestation of the design results. The goals must be determined in the project planning stage, and the specific implementation plan must be determined in the design stage. Through a reasonable design plan, the carbon emissions of the building's life cycle can be reduced. Architectural design, as a planning before building construction, integrates the requirements of

architectural function, architectural technology, and architectural art and is a comprehensive display of various technical means on the basis of satisfying the use of functions. Therefore, this article has carried out an evaluation of the effect of architectural design. At present, the research on building energy efficiency mainly focuses on building design or the whole life cycle. There are not many researches on the operation phase. The existing research mainly includes the discussion of the owner and property management mode and the development of the energy-consuming equipment database during the operation. The research on energy consumption evaluation standards needs to be further in-depth. Building energy efficiency is a hot topic today. In the face of my country's current national conditions, the most direct and effective energy saving should start from the operation of existing buildings. The research done on this subject still needs to be expanded in the following aspects. The research on the energy-saving coefficient during operation still needs to be further explored, guided by practicality, operability, and effectiveness, to provide effective theoretical tools and measurement scales for building energy saving. This paper also presented the IDS system deployment model at the edge computing side for data traffic detection and prevention form any malicious activities in the network. Based on the research content of this article, in the next step, we will try to place the sensing method in different experimental environments, further enrich the sensing model, establish a complete sensor information database, and facilitate the addition and identification of various sensors, while also standardizing the manufacture of sensors.

Data Availability

The data in the paper has been included in the article.

Conflicts of Interest

The authors declare that they have no conflicts of interest.

References

[1] X. Shi and W. Yang, "Performance-driven architectural design and optimization technique from a perspective of architects," *Automation in Construction*, vol. 32, pp. 125–135, 2013.

[2] V. Granadeiro, J. P. Duarte, J. R. Correia, and V. M. Leal, "Building envelope shape design in early stages of the design process: integrating architectural design systems and energy simulation," *Automation in Construction*, vol. 32, pp. 196–209, 2013.

[3] U. Zdun, R. Capilla, H. Tran, and O. Zimmermann, "Sustainable architectural design decisions," *IEEE Software*, vol. 30, no. 6, pp. 46–53, 2013.

[4] A. Hollberg and J. Ruth, "LCA in architectural design–a parametric approach," *The International Journal of Life Cycle Assessment*, vol. 21, no. 7, pp. 943–960, 2016.

[5] L. Su, "An automatic grid generation approach over free-form surface for architectural design," *Journal of Central South University*, vol. 21, no. 6, pp. 2444–2453, 2014.

[6] J. I. Kim, H. Jung, and S. J. Koh, "Mobile oriented future internet (MOFI): architectural design and implementations," *ETRI Journal*, vol. 35, no. 4, pp. 666–676, 2013.

[7] Y. Yu, Q. Zhang, Q. Yao, J. Xie, and J. Y. Lee, "Architectural design of heterogeneous metallic nanocrystals principles and processes," *Accounts of Chemical Research*, vol. 47, no. 12, pp. 3530–3540, 2014.

[8] C. Dapogny, A. Faure, G. Michailidis, G. Allaire, A. Couvelas, and R. Estevez, "Geometric constraints for shape and topology optimization in architectural design," *Computational Mechanics*, vol. 59, no. 6, pp. 933–965, 2017.

[9] W. Jianguo, "Tentative suggestions on the development paths of architectural design in the context of new-type urbanization in China," *Architectural Journal*, vol. 2, 2015.

[10] C.-H. Hsu, C.-K. Chen, and M.-J. Hwang, "The architectural design of networks of protein domain architectures," *Biology Letters*, vol. 9, no. 4, article 20130268, 2013.

[11] J. Kneifel, "Life-cycle carbon and cost analysis of energy efficiency measures in new commercial buildings," *Energy and Buildings*, vol. 42, no. 3, pp. 333–340, 2010.

[12] R. M. Dowd and M. Mourshed, "Low carbon buildings: sensitivity of thermal properties of opaque envelope construction and glazing," *Energy Procedia*, vol. 75, pp. 1284–1289, 2015.

[13] A. Säynäjoki, J. Heinonen, and S. Junnila, "A scenario analysis of the life cycle greenhouse gas emissions of a new residential area," *Environmental Research Letters*, vol. 7, no. 3, article 034037, 2012.

[14] P. H. Shaikh, N. B. M. Nor, P. Nallagownden, I. Elamvazuthi, and T. Ibrahim, "A review on optimized control systems for building energy and comfort management of smart sustainable buildings," *Renewable and Sustainable Energy Reviews*, vol. 34, pp. 409–429, 2014.

[15] S. Chatterjee, A. J. Matas, T. Isaacson, C. Kehlet, J. K. Rose, and R. E. Stark, "Solid-State13C NMR delineates the architectural design of biopolymers in native and genetically altered tomato fruit cuticles," *Biomacromolecules*, vol. 17, no. 1, pp. 215–224, 2016.

[16] Y. Wu, S. S. Mechael, Y. Chen, and T. B. Carmichael, "Velour fabric as an island-bridge architectural design for stretchable textile-based lithium-ion battery electrodes," *ACS Applied Materials & Interfaces*, vol. 12, no. 46, pp. 51679–51687, 2020.

[17] B. Cao, M. Hu, Y. Cheng et al., "Tailoring the d -band center of N-doped carbon nanotube arrays with Co_4N nanoparticles and single-atom Co for a superior hydrogen evolution reaction," *NPG Asia Materials*, vol. 13, no. 1, pp. 1–14, 2021.

[18] M. M. Philip, K. Natarajan, A. Ramanathan, and V. Balakrishnan, "Composite pattern to handle variation points in software architectural design of evolving application systems," *IET Software*, vol. 14, no. 2, pp. 98–105, 2020.

[19] C. D. Cadenhead, "Architectural design of critical care units: a comparison of best practice units and design," in *Pediatric Critical Care Medicine*, pp. 17–32, Springer, 2014.

[20] Y. Uchiyama, E. Blanco, and R. Kohsaka, "Application of biomimetics to architectural and urban design: a review across scales," *Sustainability*, vol. 12, no. 23, p. 9813, 2020.

[21] M. Liu, M. Zhou, L. Ma, H. Yang, and Y. Zhao, "Architectural design of hierarchically meso–macroporous carbon for microbial fuel cell anodes," *RSC Advances*, vol. 6, no. 33, pp. 27993–27998, 2016.

[22] J. Qi, L. Pan, S. Ren, F. Chang, and R. Wang, "SMTS: a swarm intelligence-inspired sensor wake-up control method for

multi-target sensing in wireless sensor networks," *Wireless Networks*, vol. 26, no. 5, pp. 3847–3859, 2020.

[23] Y. He, G. Chen, C. Potter, and R. K. Meentemeyer, "Integrating multi-sensor remote sensing and species distribution modeling to map the spread of emerging forest disease and tree mortality," *Remote Sensing of Environment*, vol. 231, article 111238, 2019.

[24] C. Li, S. Yang, Y. Guo et al., "Flexible, multi-functional sensor based on all-carbon sensing medium with low coupling for ultrahigh-performance strain, temperature and humidity sensing," *Chemical Engineering Journal*, vol. 426, article 130364, 2021.

[25] P. Zolfaghari, O. K. Erden, O. Ferhanoglu, M. Tümer, and A. D. Yalcinkaya, "MRI compatible fiber optic multi sensor platform for real time vital monitoring," *Journal of Lightwave Technology*, vol. 39, no. 12, pp. 4138–4144, 2021.

[26] M. Reddeppa, B.-G. Park, N. D. Chinh et al., "A novel low-temperature resistive NO gas sensor based on InGaN/GaN multi-quantum well-embedded p–i–n GaN nanorods," *Dalton Transactions*, vol. 48, no. 4, pp. 1367–1375, 2019.

[27] M. Ludwig, T. Morgenthal, F. Detsch et al., "Machine learning and multi-sensor based modelling of woody vegetation in the Molopo area, South Africa," *Remote Sensing of Environment*, vol. 222, pp. 195–203, 2019.

[28] X. Niu, X. Yang, H. Li, Q. Shi, and K. Wang, "Chiral voltammetric sensor for tryptophan enantiomers by using a self-assembled multiwalled carbon nanotubes/polyaniline/sodium alginate composite," *Chirality*, vol. 33, no. 5, pp. 248–260, 2021.

[29] Y. Zheng, P. P. Shum, Y. Luo et al., "High-resolution, large-dynamic-range multimode interferometer sensor based on a suspended-core microstructured optical fiber," *Optics Letters*, vol. 45, no. 4, pp. 1017–1020, 2020.

[30] J. H. Jensen, "A graph-based genetic algorithm and generative model/Monte Carlo tree search for the exploration of chemical space," *Chemical Science*, vol. 10, no. 12, pp. 3567–3572, 2019.

[31] H. Nafea, K. Kifayat, Q. Shi, K. N. Qureshi, and B. Askwith, "Efficient non-linear covert channel detection in TCP data streams," *IEEE Access*, vol. 8, pp. 1680–1690, 2020.

[32] K. N. Qureshi, S. Qayyum, M. N. Ul Islam, and G. Jeon, "A secure data parallel processing based embedded system for internet of things computer vision using field programmable gate array devices," *International Journal of Circuit Theory and Applications*, vol. 49, pp. 1450–1469, 2021.

Research Article

Performance Evaluation of Machine Learning-Based Channel Equalization Techniques: New Trends and Challenges

Shahzad Hassan,[1] **Noshaba Tariq,**[1] **Rizwan Ali Naqvi,**[2] **Ateeq Ur Rehman** [ID],[3] **and Mohammed K. A. Kaabar** [ID][4,5]

[1]*Department of Computer Engineering, Bahria University Islamabad, Pakistan*
[2]*Department of Unmanned Vehicle Engineering, Sejong University, Seoul 05006, Republic of Korea*
[3]*Department of Electrical Engineering, Government College University, Lahore 54000, Pakistan*
[4]*Gofa Camp, Near Gofa Industrial College and German Adebabay, Nifas Silk-Lafto, 26649 Addis Ababa, Ethiopia*
[5]*Institute of Mathematical Sciences, Faculty of Science, University of Malaya, Kuala Lumpur 50603, Malaysia*

Correspondence should be addressed to Ateeq Ur Rehman; ateeq.rehman@gcu.edu.pk
and Mohammed K. A. Kaabar; mohammed.kaabar@wsu.edu

Wireless communication systems have evolved and offered more smart and advanced systems like ad hoc and sensor-based infrastructure fewer networks. These networks are evaluated with two fundamental parameters including data rate and spectral efficiency. To achieve a high data rate and robust wireless communication, the most significant task is channel equalization at the receiver side. The transmitted data symbols when passing through the wireless channel suffer from various types of impairments, such as fading, Doppler shifts, and Intersymbol Interference (ISI), and degraded the overall network performance. To mitigate channel-related impairments, many channel equalization algorithms have been proposed for communication systems. The channel equalization problem can also be solved as a classification problem by using Machine Learning (ML) methods. In this paper, channel equalization is performed by using ML techniques in terms of Bit Error Rate (BER) analysis and comparison. Radial Basis Functions (RBFs), Multilayer Perceptron (MLP), Support Vector Machines (SVM), Functional Link Artificial Neural Network (FLANN), Long-Short Term Memory (LSTM), and Polynomial-based Neural Networks (NNs) are adopted for channel equalization.

1. Introduction

In wireless communication systems [1–3], the performance may be severely degraded because of wireless channel issues. The transmitted signal passes through the communication channel and has faced various impairment issues such as Intersymbol Interference (ISI), Doppler shift, and fading effects. All these effects tend to degrade and limit the data throughput during data communication [4]. To achieve higher data rates, it is mandatory to mitigate the effects of channel-induced impairments. This requires an adaptive filter for equalization to nullify the effects of the wireless channel and recover the originally transmitted data. Recently, the use of Machine Learning (ML) [5, 6] techniques especially

Artificial Neural Network- (ANN-) based methods has gained interest due to its remarkable success in the fields of Computer Vision (CV), speech recognition, and Natural Language Processing (NLP). These techniques although invented in the mid-20th century were not very popular due to the lack of required computational power. The availability of high-speed computational resources and the success of ML in various other fields have provoked its applications for the development of robust communication systems [7]. Many researchers have proposed the use of ML for designing communication systems and have demonstrated improved results in terms of Bit Error Rate (BER). However, still, there are some concerns and questions which require answers such as the following:

(i) What will be the maximum performance gain in terms of BER by using NN and its variants such as Multilayer Perceptron (MLP), Radial Basis Functions (RBFs), Functional Link Artificial Neural Network (FLANN), Support Vector Machines (SVM), and Long-Short Term Memory (LSTM)

(ii) Is it possible to train the NN to estimate a wireless channel in real time as required by the modern-day channel equalizers to mitigate the channel in real time? Typically, an equalizer is required to train its taps in less than a few microseconds. What possible methods can be used to achieve this task

During data transmission, networks have experienced various types of impairments such as path loss which results in attenuation of the signal, AWGN, and multipath effects caused by the reflections of the electromagnetic waves from various obstacles. The input digital data is fed into the source encoder which effectively transforms the bitstream into the compressed form by using Huffman encoding. The input can be an audio source, text, binary, or any other sensor input, which may require A/D conversion before feeding to the source encoder block [8].

The digital data at this stage can also be secured using encryption algorithms.

The resulting data sequence at the output of the source encoder is passed to the channel encoder which adds redundancy in a controlled manner, to help the receiver to detect and correct the channel-induced errors. This step should make the data robust against harsh channel conditions. In the next step, the output of a channel encoder is given to a modulator that applies digital modulation methods such as BPSK, QPSK, or some variants of FSK. The output of the modulator is fed to the frequency upconverter which translates the baseband signals to passband frequency, and finally, the signal is amplified to the appropriate levels and then transmitted through the antenna. The motivation of this research work is as follows.

(i) To identify the performance metrics for the existing channel estimation and equalization techniques

(ii) To identify an improved channel equalization technique for the selected wireless channel

To critically assess the performance of various channel equalization techniques by performing simulations, the mathematical formulation is presented in [8] for the communication system where they considered $s(t)$ to be the transmitted signal. It is represented mathematically in Equation (1). Figure 1 shows the transmitter and receiver block:

$$s(t) = \text{Re}\left[x(t)e^{j\omega_c t}\right], \tag{1}$$

where $x(t)$ is the baseband signal and "$\omega c = 2\pi f c$" is the center frequency of the passband signal. The received signal is given as in
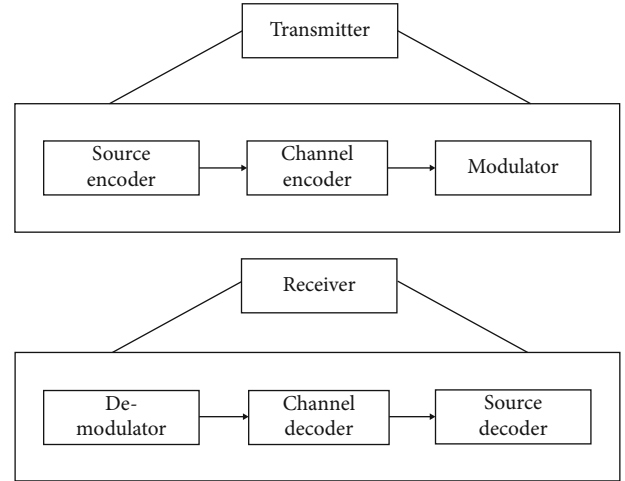
Figure 1: Transmitter and receiver block [8].

$$r(t) = \sum_{m=0}^{N-1} \gamma_m(t)s(t - \tau_m) + w(t), \tag{2}$$

where $\gamma_m(t)$ represents the complex amplitude of the channel, τ_m is the delay of the mth multipath, and N represents the total number of multipaths. $w(t)$ represents the AWGN. The resulting received signal can be written as in

$$r(t) = \sum_{m=0}^{N-1} \gamma_m(t)e^{j\omega_c \tau_m}x(t - \tau_m) + w(t), \tag{3}$$

$$r(t) = \int_{-\infty}^{\infty} h(\tau, t)x(t - \tau)d\tau + w(t), \tag{4}$$

where $h(\tau, t) = \sum_{m=0}^{N-1}\gamma_m(t)e^{j\omega_c \tau_m}\delta(t - \tau)$ is the impulse response of the time-varying channel. It is the main goal of wireless communication systems to estimate $h(\tau, t)$ which is the channel impulse response for the desired level of performance.

1.1. Performance Issues in Wireless Communications. One of the primary goals while designing a communication system is to achieve the performance as closer to Shannon's capacity definition [9] as given in

$$C = B(1 + \gamma), \tag{5}$$

where C is the capacity of the wireless channel, B represents the bandwidth, and "γ" represents the Signal to Noise Ratio (SNR). This theorem gives the fundamental bound on the achievable capacity of the wireless channel. All communication systems tend to achieve Shannon's capacity. As of today, this goal has not been fully achieved due to many reasons. Amongst the most notable reasons are

(i) the wireless channel

(ii) Signal to Noise Ratio (SNR)

(iii) link budget

FIGURE 2: The classification of equalization techniques [16].

Assuming the availability of the required bandwidth, these three objectives must be served to achieve the desired performance in wireless communication. SNR and link budget can be improved using high gain antennas, more transmit power, and better antennas; however, the effects ca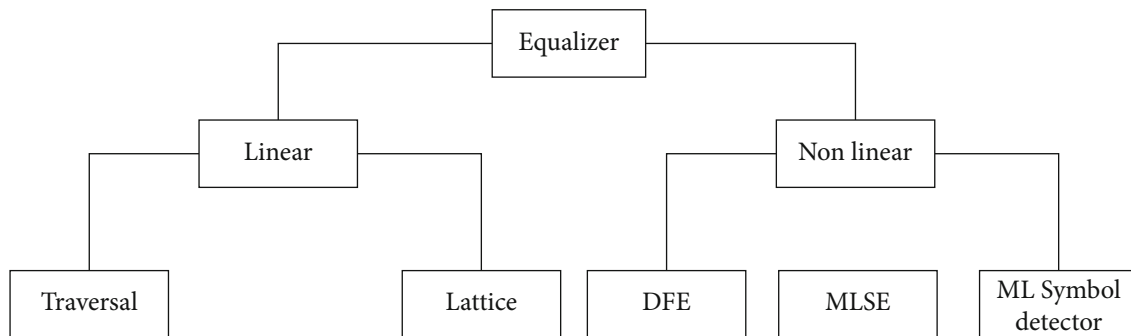used by the channel require more sophisticated handling. Its effects must be mitigated using the channel equalization method.

1.2. Channel Estimation Techniques. Channel estimation techniques are broadly categorized into three main types, the Pilot-Aided Channel Estimation (PACE) techniques, Blind and Semiblind Channel Estimation (BSB) techniques, and Decision-Directed Channel Estimation (DDCE) techniques [10]. In [10], an estimation technique was presented for the transmitter sending a known sequence of data symbols to the receiver called pilot symbols. The receiver estimates the channel with the help of received pilots using mathematical techniques.

In [11], the receiver has no information about the input signal of the channel. This technique uses the data symbols for channel estimation by employing the precoding of the symbols at the transmitter. The receiver knows the parameters of the precoding used at the transmitter and then uses correlation-based methods to estimate the channel information [12–14]. In [15], the authors used the pilot symbols and the demodulated symbols for the channel estimation. In the absence of bit errors, the symbols can be used for estimation of the channel impairments and start acting as the pilot symbols. This technique proves to be more efficient as compared to the pilot symbol based on channel estimation techniques because it reduces the bandwidth by saving the number of pilots required in pilot-based channel estimation techniques.

1.3. Channel Equalization. Channel equalization and channel estimation are interdependent. The inverse of the channel estimate can be used for channel equalization. The performance of the equalizer is proportional to the accuracy of the channel estimation.

The equalization mechanism can be divided into two modes including a training mode and a decision-directed mode. In the first mode, the equalizer is trained by sending a training sequence. The training sequence is known as a priori to the receiver. Equalizer weights are learned using the training

sequence. In the second mode, the equalizer is operated on the channel to estimate the channel. Various types of equalizers are used in the digital communication receiver. Figure 2 depicts the classification of the equalizers [16].

Equalization is generally divided into two categories including linear equalizers and nonlinear equalizers. The linear equalizers employ only a feedforward path and do not use the output of the equalizer in the equalization process. On the other hand, the nonlinear equalizers use the output of the equalizer in the determination of the future samples. Both the linear and nonlinear equalizers employ adaptive algorithms such as LMS, NLMS, RLS, and Kalman filtering for the adaptation of the equalizer weights. Amongst the nonlinear equalizers, it is the Maximum Likelihood Sequence Estimator (MLSE). This type of equalizer does not use the filter for equalizing the channel but instead uses the Viterbi algorithm to decode the sequence and chooses the sequence with maximum probability as the output.

2. Machine Learning-Based Channel Equalization Technique Results

ML is a subfield of computer science that focuses on the development of algorithms to learn and solve complex problems. Unlike the traditional approach, it does not use predefined models or a set of equations to solve the given problem; instead, it learns to solve the problem. It consists of the human brain-like neurons termed "perceptrons." A perceptron is a simple mathematical model (function) that maps the set of inputs to the set of outputs and performs three basic operations: multiplication, summation, and activation. Each input value is multiplied by its corresponding weight.

The previously weighted inputs are then summed up and passed through the activation function. The activation function determines the output of the neuron concerning its input. The commonly used activation functions are threshold, linear, sigmoid, and "ReLU." Mathematically, a perceptron can be defined in Equation (6). By subtitling the values, Equation (6) becomes (8):

$$y(x) = \varphi\left(w^T x + b\right). \tag{6}$$

Here, w is a weight vector, b is a bias, and $w^T x$ is a dot product of w and x as represented in Equation (7):

$$z = \sum_{i=1}^{N} w_i x_i, \tag{7}$$

$$y(x) = \varphi\left(\sum_{i=1}^{N} w_i x_i + b\right). \tag{8}$$

$\varphi(\cdot)$ is the activation function. A sigmoid and "ReLU" functions are defined in

$$\varphi(x) = \frac{1}{1 + e^{-x}}, \tag{9}$$

$$\varphi(x) = \max(0, x). \tag{10}$$

3. Related Work

NNs are capable of processing nonlinear data and can produce complex decision regions. A new framework based on exploiting feature selection and neural network techniques has been proposed for identifing focal and nonfocal Electro-encephalogram signals in TQWT domain [17]. Therefore, NNs can be employed for equalization purposes to overcome the difficulties associated with channel nonlinearities [18–20]. The performance of NN-based equalizers has been reported as superior to other conventional adaptive equalizers. In the recent past, the use of NNs has gained popularity in the design of software-defined radios where DNN, CNN, and RNN have been applied for classical radio operations [21–24]. In [25], the deep NNs have been used for the channel estimation of doubly selective channels which experience variations both in time and frequency. The deep learning-based algorithm is trained in three steps including the pretraining step, training stage, and testing stage. During the first two steps, the model is developed offline using training data. During the testing stage, the channel is estimated and equalized. The results show improved BER performance as compared to Linear Minimum Mean Square Error (MiMeSqEr). In [26], the ML and NN have been used in the Frequency Division Duplexing (FDD) system which is a double selective channel, and the results showed improvements in terms of MiMeSqEr in the prediction of the channel.

In [27], the NN and DL methods have been used to predict the behavior of the Rayleigh channel, and it has been reported through simulations that the MSE performance compared with the traditional algorithms has improved. In [22, 28], DL has been thoroughly investigated and provided a review of the various ML-based techniques for wireless communication. It has been shown that traditional theories do not meet the higher data rate requirements of communication and limit the efficiency due to complex undefined channel requirements, fast processing, and limited block structure. On the other hand, AI-based communication systems face some challenges that need to be addressed. These challenges include the availability of a large amount of data

and how easily it can be integrated into classical infrastructure [29]. Similarly, ML has been applied to the physical layer for modulation recognition and classification [26, 30–33].

An MLP is a feedforward NN that consists of an input layer, a hidden layer, and an output layer. It has nonlinear decision-making capabilities. The training of MLP is done through the backpropagation algorithm [34]. The MLP is the first neural network used for channel equalization [19, 20, 35–38]. Gibson et al. [20] introduced an MLP-based nonlinear equalizer structure and demonstrated its superior performance over the linear equalizer (LMS). The major drawback of the MLP network is its slow convergence [39]. This is due to the backpropagation algorithm which operates based on first-order information. A genetic algorithm [40] can be used to solve this problem. The convergence can be improved by using the second-order data like the Hessian matrix, which is defined as the second-order partial derivatives of the error performance. In [41], the authors proposed an MLP-based DF equalizer with a lattice filter to overcome the convergence problem to improve the performance of MLP. However, this improvement increased the complexity of the MLP structure.

The RBFNN is a three-layer network that comprises an input layer, a nonlinear hidden layer, and a linear output layer. The input layer contains the source symbols. In the hidden layer, the input space is transformed into a high-dimensional space by using nonlinear basis functions. The output layer linearly combines the output of the previous layers. RBFNN provides an appealing alternative to MLP for channel equalization.

Many techniques have been developed to solve the equalization problem using RBF [42–44]. In 1991 [19], the authors used RBFNN for equalization. Similarly, an RBF-based equalizer has been reported which showed satisfactory performance [45, 46]. Another work has demonstrated the use of RBFNN for equalization and found an improvement in BER [47]. The performance of RBFNN is compared with the Maximum Likelihood Sequence Estimator (MLSE) over the Rayleigh fading channel [45, 48, 49]. Simulations have confirmed that RBFNN is a reasonable choice with low computational complexity. The authors in [50, 51] proposed a complex RBF (CRBF) network, and improved performance is observed. The drawback of RBFNN is that it is not suitable for hardware implementation. The network needs a large number of hidden nodes to achieve the desired performance.

In the last few years, FLANN is very famous [52]. It is a single-layer NN that can form complex decision boundaries. FLANN provides less computational complexity and greater convergence speed than other traditional NNs. From the perspective of hardware implementation, FLANN has a simple design, less computational complexity, and higher computation performance [53, 54].

The input dimension is expanded by using nonlinear functions which may lead to better nonlinear approximation. The expansion is done using three commonly used functions, i.e., trigonometric, Chebyshev expansion, and Legendre expansion. A traditional FLANN uses trigonometric functions, whereas the other two expansions are based on Legendre [55, 56] and Chebyshev [57] polynomials. Ch-

FLANN is another computational efficient network. It has many applications in functional approximation [58], nonlinear dynamic system identification [59, 60], and nonlinear channel equalization [61]. In these networks, the expansion is performed using Chebyshev polynomials.

RNN is a popular DL technique that was first introduced for processing sequential data [24] and gained a lot of attention in the recent past. They have been proven better than traditional signal processing methods in modeling and predicting nonlinear and time series [62] in a wide variety of applications ranging from speech processing and adaptive channel equalization [63–67].

Unlike ANN, which does not have memory and cannot deal with temporal data, RNN has feedback loops which make them attractive for the equalization of nonlinear channels. This means data can be fed back to the same layers. It has been demonstrated through simulations that a reasonable size of RNN can model the inverse of the channel. RNNs are known to outperform FLANN, MLP, and RBF [68, 69]. In [70], the authors discussed that equalizers based on CNN and RNN reduce the channel's fading effects but also increase the overall coding gain by more than 1.5 dB.

RNN has one problem of exploding and vanishing gradient [71]. This problem arises when there is a long dependency in a sequence. To solve this problem, LSTM is proposed [72]. LSTM is slightly different from RNN. It has some special units in addition to standard units. These special units are called memory cells. These units can retain the information for a long period. This means that LSTM detected the patterns even in a long sequence. The sequence problems can be efficiently solved by LSTM and can also solve the channel equalization problem. In this case, future samples can be predicted by taking previous symbols into account. This means that variations in a channel can be easily tracked. We can specify the number of samples that LSTM can hold for the prediction of future sequences. If it is selected according to the delay spread of a channel, more accurate results may be observed.

SVM lies in the category of supervised learning. Originally, it is developed for binary classification. Then, it has been extended to perform regression and multiclass classification problems [73–75]. It has the potential to generalize well in classification problems by maximizing the margin. The trained classifier contains support vectors on the margin boundary and summarizes the information required to separate the data. It uses the parametric learning algorithm, in which a model has fixed learnable parameters which are adapted during the training process. Once the model is trained, these parameters are then used exclusively for testing while discarding all the training examples.

This makes the SVM more computationally efficient. On the other hand, NNs are nonparametric as the number of parameters increases with the number of layers. NN introduces nonlinearity by using nonlinear activation function whereas SVM uses kernel methods that implicitly transform the input space into higher dimensions. RBF kernel is the most commonly used kernel method. The SVM is suggested to address the number of digital communication issues due to its nonlinear processing capability. A DFE based on SVM is proposed, and it is observed that the performance of this equalizer is superior to MiMeSqEr DFE [76]. Similar work is done in [77].

This section provides a comprehensive overview of the channel estimation and equalization techniques. Different neural network structures are discussed in the context of channel equalization. The MLP network implementation is simple, but training takes a lot of time. The main disadvantage of the FLANN structure is its computational and time complexity which gradually increases as the number of input nodes increases. The RBF-based neural network equalizer is an interesting alternative and is successfully used for blind equalization. LSTM equalizers are superior to NN feedforwards, including MLPs, RBFs, and FLANNs.

4. Performance Comparison of NN-Based Channel Equalization Schemes

Channel equalization methods of the respective systems are highlighted. A critical review of the methods is provided. All the methods are found to perform well in Rayleigh communication channels. However, there is a need to compare the schemes and highlight the best possible NN scheme for channel equalization. To the best of the knowledge of the authors, this work is not being carried out in the literature. In this work, the selected NNs are used for channel equalization and their performance is compared.

4.1. Implementation of NN-Based Equalizers. ML techniques are setting a path to replace the conventional communication techniques, and the combination of these two fields has led to a lot of successful work. NNs are capable of processing nonlinear data and can produce complex decision regions. Therefore, NNs can be employed for equalization to overcome the difficulties associated with channel nonlinearities [18–20]. The simulation setup is depicted in Figure 3.

A typical NN-based channel equalizer is depicted in Figure 4. The transmitter first transmits the training symbols which are known to both the receiver and transmitter and then transmits the actual data. The equalizer uses the received training symbols to learn the equalizer weights. The optimization criterion is to minimize the MSE. Figure 4 shows the NN-based equalizer.

4.2. Data Generation and QPSK Modulation. Data is randomly generated using the MATLAB rand function. It generates uniformly distributed data between 0 and 1. The data is QPSK-modulated and then passed through the channel filter. QPSK uses two signals I and Q, where I is an in-phase signal and Q is a quadrature signal. Both of these signals are at a 90° phase difference. This modulation is popular due to its simpler design and efficient hardware realization.

The following steps are performed to produce a QPSK-modulated signal.

   (i) The incoming digital data is converted into two streams. One stream contains the odd bits, and the other takes the even bits from the original stream
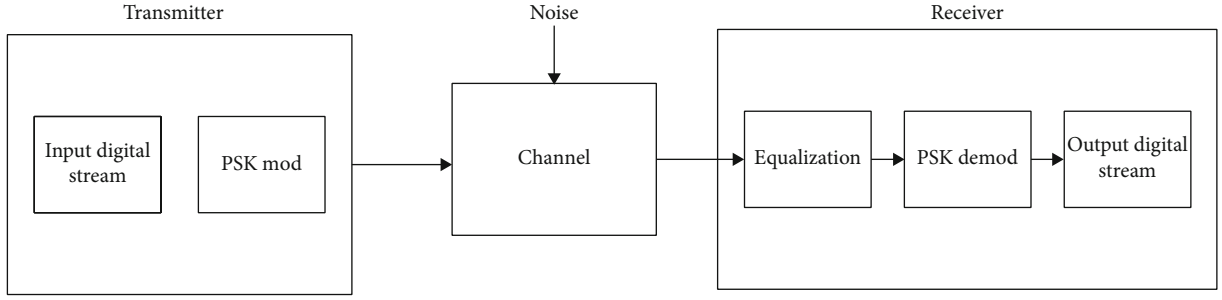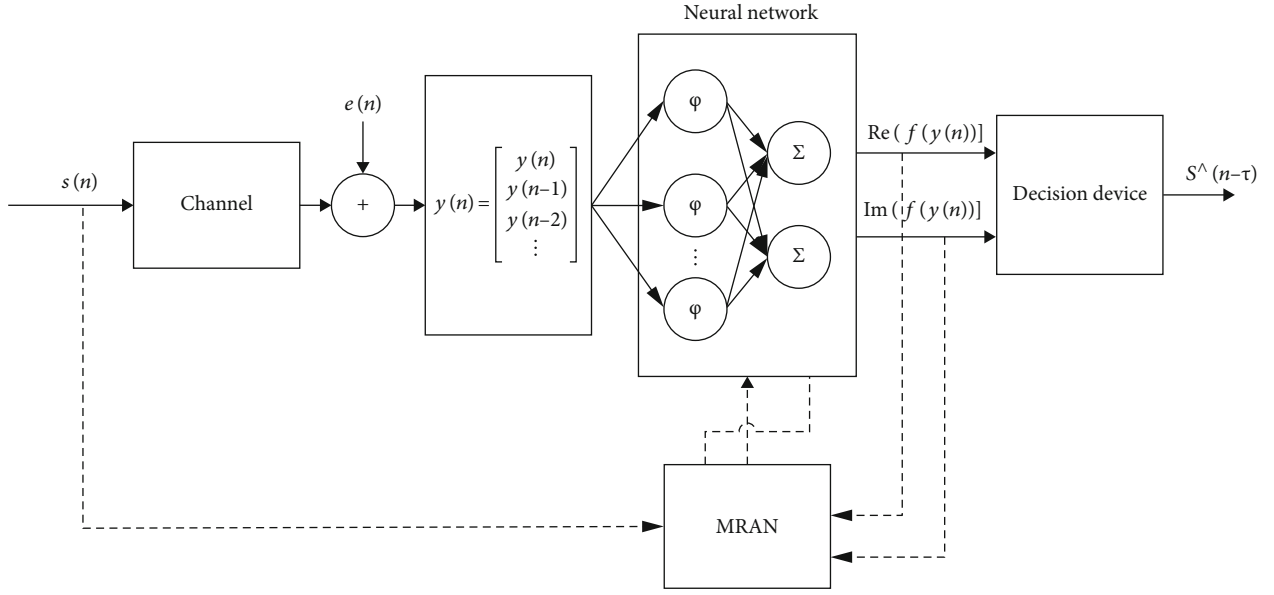
FIGURE 3: The simulation setup.

FIGURE 4: NN-based equalizer.

(ii) The streams are then pulse-shaped using root-raised cosine pulses. The duration of the pulse determines the data rate of the transmitter. In this phase, the incoming data is first upsampled by a factor "N" which corresponds to the symbol duration and then convolved with the RRC pulse. The resulting signal is termed a baseband signal

(iii) The resulting I and Q streams are then multiplied with I/Q carrier signals. In other words, these streams are amplitude-modulating using I/Q signals

(iv) Finally, the two modulated signals are summed up to form a QPSK-modulated signal. In QPSK, two bits are used in one symbol

Mathematically, QPSK modulation can be derived as follows.

Let m_k represent the message signal, where $m_k = x_i + jy_i$ is the complex representation of the ith message signal. This complex representation represents the group of bits together. One is represented as real, and the second one represents the imaginary bit. The message signal is QPSK-modulated as presented in Equation (11):

$$s_{\text{QPSK}}(t) = \text{Re}\ \left\{m_k e^{j2\pi f_o t}\right\}, \tag{11}$$

$$s_{\text{QPSK}}(t) = \text{Re}\ \left\{(x_i + jy_i)(\text{coscos}\ (2\pi f_o t) + j\sin\ (2\pi f_o t))\right\}, \tag{12}$$

$$s_{\text{QPSK}}(t) = x_i \text{coscos}(2\pi f_o t) - y_i \sin\ (2\pi f_o t), \tag{13}$$

where $x_i = 0.7071A$ and $y_i = 0.7071A$ are the amplitudes of the pulses. By substituting the values of x_i and y_i in Equation (11), Equation (14) becomes

$$s_{\text{QPSK}}(t) = 0.7071A\text{coscos}\ (2\pi f_o t) - 0.7071A \sin\ (2\pi f_o t). \tag{14}$$

Using trigonometric relations, the equation can be simplified as

$$s_{\text{QPSK}}(t) = A\text{coscos}\left(2\pi f_o t + \frac{\pi}{4}\right). \tag{15}$$

From Equation (15), the four reference constellation points of QPSK modulation are given in

$$m_i = \{0.7071 + j0.7071 - 0.7071 + j0.7071 - 0.7071 \\ - j0.7071\ 0.7071 - j0.7071. \tag{16}$$

The received signal is demodulated as follows. The received QPSK signal is multiplied with the local oscillators which are at 90 degrees' phase differences and are called I and Q. The resulting signals are low pass filtered using the RRC filters. This results in the recovery of the baseband pulses which are further downsampled by N, and the signal is received.

The received signal can be expressed mathematically in

$$r(t) = s(t) * h(t) + \eta(t). \tag{17}$$

Equation (17) shows that the received signal "$r(t)$" is the sum of convolution of "$h(t)$" with transmitted signal "$s(t)$" and with noise "$n(t)$" added.

4.3. Wireless Channel Model. The wireless channel model describes the underlying communication medium. The performance of the communication system is dependent on the condition of the channel. Rayleigh and Rician fading channel models are widely used to simulate the channel in that realistic wireless environment. The Rayleigh fading channel [78–80] is the conceptual model assuming the fact that there are several objects in the atmosphere. Due to these objects, the transmitted signal may be dispersed and replicated. It is also presumed that there is no direct path between the transmitter and the receiver. On the other hand, the Rician channel [78, 79, 81] assumes that there is a direct path between the transmitter and the receiver. The received signal contains both the dispersed and scattered (or reflected) paths. In this case, the scattered (or reflected) paths appear to be weaker than the direct path.

We have considered a complex-valued multipath channel mentioned in [51]. The coefficients of this channel are defined as in

$$c = [1 - 0.3434j\ 0.5 + 0.2912j], \tag{18}$$

$$H(z) = c_1 X(z) + c_2 z^{-1} X(z). \tag{19}$$

5. Experimental Setup and Modeling

5.1. Simulation Setup

5.1.1. Simulation Parameters of NN. Different NN equalizers are plugged into the configuration of Figure 4, and results are obtained. These configurations and the respective results are discussed in the sequel. The primary performance criteria are used in BER. Loss function analysis and the computational complexity are also calculated. The detailed results are compared and discussed in the later sections. The flowchart of the NN-based equalizer is depicted in Figure 5.

5.1.2. MLP-Based Equalizer. MLP is a simple three-layer network that maps the input to the output. MLP is designed using the "nntraintool" of MATLAB. It comprises an input layer, a hidden layer, and an output layer. The input layer
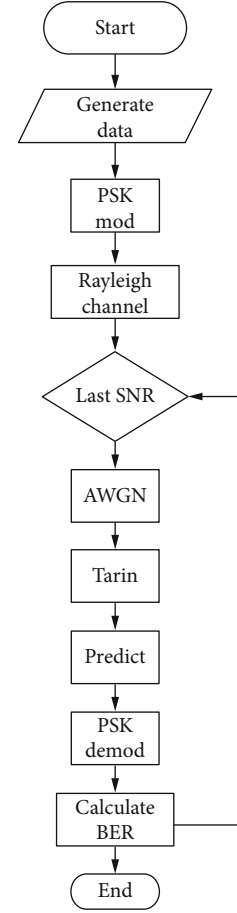
Figure 5: The flowchart of NN-based equalizer.

Table 1: The simulation parameters of MLP.

Parameter	Value
Hidden nodes	30
Input size (X)	1,000,000
Training algorithm	Scaled conjugate gradient (SCG) [77]

Table 2: Simulation parameters of the RBFNN.

Parameter	Value
Data set size	2000
Noise variance	0.01
Centers	16

contains two vectors. One vector is the real part of the input signal (X), and another is the complex part of the signal. The output layer generates four vectors "Y0" to Y3. The MLP is trained with these parameters as shown in Table 1.

5.1.3. RBFNN. RBFNN is a three-layer network that comprises an input layer, a nonlinear hidden layer, and a linear output layer. Radial functions are used as an activation function. Radial functions are special functions. The output of these functions increases or decreases monotonically with distance from a center. The K-means algorithm is used to
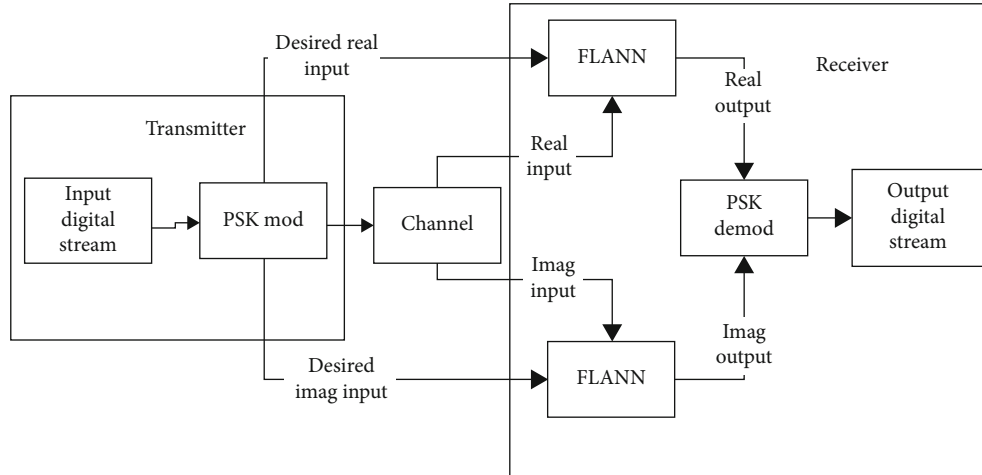
FIGURE 6: The block diagram of the implemented FLANN-based equalizer.

find the centers. So first, centers of clusters are determined in an unsupervised manner, and then, classification is performed to recover the signal. We have implemented this work [51] and observed the improved BER. The simulation parameters of RBFNN are shown in Table 2.

5.1.4. FLANN. FLANN is a single-layer neural network. The main concept of FLANN is to convert the input data to a higher dimension by using different functional expansions. Due to the absence of hidden layers, these networks have the following advantages: low computational complexity with very few adjustable parameters:

(i) Faster training time

(ii) Simple design that can be implemented on hardware

Using the work in [54, 55], we have implemented the FLANN-based equalizer. The block diagram of the equalizer is shown in Figure 6.

The simulation parameters of FLANN, Le-FLANN, and Ch-FLANN are given in Table 3.

5.1.5. SVM-Based Channel Equalizer. SVM is a supervised algorithm used for classification problems. Channel estimation is a classification problem, so it can be used to deal with the nonlinear channel effects. In this work, we have implemented a basic SVM model equalization. Simulation parameters of the SVM are shown in Table 4. The generalization error computed during simulations is 0.00001 which indicates the best performance.

5.1.6. LSTM Channel Equalizers. LSTM is a popular RNN-based DL technique. It is different from feedforward NN which does not have memory and cannot deal with temporal data. The simulation parameters are given in Table 5. The training model of LSTM is illustrated in Figure 7.

5.2. Simulation Analysis. All the simulations are executed and compared in this section. Figure 8 depicts the BER comparison of all the simulated NNs. Generally, the trend ver-

TABLE 3: Simulation parameters.

Parameters	Value
Length of input	2000
FLANN order	30
Input size	4
μ	0.01
No. of iterations	10
Channel noise variance	0.01

TABLE 4: Simulation parameters of SVM.

Parameters	Value
Input size	1,000,000
Kernel function	KNN

TABLE 5: Simulation parameters of LSTM model.

Parameters	Value
Training SNR	12 dB
Channel noise variance	0.01
LSTM nodes	16
Learning rate	0.01

ifies already established theories. As the SNR increases, the BER performance is getting better and better. The performance of FLANN is slightly worse as compared to the rest of the schemes due to its single-layer architecture. The performance of the traditional LMS algorithm is the worst. In [51], similar results are observed. All the other ML-based schemes are having the same BER performance.

In Figure 9, the zoomed version of the BER graph is depicted. The LSTM is slightly bearing higher BER than SVM and RBF-based ML methods. The performance of FLANN when compared with the rest is almost 4 dB poorer than the rest. The performance of LSTM is about 0.7 dB poorer than the RBF and SVM and MLP. This may be
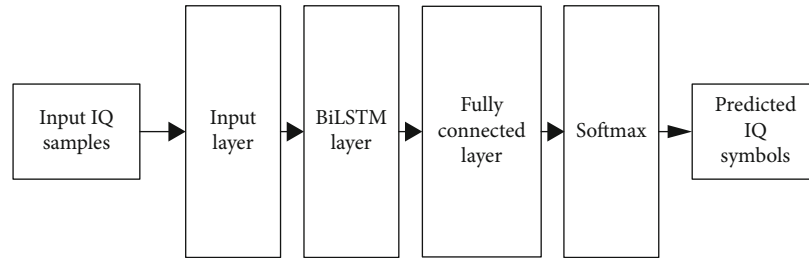
FIGURE 7: The LSTM model.
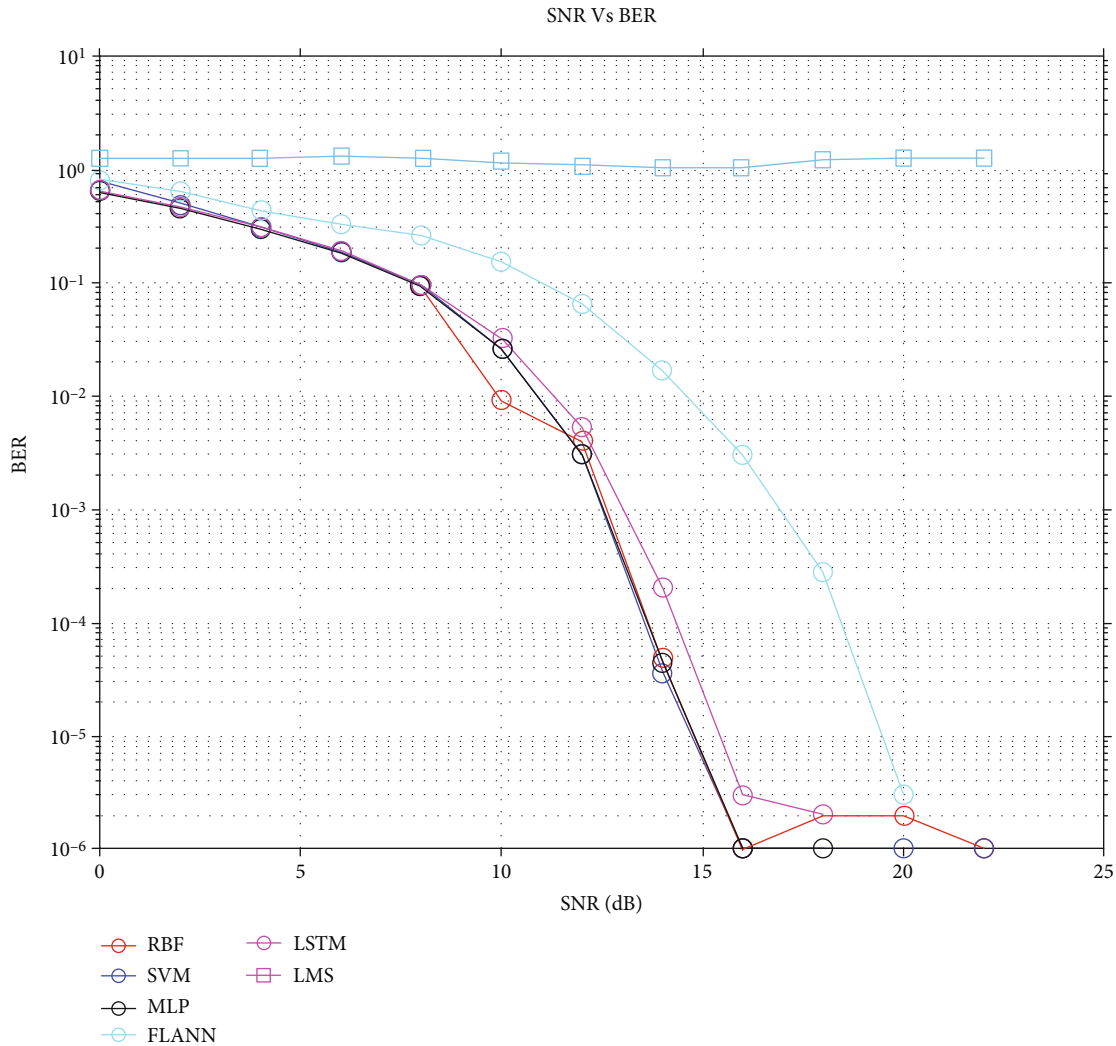
FIGURE 8: The comparison of NN techniques.

reduced by further tuning or by increasing the size of the neural network. However, this will be at the cost of time and computational resources which can be very expensive in the communication systems.

The loss function is an important parameter of the optimization and is therefore discussed. The lesser the value of the loss function, the better performance is considered. In Table 6, the values of the loss function for all the algorithms used in this text are depicted. It shows that all the NNs are well trained.

The minimum value of the loss function achieved is in the case of SVN where the value is 0.00001. The BER results depicted in Figure 9 are very much in line with these results. The loss function values of RBF, FLANN, and LSTM can be further reduced by using more training data and by using better optimization algorithms.

5.3. *Computational Complexity.* Computational complexity analysis of the algorithms is presented. This presents the number of computation resources required to perform the

SNR Vs BER

FIGURE 9: The zoomed comparison plot of BER.

TABLE 6: Loss function values.

ANN	Loss function value
Radial Basis Function	0.001
SVN (KNN-based)	0.00001
MLP	0.003
FLANN	0.005
LSTM	0.003

respective ANN. Table 7 presents the computational complexity of various algorithms. The number of additions, multiplications, and other computational resources such as exponentiation, powers, and trigonometric functions is enlisted [82]. This analysis is useful for the HW implementations and for estimating the computational requirements for embedded systems.

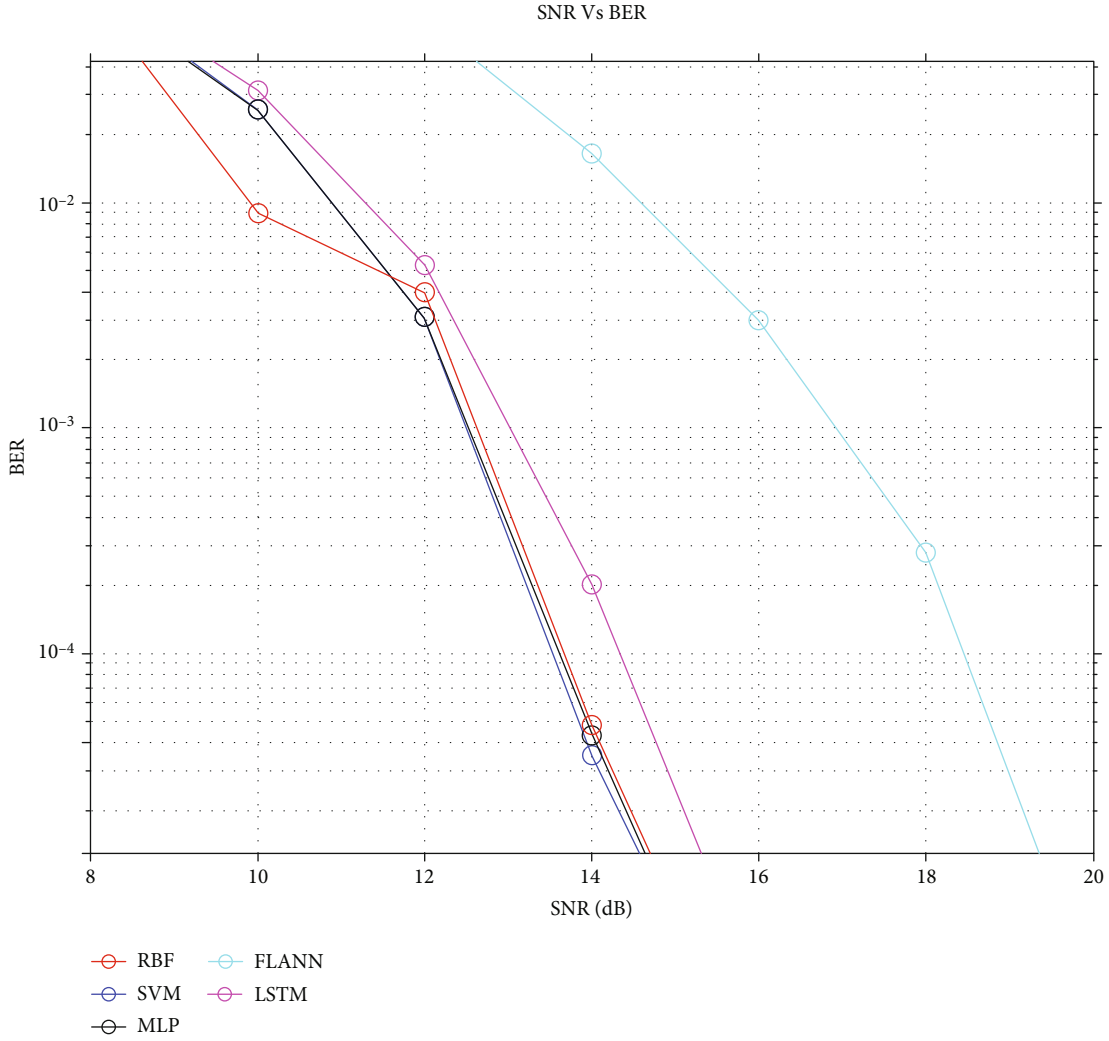The computational complexity analysis of the mentioned algorithms is verified by timing the MATLAB® implementations. The time of all the algorithms used in this work is measured using the MATLAB® built-in function called "timeit." The number of iterations performed for each algo-

rithm is 10^6. The machine used for the computation is DELL® 7920 running MATLAB® 2019b. The CPU is Intel® Xeon® Silver 4116 CPU running at 2.1 GHz. The time is enlisted in Table 8. The computational time computed endorses the computational complexity as given in Table 7. The minimum computational time achieved is for the SVM. SVM is running a KNN algorithm that is computationally efficient. Its BER results are also amongst the best. RBF and MLP bear good performance, but their computational time is more.

6. Conclusions

The communication system is an ever-evolving, well-established field of research and has shown major advances in signal estimation, equalization, and other fields such as channel coding. Channel equalization is very critical for achieving high data rates and improved spectral efficiency and has been achieved using the traditional theory of least squares estimation and minimum mean squares estimation techniques such as LMS, NLMS, RLS, and Kalman filtering. The use of NN- and SVM-based channel equalization

TABLE 7: Computational complexity.

| ANN | Computational complexity | | | | |
	No. of multiplications	No. of additions	Division	Tan$h$	Exp()
RBF	$n_0 n_1 + 2n_1 + n_0 + 1$	$2n_0 n_1 + n_0 + n_1 + 1$	$n_0 + n_1$	—	n_o
FLANN	$3n_1(n_0 + 1) + n_0$	$2n_1(n_0 + 1) + n_1$	—	n_1	—
MLP	$4\sum_{i=0}^{L-1} n_i n_{i+1} + 3\sum_{i=0}^{L-1} n_i - n_0 n_1 + 2n_L$	$3\sum_{i=0}^{L-1} n_i n_{i+1} + 3n_L - n_0 n_1$	—	—	—
SVM	$4T_d$	$3T_d$			T_d
LSTM	$2N + 2N$	$N_0 N_1$			

n_0 is the number of input nodes. n_i is the ith node in the network. T_d is the total number of Euclidean distances in the KNN-based SVM. N is the number of nodes in the convolution layer of the LSTM network. $N_0 N_1$ is the number of neurons in the BiLSTM layers [82].

TABLE 8: Time of various ANN algorithms.

ANN	Total time in seconds	Iterations	Time single iteration (seconds)
SVM	5.231	1,000,000	5.2315×10^{-6}
LSTM	102.957	1,000,000	1.029576×10^{-4}
RBF	12.2729	1,000,000	1.2273×10^{-5}
FLANN	36.3450	1,000,000	3.6345×10^{-5}
MLP	13.0859	1,000,000	1.3086×10^{-5}

methods is currently under research and is proving to be performing better than the conventional methods mentioned above.

In this article, we have addressed the application of information theory-based methods for channel equalization comprising of neural networks and SVM techniques. It revealed that the methods used in traditional communication systems are difficult to understand and implement as compared to the ANN-based methods. Channel equalization when treated as a classification problem using ANN techniques resulted in simpler receiver structures especially in the case of OFDM. The results achieved are also found to be improved in terms of BER. Another advantage with the use of ANN-based methods is that this has resulted in a relatively simpler way to understand the communication systems, and many of the computer scientists who are not well versed with the communication system theories can also attempt to develop better communication systems by using their computer science and software development skills.

This work can be extended in many ways. The following is the list of possible emerging research areas. Computational complexity analysis and computing platform optimizations of the algorithms are mandatory for efficient implementation on hardware platforms such as ARM processors and FPGA and GPUs. In this work, the preliminary computational complexity analysis has been worked out. However, this can be further extended when the implementation of these algorithms will be carried out on the FPGAs or when optimized for the implementation on the microcontrollers and DSP processors. Two-dimensional treatment of the received signal is similar to time-frequency analysis where several frames are gathered and then processed as a block. This will enable the use of advanced neural network methods such as CNN, DNN, and RNN methods. Existing frameworks such as AlexNet may also be used. Currently, performance evaluation is performed using QPSK modulation. Performance evaluation using higher-order constellations such as 16QAM, 64QAM, and 8PSK may also be carried out in the future. Validation by developing hardware may be carried out.

Data Availability

No data were used to support this study.

Conflicts of Interest

The authors declare no conflict of interest.

References

[1] O. Kaiwartya, S. Kumar, and R. Kasana, "Traffic light-based time stable geocast (T-TSG) routing for urban VANETs," in *2013 Sixth International Conference on Contemporary Computing (IC3)*, pp. 113–117, Noida, India, 2013.

[2] M. Prasad, Y.-T. Liu, D.-L. Li, C.-T. Lin, R. R. Shah, and O. P. Kaiwartya, "A new mechanism for data visualization with TSK-type preprocessed collaborative fuzzy rule based system," *Journal of Artificial Intelligence and Soft Computing Research*, vol. 7, no. 1, pp. 33–46, 2017.

[3] O. Kaiwartya and S. Kumar, "Geocast routing: recent advances and future challenges in vehicular adhoc networks," in *2014 International Conference on Signal Processing and Integrated Networks (SPIN)*, pp. 291–296, Noida, India, 2014.

[4] S. Iqbal, A. H. Abdullah, and K. N. Qureshi, "Channel quality and utilization metric for interference estimation in wireless mesh networks," *Computers Electrical Engineering*, vol. 64, pp. 420–435, 2017.

[5] S. Iqbal, H. Maryam, K. N. Qureshi, I. T. Javed, and N. Crespi, "Automised flow rule formation by using machine learning in software defined networks based edge computing," *Egyptian Informatics Journal*, 2021.

[6] H. O. Alanazi, A. H. Abdullah, and K. N. Qureshi, "A critical review for developing accurate and dynamic predictive models using machine learning methods in medicine and health care," *Journal of Medical Systems*, vol. 41, no. 4, p. 69, 2017.

[7] K. N. Qureshi, S. Din, G. Jeon, and F. Piccialli, "An accurate and dynamic predictive model for a smart M-health system using machine learning," *Information Sciences*, vol. 538, pp. 486–502, 2020.

[8] A. Goldsmith, *Wireless Communications*, Cambridge university press, 2005.

[9] C. E. Shannon, "A mathematical theory of communication," *The Bell System Technical Journal*, vol. 27, no. 3, pp. 379–423, 1948.

[10] Z. Zhang and M. Ma, "Research on pilot-aided channel estimation techniques in OFDM system," in *2011 7th International Conference on Wireless Communications, Networking and Mobile Computing*, pp. 1–4, Wuhan, China, 2011.

[11] S. Lasaulce, P. Loubaton, and E. Moulines, "A semi-blind channel estimation technique based on second-order blind method for CDMA systems," *IEEE Transactions on Signal Processing*, vol. 51, no. 7, pp. 1894–1904, 2003.

[12] A. Petropulu, R. Zhang, and R. Lin, "Blind OFDM channel estimation through simple linear precoding," *IEEE Transactions on Wireless Communications*, vol. 3, no. 2, pp. 647–655, 2004.

[13] H. H. Zeng and L. Tong, "Blind channel estimation using the second-order statistics: algorithms," *IEEE Transactions on Signal Processing*, vol. 45, no. 8, pp. 1919–1930, 1997.

[14] E. De Carvalho and D. T. Slock, "Cramer-Rao bounds for semi-blind, blind and training sequence based channel estimation," *First IEEE Signal Processing Workshop on Signal Processing Advances in Wireless Communications*, pp. 129–132, 1997.

[15] F. Yang, K. Peng, J. Wang, J. Song, and Z. Yang, "Simplified decision-directed channel estimation method for OFDM system with transmit diversity," in *VTC Spring 2009-IEEE 69th Vehicular Technology Conference*, pp. 1–5, Barcelona, Spain, 2009.

[16] T. S. Rappaport, *Wireless Communications: Principles and Practice*, Prentice hall PTR New Jersey, 1996.

[17] M. T. Sadiq, H. Akbari, A. U. Rehman et al., "Exploiting feature selection and neural network techniques for identification of focal and nonfocal EEG signals in TQWT domain," *Journal of Healthcare Engineering*, p. 24, 2021.

[18] G. J. Gibson, S. Siu, and C. F. Cowan, "The application of nonlinear structures to the reconstruction of binary signals," *IEEE Transactions on Signal Processing*, vol. 39, no. 8, pp. 1877–1884, 1991.

[19] S. Chen, G. J. Gibson, C. Cowan, and P. M. Grant, "Reconstruction of binary signals using an adaptive radial-basis-function equalizer," *Signal Processing*, vol. 22, no. 1, pp. 77–93, 1991.

[20] G. J. Gibson, S. Siu, and C. F. Cowan, "Application of multilayer perceptrons as adaptive channel equalisers," in *Adaptive Systems in Control and Signal Processing 1989*, pp. 573–578, Elsevier, 1990.

[21] T. O'shea and J. Hoydis, "An introduction to deep learning for the physical layer," *IEEE Transactions on Cognitive Communications Networking*, vol. 3, no. 4, pp. 563–575, 2017.

[22] T. Wang, C.-K. Wen, H. Wang, F. Gao, T. Jiang, and S. Jin, "Deep learning for wireless physical layer: opportunities and challenges," *China Communications*, vol. 14, no. 11, pp. 92–111, 2017.

[23] C. Zhang, P. Patras, and H. Haddadi, "Deep learning in mobile and wireless networking: a survey," *IEEE Communications surveys & tutorials*, vol. 21, no. 3, pp. 2224–2287, 2019.

[24] G. Gui, H. Huang, Y. Song, and H. Sari, "Deep learning for an effective nonorthogonal multiple access scheme," *IEEE Transactions on Vehicular Technology*, vol. 67, no. 9, pp. 8440–8450, 2018.

[25] Y. Yang, F. Gao, X. Ma, and S. Zhang, "Deep learning-based channel estimation for doubly selective fading channels," *IEEE Access*, vol. 7, pp. 36579–36589, 2019.

[26] Y. Yang, F. Gao, G. Y. Li, and M. Jian, "Deep learning-based downlink channel prediction for FDD massive MIMO system," *IEEE Communications Letters*, vol. 23, no. 11, pp. 1994–1998, 2019.

[27] Q. Bai, J. Wang, Y. Zhang, and J. Song, "Deep learning-based channel estimation algorithm over time selective fading channels," *IEEE Transactions on Cognitive Communications Networking*, vol. 6, no. 1, pp. 125–134, 2019.

[28] M. Ibnkahla, "Applications of neural networks to digital communications–a survey," *Signal Processing*, vol. 80, no. 7, pp. 1185–1215, 2000.

[29] A. Zappone, M. Di Renzo, and M. Debbah, "Wireless networks design in the era of deep learning: model-based, AI-based, or both?," *IEEE Transactions on Communications*, vol. 67, no. 10, pp. 7331–7376, 2019.

[30] E. Azzouz and A. K. Nandi, *Automatic Modulation Recognition of Communication Signals*, 2013.

[31] T. J. O'Shea, T. Erpek, and T. C. Clancy, "Deep learning based MIMO communications," 2017, https://arxiv.org/abs/1707.07980.

[32] T. J. O'Shea, T. Roy, and T. C. Clancy, "Over-the-air deep learning based radio signal classification," *IEEE Journal of Selected Topics in Signal Processing*, vol. 12, no. 1, pp. 168–179, 2018.

[33] T. J. O'Shea, J. Corgan, and T. C. Clancy, "Convolutional radio modulation recognition networks," in *International conference on engineering applications of neural networks*, pp. 213–226, Aberdeen, UK, 2016.

[34] D. E. Rumelhart, G. E. Hinton, and R. J. Williams, "Learning representations by back-propagating errors," *Nature*, vol. 323, no. 6088, pp. 533–536, 1986.

[35] G. J. Gibson, S. Siu, and C. Cowen, "Multilayer perceptron structures applied to adaptive equalisers for data communications," in *International Conference on Acoustics, Speech, and Signal Processing*, pp. 1183–1186, Glasgow, UK, 1989.

[36] S. Chen, G. Gibson, C. Cowan, and P. Grant, "Adaptive equalization of finite non-linear channels using multilayer perceptrons," *Signal Processing*, vol. 20, no. 2, pp. 107–119, 1990.

[37] D. P. Mandic, "A generalized normalized gradient descent algorithm," *IEEE Signal Processing Letters*, vol. 11, no. 2, pp. 115–118, 2004.

[38] S. Siu, G. Gibson, and C. Cowan, "Decision feedback equalisation using neural network structures and performance comparison with standard architecture," *IEE Proceedings I-Communications, Speech and Vision*, vol. 137, no. 4, pp. 221–225, 1990.

[39] A. Sarangi, S. Priyadarshini, and S. K. Sarangi, "A MLP equalizer trained by variable step size firefly algorithm for channel equalization," in *2016 IEEE 1st International Conference on Power Electronics, Intelligent Control and Energy Systems (ICPEICES)*, pp. 1–5, Delhi, India, 2016.

[40] X. Lyu, W. Feng, R. Shi, Y. Pei, and N. Ge, "Artificial neural network-based nonlinear channel equalization: a soft-output perspective," in *2015 22nd International Conference on*

Telecommunications (ICT), pp. 243–248, Sydney, NSW, Australia, 2015.

[41] A. Zerguine, A. Shafi, and M. Bettayeb, "Multilayer perceptron-based DFE with lattice structure," *IEEE Transactions on Neural Networks*, vol. 12, no. 3, pp. 532–545, 2001.

[42] Y. Tan, J. Wang, and J. M. Zurada, "Nonlinear blind source separation using a radial basis function network," *IEEE Transactions on Neural Networks*, vol. 12, no. 1, pp. 124–134, 2001.

[43] A. Uncini and F. Piazza, "Blind signal processing by complex domain adaptive spline neural networks," *IEEE Transactions on Neural Networks*, vol. 14, no. 2, pp. 399–412, 2003.

[44] N. Xie and H. Leung, "Blind equalization using a predictive radial basis function neural network," *IEEE Transactions on Neural Networks*, vol. 16, no. 3, pp. 709–720, 2005.

[45] S. Chen, B. Mulgrew, and P. M. Grant, "A clustering technique for digital communications channel equalization using radial basis function networks," *IEEE Transactions on Neural Networks*, vol. 4, no. 4, pp. 570–590, 1993.

[46] P. C. Kumar, P. Saratchandran, and N. Sundararajan, "Minimal radial basis function neural networks for nonlinear channel equalisation," *IEE Proceedings I-Communications, Speech and Vision*, vol. 147, no. 5, pp. 428–435, 2000.

[47] J. Satapathy, K. Subhashini, and G. L. Manohar, "A highly efficient channel equalizer for digital communication system in neural network paradigm," in *2009 Innovative Technologies in Intelligent Systems and Industrial Applications*, pp. 11–16, Kuala Lumpur, Malaysia, 2009.

[48] S. Chen, B. Mulgrew, and S. McLaughlin, "Adaptive Bayesian decision feedback equaliser based on a radial basis function network," in *[Conference Record] SUPERCOMM/ICC'92 Discovering a New World of Communications*, pp. 1267–1271, Chicago, IL, USA, 1992.

[49] S. Chen, B. Mulgrew, and S. McLaughlin, "Adaptive Bayesian equalizer with decision feedback," *IEEE Transactions on Signal Processing*, vol. 41, no. 9, pp. 2918–2927, 1993.

[50] S. Chen, S. McLaughlin, and B. Mulgrew, "Complex-valued radial basis function network, part II: application to digital communications channel equalisation," *Signal Processing*, vol. 36, no. 2, pp. 175–188, 1994.

[51] I. Cha and S. A. Kassam, "Channel equalization using adaptive complex radial basis function networks," *IEEE Journal on Selected Areas in Communications*, vol. 13, no. 1, pp. 122–131, 1995.

[52] S. S. Ranhotra, A. Kumar, M. Magarini, and A. Mishra, "Performance comparison of blind and non-blind channel equalizers using artificial neural networks," in *2017 Ninth International Conference on Ubiquitous and Future Networks (ICUFN)*, pp. 243–248, Milan, Italy, July 2017.

[53] G. Panda and D. P. Das, "Functional link artificial neural network for active control of nonlinear noise processes," in *International Workshop on Acoustic Echo and Noise Control*, vol. 2003, pp. 163–166, Kyoto, Japan, 2003.

[54] J. C. Patra and R. N. Pal, "A functional link artificial neural network for adaptive channel equalization," *Signal Processing*, vol. 43, no. 2, pp. 181–195, 1995.

[55] J. C. Patra, W. C. Chin, P. K. Meher, and G. Chakraborty, "Legendre-FLANN-based nonlinear channel equalization in wireless communication system," in *2008 IEEE International Conference on Systems, Man and Cybernetics*, pp. 1826–1831, Singapore, 2008.

[56] D. M. Sahoo and S. Chakraverty, "Functional link neural network approach to solve structural system identification problems," *Neural Computing and Applications*, vol. 30, no. 11, pp. 3327–3338, 2018.

[57] T. J. Rivlin, *Chebyshev Polynomials*, Courier Dover Publications, 2020.

[58] T.-T. Lee and J.-T. Jeng, "The Chebyshev-polynomials-based unified model neural networks for function approximation," *IEEE Transactions on Systems, Man, Cybernetics, Part B*, vol. 28, no. 6, pp. 925–935, 1998.

[59] J. Liu, K. Mei, X. Zhang, D. Ma, and J. Wei, "Online extreme learning machine-based channel estimation and equalization for OFDM systems," *IEEE Communications Letters*, vol. 23, no. 7, pp. 1276–1279, 2019.

[60] J. C. Patra and A. C. Kot, "Nonlinear dynamic system identification using Chebyshev functional link artificial neural networks," *IEEE Transactions on Systems, Man, Cybernetics, Part B*, vol. 32, no. 4, pp. 505–511, 2002.

[61] J. C. Patra, W. B. Poh, N. S. Chaudhari, and A. Das, "Nonlinear channel equalization with QAM signal using Chebyshev artificial neural network," in *Proceedings. 2005 IEEE International Joint Conference on Neural Networks, 2005*, vol. 5, pp. 3214–3219, Montreal, QC, Canada, 2005.

[62] G. I. Kechriotis and E. S. Manolakos, "Using neural networks for nonlinear and chaotic signal processing," in *1993 IEEE International Conference on Acoustics, Speech, and Signal Processing*, vol. 1, pp. 465–468, Minneapolis, MN, USA, 1993.

[63] A. Waibel, T. Hanazawa, G. Hinton, K. Shikano, and K. J. Lang, "Phoneme recognition using time-delay neural networks," *IEEE transactions on acoustics, speech, signal processing*, vol. 37, no. 3, pp. 328–339, 1989.

[64] G. Kechriotis, E. Zervas, and E. Manolakos, "Using recurrent neural networks for blind equalization of linear and nonlinear communications channels," in *MILCOM 92 Conference Record*, pp. 784–788, San Diego, CA, USA, 1992.

[65] M. J. Bradley and P. Mars, "Application of recurrent neural networks to communication channel equalization," in *1995 International Conference on Acoustics, Speech, and Signal Processing*, vol. 5, pp. 3399–3402, Detroit, MI, USA, 1995.

[66] J. D. Ortiz-Fuentes and M. L. Forcada, "A comparison between recurrent neural network architectures for digital equalization," in *1997 IEEE International Conference on Acoustics, Speech, and Signal Processing*, vol. 4, pp. 3281–3284, Munich, Germany, 1997.

[67] S. Hu, Y. Pei, P. P. Liang, and Y.-C. Liang, "Robust modulation classification under uncertain noise condition using recurrent neural network," in *2018 IEEE Global Communications Conference (GLOBECOM)*, pp. 1–7, Abu Dhabi, UAE, 2018.

[68] A. D. Back and A. C. Tsoi, "FIR and IIR synapses, a new neural network architecture for time series modeling," *Neural Computation*, vol. 3, no. 3, pp. 375–385, 1991.

[69] G. Kechriotis, E. Zervas, and E. S. Manolakos, "Using recurrent neural networks for adaptive communication channel equalization," *IEEE Transactions on Neural Networks*, vol. 5, no. 2, pp. 267–278, 1994.

[70] C.-F. Teng, H.-M. Ou, and A.-Y. A. Wu, "Neural network-based equalizer by utilizing coding gain in advance," in *2019 IEEE Global Conference on Signal and Information Processing (GlobalSIP)*, pp. 1–5, Ottawa, ON, Canada, 2019.

[71] S. Hochreiter, "The vanishing gradient problem during learning recurrent neural nets and problem solutions," *International*

Journal of Uncertainty, Fuzziness and Knowledge-Based Systems, vol. 6, no. 2, pp. 107–116, 1998.

[72] S. Hochreiter and J. Schmidhuber, "Long short-term memory," *Neural Computation*, vol. 9, no. 8, pp. 1735–1780, 1997.

[73] C. Cortes and V. Vapnik, "Support-vector networks," *Machine Learning*, vol. 20, no. 3, pp. 273–297, 1995.

[74] V. Vapnik, S. Golowich, and A. Smola, "Support vector method for function approximation, regression estimation and signal processing," *Advances in Neural Information Processing Systems*, vol. 9, 1996.

[75] S. R. Gunn, "Support vector machines for classification and regression," *ISIS technical report*, vol. 14, no. 1, pp. 5–16, 1998.

[76] S. Chen, S. Gunn, and C. Harris, "Decision feedback equaliser design using support vector machines," *IEE Proceedings-Vision, Image Signal Processing*, vol. 147, no. 3, pp. 213–219, 2000.

[77] D. J. Sebald and J. A. Bucklew, "Support vector machine techniques for nonlinear equalization," *IEEE Transactions on Signal Processing*, vol. 48, no. 11, pp. 3217–3226, 2000.

[78] S. S. Haykin and M. Moher, *Modern Wireless Communications*, Pearson Education India, 2011.

[79] A. Doukas and G. Kalivas, "Rician K factor estimation for wireless communication systems," in *2006 International Conference on Wireless and Mobile Communications (ICWMC'06)*, pp. 69–69, Bucharest, Romania, 2006.

[80] U. Madhow, *Fundamentals of Digital Communication*, Cambridge university press, 2008.

[81] P. M. Shankar, *Introduction to Wireless Systems*, Wiley, New York, 2002.

[82] J. C. Patra, R. N. Pal, B. Chatterji, and G. Panda, "Identification of nonlinear dynamic systems using functional link artificial neural networks," *IEEE transactions on systems, man, cybernetics, part b*, vol. 29, no. 2, pp. 254–262, 1999.

Research Article

Approach for Collision Minimization and Enhancement of Power Allocation in WSNs

Debabrata Singh [ID],[1] **Jyotishree Bhanipati,**[2] **Anil Kumar Biswal,**[2] **Debabrata Samanta** [ID],[3] **Shubham Joshi** [ID],[4] **Piyush Kumar Shukla** [ID],[5] **and Stephen Jeswinde Nuagah** [ID][6]

[1]*Department of CA, ITER, SOA Deemed To Be University, Bhubaneswar, Odisha 751030, India*
[2]*Department of CSE, ITER, SOA Deemed To Be University, Bhubaneswar, Odisha 751030, India*
[3]*Department of Computer Science, CHRIST (Deemed To Be University), Bengaluru, Karnataka 560029, India*
[4]*Department of Computer Engineering, SVKM'S NMIMS MPSTME Shirpur Campus, Savalade, Maharashtra 425405, India*
[5]*Department of CSE, University Institute of Technology, Rajiv Gandhi Proudyogiki Vishwavidyalaya (Technological University of Madhya Pradesh), Bhopal 462033, India*
[6]*Department of Electrical Engineering, Tamale Technical University, P.O. Box 3 E/R. Tamale, Ghana*

Correspondence should be addressed to Stephen Jeswinde Nuagah; jeswinde@tatu.edu.gh

Wireless sensor networks (WSNs) have attracted much more attention in recent years. Hence, nowadays, WSN is considered one of the most popular technologies in the networking field. The reason behind its increasing rate is only for its adaptability as it works through batteries which are energy efficient, and for these characteristics, it has covered a wide market worldwide. Transmission collision is one of the key reasons for the decrease in performance in WSNs which results in excessive delay and packet loss. The collision range should be minimized in order to mitigate the risk of these packet collisions. The WSNs that contribute to minimize the collision area and the statistics show that the collision area which exceeds equivalents transmission power has been significantly reduced by this technique. This proposed paper optimally reduced the power consumption and data loss through proper routing of packets and the method of congestion detection. WSNs typically require high data reliability to preserve identification and responsiveness capacity while also improving data reliability, transmission, and redundancy. Retransmission is determined by the probability of packet arrival as well as the average energy consumption.

1. Introduction

In a recent situation, the most important part of WSNs is data transmission, as it is used for transferring the message from the source to the destination. Data transmission is an energy-intensive activity that necessitates an efficient routing mechanism to avoid data loss [1]. WSN was originated from the technology named distributed sensing technology. WSNs were one of the valuable technologies that the researchers came up with, and it was a huge success [2, 3]. This helps many types of physical situations, processing data, etc. WSN also helps in monitoring environmental conditions from distant locations with perfection [4, 5]. The

most important part of data transmission is the flow of data in WSNs, because each data packet consists of events (energy consumption, storage capacity with some security features, etc.) that are more important for some applications [6]. WSNs, a subset of larger IoT networks, are wirelessly interconnected networks of small low-power sensor devices that sense environmental parameters at regular intervals and send them to some central storage or database [7, 8]. WSN protocols that maximise sensor node performance, minimise communication latency, and reduce power consumption are currently being researched. In this section, we will look at various works and research on traditional and core networking concepts, as well as wireless sensor networks [9].

As a result, data transmission should be secure; however, the fundamental difficulty is that data nodes have limited energy due to their low memory capacities, making maintaining security extremely challenging [3]. To make a safe data transfer, certain components of security must be maintained during transmission. Retransmission is done for a variety of reasons, the most important of which is to ensure that data is not lost during wireless connection [10, 11]. The retransmitting method is primarily used by WSN to ensure that reliability is a top priority. As a result, the higher the dependability of prioritising data packets, the higher the maximum number of retransmissions, and if the delay is more than multiple retransmissions will occur [12–14]. In a WSN, sensor nodes are comprised of a maximum number of sensing data packets that combined perceive, collect the information, and process it from the sensing objects, and then, it transfers required data to the receiver or the user through the medium of wireless communication [15–17]. The wireless sensor network's working period is limited due to the limited power of the battery, and as a result, there is a congestion of data transmission [18]. Hence, during transmission, if the data meant for reliable and complete, then in that case, many nodes are required. The most necessary part of WSN is to update the codes that are running on the sensors and these codes require a reliable circulation of huge data to each sensor along with energy efficiency [19, 20].

As there is a sleep schedule operated in sensors for energy efficiency, some of the sensors will be in sleep mode for which they miss out on some packets during the data circulation [21]. At some time, the sensor may not receive the packets successfully due to the unreliable state of wireless links, hence, for which retransmission of messages of those sensors is necessary, and for this, more amount of power is consumed. Due to that, the advanced research trend area of the IoT is applied to build the automaton process with the help of an energy-optimized range of sensors that provides better performance at the time of processing [22, 23].

1.1. Motivation. At present, wireless sensors are being deployed on roads, in cities, and in many other sectors of application for an optimal way of sensing and monitoring the data packets, which is explained below:

(1) Whenever the data packets are forwarded from the sending end to receiving end then there are more chances of loss of packets due to collision

(2) However, this collision is primarily caused by increased energy consumption, which causes significant interruption during transmission in WSNs

(3) So, this paper proposed optimal energy harvesting method, data reliability with retransmission of corrupted, or delayed data packet in the transmission which acts through optimal power consumption

The remaining part of the paper is structured as, in Section 2, we discuss the literature review. Section 3 highlights on the proposed model and methodology. In Section 4, we describe the simulation setup and result analysis. Finally, Section 5 suggests for future research and conclusion.

2. Literature Survey

Mamun-Or-Rashid [24] and other authors proposed for "reliable event detection and congestion avoidance in WSNs." wireless sensor networks (WSNs) are implemented by dense and endless signaling at the time of data communication. So, this paper introduced a collision avoidance protocol like source count-based HMAC and WRRF.

Wan [25] and other authors proposed for "congestion detection and avoidance networks." The authors provide a simulation and exploration for strategy, execution, and measurement of CODA by using three techniques such as receiver side congestion detection, hop-by-hop open-loop backpressure, and multisource closed-loop control.

Sankarasubramaniam [26] and other authors proposed for "ESRT in WSNs." WSNs are event-based systems which rely on several microsensor nodes' collective efforts. Reliable event detection at the sink is based on information collected. Source nodes were provided and not on a single article. This paper describes the reliable ESRT protocol. It is a new transport scheme that is designed with minimal energy costs to achieve efficient event detection in WSNs. It contains a collision control component designed to achieve reliability and energy conservation.

Intanagonwiwat [27] and other authors proposed "a scalable and robust communication networks." The developments in processor, memory, and radio technology would make it possible to detect, communicate, and compute small or inexpensive nodes. The purpose of this paper is to explore the directed model of this coordination. Wang [28] and other authors proposed "a study of transport protocols." First, the authors of the study of WSNs on transport protocols highlight many specific features of WSN and identify the simple design requirements and transport protocol tasks, with effectiveness of power, service quality, reliability, and collision management.

Woo and Culler [29] proposed a transmission control scheme that is applied for media access in WSNs. In a novel sensor network regime, the authors examine the issue of control over media access. Sensor network media access control should not only be energy efficient, they should also allow the equal allotment of all nodes within a multihop network to the infrastructure. The author proposes to support these two objectives an adaptive rate control system and considers that it is very successful in achieving our objective for justice, while being power efficient for both low- and high-speed network transport cycles.

Alzahrani and Bouabdallah [30] proposed a method QMMAC protocol for multichannel data transmission concept in the WSNs. This paper provided a method to enhance the level of throughput while consuming power. By using this protocol avoided the cause of the collision and overhearing with the help of a multichannel communication feature, the consequence of this paper performed optimal energy efficiency and end to end delay. Thus, this paper was examined by taking very limited parameters, but it requires

increasing the range of parameters to get good performance in multiple parameters.

3. Proposed Model and Methodology

WSNs consist of a huge amount of battery-driven nodes which should be taken into account in terms of power efficiency, failure tolerance, and scalability during WSN architecture design. However, during a state of emergency, urgent info should be delivered as soon as possible, keeping reliability low latency as the main aspects. Many works had been done on data gathering schemes which are applied during a normal situation like ample. We approach the integration by any scheme for data collection that is well configured for application-oriented communication of mechanisms for quick delivery. In evolving circumstances, a certain number of measures are taken to provide urgent information to BS and any information which does not occur in an emergency remains in a natural position.

3.1. Optimal Reliability and Low Latency. The reliability and delay of urgent delivery are the most critical concerns. As it stands, the material should be designated as urgent and subject to preferred restrictions [31]. Keep in mind that the energy efficiency during transmission can be sacrificed for some time. Nodes with a small memory capacity and mechanisms to facilitate rapid and efficient urgent data transmission low energy consumption also lead to simplicity, with fewer errors of programming [32].

3.2. Technical Approach

3.2.1. Retransmission in Wireless Sensor Networks (WSNs). Retransmission is based on packet arrival probability, including average energy consumption. As WSNs require high data reliability for better performance in maintaining detection and response capability and to enhance this data reliability, retransmission is used. For each single-hop transmission, a recognition packet is sent after receiving a single data packet, and retransmission is caused by loss of the acknowledgement packet [33, 34].

One-hop loss probability P_{hl} for the loss of information acknowledgement (ACK) packet is expressed as

$$P_{hl} = 1 - \pi_0^2. \tag{1}$$

The relation between P_{hl} and retransmission time x is represented by

$$P_{hl}^r = 1 - (P_{hl})^x. \tag{2}$$

And here,

$$x = \log_{P_{hl}}(1 - P_{hl}^r). \tag{3}$$

Then, average energy consumed by a failed one-hop transmission during the event of loss is

$$E_h{}' = \varepsilon \times \pi_1 \times 1 + \varepsilon(\pi_0\pi_1) \times 2 = \varepsilon\pi_1(1 + 2\pi_0). \tag{4}$$

Here, $\varepsilon\pi_1$ = energy consumption during data packet loss. $2\varepsilon\pi_0\pi_1$ = energy consumption during ACK packet is dropped. So, average of energy consumed for one data packet through one hop is

$$E_h{}^r = (P_{hl})^t t E_h{}' + \Sigma_{i=1}^t (P_{hl})^{i-1} \pi_0^2 \left[(i-1)E_h{}' + 2\varepsilon \right], \tag{5}$$

where $(P_{hl})^t$ = process probability for all t transmission failed through single hop.

$tE_h{}'$ = corresponding power consumption.
$P_{hl}^{(i-1)}\pi_0^2$ = event probability for i_{th} transmission.
$(i-1)E_h' + 2_\varepsilon$ = corresponding energy consumption. So, overall power consumption for "n" hops is

$$E_e^r = \Sigma_{i=1}^n N(P_{hl}^r)^{i-1} E_h^r, \tag{6}$$

where $N(P_{hl}^r)^{i-1}$ = no. of arrival packets after i_{th} hop. Hence, for one successful arrival packet, the average energy consumption will be

$$E_{avg}^r = \frac{E_e^r}{M(P_h^r)^n} = \Sigma_{i=1}^n (P_h^r)^{i-n-1} E_h^r. \tag{7}$$

Figure 1 shows retransmission in wireless sensor networks.

3.2.2. Optimal Power Allocation in WSNs. The power allocation is the major topic in WSN, where a lot of remote sensors send data to the fusion centre via several channels in a high-traffic environment [35].

3.2.3. Routing of WSNs and Flow Conservation. We are discussing the rate of message packet communication and message packet routing via the network flow conservation equation here.

$$\Sigma a\varepsilon S_b(x_{ab}(t) - (t)) = X_{ab}(t), \quad \forall b\varepsilon S, a\varepsilon S_b,$$
$$\Sigma b\varepsilon S_a(x_{ab}(t) - (t)) = X_{ab}(t), \quad \forall a\varepsilon S_b, bS_a, \tag{8}$$

where x_{ab} = amount of flow of energy from node.
X_{ab} = sum information collected at source node to the sink node $j\varepsilon$.
S = sensor nodes set.
a = incoming sensor node.
b = outgoing sensor node.

3.2.4. Energy Cost Model. Lifetime of the network is dependable on utilization amount of power from the sensor node P_i and active time slot T_i of anode. $E_{RX}(t_s)$ and $E_{TX}(t_s)$ are the energy transmitted by $E_{trans}(t_s)$ time slot. The computed energy consists (t_s) and $E(t_s)$. Assume (t_s) 0 represents our whole leftover energy, the power consumption for t is

$$P_a(t_s) = \Sigma r_{ab}(t_s)E_{TX}(t_s) + \Sigma r_{ab}(t_s)E_{RX}(t_s)a\varepsilon N_b$$
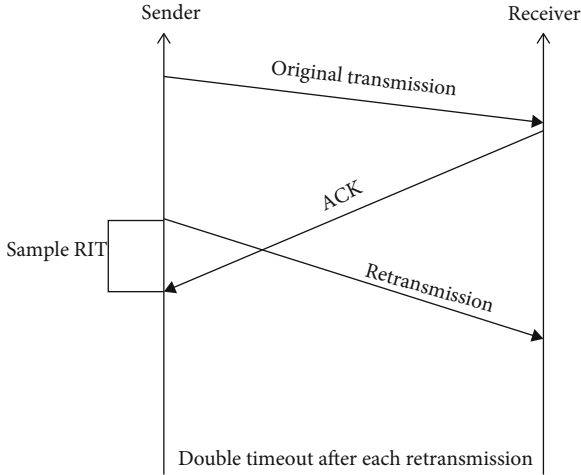$$+ \Sigma R_{ab}(t_s)E_{PR}(t_s)\Sigma R_{ab}(t_s)E_{SN}(t_s), \tag{9}$$

Figure 1: Retransmission in wireless sensor networks.

where $P_a(t_s)$ = power consumption in (t_s)

$$
\begin{aligned}
E_{TX}(t) &= \text{Transmitted energy } (t) \\
E_{RX}(t) &= \text{Receiver energy } (t) \\
E_{PR}(t) &= \text{Processing energy } (t) \\
E_{SN}(t) &= \text{Sensing energy } (t)
\end{aligned}
\tag{10}
$$

For sending a one bit of data by sender energy from $a\varepsilon N_b$ to $b\varepsilon N_a$ over a distance (dt) is

$$
E_{TX} = a_1 + a_2 * d^y, \tag{11}
$$

where y = path loss exponent.

d = distance of communication; a_1 and a_2 = constants depending upon T_c.

3.2.5. Loss in Packet and Retransmission of Data. Anatomy of packet error: the data is decrypted through a technique called CRC by

$$
P_{ARQ} = 1 - (1 - P_{be})^{L_{pt}}, \tag{12}
$$

where L_{pt} = packet size

$$
\begin{aligned}
P_{lr} &= \text{loss rate of packets} \\
P_{be} &= \text{Bit error rate.}
\end{aligned}
\tag{13}
$$

3.2.6. Analysis of Packet Error: (ECC Scheme). In this example, the packets are transferred between the sink node and the sensor node. The rate of packet loss at the sink node is

$$
P_{lr}^{ECC} = 1 - \left(1 - \Sigma_{i=a+1}^{n} \binom{m}{i} P_b^i (1 - P_b)^{m-i}\right)^{L_{pt}/k}. \tag{14}
$$

Let P_{lr} be the probability of an event. The number of retransmissions is calculated as follows:

$$
EN(R_t) = \frac{1}{(1 - P_{lr})}, \tag{15}
$$

where $EN(R_t)$ = expected number of retransmissions. The packet loss rate of ARQ or ECC schemes is denoted P_{lr}. Packet loss rate for the h-hop state when every node is communicated independently.

$$
E(R_t, h) = \frac{h}{(1 - P_{lr})}, \tag{16}
$$

where h = number of hops.

3.2.7. Error Correction Scheme through RRA. A residue system of number is truly a prime base as modules set over Galois field of b-bits (GF (2_b)).

It is a set of β modules from m_1, m_2, and m_β. Let "A" be an integer data which is represented by Γ_1, Γ_2, and Γ_β.

$$
\Gamma_j = B \bmod m_j, j = 1, 2, \cdots n, \tag{17}
$$

$$
\Theta = \Pi_{j=1}^{\beta} m_j. \tag{18}
$$

The highest operational range of the RNS is Θ specified by Equation (18).

The theorem of Chinese remainder as:

$$
\begin{aligned}
B &= \Sigma_{j=1}^{t} \Gamma_j * MI_j^{-1} * MI_j, \\
MI_J &= \frac{\Theta}{m_j},
\end{aligned}
\tag{19}
$$

where MI_j^{-1} = integers are the multiplicative inverses of MI_j.

In Pseudocode 1, at the top of the following page is shown pseudocode for the Proposed Move Right algorithm (PMR-Algo) which is a nonmonotonic energy method to resolve offline structured tree of PTP. In the pseudocode, τ_a^x represents the value of a in the ath repetition and the sink (a, m) is set to min $\{\Gamma, n_a\}$ for transmission time to each of the links, but the rest of the links is set to 0 for the transmission time (steps 2 and 3). The initial times of packet transmission (moving right) are iteratively increased so that every step locally optimizes the overall power method. This local optimization finally leads to an optimum consequence worldwide.

The transmission of all links not included in the subtree, i.e., transmissions for an initial period from n sensor nodes (Sn) children and the subtree, is finding the end period of transmission by the best.

(•) function around the Sn. We may prove that Sn start times are never reduced through the best

(•) function which provides a binary search between the actual initial and the end time of the transmission for a locally optimal initial time for the transmission from Sn. Step 10 is critical as the entire transmission time on the sink links moves correctly. When the latency limit is reached, this movement ceases.

Start 1:Setx $\longleftarrow$ 02 : For(a,m) εP, $set\tau_a^x \longleftarrow$ min $\{\Gamma, n_a\}$3:For$(a,m)\varepsilon P$,such that b m,set τ_a^x04 : *Set* f $\longleftarrow$05 :While $f = 06$:x $x + 1$
7 :ForeachV_a $\quad$ *withafromm* $- 1downtoN + 18 :$ $(\{\tau_a^x\}_{(a,b)\varepsilon P}, \tau_a^x)$best $\quad$ $(\{_a\wedge x - 1\},_a\wedge x - 1)$9 :For(a,m) $\quad$ P10:Set_
a^xmin$\{n_a, \Gamma - (\max V_{a_a}\{L_b\} - \tau_a^x)\}$11:IF k= k-1,$f \longleftarrow 1$
Stop

PSEUDOCODE 1: For Proposed Move Right algorithm (PRM-Algo) (PMR) algorithm (PMR-Algo).

3.3. Collision in Wireless Sensor Networks.
WSN's impact happens with at least two nodes of their information over the organization simultaneously. For evading crash in WSN, the information must be surrendered and, afterward, retransmitted.

3.4. Collision Minimization.
A collision during data transmission is one of the prime causes for the degradation of performance, which is practically expected in wireless sensor networks [36]. This collision could lead to unnecessary delay and loss of the packet. In order to reduce the risk of a packet collision, the area where the data packet crash occurs should be minimised.

Cooperative transmissions and optimal power allocations are used for minimizing the probability of collision during data transmission [37, 38]. Network collision is avoided by incorporating optimised algorithms, which can be achieved by using parameters such as the number of sources to maximise the size of the containment windows. If a node has a low containment window, it causes a collision, and if the containment window sizes of a node are high, then an average delay of access and a crash-free transmission are created [39].

(a) Congestion detection strategies: the most popular techniques of congestion detection are packet loss, queue length, service time, and time delay

(b) Packet loss: the receiver with the number of sequence used will calculate the packet loss. The congestion detection packet CTS (Clear to Send) can be used. It can be used as a signal for congestion to repair losses. Wireless errors are causing losses instead of packet collision

(c) Queue length: each node has a buffer to allow its duration to indicate congestion easily and properly. Congestion is indicated when the duration of the buffer reaches the fixed threshold. The excess rate is the rate of traffic. The rate of traffic is the difference between the output and the number of the rates supplied and forwarded. Several nonempty tails may show the degree of congestion

(d) Packet service period: packet's service period is different from the packet rate; the interval of the packet reaches the MAC layer and its efficient transmission. Incoming traffic through the overloaded channel is equal or less than the outgoing traffic

(e) Delay: delay quantifies the time required from the sender to the endpoint receipt from packet genera-

tion. The greatest delay is due to the usage of MAC responsibilities, which costs sleep latency

(f) Congestion detection and avoidance in sensor networks (CODA): it is a WSN-specific energy-efficient congestion control method. It helps with the detection of congestion by observing the sensor node buffer size and the use of a wireless channel. It is made up of three mechanisms

When a large number of messages are used for transmission, the crossover condition occurs, and messages are queued based on their priorities. The successors are generated during processing by crossover action. It requires optimal scheduling, so we can select crossover probability 1.0. Again, this process has improved the optimization by using efficient transformation probability as follows:

3.5. Congestion Detection.
Precise and efficient detection of congestion in wireless network congestion is critical [40]. CODA uses an efficient congestion detection on every low-priced recipient to derive a combination of present and past channel load and current buffer occupancy [41]. Since the transmitters are shared and traffic between other devices is congested in the neighbourhood [42], the channel state must be recognized by sensor networks. When the channel is listened to in order for local loading to be measured, the cost of energy is high. CODA uses a sampling system, therefore, which initiates local channel monitoring, to reduce costs while forming a reliable estimate at the appropriate time. Upon detection of congestion, nodes signal their upstream neighbours through a backpressure system.

(a) Channel loading

It provides the optimal data about how busy the adjacent network is, but it is a local modification mechanism. It has a limited effect.

(b) Buffer queue length

In conventional data networks, tail management is also used to detect congestion [43]. Nevertheless, the buffer use or queue size cannot be followed as a congestion signal without a connector layer admissions (some applications do not need this and thus will not use it to save its overhead). Since conventional methods for congestive recognition are not up to the mark, other techniques such as hop backpressure and multisource control in the closed-loop are needed.

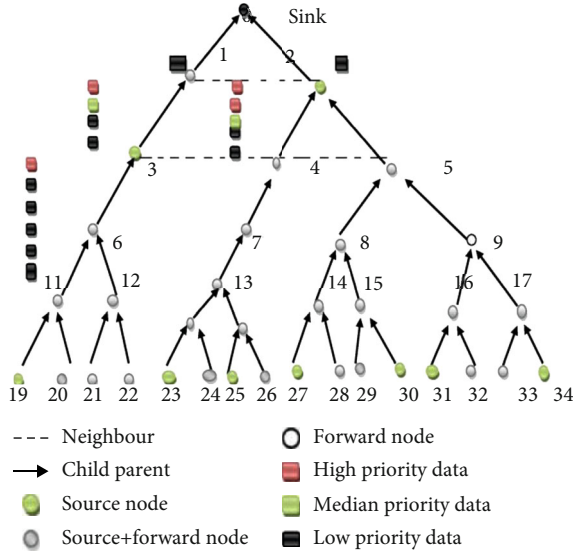(c) Use buffer and weighted buffer difference for congestion detection

FIGURE 2: Network topology for source node arrangement.

Congestion detection uses queue management. The congestion cannot be detected by the buffer. Nodes directly or implicitly send backpressure messages to their neighbour using a congestion sensing buffer. The solution for the detection of congestion [44] is to adjust the buffer and weighted buffer gap. Figure 2 represents network topology for source node arrangement.

A buffer and weighted buffer variation to detect congestion are used to solve this problem. If we take the weight of high, medium, and low priority data to be $P_h=3$, $P_m=2$, $P_l=1$, as shown in Figure 2, the $node_6$ is considered as a length of a weighted buffer WBL_6 by

$$WBL_6 = 2 * P_h + 1 * P_m + 3 * P_l = 2 * 3 + 1 * 2 + 3 * 1 = 11. \tag{20}$$

If we denote weighted buffer variance as WBV $WBV(node_6, node_3) = 6$,

$$
\begin{aligned}
WBV(node_4, node_3) &= 5, \\
WBV(node_4, node_8) &= 7, \\
WBV(node_4, node_2) &= 9, \\
WBV(node_8, node_4) &= -7, \\
WBV(node_3, node_4) &= -5.
\end{aligned} \tag{21}
$$

We propose buffer and weighted buffer differences in congestion detection for two local congestion measuring levels at each node. The length of weighted queue is expressed as:

$$WB = \Sigma_{j=1}^{N} DP(Packet_j), \tag{22}$$

where the priority of data packet dynamic is defined as:

$$DP(Pack) = \frac{\alpha^* hop + SP(Pack)}{1 + \beta^* delay}. \tag{23}$$

N is the total number of buffer packets. A weighted buffer with length WB (b), after Δb, it becomes

$$WB(b + \Delta b) = WB(b)WR * \Delta b. \tag{24}$$

The weighted buffer difference at time $t + \Delta t$ is

$$WBD_n ode_i(p + \Delta p) = \Sigma_{j=1}^{N} DP(Pack_j) - Max(WB_k(p + \Delta p)). \tag{25}$$

If $WBD_{node_i}(p + \Delta p)$, it means that the data of $node_i$ is the most important among its neighbors.

3.6. Open-Loop Hop-by-Hop Back Pressure. Sensor network CODA uses a backpressure to message anywhere congestion is detected [45, 46]. Backpressure signals pass to the source point directly. Backpressure is directly at the source in the case of impulse data in dense network conditions. The backpressure nodes of the recipient raise the rate of return of local congelation and settle on a method based upon the local network situation when an upstream node receives the backpressure node (backpressure nodes).

3.7. Regulation of Closed-Loop Multisource. It helps regulate congestion from a sink under persistent congestion over multiple sources. If the rate of source events is smaller in a channel, then the source controls itself, and the value is greater, so there is a greater likelihood of congestion [47, 48]. Only when a certain threshold is reached will the source reach the sink. This means that in order to maintain its rate, the source requires continuous, slow-term input from the sink. ACKs here act as a self-clocking system to keep the current rate of events.

4. Simulation Setup and Result Discussion

Consider each node in networking having a higher number of packets for transforming towards downstream nodes in the network. For this, there should be a small contention window; hence, its size is increased, and hence, it is found that congestion is diminished. Consequently, a small quantity of power is stored through a reduction in idle listening when a medium access delay happens. This reduces the energy loss feature. This simulation is performed in two distinct setups with several nodes like 0 to 8 and also 9 to 17 in various measuring factors which are discussed below.

4.1. Nodes vs. Contention Window. Figures 3(a) and 3(b) depicted that contention window is a time bound parameter. It specifies the flow rate and medium time of access of the data packets. In the communication process, the contention window value is considered for each node. Now, in this figure, one contention window initial value and idealized value is plotted for each of the nodes. Contention window value is evaluated by

(a)

(b)
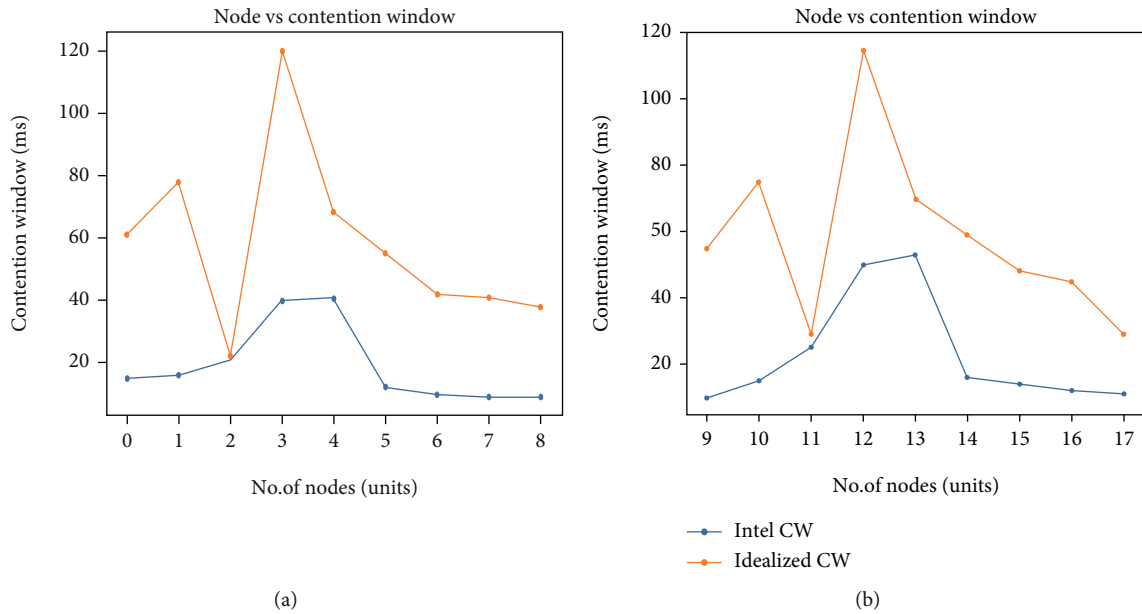
FIGURE 3: The initial contention window and idealized contention window for (a) nodes 0 to 8 and (b) nodes 9 to 17.

(a)

(b)
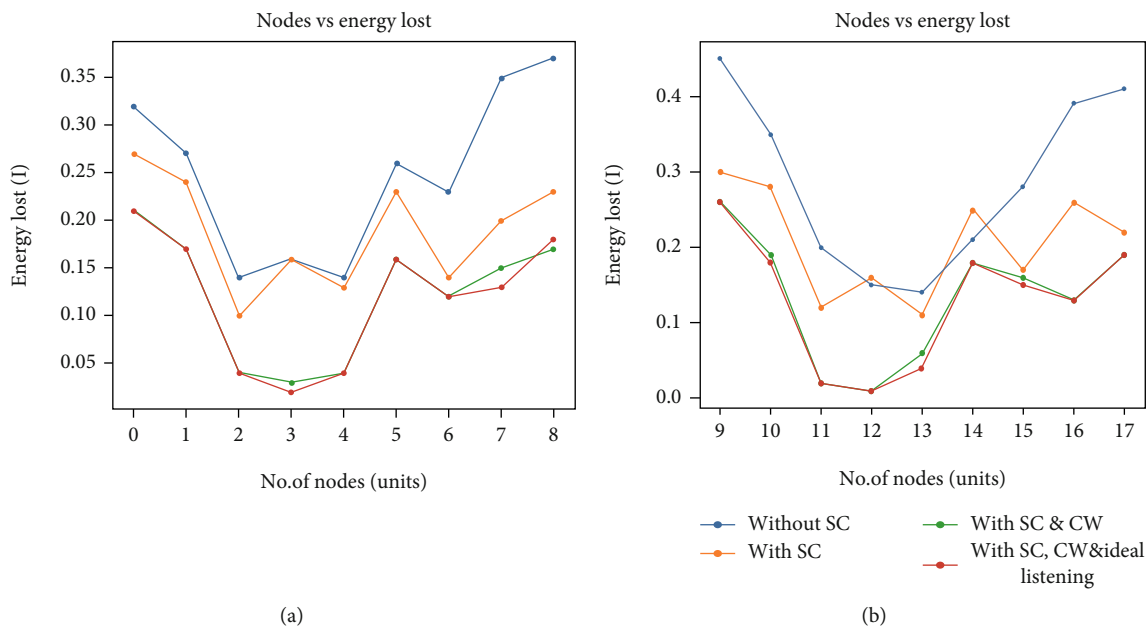
FIGURE 4: The energy lost comparison after applying the various causes for (a) nodes 0 to 8 and (b) nodes 9 to 17.

$$CW(x) = CW_{min}\left(\frac{S_n}{SC_x}\right), \qquad (26)$$

where $CW(x)$ = contention window value for any node x,

CW_{min} = minimum contention window value,

S_n = estimated number of nodes within the detecting radius,

SC_x = source count value of any node x.

$$(27)$$

4.2. Nodes vs. Energy Lost (J). In Figures 4(a) and 4(b), energy loss at each node is plotted for various conditions like with and without source-count, with combining source-count, contention window, and ideal listening.

4.3. Nodes vs. Collision. To minimise the collision of network packets. The source value prioritises data packet communication of each sensor node, which decreases the congestion of data packets and the access time for the medium node. The value of the source count priority is to communicate packets from every node, hence, reducing data packet congestion and medium node access time. Figures 5(a) and

(a)   (b)

FIGURE 5: The collision occurring and the collision which has been minimized for (a) nodes 0 to 8 and (b) nodes 9 to 17.

(a)   (b)

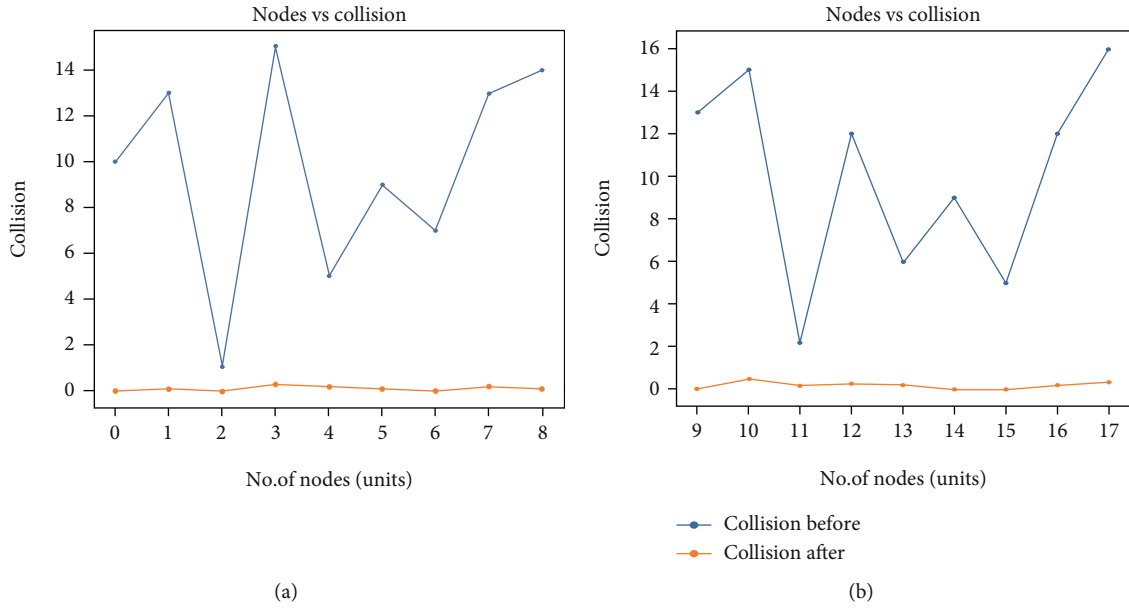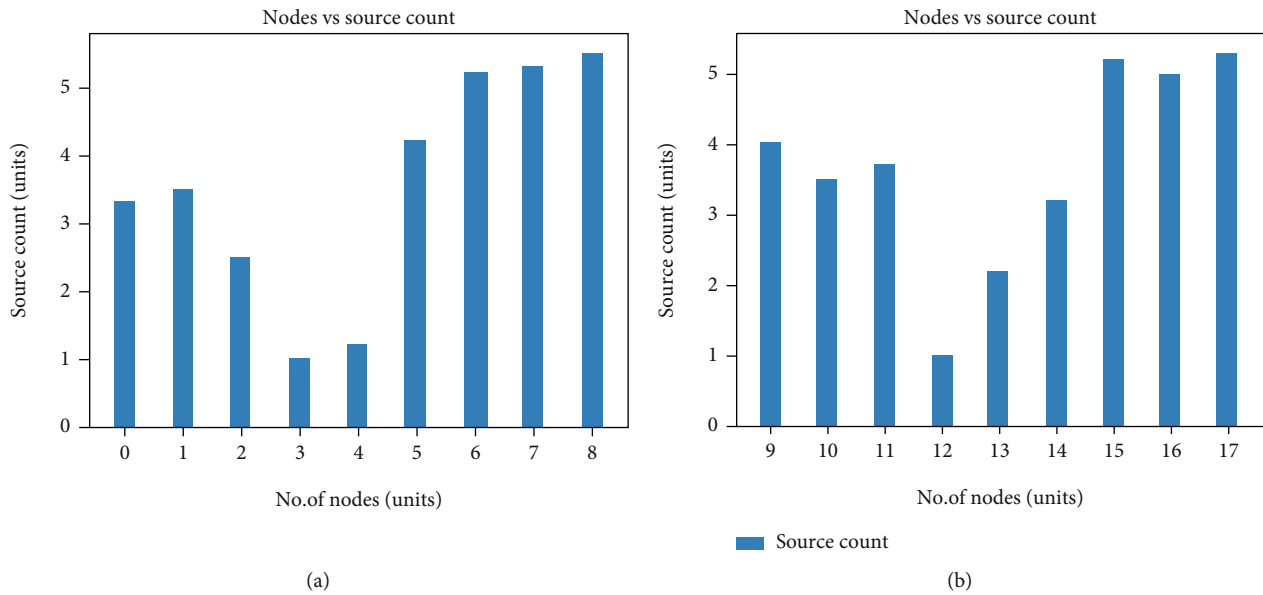FIGURE 6: The source count value for each (a) nodes 0 to 8 and (b) nodes 9 to 17.

5(b) display before and after variation of collision in respective nodes.

4.4. Nodes vs. Source Count (SC).

The whole number of source nodes to which data can be transmitted, the value of any node *x*, referred to as SC, is specified. Because when a node has packets to transmit, it needs to understand its source count (SC); it is enough to transmit SC value along with the packet. Figures 6(a) and 6(b) depicted that the SC for each node is represented.

The contention window should be greater than the user for each node with a smaller amount of data packets that can be forwarded to downstream nodes in the network.

The situation varies in a way which makes medium access delay insignificant and ultimately prevents collisions. It has been observed that medium access delays and the impact of collisions have been reduced which have contributed to increased network performance.

4.5. Nodes vs. Network Lifetime (NL).

The standard simple network topology is explained about the improvement of performance for the proposed condition method attains globally optimal solution by allocating the traffic into each node equally, then it is required to maximize the network lifetime (NL). Figures 7(a) and 7(b) show the effect of the number of nodes on the output of NL under this condition

FIGURE 7: The network lifetime for each (a) nodes 0 to 8 and (b) nodes 9 to 17.

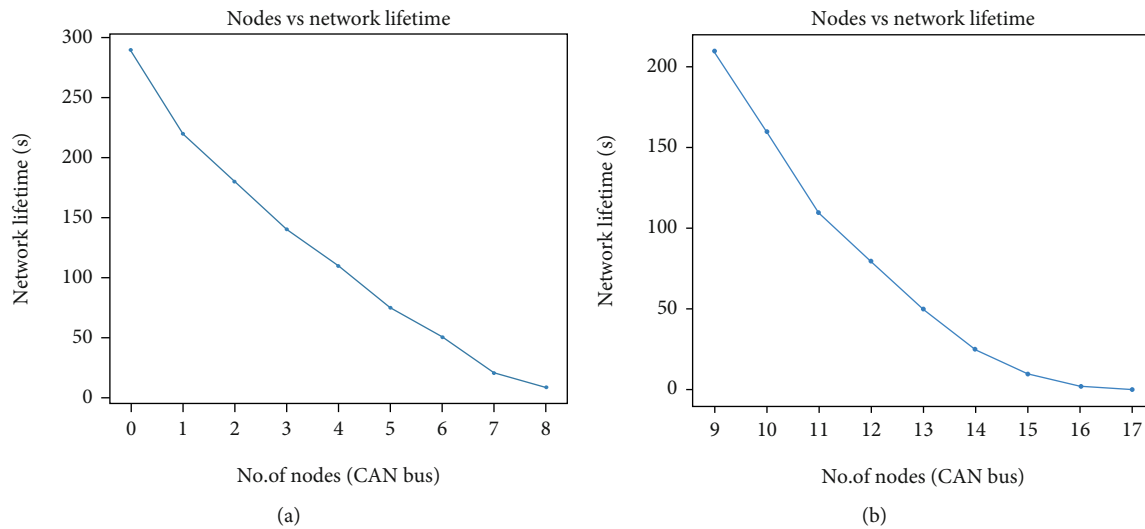method. While the number of nodes rises, the NL drops exponentially. It will be therefore easy and effective to extend the NL by limiting the network utilization in the small case.

5. Conclusion and Future Work

In this assessment work, an audit on WSN and their developments, standards, and applications were finished. Far off sensor networks include little centre with identifying, estimation, and wireless trade limits. Many coordinating, power the chiefs, and data communication shows have been unequivocally expected for WSNs where imperativeness care is a basic arrangement issue. WSNs include little centre points with recognizing, computation, and wireless correspondence limits. Many coordinating, power the heads, and data correspondence shows have been expressly proposed for WSNs where imperativeness care is a crucial arrangement issue. Future work is focused on a more optimal power efficiency model for cloud servers, smart devices, and wireless sensors that would improve the accuracy of the simulation results.

Data Availability

The 'Nodes' data used to support the findings of this study are available from the corresponding author upon request.

Conflicts of Interest

The authors of this manuscript declared that they do not have any conflict of interest.

References

[1] A. Jarwan, A. Sabbah, and M. Ibnkahla, "Data transmission reduction schemes in WSNs for efficient IoT systems," *IEEE Journal on Selected Areas in Communications*, vol. 37, no. 6, pp. 1307–1324, 2019.

[2] D.-G. Zhang, H. Wu, P. Z. Zhao et al., "New approach of multi-path reliable transmission for marginal wireless sensor network," *Wireless Networks*, vol. 26, no. 2, pp. 1503–1517, 2020.

[3] A. Jari and A. Avokh, "PSO-based sink placement and load-balanced anycast routing in multi-sink WSNs considering compressive sensing theory," *Engineering Applications of Artificial Intelligence*, vol. 100, article 104164, 2021.

[4] M. Faheem, R. A. Butt, B. Raza et al., "FFRP: dynamic firefly mating optimization inspired energy efficient routing protocol for internet of underwater wireless sensor networks," *IEEE Access*, vol. 8, pp. 39587–39604, 2020.

[5] N. S. Kumar, E. Suryaprabha, and K. Hariprasath, "Machine learning based hybrid model for energy efficient secured transmission in wireless sensor networks," *Journal of Ambient Intelligence and Humanized Computing*, vol. 11, pp. 1–16, 2021.

[6] S. M. Chowdhury and A. Hossain, "Different energy saving schemes in wireless sensor networks: a survey," *Wireless Personal Communications*, vol. 114, no. 3, pp. 2043–2062, 2020.

[7] A. Amin, X.-H. Liu, M. A. Saleem et al., "Collaborative wireless power transfer in wireless rechargeable sensor networks," *Wireless Communications and Mobile Computing*, vol. 2020, Article ID 9701531, 13 pages, 2020.

[8] L. Mishra and S. Varma, "Middleware technologies for smart wireless sensor networks towards internet of things: a comparative review," *Wireless Personal Communications*, vol. 116, no. 3, pp. 1539–1574, 2021.

[9] S. L. Yadav, R. Ujjwal, S. Kumar, O. Kaiwartya, M. Kumar, and P. K. Kashyap, "Traffic and energy aware optimization for congestion control in next generation wireless sensor networks," *Journal of Sensors*, vol. 2021, 2021.

[10] B. Jiang, G. Huang, F. Li, and S. Zhang, "Compressed sensing with dynamic retransmission algorithm in lossy wireless IoT," *IEEE Access*, vol. 8, pp. 133827–133842, 2020.

[11] C. Seneviratne, P. A. D. S. N. Wijesekara, and H. Leung, "Performance analysis of distributed estimation for data fusion using a statistical approach in smart grid noisy wireless sensor networks," *Sensors*, vol. 20, no. 2, p. 567, 2020.

[12] I. Nikol'skii and K. Furmanov, "Efficiency of retransmission in sensor networks," *Computational Mathematics and Modeling*, vol. 31, no. 4, pp. 471–476, 2020.

[13] R. Gurunath, A. H. Alahmadi, D. Samanta, M. Z. Khan, and A. Alahmadi, "A novel approach for linguistic steganography evaluation based on artificial neural networks," *IEEE Access*, vol. 9, pp. 120869–120879, 2021.

[14] H. S. Z. Kazmi, N. Javaid, M. Awais, M. Tahir, S.-O. Shim, and Y. B. Zikria, "Congestion avoidance and fault detection in WSNs using data science techniques," *Transactions on Emerging Telecommunications Technologies*, vol. 107, no. article e3756, 2019.

[15] A. K. Biswal and M. Samantaray, "A novel approach for localization in sensor network," *International Journal of Engineering Research Technology*, vol. V9, no. 1, pp. 323–328, 2020.

[16] H. Xie, Z. Yan, Z. Yao, and M. Atiquzzaman, "Data collection for security measurement in wireless sensor networks: a survey," *IEEE Internet of Things Journal*, vol. 6, no. 2, pp. 2205–2224, 2018.

[17] A. Liu, Z. Chen, and N. N. Xiong, "An adaptive virtual relaying set scheme for loss-and-delay sensitive WSNs," *Information Sciences*, vol. 424, pp. 118–136, 2018.

[18] D. Samanta, A. H. Alahmadi, M. P. Karthikeyan et al., "Cipher block chaining support vector machine for secured decentralized cloud enabled intelligent IoT architecture," *IEEE Access*, vol. 9, pp. 98013–98025, 2021.

[19] A. K. Biswal, D. Singh, and B. K. Pattanayak, "IoT-based voice-controlled energy-efficient intelligent traffic and street light monitoring system," in *Green Technology for Smart City and Society*, pp. 43–54, Springer, 2021.

[20] S. Gopinath, K. V. Kumar, P. Elayaraja, A. Parameswari, S. Balakrishnan, and M. Thiruppathi, "Sceer: secure cluster based efficient energy routing scheme for wireless sensor networks," *Materials Today: Proceedings*, vol. 45, pp. 3579–3584, 2021.

[21] S. Gorgich and S. Tabatabaei, "Proposing an energy-aware routing protocol by using fish swarm optimization algorithm in WSN (wireless sensor networks)," *Wireless Personal Communications*, vol. 107, pp. 1–21, 2021.

[22] Y.-W. Kuo, C.-L. Li, J.-H. Jhang, and S. Lin, "Design of a wireless sensor network-based IoT platform for wide area and heterogeneous applications," *IEEE Sensors Journal*, vol. 18, no. 12, pp. 5187–5197, 2018.

[23] A. Lavric, "Lora (long-range) high-density sensors for internet of things," *Journal of Sensors*, vol. 2019, Article ID 3502987, 9 pages, 2019.

[24] M. Mamun-Or-Rashid, M. M. Alam, M. A. Razzaque, and C. S. Hong, "Reliable event detection and congestion avoidance in wireless sensor networks," in *International Conference on High Performance Computing and Communications*, pp. 521–532, Springer, 2007.

[25] C.-Y. Wan, S. B. Eisenman, and A. T. Campbell, "Coda: congestion detection and avoidance in sensor networks," in *Proceedings of the 1st international conference on Embedded networked sensor systems*, pp. 266–279, Los Angeles, California, USA, 2003.

[26] Y. Sankarasubramaniam, O. B. Akan, and I. F. Akyildiz, "Esrt: event-to-sink reliable transport in wireless sensor networks," in *Proceedings of the 4th ACM international symposium on Mobile ad hoc networking & computing*, pp. 177–188, Annapolis, Maryland, USA, 2003.

[27] C. Intanagonwiwat, R. Govindan, and D. Estrin, "Directed diffusion: a scalable and robust communication paradigm for sensor networks," in *Proceedings of the 6th annual international conference on Mobile computing and networking*, pp. 56–67, Boston, Massachusetts, USA, 2000.

[28] C. Wang, K. Sohraby, B. Li, M. Daneshmand, and Y. Hu, "A survey of transport protocols for wireless sensor networks," *IEEE Network*, vol. 20, no. 3, pp. 34–40, 2006.

[29] A. Woo and D. E. Culler, "A transmission control scheme for media access in sensor networks," in *Proceedings of the 7th annual international conference on Mobile computing and networking*, pp. 221–235, Rome, Italy, 2001.

[30] E. Alzahrani and F. Bouabdallah, "Qmmac: quorum-based multichannel mac protocol for wireless sensor networks," *Sensors*, vol. 21, no. 11, p. 3789, 2021.

[31] P. Mukherjee and A. Das, "Nature-inspired algorithms for reliable, low-latency communication in wireless sensor networks for pervasive healthcare applications," in *Nature Inspired Computing for Wireless Sensor Networks*, pp. 321–341, Springer, 2020.

[32] Z. Chen and H. Shen, "A grid-based reliable multi-hop routing protocol for energy-efficient wireless sensor networks," *International Journal of Distributed Sensor Networks*, vol. 14, no. 3, 2018.

[33] M. A. Hassanien, P. Loskot, S. M. al-Shehri, T. Numanoğlu, and M. Mert, "Design and performance evaluation of bitwise retransmission schemes in wireless sensor networks," *Physical Communication*, vol. 37, article 100876, 2019.

[34] A. K. Biswal, D. Singh, B. K. Pattanayak, D. Samanta, S. A. Chaudhry, and A. Irshad, "Adaptive fault-tolerant system and optimal power allocation for smart vehicles in smart cities using controller area network," *Security and Communication Networks*, vol. 2021, Article ID 2147958, 15 pages, 2021.

[35] V. Sundararaj, S. Muthukumar, and R. Kumar, "An optimal cluster formation based energy efficient dynamic scheduling hybrid mac protocol for heavy traffic load in wireless sensor networks," *Computers & Security*, vol. 77, pp. 277–288, 2018.

[36] F. Wang, W. Liu, T. Wang et al., "To reduce delay, energy consumption and collision through optimization duty-cycle and size of forwarding node set in WSNs," *IEEE Access*, vol. 7, pp. 55983–56015, 2019.

[37] J. Zhang, L. Xu, P.-W. Tsai, and Z. Lin, "Minimization of delay and collision with cross cube spanning tree in wireless sensor networks," *Wireless Networks*, vol. 25, no. 4, pp. 1875–1893, 2019.

[38] S. W. H. Shah, A. N. Mian, A. Aijaz, J. Qadir, and J. Crowcroft, "Energy-efficient mac for cellular IoT: state-of-the-art, challenges, and standardization," *IEEE Transactions on Green Communications and Networking*, vol. 5, no. 2, pp. 587–599, 2021.

[39] G. M. J'unior and L. H. Correia, "Sm3-mac: a multichannel collision-free mac protocol for wireless sensor networks," in *2018 IEEE Symposium on Computers and Communications (ISCC)*, pp. 00550–00555, Natal, Brazil, 2018.

[40] C. Lim, "A survey on congestion control for RPL-based wireless sensor networks," *Sensors*, vol. 19, no. 11, p. 2567, 2019.

[41] P. Aimtongkham, S. Heng, P. Horkaew, T. G. Nguyen, and C. So-In, "Fuzzy logic rate adjustment controls using a circuit breaker for persistent congestion in wireless sensor networks," *Wireless Networks*, vol. 26, no. 5, pp. 3603–3627, 2020.

[42] M. Vadivel, A. Ali, and V. Sivakumar, "A study on congestion control in WSN using dynamic alternative path selection approach," in *2018 2nd International Conference on I-SMAC (IoT in Social, Mobile, Analytics and Cloud)(I-SMAC) I-*

SMAC (IoT in Social, Mobile, Analytics and Cloud)(I-SMAC), pp. 346–349, Palladam, India, 2018.

[43] K. Le, B. Pham, Q. Tram, T. Bui, and T. Quan, "Code-WSN: a formal modelling tool for congestion detection on wireless sensor networks," in *2018 IEEE World Symposium on Communication Engineering (WSCE)*, pp. 1–7, Singapore, 2018.

[44] N. Ababs and F. Yu, "A dual-buffer based congestion control algorithm for wireless multimedia sensor networks," in *2019 International Conference on Internet of Things (iThings) and IEEE Green Computing and Communications (GreenCom) and IEEE Cyber, Physical and Social Computing (CPSCom) and IEEE Smart Data (SmartData)*, pp. 1177–1184, Atlanta, GA, USA, 2019.

[45] N. Pant, "Priority aware congestion control scheme using dual thresholds," in *2018 First International Conference on Secure Cyber Computing and Communication (ICSCCC)*, pp. 610–613, Jalandhar, India, 2018.

[46] Anisha and S. S. Chauhan, "A survey on transport layer protocols for reliable and secure wireless sensor networks," in *Evolving Technologies for Computing, Communication and Smart World*, pp. 151–163, Springer, 2021.

[47] S. A. Chelloug, "An intelligent closed-loop learning automaton for real-time congestion control in wireless body area networks," *International Journal of Sensor Networks*, vol. 26, no. 3, pp. 190–199, 2018.

[48] Y. Yu, V. K. Prasanna, and B. Krishnamachari, "Energy minimization for real-time data gathering in wireless sensor networks," *IEEE Transactions on Wireless Communications*, vol. 5, no. 11, pp. 3087–3096, 2006.

Research Article

Financial Security Analysis of E-Commerce Platform Based on Supply Chain for Heterogeneous Network Location Verification

Qiao Qu [ID],[1] Cheng Liu,[1] and Xinzhong Bao [ID][2]

[1]*School of Economics and Management, University of Science and Technology Beijing, Beijing 100083, China*
[2]*School of Management, Beijing Union University, Beijing 100101, China*

Correspondence should be addressed to Qiao Qu; qq0069aa@163.com

The development of supply chain finance, its pricing strategy for bilateral business cooperation between e-commerce, banking institutions, and fourth-party logistics services providers has gained the attention of researchers. This paper combines the heterogeneous network location verification technology, starting from information asymmetry and Rubens bargaining game ideas, and combines it with game theory methods to provide a reference for bilateral cooperation decision-making on e-commerce platforms. The experiment results indicated the pricing decisions of e-commerce platforms which are affected by the efforts of the other party and the ability of bargaining. The quoted price increases with the decrease of the bank's ability and the increase of the service provider's ability. The pricing decisions of banks and service providers are only affected by the direct proportion of their respective business costs. When considering the introduction of incentive mechanism conditions, it is found that appropriate incentive conditions can increase the quotation of the e-commerce platform. The price quoted by the e-commerce platform that chooses to bargain with the bank is higher than the price quoted by the bank after negotiating with the service provider, which will help to better realize the benefits. Finally, the paper numerically analyzes the results of the bargaining game between e-commerce platforms and banks and fourth-party logistics service providers, and the numerical results verify the better performance.

1. Introduction

In recent years, with the rapid development of Information and Communication Technologies (ICTs), Internet of Things (IoTs), new retail, and digital finance, the supply chain finance model has been innovated. This strategy helps further to ease the financing difficulties and financial pressures in small and medium-sized enterprises [1]. The collaborative development model of e-commerce platforms, finance, and logistics systems has gradually emerged. The main links of the supply chain operation are completed online and promote the circulation of data information and resources between different enterprise entities. The multiagent collaboration platform-based supply chain finance has gradually become a development trend. At the same time, e-commerce platforms play an increasingly important role in the operation of supply chain finance and promote the optimal allocation of online and offline resources and information sharing. This development trend towards multiplatform cooperation has gained the interest. Business cooperation channels continue to expand [2, 3]. However, the development of supply chain finance has been still faced challenges and has certain operational and cooperation risks. The problems of cooperative relations and benefit distribution among multiple entities have become more complicated, and related business cooperation pricing issues are worthy and need further discussion and research [4]. Since banks and fourth-party logistics service providers are, respectively, the main funders and logistics service providers for the online operation of supply chain finance. It is important to coordinate the cooperative pricing relationship between the e-commerce platform and the two parties to improve online resource circulation and business efficiency.

In the context of the gradual development of e-commerce, the government encourages the innovation of supply chain financial models that coordinate the development of e-

commerce platforms with banks and logistics service providers. The relevant analysis of the cooperative pricing strategy of e-commerce platforms helps to reduce the cooperation crisis of participants and increase economic benefits [5, 6]. At present, many scholars have carried out research on relevant aspects of supply chain finance, and their main content is concentrated on model development and operation, online, and offline risk management issues but there are few studies on bilateral cooperation pricing of e-commerce platforms. First of all, in the research on the development of the supply chain finance model, authors in [7] showed that the supply chain finance network structure shows the characteristics of platform and network, which promotes the information sharing and the improvement of the credit quality of small and medium-sized enterprises. Authors believed that the e-commerce environment provides opportunities for banks and financial institutions for innovate using technology and business practices [8]. Authors in [9] discussed that the logistics service providers in the supply chain can help to improve the organizational efficiency of enterprises and the level of supply chain management.

In [10], the authors found that the improvement of supply chain management has a positive impact on banks' participation in supply chain finance, the establishment of bank credit mechanisms, and risk management. Authors in [11] pointed out that the development of digital credit has the advantage of reducing transaction costs. Second, a reasonable pricing strategy will help to achieve multiplatform cooperation in the supply chain to effectively improve the efficiency of supply chain operations and corporate financing efficiency and promote the further extension of the supply chain industry chain. The authors in [12] used system dynamics to improve the supply chain of product distribution systems. The authors in [13] used the analytic hierarchy process and fuzzy set theory to study the supply chain performance and strategy issues of the purchasing department. By introducing contracts to coordinate the supply chain with capital constraints, the total benefits under centralized decision-making can be realized, and the overall efficiency of the supply chain and the cooperation and win-win of the main body can be improved. At the same time, game theory research methods have been well used, including the study of the profit distribution game model of upstream and downstream enterprises in the supply chain [14, 15]. Use the optimized game model to study corporate financing operation decisions and build a Stackelberg game model to discuss the collaborative innovation of supply chain companies [16, 17].

This paper combines the heterogeneous network location verification technology and draws the idea of dynamic bargaining game to analyze the bilateral pricing strategy of e-commerce platforms. To sum up, although the existing literature studies mostly focused on the traditional supply chain finance model and its development, supply chain financing and risk issues, and product distribution strategies and discussed the cooperation model of the participants and the platform distribution channels. But still, from the perspective of e-commerce platforms, it is rare to use bilateral bargaining models to analyze the pricing issues of cooperating with banking institutions and service providers at the same time. Based on this, the main contribution of the paper is combining the heterogeneous network location verification technology, drawing on the idea of dynamic bargaining game, and analyzing the bilateral pricing strategy of e-commerce platforms.

The structure of the paper is organized as follows: Section 1 presents the model description and model assumptions, explaining the brief process of parameter setting and bargaining on the e-commerce platform. Section 2 discusses the game model of bargaining with fourth-party service providers and banking institutions and analyzes the results of the e-commerce platform. Section 3 illustrates the numerical analysis, combining the research results to analyze the influence of relevant factors on the pricing decisions of the partners. Section 4 presents the conclusion, which puts forward the deficiencies and prospects of the research in this paper, and tries to make relevant suggestions based on the conclusion.

2. Model Description and Model Assumptions

2.1. Heterogeneous Network Location Verification. The location management technology of heterogeneous networks is one of the research area. There are various studies that discussed the location management technology for heterogeneous wireless networks, including link layer location management technology, network layer location management technology, and application layer location management technology [18]. In the network architecture of wide local area network (WLAN) and mobile communication network interconnection, 3Gpp and 3GppZ both decided to adopt the mobile Internet Protocol (IP) proposed by Internet Engineering Task Force (IETF) to realize the location management of WLAN terminal [19, 20]. However, the mobile communication network itself has a very mature mechanism for location management, and the network architecture of the mobile communication network is constantly evolving. In this case, how to use the mobile IP protocol to realize the location management function of WLAN and mobile communication network interconnection still needs a lot of research work [21–23]. However, in the HMIPv6 mobility architecture, all packets sent by the communication peer to all mobile nodes (MNs) in the anchor area network and must pass through a fixed MAP. The MAP receives all the data packets on behalf of the mobile terminal it serves and encapsulates these data packets and forward to the current address of the terminal [24, 25]. Therefore, MAP consumes a lot of processing power in route search and packet forwarding, which seriously affect the overall performance of the network. The performance of MAP becomes a bottleneck for the entire network. In the future heterogeneous and convergent network environment, existing wireless access technologies are evolving with an advanced stage, new wireless access technologies continue to emerge, and they complement each other to form a network with overlapping coverage. Figure 1 reflects the
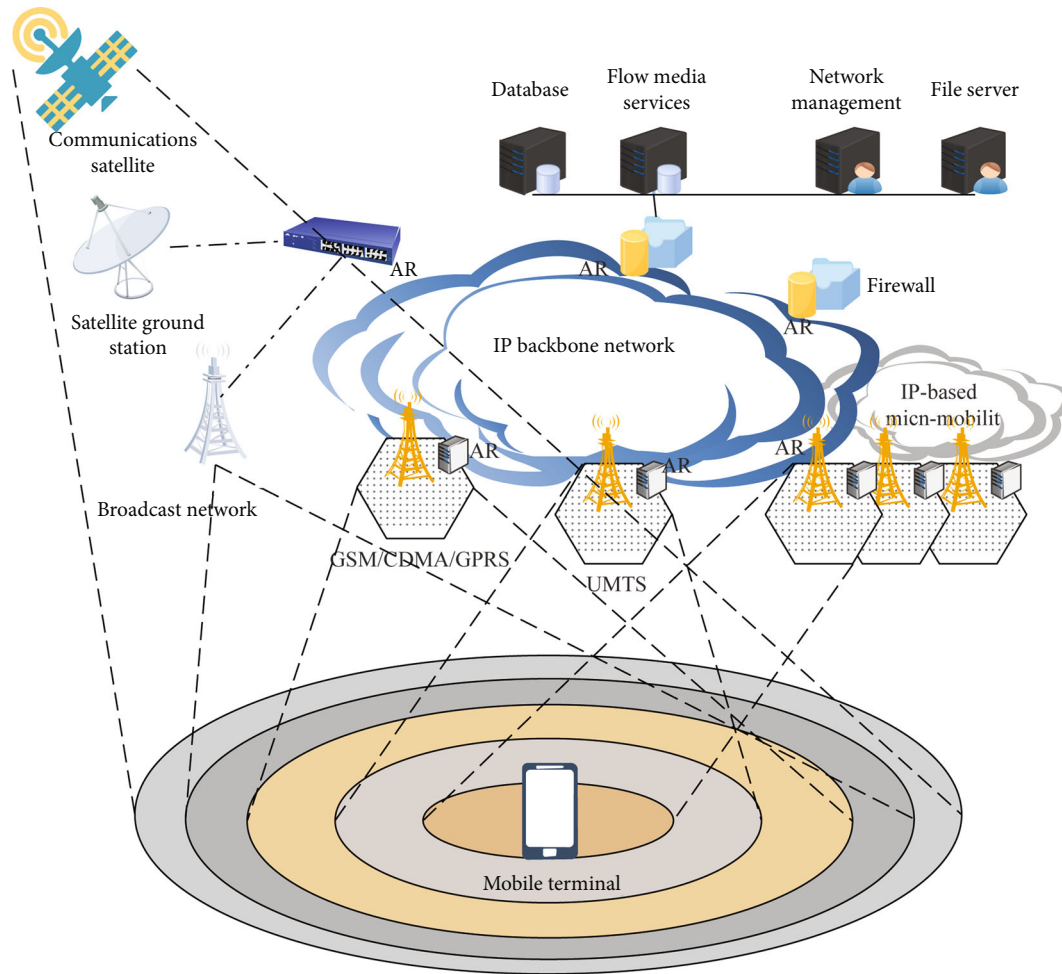
FIGURE 1: Future heterogeneous converged network environment.

schematic diagram of the future heterogeneous converged network environment.

From the current technology perspective, mobile IP-based network layer mobility management is adopted for terminal roaming in a heterogeneous network environment, which can better shield various lower-layer wireless communication technologies and realize seamless user roaming and unified mobility management to achieve the ultimate goal of personal communication [26]. For the movement within the anchor domain, the MN only moves between subnets, and the MAP to which the MN belongs before and after the movement does not change. For the movement between the anchor domains, the MAP that the MN belongs to before and after the movement changes, but the MAP before and after the movement still belongs to the same access network and is controlled by the same CMAP (Or HA) management [27]. For the movement between visiting networks, the MAPs before and after the MN moves are in different visits and are managed by different CMAPs.

2.2. E-Commerce Platform Supply Chain Model Description. This paper is based on the important position of e-commerce platform in the supply chain financial business, and it is playing an increasingly important role in the multi-platform cooperation model. Based on the e-commerce platform undertaking the credit entrusted business of banking institutions and the logistics integrated service business outsourcing to the fourth-party logistics service provider, this paper establishes the bilateral bargaining model of the e-commerce platform in business cooperation and discusses the different bargaining orders. That is, the platform first bargained with service providers, and then with the banking institutions bargaining strategy, and the platform first bargained with banking institutions, and then bargaining strategies with service providers, and based on the relevant conclusions drawn, consider the introduction of incentive mechanism conditions for analysis. This will not only help banks expand their customer base and business channels but also promote fourth-party service providers to further build a comprehensive service system that integrates warehousing and transportation, circulation processing, technical consultation, and resource integration. The brief schematic flow of bilateral bargaining on the e-commerce platform can be represented in Figure 2.

Using the bargaining game method, we can simulate and solve the real transaction and interest coordination issues through negotiation between the two parties. For the party undertaking bilateral bargaining, the reasonable pricing
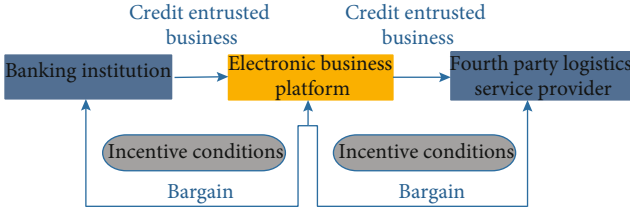
FIGURE 2: Schematic diagram of bilateral bargaining on e-commerce platforms.

issues discussed are also affected by the game decisions of other parties. From the perspective of revenue, e-commerce platforms play an important role in information sharing and resource integration, building a bridge for cooperation between multiple platforms in supply chain finance. When establishing the game model, this paper considers that the platform revenue is mainly derived from the pricing income of the bank's credit entrustment business and deducts the pricing expenses of the product logistics service business with the fourth-party service provider. In addition, it does not consider the business cooperation to the parties. The related hidden income is brought by it, such as the trust and satisfaction of the client enterprise, the stickiness and intensity of cooperation between the parties and the bank, the improvement of platform information management level, the improvement of transportation logistics, and product quality service system.

2.3. Model Assumptions and Parameter Description

Hypothesis 1. E-commerce platforms, banks, and fourth-party service providers have the ability to learn in the game and can make decisions and anticipate adjustments based on the behavior of another game party. The pricing and cooperation plans reached by the parties in the bargaining game are mainly affected by factors such as their respective business costs, effort level, affordability, bargaining ability, and order.

Hypothesis 2. E-commerce platforms can obtain certain benefits from participating in cooperation and promote the circulation and sharing of information resources in the supply chain. In addition, in the information age, banks gradually give way to the e-commerce platform and the fourth party in cooperation. Here, C_b can be used to indicate that the bank alone bears the cost of the business, including the collection and review of customer enterprise credit information, product pledge, and supervision [28]. Let C_e denote the final business price reached between the e-commerce platform and the bank. If the incentive mechanism is considered, the bank sets incentive coefficients $\alpha, \alpha \geq 1$ for the e-commerce platform, that is, αC_e is used to represent the bank's subsidies and sharing of costs such as technical input and information management when developing business on the e-commerce platform, which can also mobilize electricity. The investment enthusiasm and effort level of the business platform can obtain hidden benefits. At the same time, by setting an incentive factor T, it means the amount of penalties imposed by banks on e-commerce platforms

withdrawing from cooperation or business violations, in order to deal with online operations and moral hazards that may be involved in e-commerce platforms, or to seek better partners and withdraw from the constraints of the cooperation [29].

Hypothesis 3. In cooperation with fourth-party service providers, e-commerce platforms can not only use the advantages of service providers in product pledge, circulation processing, quality and safety, technical consultation, and resource integration, to entrust enterprise product circulation services. Here, C_f is used to represent the business cost of the fourth party service provider. Let C_s denote the final business price reached between the e-commerce platform and the fourth-party service provider. If the incentive mechanism is considered, the e-commerce platform has an incentive coefficient $\beta, \beta \geq 1$ for the fourth-party service provider, that is, βC is used to represent the subsidy of the e-commerce platform to the service provider's business cost or the reward in the supervision process, which can also promote service providers actively promote business processes and improve logistics management to obtain hidden benefits; at the same time, by setting up incentive factors, it means that the e-commerce platform imposes penalties on fourth-party service providers' withdrawal from cooperation or business violations to provide services The business risks and issues that may be involved in the cooperation are constrained.

Hypothesis 4. Each party in the game can estimate the cost of benefits of other parties based on experience. Therefore, it is assumed that the e-commerce platform can estimate C_b, C_f according to experience. All follow the uniform distribution of F. The bank estimates that F obeys the uniform distribution of $[m, n]$. Fourth, the service provider estimates that C_s obeys the uniform distribution of $[m, n]$. If there is $C_b \geq C_e \geq C_s$, the intermediate business transaction will be reached, and vice versa.

Hypothesis 5. Taking $\lambda_e, \lambda_b, \lambda_f$ as the discount factor for e-commerce platforms, banks, and fourth-party service providers, respectively, it can be regarded as the degree of cooperation and bargaining power of all parties in the game process, and $0 < \lambda_e, \lambda_b, \lambda_f < 1$ mainly refers to the fact that all parties are if the cooperation agreement is reached late, the price will be paid, otherwise, the parties will tend to reach the cooperation late [30].

Hypothesis 6. In terms of revenue, the revenue of the e-commerce platform mainly comes from the pricing revenue of the bank and the difference between the pricing expenditure of the fourth-party service provider, and other hidden benefits and other costs are not considered here. When choosing a strategy, when the e-commerce platform chooses to bargain with the bank first, the quoted price is represented by $P_{ei}(i = 1, 3, 5 \cdots)$, and $P_{bj}(j = 2, 4, 6 \cdots)$ is the quoted price when the bank is playing with the e-commerce platform. At this time, if the price quoted by the e-commerce

platform is higher than the bank's expectations estimate that the bank may choose not to cooperate and complete the business on its own. Then, the e-commerce platform then bargained with the fourth-party service provider's quotation is represented by $P_{si}(i = 1, 3, 5 \cdots)$, $P_{fj}(j = 2, 4, 6 \cdots)$ is the quotation provided by the fourth-party service provider in the game with the e-commerce platform, if the e-commerce platform first communicates with the bank, the price offered is low, and it may have a weaker advantage when bargaining with service providers. The paper mainly analyzes the two-stage game model of the parties to the game, regardless of the situation of the financing company. The symbols and meanings of the relevant parameters can be seen in Table 1.

3. Model Establishment and Analysis

(a) The e-commerce platform first negotiates with the fourth-party logistics service provider

In this strategy, if the two parties first reach a deal, it is equivalent to that the e-commerce platform can have relative psychological expectations and estimates when it knows its own cost function and then bargain with the bank, which can guarantee better returns; on the contrary, if the two parties do not reach a deal, the game ends.

(b) The game between e-commerce platforms and fourth-party logistics service providers

In the first stage of the game, if the fourth-party logistics service provider does not accept the offer from the e-commerce platform, the two parties enter the second stage of the game and the service provider will make an offer. Use the reverse induction method to solve, first discuss the second stage of the game [31]. If the quotation P_{f2} provided by the service provider satisfies the condition that the income of the e-commerce platform is positive, that is, $\lambda_e(C_e - P_{f2})q \geq 0, C_e \geq P_{f2}$, where q is the workload of the two parties to undertake the business, the e-commerce platform will accept the quotation and the game process ends. Therefore, the service provider can use condition $C_e \geq P_{f2}$ as the criterion for judging whether the e-commerce platform chooses to accept, and modify the estimate that C_e is a uniform distribution in the P_{s1}, n interval. If π_f is used to represent the service provider's own income, P_{ea}, P_{er} is the e-commerce platform's choice to accept and reject the probability of quotation, then:

$$\max_{P_{f2}} \pi = 0 P_{er} + \lambda_f \left(P_{f2} - Cf\right) q P_{ea}, \tag{1}$$

$$P_{ea} = P\left(C_e \geq P_{f2}\right) = \frac{n - P_{f2}}{n - P_{s1}}, \tag{2}$$

$$P_{er} = P\left(C_e < P_{f2}\right) = \frac{P_{f2} - P_{s1}}{n - P_{s1}}. \tag{3}$$

Substituting formulas (2) and (3) into formula (1), the

maximum profit that the service provider can guarantee can be found, the two sides of the obtained formula are derived from P_{f2}, and the service provider's quotation in the second stage of the game can be obtained as

$$\max_{P_{f2}} \pi_f = \max_{P_{f2}} \left[\lambda_f \left(P_{f2} - C_f\right) q \frac{n - P_{f2}}{n - P_{s1}}\right], \tag{4}$$

$$P_{f2} = \frac{(n + C_f)}{2}. \tag{5}$$

If the e-commerce platform chooses to accept, the e-commerce platform and the service provider will obtain the following benefits:

$$\lambda_f \left(P_{f2} - C_f\right) q = \lambda_f \frac{(n - C_f)q}{2}, \tag{6}$$

$$\lambda_e \left(C_e - P_{f2}\right) q = \lambda_e \frac{(2C_e - n - C_f)q}{2}. \tag{7}$$

When looking at the first stage of the game between the two parties and the e-commerce platform proposes a quotation P_{s1}, the service provider obtains revenue $(P_{s1} - C_f)q$. In order to satisfy the higher revenue obtained by the service provider at this stage, it should be at P_{s1}, that is, $(P_{s1} - C_f)q \geq \lambda_f(n - C_f)q/2$. The service provider will tend to choose accept [32]. If E is used to represent the revenue π_e of the e-commerce platform, and P_{fa}, P_{fra} is the probability that the service provider chooses to accept the quotation in the first stage and the second stage, respectively, then,

$$\max_{P_{s1}} \pi_e = (C_e - P_{s1})q P_{fa} + \left[\lambda_e(2C_e - n - C_f)\frac{q}{2}\right]P_{fra}, \tag{8}$$

$$P_{fa} = P\left(C_f \leq \frac{2P_{s1} - \lambda_f n}{2 - \lambda_f}\right) = \frac{[2(P_{s1} - m) - \lambda_f(n - m)]}{(2 - \lambda_f)(n - m)}, \tag{9}$$

$$P_{fra} = P\left(C_f > \frac{2P_{s1} - \lambda_f n}{2 - \lambda_f}\right) P\left(C_e \geq P_{f2}\right) = \frac{2(n - P_{f2})}{(2 - \lambda_f)(n - m)}. \tag{10}$$

Substituting equations (5) and (6) into equation (4) can find the maximum benefit that the e-commerce platform can guarantee, and deriving the two sides of the obtained formula with respect to P_{s1}, we can get

$$P_{s1} = \frac{[2(C_e + m) + \lambda_f(n - m)]}{4}. \tag{11}$$

That is, under normal circumstances, the quotation of the e-commerce platform in the first stage, the condition that is met at this time is $C_f \leq [2(C_e + m) - \lambda_f(n + m)]/2(2 - \lambda_f)$. If considering the addition of incentive factors, let the quotation be P_{s1}', $P_{s1}' = [2(\alpha C_e - T + m) + \lambda_f(n - m)]/4$, and the condition that is satisfied at this time is $C_f \leq [2($

TABLE 1: Parameter symbols and their description.

Parameter	Meaning
C_b	Cost borne by the bank
C_f	Costs borne by fourth-party logistics service providers
C_e	E-commerce platform and bank bargaining the final price
a, T	Respectively, the bank's incentives for e-commerce platforms
C_s	The e-commerce platform negotiates the final price with the fourth-party logistics service provider
β, I	Respectively, the incentive factors of e-commerce platforms for fourth-party logistics service providers
$\lambda_e, \lambda_b, \lambda_f$	The discount factors of e-commerce platforms, banks, and fourth-party logistics service providers, respectively
$P_{ei}(i = 1, 3, 5 \cdots)$	Quotations made by the e-commerce platform in the game with the bank game with the fourth-party logistics service provider Quotations made by the e-commerce platform in the game with the bank
$P_{si}(i = 1, 3, 5 \cdots)$	The price quoted by the e-commerce platform during the game with the fourth-party logistics service provider
$P_{bj}(j = 2, 4, 6 \cdots)$	Quotations made by banks in gaming with e-commerce platforms
$P_{fj}(j = 2, 4, 6 \cdots)$	Quotations made by a fourth-party logistics service provider in a game with an e-commerce platform

$\alpha C_e - T + m) - \lambda_f(n + m)]/2(2 - \lambda_f)$, so considering the incentive mechanism will have a certain impact on the final price reached by the cooperation. In summary, the equilibrium solution results of the game between the two parties can be seen in Table 2.

(c) The game between e-commerce platforms and banks

The research in this section is based on the situation that the abovementioned fourth-party logistics service providers first choose to accept the e-commerce platform quotation, that is, under condition $C_f \leq (2P_{s1} - \lambda_f n)/(2 - \lambda_f)$, discuss the bargaining game between the e-commerce platform and the bank. For the same reason, refer to the above section for the solution process, and the game results can be seen in Table 2.

Proposition 7. *Combined with the above analysis, it can be seen that in the process of bilateral bargaining, e-commerce platforms need to combine the pricing decisions of fourth-party service providers and the business pricing decisions of banks to ensure profit.*

Proposition 8. *In the strategy of bargaining between the e-commerce platform and the fourth-party service provider, the service price of the first stage of the e-commerce platform is P_{s1}, and the price under the condition of considering the incentive factor is $P_{s1}{}'$. The comparison can be obtained:*

$$P_{s1}{}' = \frac{\left[2(\alpha C_e - T + m) + \lambda_f(n - m)\right]}{4}, \tag{12}$$

$$P_{s1}{}' - P_{s1} = \frac{C_e(\alpha - 1)T}{2}. \tag{13}$$

And there is $\alpha \geq 1$.

Proposition 8 shows that under normal circumstances and considering incentive conditions, the cooperative pric-

ing proposed by the e-commerce platform is different. Incentive factors have a certain impact on the behavioral decision-making of the e-commerce platform, and only affect the pricing reached in the first stage of the game between the two parties. If it is shown that the higher the subsidy and allocation amount between the incentive factors set by the bank for the e-commerce platform, and the higher the penalty amount, the greater the e-commerce revenue function platform will be. Under the premise of guaranteeing income, the price of the fourth-party service provider will be higher, which is conducive to increasing the service provider's business income [31]. If there is $T > C_e(\alpha - 1) > 0$ at $P_{s1}{}' < P_{s1}$, it means that when the amount of subsidy and sharing is lower and lower than the amount of penalty imposed, the income function of the e-commerce platform is smaller, and the cost and benefit protection considerations will restrict the provision price the service provider's business.

3.1. E-Commerce Platform First Bargaining Strategy with Banks. In this strategy, if the two parties first reach a deal, the e-commerce platform will be more cautious in bargaining because they cannot determine whether they can accept the fourth-party logistics service provider's quotation later; otherwise, if the two parties do not reach a deal, the game ends.

(a) The game between e-commerce platforms and banks

In the same way, use the reverse induction method to solve the problem, first discuss the second stage of the game and let the bank make a quotation first. If the bank's quotation P_{b2} meets the condition that the income of the e-commerce platform is positive, that is, at time $\lambda_e(P_{b2} - C_s) q \geq 0\ P_{b2} \geq C_s$, where q is the workload of the two parties to undertake the business, the e-commerce platform will accept the quotation and the game process ends [33]. Therefore, the bank can modify the estimation that $[m, P_{ei}]$ is a uniform

TABLE 2: Results of bargaining strategies between E-commerce platforms and service providers and banks.

E-commerce platform first game with service provider	Phase 1	E-commerce platform quotation	$P_{s1} = [2(C_e + m) + \lambda_f(n - m)]/4$
		To meet the conditions	$C_f \leq [2(C_e + m) - \lambda_f(n + m)]/2(2 - \lambda_f)$
	Phase 2	Service provider quotation	$P_{f2} = (n + C_f)/2$
		To meet the conditions	$C_e \geq P_{f2}$
E-commerce platform and silver game again	Phase 3	E-commerce platform quotation	$P_{e1} = [\lambda_b(m - n) + 2(n + C_e)]/4$
		To meet the conditions	$C_b \geq (2P_{e1} - \lambda_b m)/(2 - \lambda_b)$
	Phase 4	Bank quote	$P_{b2} = (C_b + m)/2$
		To meet the conditions	$P_{b2} \geq C_e$

distribution in the C_s interval. If π_b is used to represent the bank's own income, and P_{ea}, P_{er} is the probability that the e-commerce platform chooses to accept and reject the offer, then

$$\max_{P_{b2}} \pi_b = 0 \, P_{er} + \lambda_b(C_b - P_{b2})q P_{ea}, \tag{14}$$

$$P_{ea} = P(P_{b2} \geq C_s) = \frac{P_{b2} - m}{P_{e1} - m}, \tag{15}$$

$$P_{er} = P(P_{b2} < C_s) = \frac{P_{e1} - P_{b2}}{P_{e1} - m}. \tag{16}$$

Substituting equations (8) and (9) into equation (7) can find the maximum income that the bank can guarantee, and deriving the two sides of the obtained formula, we can get the bank's quotation in the second stage of the game:

$$P_{b2} = \frac{(C_b + m)}{2}, \tag{17}$$

If the e-commerce platform chooses to accept, the bank and the e-commerce platform will obtain the following benefits:

$$\lambda_b(C_b - P_{b2})q = \lambda_b \frac{(C_b - m)q}{2}, \tag{18}$$

$$\lambda_e(P_{b2} - C_s)q = \lambda_e \frac{(C_b + m - 2C_s)q}{2}. \tag{19}$$

Looking at the first stage of the game between the two parties and the e-commerce platform proposes a quotation P_{e1}, the bank will obtain income $(C_b - P_{e1})q$. In order to satisfy the bank's higher income at this stage, it should be at $(C_b - P_{e1})q \geq \lambda_b(C_b - m)q/2$, that is, $C_b \geq (2P_{e1} - \lambda_b m)/(2 - \lambda_b)$, the bank will choose to accept. If π_e is used to represent the income of the e-commerce platform itself, and P_{ba}, P_{bra} is the probability that the bank chooses to accept the quotation in the first and sec-

ond stages, respectively, then,

$$\max_{P_{e1}} \pi_e = (P_{e1} - C_s)q P_{ba} + \lambda_e \frac{(C_b + m - 2C_s)q P_{bra}}{2}, \tag{20}$$

$$P_{ba} = P\left(C_b \geq \frac{2P_{e1} - \lambda_b m}{2 - \lambda_b}\right) = \frac{[2(n - P_{e1}) + \lambda_b(m - n)]}{(2 - \lambda_b)(n - m)}, \tag{21}$$

$$P_{bra} = P\left(C_b < \frac{2P_{e1} - \lambda_b m}{2 - \lambda_b}\right) P(P_{b2} \geq C_s) = \frac{2(P_{b2} - m)}{(2 - \lambda_b)(n - m)}. \tag{22}$$

Substituting equations (11) and (12) into equation (10) to find the maximum profit that the e-commerce platform can guarantee, and deriving the two sides of the formula to P_{e1}, we can get

$$P_{e1} = \frac{[2(n + C_s) + \lambda_b(m - n)]}{4}. \tag{23}$$

That is, in general, the quotation of the e-commerce platform in the first stage, the condition that is satisfied at this time is $C_b \geq [2(C_s + n) - \lambda_b(n + m)/2(2 - \lambda_b)]$; if the condition of adding an incentive factor is considered, the quotation is set to $P_{e1}', P_{e1}' = [2n + 2(\beta C_s - I) + \lambda_b(m - n)]/4$. The condition that is satisfied at this time is $C_b \geq [2(n + \beta C_s - I) - \lambda_b(m + n)]/2(2 - \lambda_b)$, so consider the incentive The mechanism will have an impact on the final price of the cooperation. In summary, the equilibrium solution results of the game between the two parties can be seen in Table 3.

3.1.1. The Game between E-Commerce Platforms and Fourth-Party Logistics Service Providers. This study is based on the abovementioned bank's acceptance of e-commerce platform quotations in the first stage of the game, that is, under condition $C_b \geq [2(C_s + n) - \lambda_b(n + m)/2(2 - \lambda_b)]$, discussing the bargaining game between the e-commerce platform and the fourth-party logistics service provider. Refer to the above section for the process. The game results can be seen in Table 3.

TABLE 3: Results of bargaining strategies between E-commerce platforms and banks and service providers.

E-commerce platform first game with banks	Phase 1	E-commerce platform quotation	$P_{e1} = [2(n + C_s) + \lambda_b(m - n)]/4$
		To meet the conditions	$C_b \geq [2(C_s + n) - \lambda_b(n + m)]/2(2 - \lambda_b)$
	Phase 2	Service provider quotation	$P_{b2} = (C_b + m)/2$
		To meet the conditions	$P_{b2} \geq C_s$
E-commerce platform and service provider game again	Phase 3	E-commerce platform quotation	$P_{s1} = [2(C_e + m) + \lambda_f(n - m)]/4$
		To meet the conditions	$C_f \leq (2P_{s1} - \lambda_f n)/(2 - \lambda_f)$
	Phase 4	Bank quote	$P_{f2} = (C_f + n)/2$
		To meet the conditions	$C_e \geq P_{f2}$

Proposition 9. *In the strategy of bargaining with banks on the e-commerce platform, the first stage of the e-commerce platform's business pricing is P_{e1}, and the pricing under the condition of incentive factors is $P_{e1}{}'$. The comparison can be*

$$P_{e1} = \frac{[2(n + C_s) + \lambda_b(m - n)]}{4}, \quad (24)$$

$$P_{e1}{}' = \frac{[2n + 2(\beta C_s - I) + \lambda_b(m - n)]}{4}, \quad (25)$$

$$P_{e1}{}' - P_{e1} = \frac{C_s(\beta - 1) - I}{2}. \quad (26)$$

And there is $\beta \geq 1$.

Proposition 9 indicates that no matter which strategy is chosen, the cooperative pricing proposed by the e-commerce platform will be different in general and under consideration of incentive conditions, indicating that the incentive factor has a certain impact on the behavioral decision-making of the e-commerce platform and only affects the game between the two parties. The pricing reached in the first stage has an impact. Among them, if $0 \leq I < C_s(\beta - 1)$, there is $P_{e1}{}' \geq P_{e1}$, indicating that the higher the amount of subsidies and rewards, and the higher the amount of penalty imposed by the e-commerce platform, the higher the cost of the e-commerce platform. The function is larger, and the constraint and punishment on the service provider are smaller. In order to protect the platform's revenue, the bank will offer a higher price. If there is $I > C_s (\beta - 1) > 0$ at $P_{e1}{}' < P_{e1}$, it means that when the amount of subsidies and rewards is lower and lower than the amount of penalties levied, for the e-commerce platform, through the restraint and supervision of service providers, a certain amount of income is guaranteed, which helps to increase the enthusiasm of the e-commerce platform for cooperation and investment also reflects that it has a relatively small impact on the platform's bargaining attitude with the bank, which makes it easier for the bank to consider the decision-making problem of determining reasonable pricing from its own perspective. This also shows that the e-commerce platform in Proposition 7 needs to be considered in conjunction with bilateral bargaining links. The results of

bargaining with one party and incentive factors will have an impact on the results of bargaining with the other party.

Proposition 10. *Based on the above analysis, it is known that the e-commerce platform in the bilateral bargaining price proposed by the fourth-party logistics service provider and the bank are, respectively, P_{s1} and P_{e1}. Taking the derivation of λ_f and λ_b on both sides of the formula, we can get*

$$\frac{\partial P_{s1}}{\partial \lambda_f} = \frac{n - m}{4} \geq 0, \frac{\partial P_{e1}}{\partial \lambda_b} = \frac{m - n}{4} \leq 0. \quad (27)$$

Proposition 10 shows that no matter which strategy the e-commerce platform chooses, its pricing decision is not affected by its own factors, but by the bargaining ability factors (λ_f, λ_b) of the counterparty in the game. Among them, the e-commerce platform's pricing of service providers is positively correlated with the counterparty's bargaining power, and the bank's pricing is negatively correlated with the counterparty's ability factors; while the pricing decisions of the service provider and the bank are related to their respective business costs (C_f, C_b). It is positively correlated.

Proposition 11. *First of all, in strategy 1, it is known that P_{s1} is the quotation of the e-commerce platform and the fourth-party logistics service provider, and C_e is the final business price negotiated between the e-commerce platform and the bank. Since the e-commerce platform and the bank's quotation are P_{e1}, so substituting it into the G formula to get the final price P_{s1} reached by the e-commerce platform and the service provider $P_{s1}{}'$:*

$$P_{s1} = \frac{[2(C_e + m) + \lambda_f(n - m)]}{4}, \quad (28)$$

$$P_{e1} = \frac{[\lambda_b(m - n) + 2(n + C_e)]}{4}, \quad (29)$$

$$P_{s1}{}' = \frac{[(n - m)(2\lambda_f - \lambda_b) + 4m + 2(n + C_e)]}{8}. \quad (30)$$

And if the e-commerce platform offers the same

quotation to the service provider in the first stage, $C_e = [2n - (n-m)\lambda_b]/2$ can be obtained. It can be seen that in the second stage of the game, under condition $C_f \leq [(n-m)(\lambda_f - \lambda_b) + 2(n+m) - 2\lambda_f n]/2(2-\lambda_f)$, the service provider will choose to accept the quotation offered by the e-commerce platform and reach cooperation in the first stage of the game.

Similarly, in strategy two, it is known that P_{e1} is the quotation of the e-commerce platform and the bank, and C_s is the business price reached by the bargaining between the e-commerce platform and the fourth-party logistics service provider. Substitute the quotation P_{e1} of the e-commerce platform and the service provider into the formula P_{e1}'. Available business pricing finally reached between the e-commerce platform and the bank:

$$P_{e1} = \frac{[2(n + C_s) + \lambda_b(m-n)]}{4}, \tag{31}$$

$$P_{s1} = \frac{[2(C_e + m) + \lambda_f(n-m)]}{4}, \tag{32}$$

$$P_{e1}' = \frac{[(n-m)(\lambda_f - 2\lambda_b) + 2(C_e + m) + 4n]}{8}. \tag{33}$$

And if the e-commerce platform offers the same quotation for the bank in the first stage, $C_e = [2m + (n-m)\lambda_f]/2$ can be obtained. From this, it can be seen that in the first stage of strategy $C_b \geq [(n-m)(\lambda_f - \lambda_b) + 2(n+m) - 2\lambda_b m]/2(2-\lambda_b)$, if the conditions are met, the bank will choose to accept and reach cooperation in the first stage of the game.

Compare the pricing of banks in different strategies by the e-commerce platform, that is, strategy one, after the e-commerce platform makes a quotation to the service provider, and then the quotation P_{e1} to the bank; and strategy two, the e-commerce platform to the service provider, the first stage the quotation of is substituted into the quotation for the first stage of the bank, and the quotation provided by the e-commerce platform to the bank first, that is, the final price P_{e1}' reached by the two parties, can be compared:

$$P_{e1} = \frac{[(n-m)(\lambda_f - \lambda_b) + 2(n+m)]}{4}, \tag{34}$$

$$P_{e1}' = \frac{(n-m)(\lambda_f - 3\lambda_b) + 6n + 2m]}{8}, \tag{35}$$

$$P_{e1}' - P_{e1} = \frac{[(n-m)(2 - \lambda_b - \lambda_f)]}{8}. \tag{36}$$

Because of $0 < \lambda_b, \lambda_f < 1$, so $P_{e1}' > P_{e1}$. In the same way, the pricing of service providers on e-commerce platforms is different in different strategies.

Proposition 11 indicates that the e-commerce platform's pricing decisions for banks and service providers need to consider the issues in bilateral pricing strategies at the same time. In different strategies, the price offered by the e-commerce platform to the game player is different. The price offered by the e-commerce platform to the bank will be

higher than the price offered to the bank after the service provider. Therefore, for e-commerce platforms, in the process of participating in the cooperation, first determining the cooperative pricing with the bank will help achieve better returns.

Proposition 12. *In strategy 1, if the e-commerce platform can complete the game with the fourth-party logistics service provider and the bank in the first stage:*

$$C_f \leq \frac{[(2-\lambda_f)(n+3m) + \lambda_b(m-n)]}{4(2-\lambda_f)} = r, \tag{37}$$

$$C_b \geq \frac{[(n-m)(\lambda_f - \lambda_b) + 2(n+m) - 2\lambda_b m]}{2(2-\lambda_b)} = k. \tag{38}$$

Because of $k - r > 0$, $C_b \geq C_f$ can be obtained; and it can be analyzed that the income of the e-commerce platform is positive, that is, the difference between the price P_{e1} of the e-commerce platform and the bank and the price P_{s1}' of the service provider is positive, where P_{s1}' is determined by substituting P_{e1} into P_{s1} to get, namely,

$$P_{s1} = \frac{[2(C_e + m) + \lambda_f(n-m)]}{4}, \tag{39}$$

$$P_{e1} = \frac{[2(n+m) + (n-m)(\lambda_f - \lambda_b)]}{4}, \tag{40}$$

$$P_{s1}' = \frac{[(n-m)(3\lambda_f - \lambda_b) + 2n + 6m]}{8}. \tag{41}$$

Because of $P_{e1} - P_{s1}' > 0$, the income of the e-commerce platform is positive under this condition. Similarly, in the second strategy, if the e-commerce platform can complete the game with the bank and the service provider in the first stage:

$$C_f \geq \frac{[(n+m)(2-2\lambda_b) + (n-m)(\lambda_f - \lambda_b) + 4n]}{4(2-\lambda_b)} = \varepsilon, \tag{42}$$

$$C_f \leq \frac{[(n-m)(\lambda_f - \lambda_b) + 2(n+m) - 2\lambda_f n]}{2(2-\lambda_f)} = \mu. \tag{43}$$

There may be $C_b \geq C_f$, and the e-commerce platform income may be positive.

Proposition 12 shows that if condition $C_b \geq k, C_f \leq r$, $C_f \leq C_b$ is met, the e-commerce platform can first complete the game with the service provider in one stage and then complete the game with the bank in one stage, and the return is positive. Under condition $C_b \geq \varepsilon C_f \leq \mu$, the e-commerce platform can first complete the game with the bank in one stage and then complete the game with the service provider in one stage.

Proposition 13. *In strategy 1, if the e-commerce platform first completes the game with the fourth-party logistics service provider in the first stage, and then completes the game with the bank in the second stage, it will exist when the game process between the e-commerce platform and the bank enters the second stage condition:*

$$P_{b2} = \frac{(C_b + m)}{2} \geq \frac{[2m + (n-m)\lambda_f]}{2}, \quad (44)$$

$$C_b < \frac{[(n-m)(\lambda_f - \lambda_b) + 2(n+m) - 2\lambda_b m]}{2(2-\lambda_b)} = \omega. \quad (45)$$

Therefore, there is inequality $(n-m)\lambda_f + m \leq C_b < [(n-m)\lambda_f + (n+m)(2-\lambda_b)]/(4-2\lambda_b)$, and the condition $[\lambda_f (3-2\lambda_b) + \lambda_b]/2 < 1$ can be established by observing both sides of the inequality. The first-stage game condition between the e-commerce platform and the service provider is $C_f \leq v$, combined with the condition $C_f \leq C_b$, the second inequality about C_b can be obtained as follows:

$$C_f \leq \frac{[C_b + 3m - \lambda_f(n+m)]}{2(2-\lambda_f)} = v, \quad (46)$$

$$C_b \geq \frac{[3m - \lambda_f(n+m)]}{(3-2\lambda_f)}. \quad (47)$$

After comparing the two inequalities, it is found that

$$\frac{[3m - \lambda_f(n+m)]}{(3-2\lambda_f)} - \frac{[(n-m)\lambda_f + (n+m)(2-\lambda_b)]}{(4-2\lambda_b) < 0}. \quad (48)$$

Therefore, there is an intersection between inequalities, there is $t \leq C_b < [(n-m)\lambda_f + (n+m)(2-\lambda_b)]/(4-2\lambda_b)$, where $t = \max[(n-m)\lambda_f + m, [3m - \lambda_f(n+m)]/(3-2\lambda_f)]$

Proposition 13 shows that when condition $C_f \leq v, t \leq C_b < \omega$ is met, the e-commerce platform can also choose to complete the bargaining game with the service provider in the first stage and then complete the game with the bank in the second stage.

4. Numerical Analysis

Combining the above analysis, the results of the bargaining game between e-commerce platforms and banks and fourth-party logistics service provider platforms are numerically analyzed. Suppose that the basic parameters are taken as $m = 10$, $n = 30$, λ_f, λ_b is in the interval (0,1), $\alpha, \beta \geq 1$, T, $I \geq 0$. The setting of parameters needs to meet the constraints of the above propositions. Suppose that P_{s1} and $P_{s11}{}'$ are used to represent the quotation of the service provider in the first stage of the game under normal circumstances and with the addition of incentive factors, respectively, and P_{e1} represents the general situation, the e-commerce platform first offers the quotation to the service provider, and then the quotation offered by the bank in the first stage of the game. P_{b2} represents the quotation offered by the bank during the second stage of the game between the e-commerce platform and the bank, and P_{e11} and $P_{e11}{}'$, respectively, represent general under the circumstances and with the addition of incentive factors, the e-commerce platform first quotes the bank's quotation in the first stage. $P_{e1}{}'$ indicates that considering the e-commerce platform's subsequent transaction with the service provider, the bank's first stage of the game offer.

4.1. The Impact of Incentive Factors on the Pricing Strategy of E-Commerce Platforms. When considering the inclusion of incentive factors, it will have a certain impact on the pricing behavior of the e-commerce platform. The incentive factors added by one party in the cooperation will affect the pricing decision of the other party in other cooperation. Figure 3 reflects the changes in e-commerce platform's decision-making for service providers under the influence of incentives.

According to the results of the numerical analysis, it can be seen from Figure 3 that if the amount of cost subsidies and sharing incentives invested by the bank on the e-commerce platform is higher than the amount of penalty incentives levied in advance for the platform cooperation crisis, when it meets $0 \leq T < C_e(\alpha - 1)$, there is $P_{s11}{}' > P_{s1}$, that is, the e-commerce platform will increase the price of the service provider, so that the service provider can get higher cooperation rewards in the negotiation with it. In addition, the platform's offer $P_{s11}{}'$ to the service provider will increase as α increases. Conversely, the platform's offer to service providers will decrease with the increase of. When $T > C_e(\alpha - 1) > 0$ is met and the penalty parameter is higher than the value of the subsidy parameter, the platform's offer to the service provider will be reduced. The analysis is mainly due to the decrease in the pricing income obtained by the e-commerce platform from the negotiation with the bank, and the platform is out of interest. The angle of view will reduce the cost of outsourcing by lowering the quotation of service providers. For banks, the restriction and supervision of the platform can better reduce transaction costs, mobilize the enthusiasm in the supply chain finance business, and promote the development of client enterprise financing projects on the platform. In addition, from the numerical analysis, it can be concluded that the quotation $P_{s11}{}'$ of the e-commerce platform to the service provider will not be affected by the change of the β value. Figure 4 reflects the changes in e-commerce platforms' pricing decisions for banks under the influence of incentives.

It can be seen from Figure 3 that if the amount of subsidies or business rewards invested by the e-commerce platform to the service provider is higher than the amount of penalties levied in advance, when it meets $0 \leq I < C_s(\beta - 1)$, there is $P_{e11}{}' > P_{e11}$, that is, the e-commerce platform will propose a higher level to the bank. Quotation, which is conducive to obtaining higher cooperation rewards. In addition, the platform's offer $P_{e11}{}'$ to the bank will increase as β increases. Conversely, the quotation $P_{e11}{}'$ of the platform to the bank will decrease with the increase of I; when $I > C_s(\beta - 1) > 0$ is met and the value of the penalty parameter
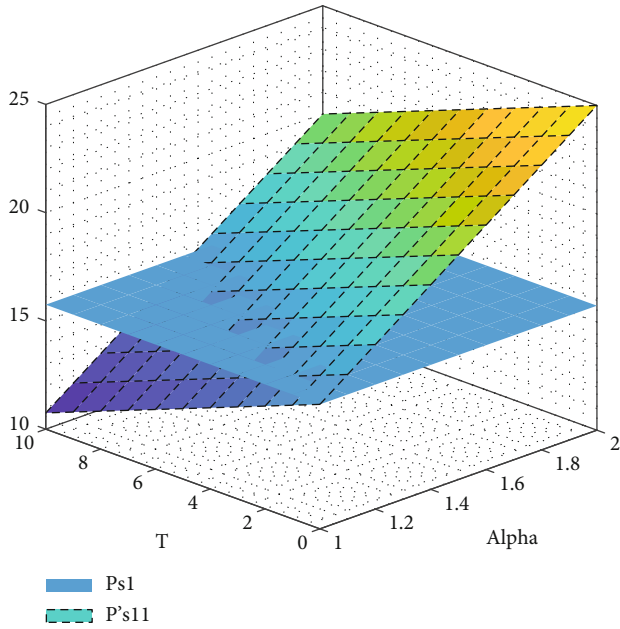
FIGURE 3: The changing trend of e-commerce platform's pricing of service providers under different incentive factors α, T.
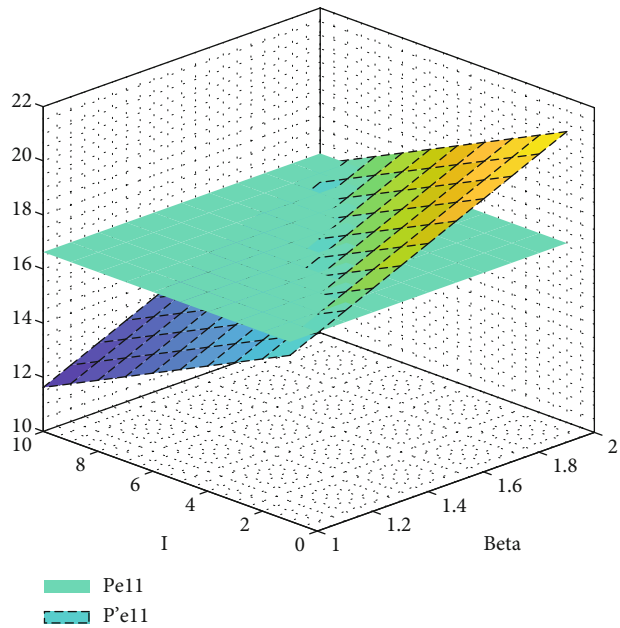

FIGURE 4: The changing trend of bank pricing by E-commerce platforms under different incentive factors β, I.

is higher, the quotation of the platform to the bank will decrease. The analysis is mainly because the platform can reach the service provider well. The purpose of the supervision of the business development process is to ensure that the bank's quotation is less demanding on the premise of ensuring its own benefits, which is beneficial to stimulate the bank's cooperation initiative. In addition, from the numerical analysis, it can be concluded that the e-

commerce platform's offer $P_{e11}{}'$ to the bank will not be affected by the change in the value of α. Therefore, each participant can make relevant pricing decisions from the perspective of their own benefits and cooperation, which is in line with the calculation results of Propositions 8 and 9. At the same time, it also shows that e-commerce platforms need to consider decision-making in conjunction with bilateral bargaining links and make timely adjustments. The results of the bargaining game with one party and the incentive conditions will affect the results of the game with the other party, which conforms to the conclusion of Proposition 7.

4.2. The Influence of the Bargaining Power of Banks and Service Providers on the Pricing Strategy of E-Commerce Platforms. While keeping the value of λ_f unchanged, observing the pricing trends of the e-commerce platform when the value of λ_b is different, it can be seen that as the value of λ_b continues to increase, no matter which pricing strategy the e-commerce platform chooses, the platform's trend of pricing P_{e1} will continue to decrease, which is negatively correlated with factors related to bank bargaining power. The impact on the pricing of the platform and the service provider is relatively small, that is, the change trend of P_{s1} is relatively flat. Figure 5 reflects the influence of banks' bargaining power on the pricing decisions of e-commerce platforms.

At the same time, when the platform chooses the strategy of bargaining with the service provider first and then with the bank, the ability influencing factor has less impact on the platform's pricing behavior, that is, the change trend of B is relatively flat. Comply with the calculation result of Proposition 10. In addition, under different values of $P_{e1}{}'$, the e-commerce platform's first offer to the bank P_{e1} will be higher than the first offer to the service provider, and then the offer to the bank E. Therefore, if the pricing strategy can be achieved, the platform chooses to first determine the pricing of business cooperation with the bank, which will help it obtain better returns, which is in line with the calculation results of Propositions 11 and 12. Figure 6 reflects the influence of service providers' bargaining power on the pricing decisions of e-commerce platforms.

As shown in Figure 6, while keeping the value of λ_b unchanged, observing the changing trend of e-commerce platform pricing with different values of λ_f, it can be seen that as the value of λ_f continues to increase, the platform's pricing trend for service providers will constantly rise, and it is positively correlated with the bargaining power factor of service providers.

4.3. The Impact of Bank and Service Provider Cost Factors on E-Commerce Platform Pricing Strategies. According to the analysis of Proposition 13, observe the pricing decision of the e-commerce platform under the condition of conforming to $C_f \leq v, l \leq C_b < \omega$, and the relationship $[\lambda_f(3 - 2\lambda_b) + \lambda_b]/2 < 1$ is established. It can be seen that no matter in general or in the presence of incentive factors, the e-commerce platform can choose to first offer a quotation with the service provider, and then offer a quotation with the
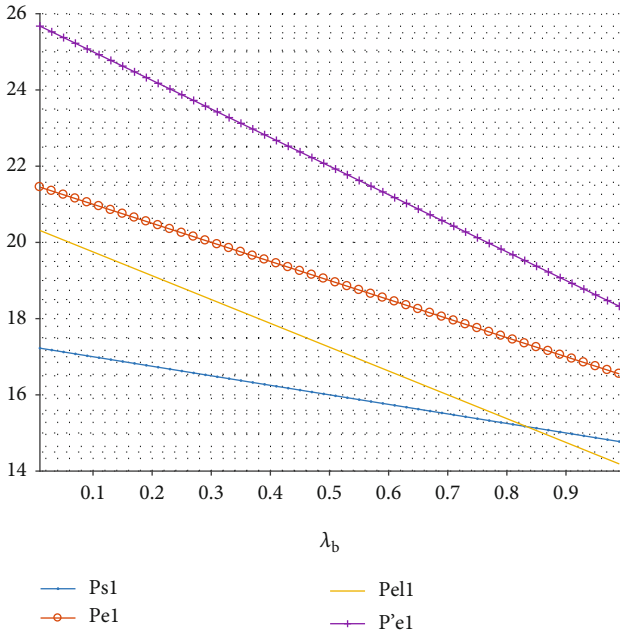
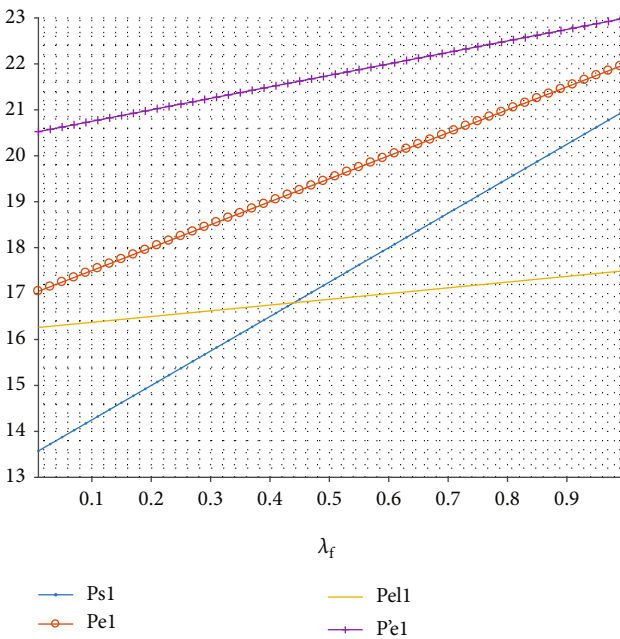Figure 5: The changing trend of E-commerce platform pricing under different bargaining power λ_b.

Figure 6: The pricing trends of E-commerce platforms under different bargaining power λ_f.

Figure 7: Changes in pricing of e-commerce platforms under the joint action of C_f and C_b.

bank in a stage of the game, and the return is positive. You can also choose to accept the quotation proposed by the bank in the second-stage game with the bank and complete the transaction. At this time, it must conform to the relational formula of λ_f, λ_b and the calculation result of Proposition 13. Figure 7 reflects the impact on the pricing strategy of e-commerce platforms under the conditions of changing the business costs of banks and service providers.
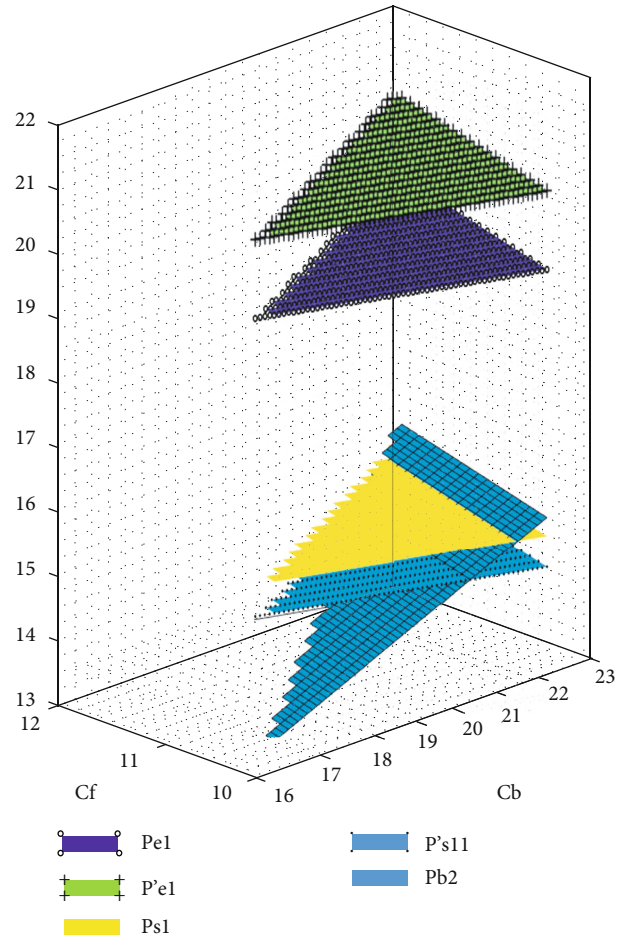
From the perspective of e-commerce platforms, this paper discussed the strategic issues of bilateral business cooperation pricing between e-commerce platforms, banking institutions, and service providers in supply chain finance and discussed the pricing decisions of e-commerce platforms under different bargaining orders. Analyze the influence of partners' bargaining power, cost and incentive factors on pricing decisions, and draw the following conclusions: first, the pricing decisions of e-commerce platforms are related to the efforts of partners, bargaining power and other factors, and e-commerce platforms. The higher the negotiated price, the more helpful it is to strengthen the cooperation between the service provider and the platform; the quotation proposed by the platform to the bank increases with the decrease of the counterpart's ability, and the negotiated price increases. High, the more helpful it is to strengthen the cooperation between the platform and banking institutions. It shows that e-commerce platforms can explore multiplatform pricing cooperation and revenue coordination strategies based on their expected benefits and partner negotiation capabilities. The second conclusion is the pricing decisions of service which providers and banks change with changes in their respective costs. Both parties can proceed from reality and adjust their decisions by

controlling relevant business costs. It shows the importance of reducing costs and improving risk control capabilities to all parties. With the introduction of incentive mechanisms for partners, under certain conditions, the cost pressure of the other party can be alleviated, playing a role in cooperation incentives and behavioral restraints, indicating that appropriate incentive conditions are considered, such as subsidies for partners' costs or risks. And incentives, constraints on cooperative business processes, etc., will help realize multiplatform mutual profit and promote cooperative alliances. In terms of strategic choice, if the e-commerce platform chooses to negotiate pricing with the bank first, the pricing reward will be higher than the reward it would obtain after negotiating the pricing with the service provider and then negotiating the pricing with the bank; at the same time, the platform can make a decision with reference to the value range and conditions of the partner's cost coefficient.

5. Conclusion

The research paper concludes that the realistic for online supply chain financial services, especially those in which e-commerce platforms, banking institutions, and fourth-party logistics service providers participate in cooperation, and coordinate the pricing decisions and interest relationships between e-commerce platforms and partners significance, help to improve the overall cooperation intensity and efficiency, and promote the optimal allocation and integration of upstream and downstream resources. However, this article also has some limitations. It does not consider the risk factors involved in the business. The value and interval uniform distribution of parameters and other ways of cooperation need to be further explored. This is also the direction of follow-up research and will be in future research. Look at the problem with a developmental perspective. Combining the research content, try to put forward the following suggestions for the development of supply chain finance and the cooperation strategy of e-commerce platforms: first, for e-commerce platforms, they should make better use of their unique network technology advantages in bilateral business cooperation and expand customer groups. Strengthen the construction of information platforms, further promote the flow of upstream and downstream information, improve the collection and management of customer enterprise information and credit evaluation, and improve bank credit entrustment services, thereby helping banks reduce transaction risks and improve review efficiency. On the other hand, it will strengthen cooperation with service providers in logistics and product services, and strengthen standardization work such as e-commerce and logistics docking and data sharing, so as to optimize the transportation and circulation efficiency of online products and improve the basic service level of products. Second, for banks, further improve financial services, achieve customer segmentation and precise marketing, reduce the cost of information asymmetry, and improve the efficiency of credit and risk management; for service providers, pay more attention to technology and resource optimization. Improve the efficiency of product operation by improving the smart logistics service system and product sales chain. Third, innovate technology and optimize the external environment. Use terminal technology, artificial intelligence, digitization, cloud computing, and other technologies to establish a digital credit system to provide risk control and technical support for operations on the supply chain; at the same time, adhere to the guidance of the government to promote leading enterprises and e-commerce enterprises to drive upstream and downstream small and medium-sized enterprises enterprise development, improve corporate financing efficiency, and provide a beneficial environment for promoting new channels and new development of supply chain finance.

Data Availability

All data has been included in the manuscript.

Conflicts of Interest

The authors declare that they have no conflicts of interest.

References

[1] A. Nagurney, P. Daniele, and S. Shukla, "A supply chain network game theory model of cybersecurity investments with nonlinear budget constraints," *Annals of Operations Research*, vol. 248, no. 1-2, pp. 405–427, 2017.

[2] Q. Hu, Z. Xu, T. Dinev, and H. Ling, "Does deterrence work in reducing information security policy abuse by employees?," *Communications of the ACM*, vol. 54, no. 6, pp. 54–60, 2011.

[3] R. W. Johnstone, "Not safe enough: fixing transportation security," *Issues in Science and Technology*, vol. 23, no. 2, pp. 51–60, 2007.

[4] N. J. Rowan and C. M. Galanakis, "Unlocking challenges and opportunities presented by COVID-19 pandemic for cross-cutting disruption in agri-food and green deal innovations: Quo Vadis?," *Science of the Total Environment*, vol. 748, p. 141362, 2020.

[5] C. Zhao and B. Chen, "China's oil security from the supply chain perspective: a review," *Applied Energy*, vol. 136, pp. 269–279, 2014.

[6] X. Wang, Y. Wu, L. Liang, and Z. Huang, "Service outsourcing and disaster response methods in a relief supply chain," *Annals of Operations Research*, vol. 240, no. 2, pp. 471–487, 2016.

[7] H. Song, K. Yu, A. Ganguly, and R. Turson, "Supply chain network, information sharing and SME credit quality," *Industrial Management & Data Systems*, vol. 116, no. 4, pp. 740–758, 2016.

[8] M. S. Heng, "Research note: implications of e-commerce for banking and finance," *SSRN Electronic Journal*, vol. 12, no. 7, pp. 392–401, 2006.

[9] R. S. Bhatti, P. Kumar, and D. Kumar, "Analytical modeling of third party service provider selection in lead logistics provider environments," *Journal of Modelling in Management*, vol. 5, no. 3, pp. 275–286, 2010.

[10] G.-S. Tang, "Supply chain governance level, bank's perception of the seller and bank credit," in *2014 International Conference on Management Science & Engineering 21th Annual Conference Proceedings*, pp. 1333–1338, IEEE, 2014.

[11] E. Francis, J. Blumenstock, and J. Robinson, *Digital Credit: A Snapshot of the Current Landscape and Open Research Questions*, CEGA White Paper, 2017.

[12] J. Wikner, D. R. Towill, and M. Naim, "Smoothing supply chain dynamics," *International Journal of Production Economics*, vol. 22, no. 3, pp. 231–248, 1991.

[13] A. Amid, S. Ghodsypour, and C. O'Brien, "A weighted max-min model for fuzzy multi-objective supplier selection in a supply chain," *International Journal of Production Economics*, vol. 131, no. 1, pp. 139–145, 2011.

[14] A. V. Iyer and M. E. Bergen, "Quick response in manufacturer-retailer channels," *Management Science*, vol. 43, no. 4, pp. 559–570, 1997.

[15] I. Triulzi, F. Di Pasquale, A. Antonel, E. Rossi, and G. Turchetti, "PP155 demand side and supply side of healthcare supply chain," *International Journal of Technology Assessment in Health Care*, vol. 35, no. S1, pp. 66-67, 2019.

[16] M. E. Ferguson, "When to commit in a serial supply chain with forecast updating," *Naval Research Logistics (NRL)*, vol. 50, no. 8, pp. 917–936, 2003.

[17] F. Mazzetto, R. A. Ortiz-Gutiérrez, D. Manca, and F. Bezzo, "Strategic design of bioethanol supply chains including commodity market dynamics," *Industrial & Engineering Chemistry Research*, vol. 52, no. 30, pp. 10305–10316, 2013.

[18] D. Lanier Jr., W. F. Wempe, and Z. G. Zacharia, "Concentrated supply chain membership and financial performance: chain- and firm-level perspectives," *Journal of Operations Management*, vol. 28, no. 1, pp. 1–16, 2010.

[19] M. Du, Q. Chen, J. Xiao, H. Yang, and X. Ma, "Supply chain finance innovation using blockchain," *IEEE Transactions on Engineering Management*, vol. 67, no. 4, pp. 1045–1058, 2020.

[20] K. N. Qureshi, R. Hussain, and G. Jeon, "A distributed software defined networking model to improve the scalability and quality of services for flexible green energy internet for smart grid systems," *Computers Electrical Engineering*, vol. 84, article 106634, 2020.

[21] M. Marques, M. F. Da Costa, M. I. D. O. Mayorga, and P. R. C. Pinheiro, "Water environments: anthropogenic pressures and ecosystem changes in the Atlantic drainage basins of Brazil," *Environment*, vol. 33, no. 1, pp. 68–77, 2004.

[22] J. Manne, C. S. Snively, M. Z. Levy, and M. R. Reich, "Supply chain problems for Chagas disease treatment," *The Lancet Infectious Diseases*, vol. 12, no. 3, pp. 173–175, 2012.

[23] K. N. Qureshi, O. Kaiwartya, G. Jeon, and F. Piccialli, "Neurocomputing for internet of things: object recognition and detection strategy," *Neurocomputing*, vol. 8, no. 22, pp. 623–635, 2021.

[24] Y.-W. Kim, S.-H. Han, J.-S. Yi, and S. Chang, "Supply chain cost model for prefabricated building material based on time-driven activity-based costing," *Canadian Journal of Civil Engineering*, vol. 43, no. 4, pp. 287–293, 2016.

[25] A. Hasan and K. Qureshi, "Internet of things device authentication scheme using hardware serialization," in *in 2018 International Conference on Applied and Engineering Mathematics (ICAEM)*, pp. 109–114, IEEE, 2018.

[26] T.-J. Yang, "Financial performance analysis of e-collaboration supply chain under transportation disruptions," in *in 2008 International Symposium on Computer Science and Computational Technology*, vol. 2, pp. 435–439, IEEE, 2008.

[27] A. Paz, G. El Boussaidi, and M. Hafedh, "checsdm: a method for ensuring consistency in heterogeneous safety-critical system design," *IEEE Transactions on Software Engineering*, vol. 5, no. 23, pp. 226–234, 2020.

[28] A. Filippov and S. Shkirskaya, "Verification of the cell (heterogeneous) model of an ion-exchange membrane and its comparison with the homogeneous model," *Colloid Journal*, vol. 81, no. 5, pp. 597–606, 2019.

[29] K. Riad and J. Cheng, "Adaptive XACML access policies for heterogeneous distributed IoT environments," *Information Sciences*, vol. 548, pp. 135–152, 2021.

[30] R. S. Jayne, H. Wu, and R. M. Pollyea, "Geologic CO_2 sequestration and permeability uncertainty in a highly heterogeneous reservoir," *International Journal of Greenhouse Gas Control*, vol. 83, pp. 128–139, 2019.

[31] E. Yang, D.-K. Kang, and C.-H. Youn, "BOA: batch orchestration algorithm for straggler mitigation of distributed DL training in heterogeneous GPU cluster," *The Journal of Supercomputing*, vol. 76, no. 1, pp. 47–67, 2020.

[32] G. Xie, W. Ma, H. Peng, R. Li, and K. Li, "Price performance-driven hardware cost optimization under functional safety requirement in large-scale heterogeneous distributed embedded systems," *IEEE Transactions on Industrial Electronics*, vol. 68, no. 5, pp. 4485–4497, 2019.

[33] Y. Yu, Z. Li, D. Zhang, L. Xing, and H. Peng, "Simulation studies of time reversal-based protoacoustic reconstruction for range and dose verification in proton therapy," *Medical Physics*, vol. 46, no. 8, pp. 3649–3662, 2019.